WT1 ROLE IN MAMMARY GLAND AND BREAST CANCER BIOLOGY

Mara Artibani

Ph.D.

The University of Edinburgh

2014

Declaration

This thesis has been composed by me and is entirely my own work.

The experiments described within this thesis, unless stated otherwise, have been carried out by me and have not been submitted for any other degree or professional qualification.

Mara Artibani

Acknowledgements

Firstly, I would like to express my gratitude to my supervisors, Peter Hohenstein and Nick Hastie: their help, support and guidance were essential for the development of this project.

Secondly, this work would have not been possible without the members of the Hohenstein and Hastie labs, who I will really miss, or my precious collaborators (Dr. A. Sims performed the bioinformatics analysis, Dr. E. Katz provided the first set of clinical samples, Dr. M. Smalley and Dr. D. Sproul sorted the different mammary populations, Dr. R. McGregor and Dr. T. Kendall provided the second set of clinical samples, Dr. S. Aitken performed the Galaxy analysis of the RNA-sequencing data, Dr. E. Freyer performed the flow cytometer analyses and sorting, Dr. J. Del Pozo and Dr. L. Morrison analysed the mammary branching, Dr. M. Diaz and J. Bailey performed the histopathological analysis of the murine mammary tumours).

Special thanks should also go to Anna Thornburn, for her amazing support with all the animal experiments, and to my colleagues of the West Wing office.

Lastly, I would like to thank all my family and friends for their patience and support, in particular my dearest friends (Manu, Flavietta, Miss Paro & Zhou Zhou), my sister Irene, my parents and my husband.

Abstract

The Wilms' Tumour Suppressor gene 1, *WT1*, encodes for a complex protein which is essential in mammals throughout life. Its roles vary with the developmental stages: in the embryo, it regulates the epithelial-mesenchymal balance required for a correct organogenesis and acts as a tumour suppressor; in the adult, it is involved in the maintenance of tissue homeostasis and has been controversially considered as an oncogene.

Breast cancer is one of the adult tumours in which *WT1* oncogenic function was first hypothesised. This malignancy is the most common in women, with more than one million cases being diagnosed worldwide every year, and represents the leading cause of cancer related deaths.

Because of its major health burden, this disease has been extensively studied and special attention has also been paid to normal mammary gland biology: several works have shown that breast cancer can be divided into many molecular subtypes, which may reflect the cell of origin of the tumour; moreover, many genes involved in the normal development of the mammary gland have been proven to also play a role in breast tumorigenesis.

WT1 expression has been previously reported in both healthy mammary glands and breast cancer samples, however, its function in this context is not well understood and the evidence gathered so far is extremely contradictory.

This thesis aimed to investigate the exact role played by WT1 in both mammary gland and breast cancer biology, using a combination of *in vivo* and *in vitro* techniques.

Following flow cytometry isolation, *Wt1* mRNA expression was detected in the myoepithelial and stem cell subpopulations of the healthy gland. To investigate the effects of WT1 loss, *Wt1* conditional mice were crossed with two different mammary specific Cre lines: the knockout animals developed, bred and lactated normally, however, they showed a significant increase of ductular branches during pregnancy, suggesting that WT1 may be involved in the regulation of branching morphogenesis.

In order to study WT1 role in mammary tumours, the gene was knocked out in a breast cancer mouse model and knocked down in several breast cancer cell lines, using both constitutive and inducible lentivirus-based systems. WT1 loss did not seem to affect cell proliferation, but resulted in a significant increase in cell migration *in vitro* and in the upregulation of mesenchymal markers.

Furthermore, bioinformatics analysis showed that the *WT1*-positive tumours mainly belong to the luminal/ER-positive subtypes and express lower levels of mesenchymal markers than the *WT1*-negative tumours.

As a whole, the findings of this thesis characterise WT1 expression in the healthy mammary gland and provide the first evidence of its possible function in this organ; moreover, this work seems to rule out an oncogenic role for WT1 in breast cancer, while suggesting that it could be an upstream regulator of cell migration. Additional experiments are required to confirm this result *in vivo* and verify whether it could lead to any clinical application.

Abbreviations

cDNA	Complementary DNA
CFA	Colony Forming Assay
Cre	Cre-Recombinase
CSCs	Cancer Stem Cells
EMT	Epithelial to Mesenchymal Transition
EYFP	Enhanced Yellow Fluorescent Protein
FACS	Fluorescence Activated Cell Sorting
FCS	Foetal Calf Serum
GD	Gestation Day
GFP	Green Fluorescent Protein
IDC	Invasive Ductal Carcinoma
IF	Immunofluorescence
IHC	Immunohistochemistry
MaSCs	Mammary Stem Cells
MET	Mesenchymal to Epithelial Transition
mRNA	messenger RNA
NOD/SCID	Non Obese Diabetic/Severe Combined Immuno Deficiency
NST	No Special Type
PABC	Pregnancy Associated Breast Cancer
PBS	Phosphate Buffered Saline

PCR	Polymerase Chain Reaction
RFP	Red Fluorescent Protein
RNAi	RNA interference
RT-PCR	Reverse-Transcription PCR
SAM	Significance Analysis of Microarray
SV40 Tag	Simian Virus 40 large Tumour Antigen
shRNA	small hairpin RNA
siRNA	small interfering RNA
TGF	Transforming Growth factor
VEGF	Vascular Endothelial Growth Factor
WT1	Wilms' Tumour Suppressor Gene 1

Table of contents

Figures and Tables

Chapter 1: Introduction

1.1 Overview

Breast cancer is the most frequent malignancy in women, with more than one million cases being diagnosed worldwide every year (Parkin and Fernández 2006, Soerjomataram, Lortet-Tieulent et al. 2012). Despite all the recent progress made in the therapeutic field, breast cancer still accounts for 14% of cancer deaths and kills annually more than 410,000 women (Coughlin and Ekwueme 2009).

The heterogeneity of this disease, which can be divided into many histological and molecular subtypes, represents a major challenge and a lot of effort is being put into finding new biomarkers and therapy targets that would help treat the patients according to their subtype of breast cancer.

Given the strong links between tumour and developmental biology, another line of research has focused on the normal mammary gland and its signalling pathways, showing that many genes involved in the normal development of the mammary gland also play a role in breast cancer (Dickson, Creer et al. 2000, Lanigan, O'Connor et al. 2007).

One such gene may be the Wilms' Tumour Suppressor gene 1, *WT1*, which encodes for a complex protein essential for mammalian development.

WT1 has been extensively studied in the fields of embryology, oncology and renal disease, however its role in both normal and cancerous mammary glands remains unclear: its expression has been reported in the myoepithelium and in the ductal lumen of the normal gland (Silberstein, Van Horn et al. 1997, Silberstein, Dressler et al. 2002) as well as in breast cancer, where it is at the centre of a controversy over a potential oncogenic or tumour suppressing function (Cheng, Wu et al. 2001, Loeb, Evron et al. 2001, Zhang, Yu et al. 2003, Wang and Wang 2008).

This project aims to shed some light on the exact role of *Wt1* in both normal gland development and breast cancer; to do so a combination of *in vivo* and *in vitro* approaches have been used, including mammary-specific *Wt1* conditional knockout mice and a breast cancer mouse model in which *Wt1* was selectively ablated.

This introduction will try to provide some context for my work and will include:

- an overview of the *WT1* gene (expression pattern, isoforms, role in development and in cancer)
- a review of mammary gland biology (normal development and breast cancer)
- a critical analysis on the current knowledge about the role of WT1 in both normal and cancerous mammary glands

1.2 The Wilms' Tumour Gene 1, *WT1*

The Wilms' Tumour Gene, *WT1*, is located on the short arm of the human chromosome 11 (11p13) and was first identified in 1990, when a series of papers was published by the Housman group (Call, Glaser et al. 1990, Haber, Buckler et al. 1990, Rose, Glaser et al. 1990). Their work linked deletions of the *WT1* locus to Wilms' tumour (the eponymous paediatric kidney cancer) and the WAGR syndrome (Wilms' tumour predisposition, Aniridia, Genitourinary anomalies and mental Retardation).

1.2.1 Gene structure, function and expression pattern

The *WT1* gene consists of ten exons and encodes a 52-54 kDa protein product with two major domains: the N-terminal is rich in proline and glutamine residues and has a transcriptional regulatory function, the C-terminal is composed of four Cys_2His_2 zinc fingers and allows sequence-specific nucleic acid binding (Figure 1.1) (Gessler, Poustka et al. 1990, Haber, Sohn et al. 1991).

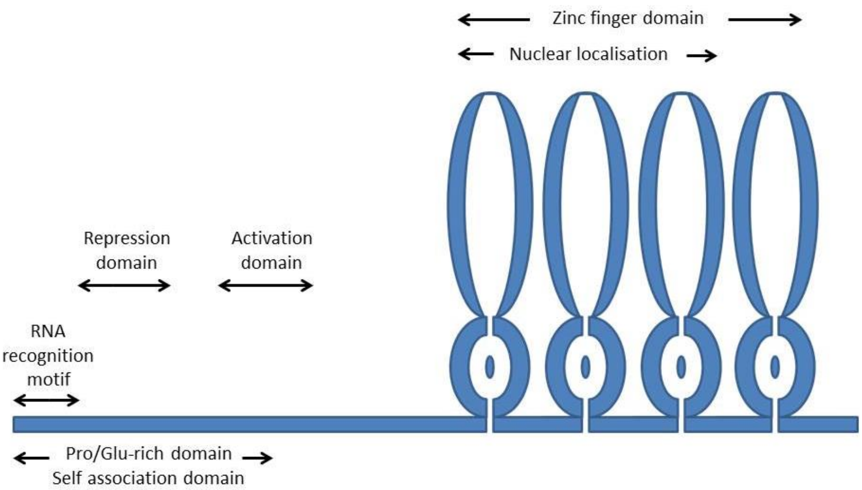

Figure 1.1 Schematic of the WT1 protein.

The C-terminal of the WT1 protein is characterised by four zinc-fingers, while the N-terminal includes an RNA recognition motif, a repression and an activation domain.

WT1 is expressed in a tightly regulated time- and tissue-specific manner: in the mammalian embryo, it is found in many tissues of mesodermal and ectodermal origin, including kidneys, gonads, heart, spleen, spinal cord, limb, brain and mesothelium (Pritchard-Jones, Fleming et al. 1990, Armstrong, Pritchard-Jones et al. 1993, Moore, Schedl et al. 1998).

Consistent with this expression pattern, homozygous *Wt1* knockout mice die in utero at E13.5 from heart malformations and show extensive defects of the urogenital system; the kidneys fail to develop owing to apoptosis of the early renal precursor cells and developmental abnormalities are also observed in the liver, spleen, diaphragm and adrenal glands (Kreidberg, Sariola et al. 1993, Moore, McInnes et al. 1999).

In the adult, *Wt1* expression was initially thought to be confined to kidney podocytes, mesothelium and granulosa/Sertoli cells of ovaries/testis (Pelletier, Schalling et al. 1991, Mundlos, Pelletier et al. 1993, Walker, Rutten et al. 1994); over the years, however, *Wt1* was also detected in the epithelial cells of the mammary gland, in the bone marrow and in the Schwann cells of human nerves (Silberstein, Van Horn et al. 1997, Hosen, Shirakata et al. 2007, Schittenhelm, Thiericke et al. 2010). In all these adult tissues, *Wt1* expression is restricted to a very small percentage of cells; nevertheless, inducible deletion of *Wt1* in adult mice leads to a drastic phenotype: within a week, the knockout animals show spleen and pancreatic atrophy, severe bone and fat reduction, kidney failure and impaired erythropoiesis (Chau, Brownstein et al. 2011).

All these observations suggest different roles for *Wt1* throughout development: while in adulthood it seems to regulate tissue homeostasis, in the embryo it prevents apoptosis and promotes cell differentiation (as discussed in more detail in chapter 1.2.2).

Additional complexity is introduced by the fact that, depending on the tissue and the context, *WT1* has also been shown to act as a transcriptional activator or repressor, a tumour suppressor gene or an oncogene, to be involved in the differentiation or maintenance of progenitor cells and in RNA metabolism (Hohenstein and Hastie 2006).

These different functions are achieved, at least in part, through the expression of multiple isoforms: these protein variants result from combinations of alternative start codons, RNA editing processes and alternative splicing events (Figure 1.2).

The WT1 locus encodes a theoretical maximum of 36 isoforms, all of which express the zinc-finger region in exons 7-10; the majority of these protein configurations, however, has not yet been characterised.

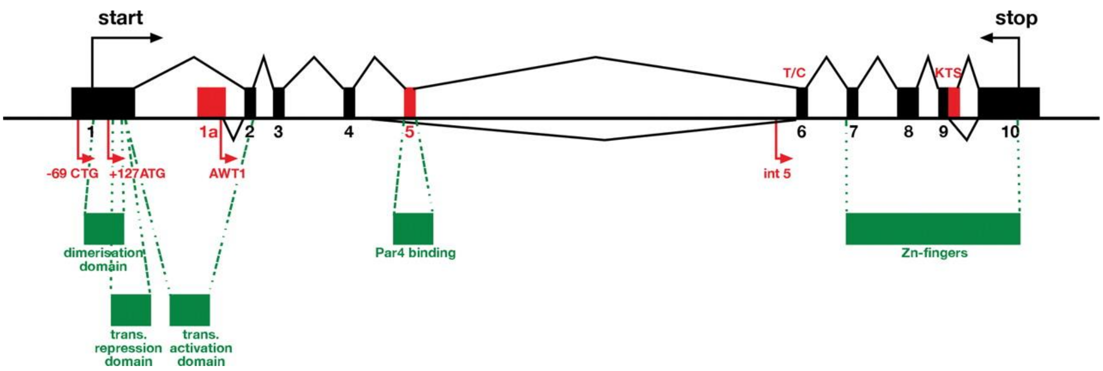

Figure 1.2 Schematic of the WT1 gene.

The alternative exons, start codons and splicing sites are shown in red while the affected functional domains are in green (from Hohenstein & Hastie 2006).

The best studied isoforms derive from two alternative splice donor sites at the end of exon 9, which include or omit 9 nucleotides encoding for lysine, threonine and serine (KTS) (Haber, Sohn et al. 1991); NMR studies have revealed that the insertion of these three amino acids increases the flexibility of the zinc finger region, which results in a much higher binding affinity for RNA than DNA (Caricasole, Duarte et al. 1996, Laity, Chung et al. 2000). The +KTS variants have been shown to co-localise and directly interact with proteins of the splicing machinery such as U2AF65 and RBM4 (Englert, Vidal et al. 1995, Larsson, Charlieu et al. 1995, Davies, Calvio et al. 1998, Ladomery, Slight et al. 1999, Markus, Heinrich et al. 2006) and also to bind the mRNA of *IGFR2*, *ACTN1* and *SCRB* (Caricasole, Duarte et al. 1996, Morrison, Venables et al. 2006, Wells, Rivera et al. 2010), supporting the idea that they mainly act at a post-transcriptional level. Despite its role in RNA processing, the best characterised WT1 function is that of a transcription factor: morphological and biochemical studies have shown that this role is predominantly exerted by the –KTS isoforms (Larsson, Charlieu et al. 1995, Laity, Chung et al. 2000) and two different consensus DNA sequences have so far been described (Rauscher, Morris et al. 1990, Madden, Cook et al. 1991).

Many different approaches have been used to identify the transcriptional targets of WT1, from *in vitro* reporter assays and overexpression experiments, to ChIP and transgenic mouse models; all these studies have recognised a series of candidate genes, which include other transcription factors, growth factors and their receptors, signal transducers, extracellular matrix and cell adhesion molecules as well as genes regulating the cell cycle and the apoptotic pathways (Table 1.1).

Depending on the cellular and temporal context, WT1 can either activate or repress the transcription of its target genes: this dichotomous behaviour was first described *in vitro* in relation to the platelet-derived growth factor (Gashler, Bonthron et al. 1992, Wang, Madden et al. 1992, Wang, Qiu et al. 1993) and then observed also for the Insulin-like growth factor II (Drummond, Madden et al. 1992, Nichols, Re et al. 1995, Ward, Pooler et al. 1995), *MYC* (Hewitt, Hamada et al. 1995, Udtha, Lee et al. 2003, Han, San-Marina et al. 2004), *SNAI1* (Martinez-Estrada, Lettice et al. 2010), *CDH1* (Hosono, Gross et al. 2000, Martinez-Estrada, Lettice et al. 2010) and *BCL-2* (Hewitt, Hamada et al. 1995, Heckman, Mochon et al. 1997, Mayo, Wang et al. 1999).

The molecular basis for this dual role of WT1 have only recently been elucidated by a study on the WNT4 gene: Essafi and colleagues have shown that in the developing kidney WT1 activates *WNT4* by recruiting p300 and Cbp as co-activators and by maintaining the chromatin of the *Wnt4* locus in an active conformation; conversely, in the developing heart, *Wt1* recruits the co-repressor Basp1 and switches the chromatin to a repressed state, which leads to *Wnt4* downregulation (Essafi, Webb et al. 2011).

Table 1.1 Transcriptional targets of WT1

Target	Effect	Reference
Growth factors		
Insulin-like growth factor II	Activation/Repression	Nichols et al. 1995, Ward e al. 1995, Drummond et al. 1992
Amphiregulin	Activation	Lee et al. 1999
Platelet derived growth factor A	Activation/Repression	Wang et al. 1992, Gashler et al. 1992, Wang et al. 1993
Colony stimulating factor 1	Repression	Harrington et al. 1993
Transforming growth factor beta	Repression	Dey et al. 1994
Inhibin alpha	Repression	Hsu et al. 1995
Midkine	Repression	Adachi et al. 1996
Müllerian-inhibiting substance	Repression	Shimamura et al. 1997
Connective tissue growth factor	Repression	Stanhope-Baker et al 2000
Vascular endothelial growth factor	Activation	Hanson et al. 2008, McCarty et al. 2011
Receptors		
Epidermal growth factor receptor	Repression	Menke et al. 1997, Englert et al. 1995
Androgen receptor	Repression	Zaia et al. 2001
Insulin receptor	Repression	Webster et al. 1997, Menke et al. 1997
Insulin-like growth factor 1 receptor	Repression	Werner et al. 1993, Werner et al. 1994
Retinoic acid receptor alpha	Repression	Goodyer et al. 1995
Vitamin D	Activation	Lee et al. 2001, Maurer et al. 2001, Wagner et al. 2001
Transcription factors		
WT1	Repression	Rupprecht et al. 1994
MYB	Repression	McCann et al. 1995
MYC	Activation/Repression	Hewitt et al. 1995, Udtha et al. 2003, Han et al. 2004
PAX2	Repression	Ryan et al. 1995
EGR1	Repression	Madden et al. 1991
SNAIL	Activation/Repression	Martinez-Estrada et al. 2009

Table 1.1 (continued)

Target	Effect	Reference
Extracellular adhesion		
E-cadherin	Activation/Repression	Hosono et al. 2000, Martinez-Estrada et al. 2009
Thrombospondin 1	Repression	Dejong et al. 1999
Syndecan 1	Activation	Cook et al. 1996
Genitourinary development		
Podocalyxin	Activation	Palmer et al. 2001
Sprouty 1	Activation	Gross et al. 2003
WNT4	Activation/Repression	Sim et al. 2002, Essafi et al. 2011
SRY	Activation	Hossain et al. 2001
SLC6A6	Activation	Han et al. 2003
NR0B1 (DAX1)	Activation	Kim et al 1999
Apoptosis		
BCL-2	Activation/Repression	Hewitt et al. 1995, Heckman et al. 1997, Mayo et al. 1999
BAK-1	Activation	Morrison et al. 2005
A1	Activation	Simpson et al. 2006
BAG3	Activation	Cesaro et al. 2010
Cell cycle		
p21	Activation	Englert et al. 1997
cyclin E	Repression	Loeb et al. 2002
cyclin G1	Activation	Wagner et al. 2001
Miscellaneous		
Erythropoietin	Activation	Dame et al. 2006
Ornithine decarboxylase	Repression	Moshier et al. 1996, Li et al. 1999
Superoxide dismutase 1	Activation	Minc et al. 1999
hTERT	Repression	Oh et al. 1999

Transgenic mouse models in which either the + or the –KTS proteins are specifically ablated show different phenotypes and demonstrate that the ratio of the different isoforms is crucial for development (Hammes, Guo et al. 2001).

Under normal physiological conditions, the ratio between + and – KTS splice variants is of approximately 5:1 in the embryo and 2:1 in the adult (Haber, Sohn et al. 1991); perturbations of this proportions either lead to kidney hypoplasia and streak gonads (if the mice only express the – KTS), or to renal failure and complete XY sex reversal (if they only express the + KTS).

In both cases, however, the homozygous knockout mice do not develop such a severe phenotype as the complete null: the pups survive embryonic development and die within 24 hours after birth, which suggests that the KTS isoforms of WT1 have both distinct and overlapping functions (Hammes, Guo et al. 2001).

Another splicing event of particular importance results in the optional transcription of exon 5, which encodes for a mammal specific 17-amino acid sequence whose function is not yet fully understood (Haber, Sohn et al. 1991).

Renshaw reported that this differential splicing appears to be regulated in a tissue-specific manner and that the highest expression levels for exon 5 are observed in the testis, kidneys and haematopoietic system (Renshaw, King-Underwood et al. 1997).

Different studies have linked the function of the +Exon 5 variants to cell cycle regulation and apoptosis, even though conflicting results were observed: in osteosarcoma cell lines, these isoforms are the most potent at inducing TP53-independent apoptosis (Englert, Hou et al. 1995) and their overexpression in mouse embryonic fibroblasts blocks cell cycle progression (Kudoh, Ishidate et al. 1995); however, the same +Exon 5 proteins are the only WT1 isoforms that can rescue HEK293 cells from the apoptotic signal induced by UV light treatment (Richard, Schumacher et al. 2001). These contradictory results can be partially explained by the fact that the Exon 5 region contains a transcriptional activation domain which requires a direct interaction with the prostate apoptosis response factor PAR4 (Richard et al. 2001): since the nuclear levels of PAR4 depend on the cellular and experimental context, the Exon 5-mediated response to apoptosis may vary accordingly.

To better characterise this isoform, Natoli and colleagues generated a mouse strain that specifically lacks Exon 5; given that this variant is only present in placental mammals, a possible role in mammal-specific reproductive functions had been hypothesised: surprisingly, however, the knockout mice show no obvious phenotype, and they develop, breed and lactate normally (Natoli, McDonald et al. 2002). This finding suggests that there is a degree of functional redundancy among the different isoforms and that, at least under physiological conditions, Exon 5 has no essential function.

In addition to the four major isoforms just described (+/- KTS and +/-Exon 5), other WT1 configurations derive from a maternally-imprinted alternative exon 1 (exon 1A, Dallosso et al. 2004), a cryptic promoter in intron 5 (Dechsukhum, Ware et al. 2000) and two alternative translation start sites (Bruening and Pelletier 1996, Scharnhorst, Dekker et al. 1999). Very little is known about these isoforms, which seem much less abundant than those translated starting from the main ATG site; noteworthy, however, is the expression profile of the truncated transcript starting from intron 5: this short protein, in fact, has only been detected in breast and pancreatic cancer cell lines and in the blood of patients affected by acute leukaemia (Bae, Jackson-Cook et al. 1994, Dechsukhum, Ware et al. 2000), suggesting that it might be a tumour-specific isoform.

1.2.2 WT1 in development: regulation of the epithelial-mesenchymal balance

As previously mentioned, WT1 plays a crucial role during embryonic development and its expression in mice can be detected as early as E8.5: at this stage WT1 is found in the intermediate and lateral plate mesoderm, which will later give rise to kidneys, gonads and adrenal glands. At E9.5 WT1-positive cells are also spotted in the septum transversum, the mesenchymal structure which contributes to the formation of the liver mesothelium, diaphragm, ventricular myocardium, peri and epicardium (Armstrong, Pritchard-Jones et al. 1993, Moore, McInnes et al. 1999, Chau and Hastie 2012).

Embryonic development is characterized by a series of bidirectional conversions between epithelial and mesenchymal phenotypes, respectively called epithelial to mesenchymal transition (EMT) and mesenchymal to epithelial transition (MET). Both these processes are essential for organogenesis and allow the embryonic cells to migrate, relocate themselves and differentiate (reviewed in Perez-Pomares and Munoz-Chapuli 2002, Thiery, Acloque et al. 2009).

During development, the vast majority of WT1-expressing tissues undergoes an EMT or an MET, and most of the developmental defects observed in the *Wt1*-deficient embryos can be explained by disturbances of these processes (reviewed in Miller-Hodges and Hohenstein 2012).

The epicardial cells, for example, go through an EMT and then migrate into the heart, where they differentiate into cardiomyocytes and cells of the coronary vasculature (Mikawa and Gourdie 1996, Zhou, Ma et al. 2008).

This epicardial EMT is regulated by WT1 through the direct repression of the epithelial marker CDH1 and the activation of SNAIL, a pro-EMT transcription factor. In epicardial-specific *Wt1* knockout mice, the epicardium develops normally but the EMT is impaired: as a result, the number of mesenchymal progenitor cells and their derivatives is drastically reduced, which leads to thinner heart walls, pericardial hemorrhage and, ultimately, heart failure (Martinez-Estrada et al. 2009).

Also the liver abnormalities of the *Wt1* null have been linked to a disturbed EMT: Ijpenberg and colleagues have shown that the *Wt1*-positive mesothelium of the developing liver undergoes an EMT and the resulting mesenchymal cells invade the liver parenchyma to give rise to hepatic stellate cells; in *Wt1* knockout mice, however, the stellate cells show an anomalous differentiation and the liver size is reduced (Ijpenberg, Perez-Pomares et al. 2007).

More complicated and diverse seems the role of WT1 in kidney development, which therefore deserves a more detailed analysis.

The early stages of nephrogenesis are characterized by reciprocal interactions between the metanephric mesenchyme and the ureteric bud, precursors of the nephron and the collecting duct system respectively. The kidneys start to develop when the epithelial ureteric bud forms an outgrowth from the Wolffian duct into the metanephric mesenchyme. In mice the first contact between the ureteric bud and the mesenchyme is approximately at E10.5-11 and it is followed by the condensation of the mesenchymal cells that surround the tips of the ureteric bud (Figure 1.3): these cells aggregate around the tips of the ureteric bud, undergo an MET, and then form the renal vesicle. The differentiation and elongation of the renal vesicle lead to the comma and S-shaped bodies, which eventually produce the renal corpuscle (or glomerulus), the proximal tubule and the loop of Henle (Saxen and Sariola 1987, Vainio and Lin 2002).

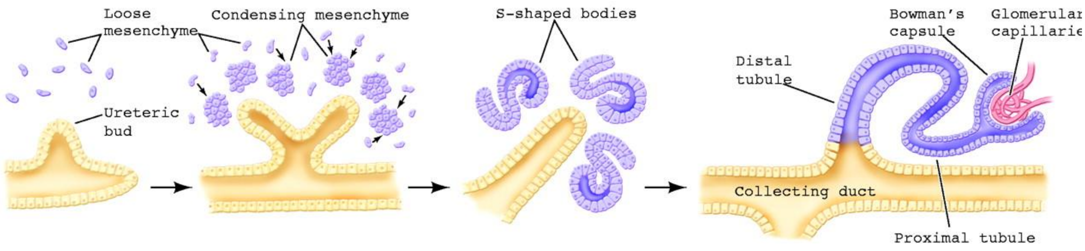

Figure 1.3 Embryonic kidney development (adapted from Scholz & Kirschner 2005). Nephrogenesis starts with the ureteric bud invasion of the metanephric mesenchyme; the mesenchymal cells around the branching ureteric bud condense, switch towards an epithelial state and give rise to the complex structures of the mature kidney.

In the *Wt1* knockout mice, the Wolffian duct develops normally but the ureteric bud is absent and the cells of the metanephric mesenchyme undergo extensive apoptosis at E11 (Kreidberg, Sariola et al. 1993): *Wt1* is therefore required in the early stages of nephrogenesis for the survival and differentiation of the renal progenitor cells.

Besides its early role as a survival factor, *Wt1* expression pattern implies also a role in later stages of kidney development, including the MET: its expression gradually increases from the metanephric mesenchyme stage till the S-shaped body and is then restricted to the proximal nephron (Armstrong, Pritchard-Jones et al. 1993); the complete absence of kidneys in the knockout embryos, however, has made the investigation on the late *Wt1* functions quite challenging.

To overcome these limitations, different approaches have been used: a complementation study has shown that a human-derived WT1 YAC construct can partially rescue the kidney defects of the knockout mice, providing also evidence for a continuous *Wt1* requirement throughout nephrogenesis (Moore, McInnes et al. 1999). Furthermore, *Wt1* siRNAs applied to kidney rudiments at the stage between ureteric bud invasion and mesenchyme condensation, block nephron development at the pre-epithelial stage, demonstrating that in organ culture experiments *Wt1* is indispensable for MET (Davies, Ladomery et al. 2004).

Recently, these findings have been confirmed *in vivo*, using a conditional *Wt1* knockout model and three different Cre lines that selectively inactivate the gene at different stages of nephron development (Berry et al. manuscript submitted).

Hence, the kidney phenotype of the *Wt1*-null mice cannot be linked to a defective MET, given that the metanephric blastema degenerates before reaching this stage; deleting *Wt1* later in development, however, has revealed that this gene plays a crucial role in the epitheliasation of the metanephric mesenchyme and it does so by directly activating *Wnt4* (Essafi et al. 2011), whose expression is both necessary and sufficient for the nephron MET to occur (Stark, Vainio et al. 1994, Kispert, Vainio et al. 1998).

In summary, WT1 can rightfully be considered as a major regulator of the epithelial-mesenchymal balance during development and its functions vary according to the tissue and the developmental stage.

1.2.3 Wt1 in cancer

Since its identification more than two decades ago, WT1 has been extensively studied in the field of cancer biology: initially discovered as a causative gene of

Wilms' tumour, it has later been associated to acute leukaemias and, more recently, to many adult solid tumours, including breast, pancreatic and colorectal cancer.

This section aims at reviewing the current knowledge of WT1 role in tumorigenesis and comparing its functions in the different types of cancer in which it is expressed/ mutated.

1.2.3.1 Wilms' tumour

Wilms' tumour, or nephroblastoma, is the most common paediatric kidney cancer, with an incidence of 1 in 10,000 children (Miller, Young et al. 1995). It is named after Dr. Max Wilms, the German pathologist who, in the far 1899, realised the embryonic origin of this malignancy; later studies confirmed that Wilms' tumour derives from pluripotent renal precursor cells, a reason why it is frequently cited as an example of defective differentiation leading to tumorigenesis (Zhuang, Merino et al. 1997).

Along with retinoblastoma and neuroblastoma, Wilms' tumour was one of the paediatric cancers upon which Knudson based his 'two-hit' model of tumour suppression, which suggests that two rate-limiting genetic events are required to initiate tumorigenesis (Knudson 1971, Knudson and Strong 1972).

The first gene found to be inactivated in Wilms' tumour was *WT1*: in accordance with the two-hit hypothesis, Haber and colleagues described a case of sporadic unilateral Wilms' tumour with an intragenic *WT1* deletion in one allele and a loss of heterozygosity in the other (Haber et al. 1990).

Subsequently, *WT1* mutations were detected in 10–15% of patients (Varanasi, Bardeesy et al. 1994) and were found to be quite heterogeneous, including whole or partial gene deletions, insertions, nonsense, missense and splicing-affecting mutations (Little and Wells 1997); all these abnormalities, however, lead to a loss of function, which clearly demonstrates that *WT1* behaves as a classic tumour suppressor gene in the etiology of Wilms' tumour.

1.2.3.2 Leukaemia

More controversial is the role of WT1 in both normal and malignant hematopoiesis (reviewed in Ariyaratana and Loeb 2007, Yang, Han et al. 2007).

Research on this topic was sparked by the finding that in adult mice both thymus and spleen show *Wt1* expression (Buckler, Pelletier et al. 1991), later detected also in the bone marrow, where it is restricted to approximately 1% of the CD34+ multipotent progenitor cells (Hosen, Sonoda et al. 2002). The use of a WT1-GFP knockin reporter mouse has helped characterise this WT1+ population of short-term stem cells, showing that it comprises both uncommitted, quiescent CD38– and committed, proliferating CD38+ cells (Hosen, Shirakata et al. 2007); methylcellulose-based cultures have also demonstrated that these WT1+ cells can differentiate in erythrocytes, leukocytes and granulocytes, while defective haematopoiesis is observed upon inducible deletion of *Wt1* in adult mice (Chau, Brownstein et al. 2011).

Multiple studies have shown that, following differentiation of the progenitor cells, *Wt1* is downregulated to such an extent that it is almost undetectable in mature blood cells (Sekiya, Adachi et al. 1994, Menssen, Renkl et al. 1997, Hosen, Shirakata et al. 2007), which suggests that it may play a role in the regulation of early hematopoietic differentiation.

Additional, but controversial evidence, is provided by the fact that wildtype WT1 is strongly expressed in the immature tumour cells of almost all acute leukaemias, whereas it is absent in non-Hodgkin’s lymphoma, whose cells originate from a more mature lymphoid population (Inoue, Sugiyama et al. 1994). However, WT1 expression in acute myelogenous and lymphocytic leukaemias, as well as in the blast crisis of chronic myeloid leukemia, has been interpreted by some investigators as an indicator of an oncogenic role for WT1 and not as a marker of their original cell lineage.

Data in this field have been extremely contradictory, as illustrated by the correlation between WT1 expression and prognosis: elevated WT1 levels in leukemia patients have been associated to either positive (Rodrigues, Oliveira et al. 2007) or negative

(Inoue, Sugiyama et al. 1994, Bergmann, Miething et al. 1997, Trka, Kalinova et al. 2002, Barragan, Cervera et al. 2004) outcomes, but also described to be of no prognostic value whatsoever (Schmid, Heinze et al. 1997, Yanada, Terakura et al. 2004). These conflicting results are unlikely to reflect real biological functions of WT1: the discrepancies are more probably due to the presence of confounding factors, such as differences in the patient age, detection techniques and histological/cytogenetic tumour subtypes.

Weighing in favour of an oncogenic WT1, is the fact that its expression levels are much higher in leukemia than in physiologic conditions (Inoue, Ogawa et al. 1997, Menssen, Renkl et al. 1997); as a consequence of this overexpression in the malignant phenotype, WT1 is considered as a robust marker for the detection of minimal residual disease (Inoue, Sugiyama et al. 1994, Ogawa, Tamaki et al. 2003) and also an independent risk factor for relapse (Inoue, Ogawa et al. 1996, Lapillonne, Renneville et al. 2006).

In keeping with these findings, treatment with WT1 antisense oligomers has been shown to inhibit the proliferation of leukemic cells *in vitro* and to induce apoptosis (Algar, Khromykh et al. 1996, Yamagami, Sugiyama et al. 1996).

Moreover, WT1 has recently been indicated as a promising tumour antigen that can be targeted through immunotherapy (reviewed in Keilholz, Menssen et al. 2005). Several studies in mice revealed that the immunization with WT1 peptide or cDNA triggers the response of cytotoxic T-lymphocites which selectively kill the WT1 expressing tumour cells, leading to prolonged survival (Gaiger, Reese et al. 2000, Oka, Udaka et al. 2000, Tsuboi, Oka et al. 2000).

These observations have paved the way to human WT1 vaccine for patients affected by leukemia (Mailander, Scheibenbogen et al. 2004, Oka, Tsuboi et al. 2004). The clinical studies, mainly performed in Japan and Germany, are now in phase-II and have so far obtained encouraging results: a statistical analysis carried out on all the WT1-based vaccine trials published until 2012, reveals that out of the 83 patients with haematological malignancies, 13 achieved complete remission and an additional

18 showed stabilization of the disease after vaccination (Van Driessche, Berneman et al. 2012).

Some findings, however, are difficult to reconcile with a presumed oncogenic function and would support a tumour-supressing role: firstly, *WT1* mutations have been found in 15-20% of leukemia patients (King-Underwood, Renshaw et al. 1996), similar to what is observed in Wilms' tumour; these alterations include nonsense, missense, and frameshift mutations and are predicted to produce a truncated protein with defective DNA-binding ability (King-Underwood et al. 1996).

Secondly, several independent studies have associated these mutations to poor prognosis, and hypothesised that they may confer drug resistance by altering the apoptotic response to cytotoxic agents (King-Underwood and Pritchard-Jones 1998, Summers, Stevens et al. 2007, Paschka, Marcucci et al. 2008, Hollink, van den Heuvel-Eibrink et al. 2009). Lastly, Wilms' tumour survivors have a high risk of developing secondary malignances, 20% of which are haematological (Breslow, Takashima et al. 1995, Shearer, Kapoor et al. 2001); these statistics could merely reflect the higher susceptibility of bone marrow cells to chemo/radiotherapy, but the hypothesis that *WT1* mutations may represent a predisposition factor for leukemia cannot be ruled out.

All in all, at the actual state of research, uncertainty remains over the exact role of *WT1* in leukemogenesis and further investigation is required.

1.2.3.3 Adult solid tumours

Over the past few years, WT1 expression has been detected not only in leukaemia, but also in a variety of non haematological malignancies, ranging from brain tumour to prostate cancer (Table 1.2).

Table 1.2 Expression of WT1 in solid tumours

Tumour type	Detection method	Reference
Biliary cancer	IHC	Nakatsuka et al. 2006
Bone and soft tissue carcinoma	RT-PCR, IHC, WB	Ueda et al. 2003
Brain tumour	IHC	Nakatsuka et al. 2006
Breast cancer	RT-PCR, IHC, SB	Silberstein et al. 1997, Loeb et al 2001, Nakatsuka et al. 2006, Gillmore et al. 2006
Cervical cancer	IHC	Nakatsuka et al. 2006
Colon cancer	RT-PCR, WB	Koesters et al. 2004
Colorectal adenocarcinoma	RT-PCR, IHC	Oji et al. 2003
Colorectal cancer	IHC	Nakatsuka et al. 2006
Desmoid tumour	RT-PCR, IHC	Amini Nik et al. 2005
Endometrial cancer	IHC	Nakatsuka et al. 2006
Esophageal cancer	RT-PCR, IHC	Nakatsuka et al. 2006, Oji et al. 2004
Gastric adenocarcinoma	IHC	Nakatsuka et al. 2006
Glioblastoma multiforme	RT-PCR	Clark et al. 2007
Endometrial cancer	IHC	Ohno et al. 2009
Head & neck squamous cell carcinoma	RT-PCR, IHC	Oji et al. 2003a
Lung cancer	RT-PCR, IHC	Oji et al. 1999, Menssen et al 2000, Oji et al. 2002, Nakatsuka et al. 2006
Malignant melanoma	IHC	Nakatsuka et al. 2006
Malignant mesothelioma	IHC	Kumar-Singh et al. 1997, Foster et al. 2001
Neuroblastoma	RT-PCR	Denis et al. 2002
Osteosarcoma	IHC	Nakatsuka et al. 2006
Ovarian cancer	IHC	Nakatsuka et al. 2006, Hylander et al. 2006, Waldstrom et al. 2005
Pancreatic cancer	IHC	Nakatsuka et al. 2006
Pancreatic ductal adenocarcinoma	IHC	Oji et al. 2004a
Primary astrocytic tumour	RT-PCR, IHC	Oji et al. 2004b
Primary thyroid cancer	RT-PCR, IHC	Oji et al. 2003b
Prostate cancer	IHC	Nakatsuka et al. 2006, Devilard et al. 2006, King et al. 2009
Renal cell carcinoma	NB, IHC	Campbell et al. 1998, Nakatsuka et al. 2006
Rhabdomyosarcoma	RT-PCR, WB	Carpentieri et al. 2002
Soft tissue sarcoma	IHC	Nakatsuka et al. 2006
Urothelial cancer	IHC	Nakatsuka et al. 2006
Uterine sarcoma	RT-PCR, IHC	Coosemans et al. 2007

Abbreviations: RT-PCR, Real-Time Polymerase Chain Reaction; IHC, Immunohistochemistry; SB, Southern Blot; NB, Northern Blot; WB, Western Blot

Several studies have shown that *WT1* levels are much higher in the tumours than in the respective normal tissues and that no *WT1* mutations or splicing anomalies can be detected in the neoplastic samples (Campbell, Kuriyan et al. 1998, Menssen, Bertelmann et al. 2000, Loeb, Evron et al. 2001, Dennis, Manji et al. 2002, Oji, Miyoshi et al. 2003, Ueda, Oji et al. 2003, Koesters, Linnebacher et al. 2004, Oji, Nakamori et al. 2004, Oji, Suzuki et al. 2004, Amini Nik, Hohenstein et al. 2005, Clark, Dos Santos et al. 2007). In some tumour types *WT1* expression has also been reported to correlate with higher histological grade and worse prognosis (Miyoshi, Ando et al. 2002, Oji, Miyoshi et al. 2003, Oji, Nakamori et al. 2004, Ohno, Dohi et al. 2009); this observation is consistent with the fact that *WT1* seems to play an important role in the growth of cancer cells: similarly to what observed in leukemic cell lines (Algar, Khromykh et al. 1996, Yamagami, Sugiyama et al. 1996), RNAi silencing of *WT1* has been shown to inhibit proliferation and to induce apoptosis in cell cultures originated from melanoma, glioblastoma, fibrosarcoma, gastric, lung, ovarian and pancreatic cancers (Oji, Nakamori et al. 2004, Oji, Suzuki et al. 2004, Zamora-Avila, Franco-Molina et al. 2007, Tatsumi, Oji et al. 2008).

An additional similarity between hematological and solid malignancies is the immunogenicity of the WT1 protein: in both cases this antigen can stimulate a response from cytotoxic T-lymphocites which is of sufficient avidity to kill the tumor cells (Koesters, Linnebacher et al. 2004, Gillmore, Xue et al. 2006).

The vaccine trials, however, show a lower response rate for the solid tumours: out of the 75 patients in the clinical studies only two achieved a complete remission, while an additional eight had partial remission and decrease in tumour size (Van Driessche, Berneman et al. 2012).

All these findings would suggest an oncogenic role for *WT1* in adult solid tumours, however, once again, there are some controversial data to consider: *WT1* has been shown to inhibit the transformed phenotype of breast cancer cells and the malignant progression of mammary epithelial cells (Zhang, Yu et al. 2003, Wang and Wang 2008); moreover, a study on IDC reported that *WT1* is undetectable in the vast majority of the tumours analysed as a result of genetic deletion and promoter hypermethylation, suggesting that *WT1* loss may be an important event in breast tumorigenesis (Cheng, Wu et al. 2001).

Since this debate is particularly important to put my project in context, it will be analysed in more detail in chapter 1.4, following an introductory section on mammary gland biology and breast cancer.

1.2.3.4 Possible roles of WT1 in tumorigenesis

As mentioned earlier, *WT1* expression seems to correlate with poor prognosis, at least in breast and endometrial cancer (Miyoshi et al. 2002, Ohno et al. 2009); the biological basis for this finding have not yet been identified, but different hypotheses can be formulated.

First of all, tumours expressing high levels of *WT1* may have a proliferative advantage since silencing *WT1* leads to growth arrest and apoptosis (Yamagami et al. 1996, Algar et al. 1996, Zamora-Avila et al. 2007, Oji et al. 2004b, Tatsumi et al. 2008, Oji et al. 2004a). Investigations on the molecular mechanisms involved in this process have revealed that WT1 can modulate many genes of the bcl-2 family, including *BAK*, *BAG3*, *A1* and *BCL-2* itself (Hewitt, Hamada et al. 1995, Heckman, Mochon et al. 1997, Mayo, Wang et al. 1999, Morrison, English et al. 2005, Simpson, Burwell et al. 2006, Cesaro, Montano et al. 2010) as well as regulate the Fas-related death signaling pathway (Uesugi, Hiasa et al. 2013); moreover, there is strong evidence suggesting that *WT1* can promote cell proliferation by up-regulating cyclin D1 (Caldon, Lee et al. 2008, Xu, Wu et al. 2013).

A second hypothesis is related to the formation of blood vessels: WT1 has been detected in the vasculature of different tumour types (Timar, Meszaros et al. 2005, Wagner, Michiels et al. 2008) and its expression in endometrial cancer has been associated with the induction of angiogenesis (Dohi, Ohno et al. 2010). In addition, two different groups showed that WT1 directly upregulates the expression of the vascular endothelial growth factor (VEGF) (Hanson, Gorman et al. 2007, McCarty, Awad et al. 2011) and many other vascular genes have been identified as potential

WT1 targets, including the vascular endothelial cadherin, angiopoietin-2, vascular endothelial growth factor receptors 1 and 2 (Kirschner, Sciesielski et al. 2010).

Hence, the correlation with poor outcome may be explained by a pro-angiogenic function of *WT1*: the tumours with higher levels of this gene are more abundant in blood vessels, which increases the proliferative rate of the cancer cells but also grants them easy access to the vascular system, from where they can spread and metastasise.

Finally, a last hypothesis is based on the fact that *WT1* is a key regulator of the epithelial/mesenchymal balance and therefore it may play a role in the EMT of tumour cells.

The epithelial-to-mesenchymal transition is a key biological process for embryonic development, tissue differentiation and repair (reviewed in Thiery, Acloque et al. 2009): it consists of a highly coordinated series of events starting with the loss of cell-cell adhesion and the replacement of the baso-apical polarisation by front-rear polarisation; the next step involves changes in the cytoskeleton organisation and the trigger of proteolytic enzymes such as matrix metalloproteases which alter cell-matrix adhesion. Eventually, the cells start to secret extra-cellular matrix components and show a migratory phenotype (Figure 1.4) (Zavadil and Bottinger 2005).

As a whole, these drastic changes in cell morphology are achieved through the synergic action of many transcription factors, including ZEB1, ZEB2, SIP1, TWIST1, SLUG and SNAIL, whose function is to repress epithelial markers such as E-cadherin and simultaneously induce mesenchymal markers like vimentin and N-cadherin (Batlle, Sancho et al. 2000, Comijn, Berx et al. 2001, Hajra, Chen et al. 2002, Yang, Mani et al. 2004, Peinado, Olmeda et al. 2007).

Most scientists agree in classifying the EMT into three different types, according to the biological setting in which it takes place: type I is associated with embryogenesis, type II with wound healing and tissue regeneration while type III is observed in neoplastic cells (Kalluri and Weinberg 2009).

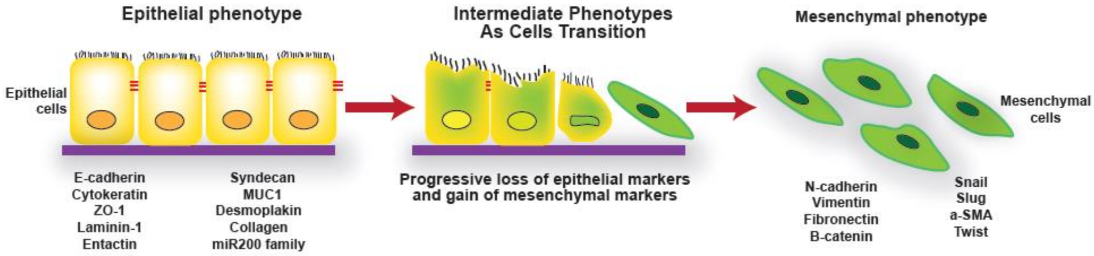

Figure 1.4 Epithelial-to-mesenchymal transition.

The epithelial-to-mesenchymal transition is a multi-step process characterised by the progressive loss of epithelial markers such as E-cadherin and the gain of mesenchymal markers like vimentin and N-cadherin.

Recently, this third type of EMT has been linked to the acquisition of a malignant phenotype by the epithelial cancer cells: features of EMT have been described in breast (Trimboli, Fukino et al. 2008) and colorectal cancer (Brabletz, Jung et al. 2005), mainly at the invasive front of the tumour (Brabletz, Jung et al. 2001, Prall 2007), suggesting that the EMT may generate migratory cells which leave the primary site, invade the blood vessels and potentially metastasise (Iwatsuki, Mimori et al. 2010, Micalizzi, Farabaugh et al. 2010).

This theory on EMT contribution to tumour progression (Figure 1.5) seems to be supported by the fact that many developmental EMT drivers, including SNAIL, SLUG, TWIST and ZEB1, are mis-expressed in cancer and significantly correlate with relapse and poor clinical outcomes (Savagner, Yamada et al. 1997, Blanco, Moreno-Bueno et al. 2002, Yang, Mani et al. 2004, Huber, Kraut et al. 2005, Wellner, Schubert et al. 2009).

Recent work has also suggested that the EMT process may be linked to cancer stem cells (CSCs): the cells undergoing this transition have been shown to acquire stem-cell properties such as the expression of stem-cell markers and an increased ability to form spheres in colony-forming assays (Mani, Guo et al. 2008, Morel, Lievre et al. 2008).

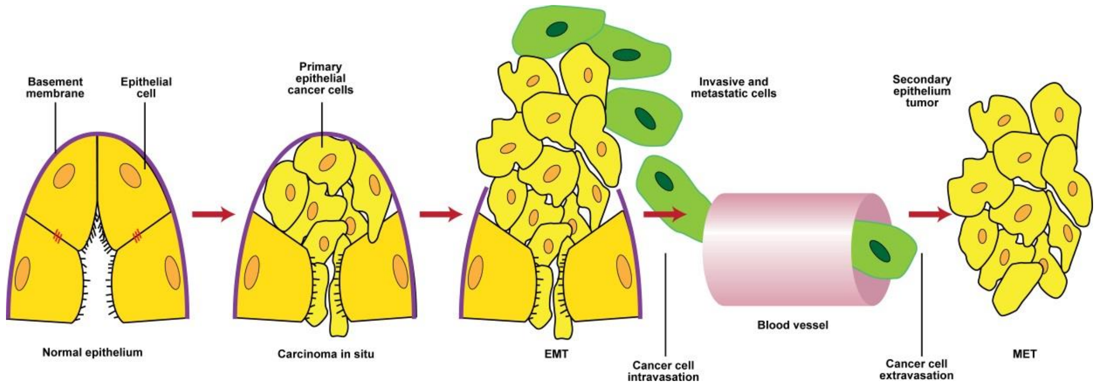

Figure 1.5 EMT contribution to tumour progression.

The epithelial-to-mesenchymal transition is believed to play a role in the formation of secondary tumours by promoting the motility of cancer cells.

It is not clear how *WT1* may come into play in this process, but investigations on the topic seem worthwhile, given the strong circumstantial evidence linking *WT1* to the cancer-related EMT: among the transcriptional targets of WT1 there are many pro-EMT genes, including *SNAIL*, *SLUG* and *TGF-β* (Dey, Sukhatme et al. 1994, Martinez-Estrada, Lettice et al. 2010, Takeichi, Nimura et al. 2013); of particular importance is the fact that the latter can induce an EMT in different types of tumour cells (Song 2007) and through multiple signalling pathways (Bhowmick, Ghiassi et al. 2001, Roberts, Tian et al. 2006).

In conclusion, there are at least three possible explanations for the correlation between *WT1* expression and poor survival in cancer patients (altered proliferation/apoptosis, increased angiogenesis, induction of EMT/CSCs); since these theories are not mutually exclusive, they may all contribute to the aggressive phenotype observed in the WT1 positive tumours. Further research is however required to validate these hypothesis, and especially to investigate a potential role of *WT1* in the induction of cancer-specific EMT.

1.3 Overview of mammary gland biology

Mammary glands and milk production are distinctive features of mammals and have evolved as a unique survival strategy that provides the offspring with both nutrition and immunological protection (Oftedal 2002, reviewed in Khokha and Werb 2011).

Despite some structural differences among species, the mammary glands of all mammals are made up by two main compartments, the ductal epithelium and the surrounding stroma (Figure 1.6).

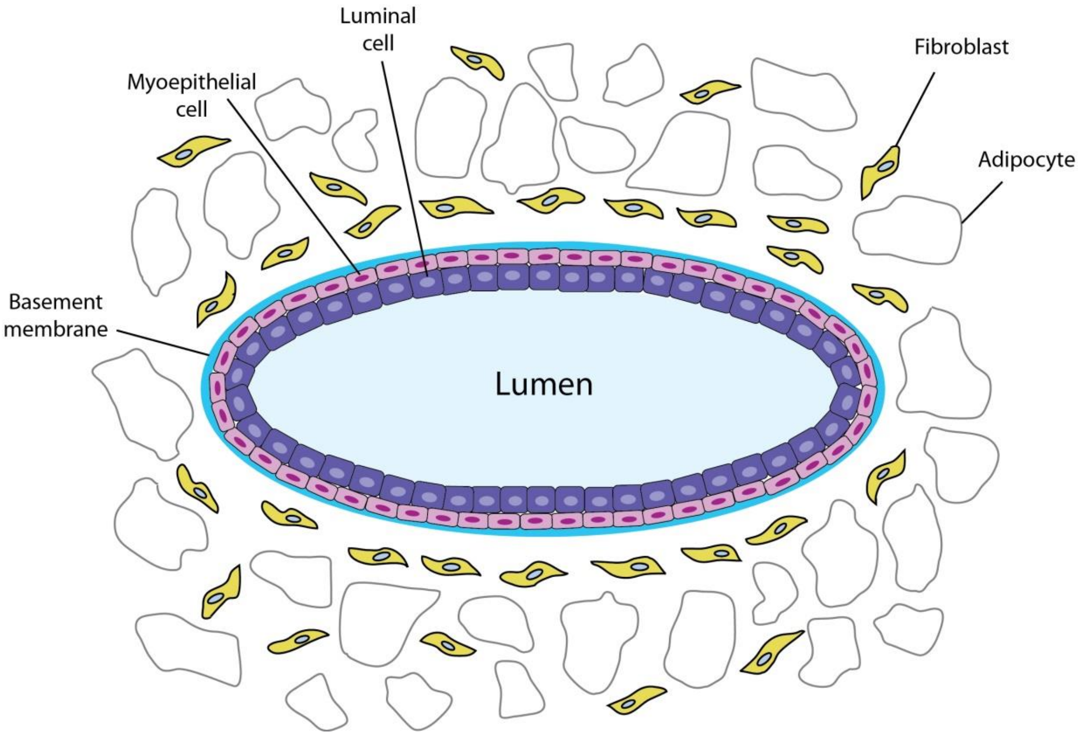

Figure 1.6 Structure of a mammary gland duct.

The mammary ducts are surrounded by an inner layer of luminal cells and an outer layer of myoepithelial cells.

The epithelium of the ducts is bilayered, with an inner ring of luminal cells connected by tight junctions and an outer, basal layer which includes myoepithelial and progenitor cells. With pregnancy, the luminal sheet differentiates into secretory cells and rearranges to form the alveoli: during lactation these hollow cavities will develop into milk-secreting lobules while the myoepithelial cells contract to facilitate the delivery of milk to the pups. The stroma, also called mammary fat pad, is the connective tissue that surrounds and supports the epithelial structures; it mainly consists of adipocytes but there are also fibroblasts, blood vessels and hematopoietic cells (reviewed in Richert, Schwertfeger et al. 2000).

This basic organization of the mammary gland is very dynamic and undergoes dramatic changes throughout its existence; these remodeling programs depend on the physiological stimuli that characterise the different phases of sexual development/reproduction and, if harnessed, can lead to breast tumorigenesis (Lanigan, O'Connor et al. 2007).

In this section I will cover the basics of mammary gland biology, first describing the development of this organ from embryogenesis to senescence, then focusing on breast cancer, its different histological and molecular subtypes and the treatment options currently available.

1.3.1 Development of the mouse mammary gland

The mammary gland is a unique organ, in that only a rudimentary ductal tree is present at birth, with most of the development occurring postnatally (Richert et al. 2000).

During mouse embryogenesis, the mammary anlage starts developing at E10.5, when a thickening in the ventral skin gives rise to the milk line (Figure 1.7); by E11.5 the mammary epithelium and mesenchyme can be distinguished and the reciprocal interactions between these two tissues will form a primary sprout that branches into a small ductal system just before birth (reviewed in Robinson 2007). This rudimentary gland will keep growing in an isometric way with the rest of the body until puberty.

Unlike these earlier stages of development, which are hormone-independent, the phases from puberty onwards strongly rely on the action of the endocrine system and oestrogen, progesterone, prolactin, cortisol and somatotropine have been identified as indispensable mammotropic hormones (reviewed in Brisken and O'Malley 2010).

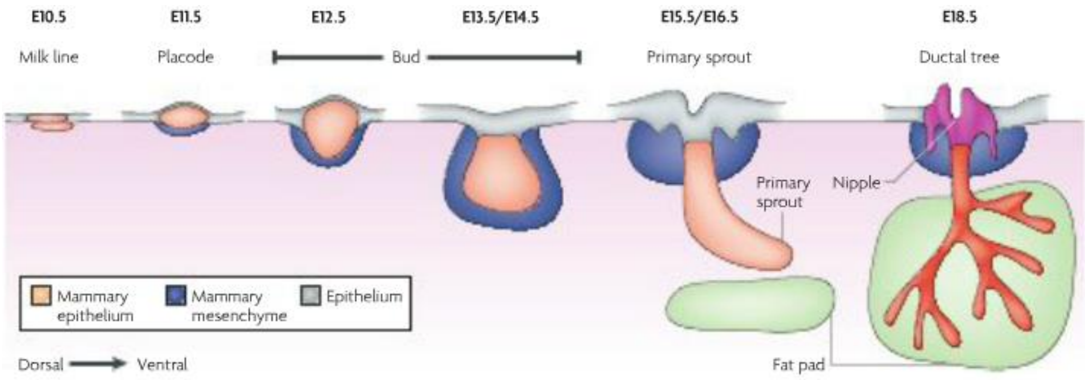

Figure 1.7 Embryonic development of the mouse mammary gland (from Robinson 2007). The mammary gland has an ectodermal origin and derives from a thickening in the ventral skin (the milk line).

During puberty the glands develop highly motile and proliferating structures at the forefront of the ducts (Figure 1.8): these terminal end buds (TEB) guide the elongation of the ductal tree, which forms primary ducts by invading the surrounding stroma until it reaches the distal portion of the fat pad; simultaneously, secondary and tertiary side branches are formed by lateral bud sprouting (Hinck and Silberstein 2005, Lu, Sternlicht et al. 2006).

This whole process of branching morphogenesis depends on the mitogenic stimulus of the ovarian oestrogens and their paracrine mediator amphiregulin, which regulates the stromal-epithelial cross-talk (Sternlicht 2006).

After puberty the female mice reach sexually maturity and are able to reproduce but, like other mammals, their fertility is limited to a specific phase of the reproductive cycle, which in rodents is called estrous cycle.

Despite being much shorter than the human menstrual cycle (4 vs 28 days), the mouse estrous cycle is regulated by the same complex network of hormones belonging to the hypothalamus-pituitary-ovary axis (Figure 1.9): the gonadotropin-releasing hormone (GnRH) secreted by the hypothalamus stimulates the anterior pituitary gland to produce follicle-stimulating hormone (FSH) and luteinizing hormone (LH), which in turn induce the ovarian follicle to synthesise oestrogen and progesterone (reviewed in Hawkins and Matzuk 2008, Joshi, Di Grappa et al. 2012).

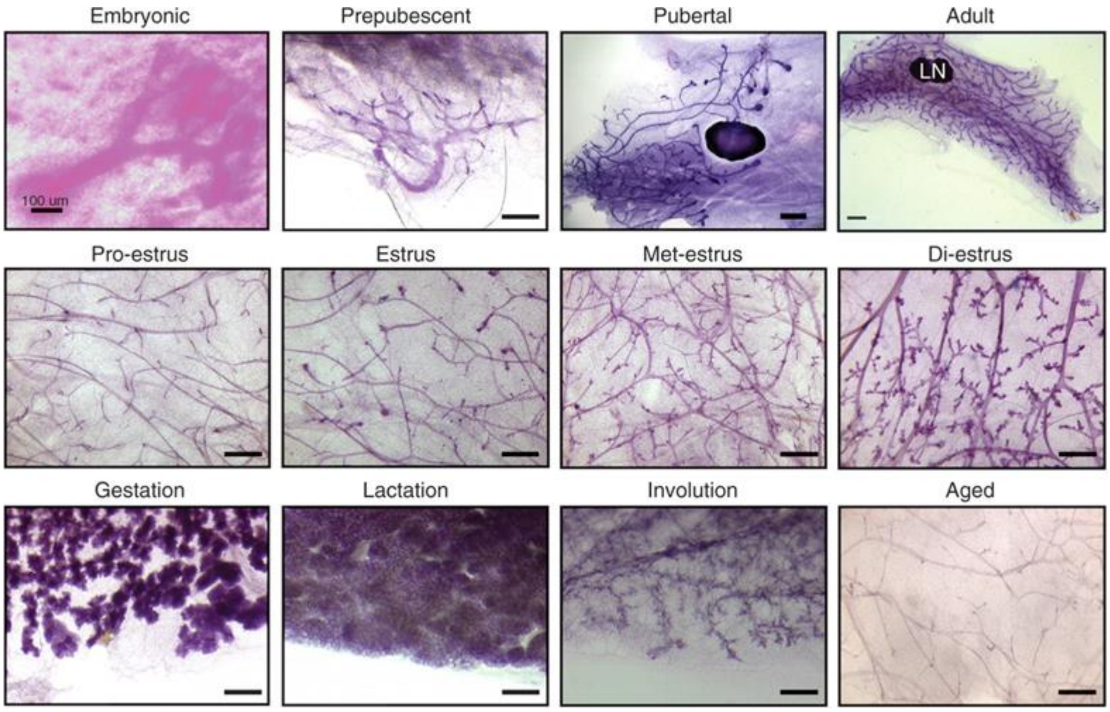

Figure 1.8 Stages of mammary gland remodeling (from Khokha & Werb 2011).

Murine mammary gland wholemounts showing the remodeling occurring in this organ from the embryonic (E18.5) to aged stage (20 month-old).

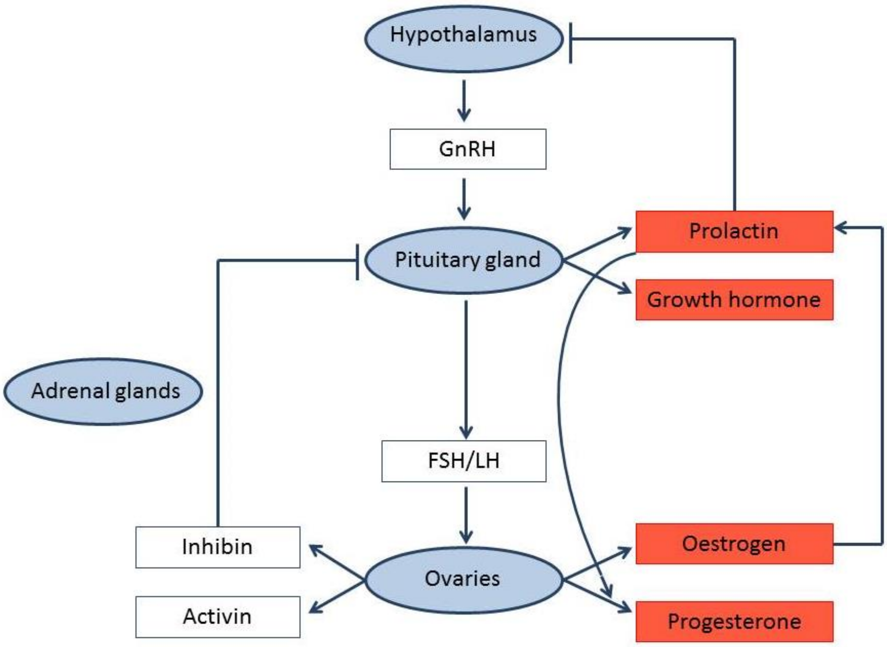

Figure 1.9 Scheme of the female endocrine system.

Different endocrine glands belonging to the hypothalamus-pituitary-ovary axis secrete mammotropic hormones (highlighted in red).

Figure 1.10 illustrates how the rodent proestrus, equivalent to the human follicular phase, is characterised by a rise in the serum levels of oestrogen, which then triggers the LH surge leading to ovulation: once the ovarian follicle burst, its egg is released in the fallopian tube ready to be fertilised, while the ruptured follicle develops into the corpus luteum; this structure is responsible for the progesterone peak of the diestrus/luteal phase which induces the decidualization of the uterine membrane in preparation for a potential pregnancy. If the egg is indeed fertilised, the progesterone secretion will be eventually taken over by the placenta; if not, the corpus luteum will degenerate, leading to a drop in progesterone levels and the reabsorption of the uterine lining (Silverthorn 2004).

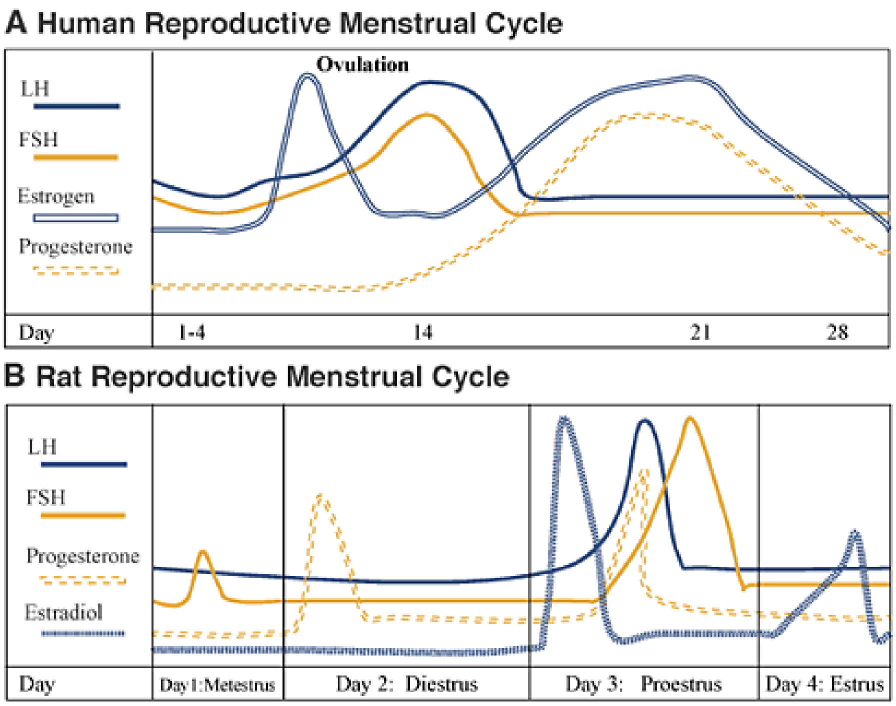

Figure 1.10 Hormone fluctuations during the reproductive cycle.

The graphs represent the reproductive cycles of humans (A) and rodents (B) (adapted from http://pubs.niaaa.nih.gov/publications/arh26-4/274-281.htm).

The cyclical thickening and regression of the endometrium, however, is not the only morphological change induced by the fluctuations in sex hormones levels: also the mammary gland undergoes remodeling with each reproductive cycle, displaying a peak of additional side branching and alveolar bud development in the mouse diestrus (Figure 1.8), most likely in response to progesterone signaling (Fata, Chaudhary et al. 2001).

The most extensive remodeling, however, occurs during pregnancy, when the high levels of progesterone and prolactin drive epithelial proliferation and differentiation into secretory milk-producing cells.

In the first stages of pregnancy the epithelial compartment undergoes a 100-fold increase in cell number and an intensive side branching which is induced by the expression of WNT4; subsequently, the alveolar buds differentiate into individual alveoli and group together to form lobular units, a process called lobuloalveologenesis (Richert, Schwertfeger et al. 2000, Oakes, Hilton et al. 2006, Khokha and Werb 2011).

With parturition, the drop in progesterone levels leads to the secretion of milk from the fully matured alveoli into the lumen; lactation continues as long as the suckling stimulus does and relies on the action of two hormones: prolactin, which maintains milk secretion from the luminal cells, and oxytocin, which acts on the myoepithelial cells inducing their contraction (Neville, McFadden et al. 2002).

Upon weaning, the build-up of milk in the glands triggers involution; this process restores the simple pre-gestation ductal structure and consists of two phases: the first is potentially reversible, if the suckling stimulus resumes within 48h involution is halted and lactation starts again; during this phase many luminal cells undergo apoptosis but the overall architecture of the gland is not altered. The second phase is characterized by the irreversible remodeling of the mammary structure: cell death intensifies, the alveoli collapse and most of the epithelial cells are replaced by adipocytes (Lund, Romer et al. 1996, Watson 2006). While the extracellular matrix remodeling depends on the activity of specific matrix metalloproteinases (mainly MMP-2, MMP-3, MMP-9 and MMP-11) (Green and Lund 2005), multiple pathways contribute to the destruction of the secretory epithelium, including canonical apoptosis, phagocytosis by macrophages and epithelial cell autophagy (reviewed by Watson 2006).

At the end of involution the gland is back to a pre-gestation state and is ready for the new round of epithelial proliferation and differentiation that will start with the next pregnancy.

Finally, with aging, the reproductive cycle stops and the gland undergoes an irreversible lobular involution which leads to gradual loss of the mammary epithelium and the formation of a dormant ductal tree (Figure 1.8) (reviewed in Radisky and Hartmann 2009, Khokha and Werb 2011).

1.3.2 Breast cancer

1.3.2.1 Epidemiology, risk factors and genetics

Breast cancer is the most common malignancy in women as well as the main cause of cancer related deaths (Soerjomataram et al. 2012, Parkin et al. 2006).

It has been estimated that in the European Union alone there are one million women living with breast cancer (Dixon 2009) and this reflects in an annual economic burden of € 15 billion, which makes the health-care costs associated with breast cancer the highest of all oncology-related health-care: even colorectal cancer, the tumour with the highest incidence across the EU, has lower costs (€13.1 billion), which can be explained by different treatment regimens (surgery vs radiation) and also by the prohibitive price of some breast cancer drugs (Luengo-Fernandez, Leal et al. 2013).

In the United Kingdom, age-standardised incidence and mortality of breast cancer are among the highest worldwide (Figure 1.11), probably due to risk factors like smoking and diet: every year this malignancy kills more than 13 000 people and the incidence is particularly elevated for women in their fifties, bordering a rate of 2% (Dixon 2009, Murray, Richards et al. 2013).

It has long been established that ageing is a fundamental risk factor for tumorigenesis and breast cancer is no exception, since the incidence increases with age and doubles every 10 years; unlike other tumour types, however, the rate of increase slows down at the onset of menopause, an observation which fits with a potential role of oestrogen and progesterone in the development of breast cancer (Dixon 2009).

Several epidemiology studies have unequivocally shown that a woman’s risk of developing breast cancer is closely related to her lifetime hormonal exposure: early menarche, late menopause, nulliparity and lack of breastfeeding are all factors that increase a woman's total number of menstrual cycles and have all been associated to higher risk of breast cancer (Dixon 2009).

Further evidence is provided by the fact that reducing the oestrogen levels with a bilateral oophorectomy has a protective effect (Kauff and Barakat 2007), while hormone replacement therapies and oral contraceptives increase the relative risk of developing breast cancer (Dixon 2009).

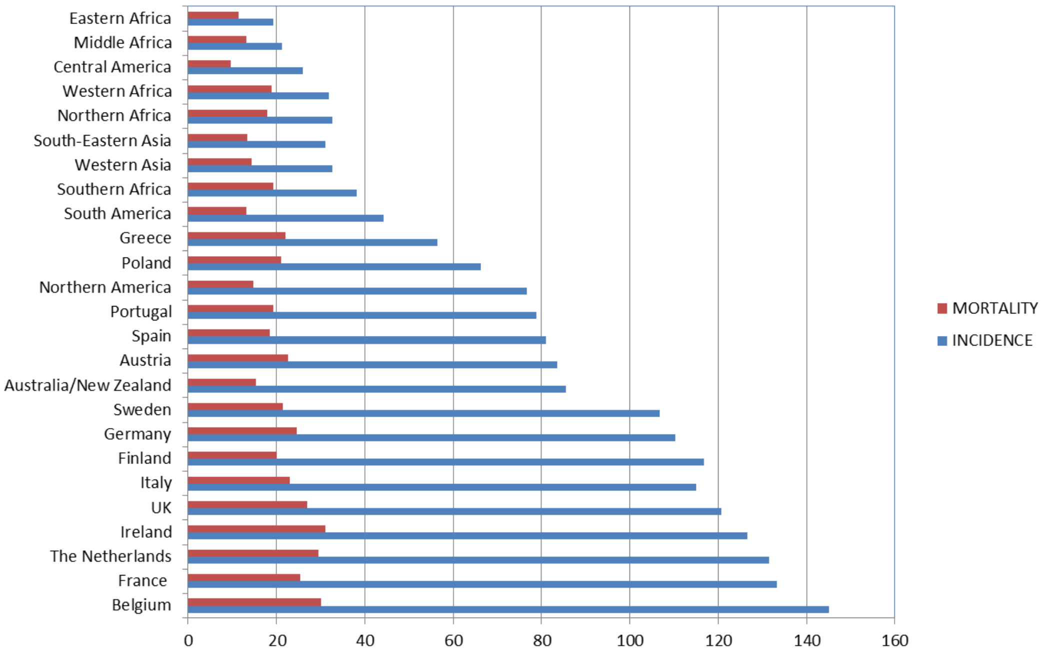

Figure 1.11 Age standardised world incidence and mortality rates of breast cancer.
The graph shows the rates calculated per 100 000 women (adapted from Cancer Stats, Cancer Research UK, 2008 http://www.cancerresearchuk.org/cancer-info/cancerstats/).

Prolonged exposure to oestrogen and progesterone is therefore an established risk factor and it has been shown to contribute to breast tumorigenesis in different ways: firstly, these steroids are key mitogens for mammary cells, their binding to specific membrane receptors activates the transcription of proliferation genes and with each cell division there is a chance for DNA mutations to occur (Clemons and Goss 2001); secondly, estradiol, the predominant type of oestrogen in fertile non-pregnant women, can be metabolized to quinone derivatives that directly damage DNA (Yue, Santen et al. 2003). Lastly, mammary stem cells (MaSCs), which are responsible for the epithelial expansion during puberty, diestrus and pregnancy (Shackleton, Vaillant et al. 2006), are highly responsive to steroid hormone signaling (Asselin-Labat, Vaillant et al. 2010, Joshi, Jackson et al. 2010) and have recently been implicated in the initiation of breast cancer (reviewed in Tiede and Kang 2011).

Additional risk factors are related to lifestyle and include obesity (Pierobon and Frankenfeld 2013), smoking (Reynolds 2013), lack of physical activity (Kossman, Williams et al. 2011) and excessive alcohol intake (de Menezes, Bergmann et al. 2013).

Alongside with these hormonal and behavioural factors, a major role is also played by genetic predisposition, which is responsible for approximately 10% of all breast carcinomas (Dixon 2009).

Several studies have now demonstrated that mutations in specific genes are strongly associated with breast cancer and these susceptibility genes can be divided according to the relative risk that they confer (Table 1.3): interestingly, almost all of them are involved in the maintenance of genomic stability and in DNA damage signaling/repair pathways (reviewed in Tan, Marchio et al. 2008).

The most common mutations are found in the Breast Cancer Susceptibility Gene 1 (*BRCA1*) and 2 (*BRCA2*), which account for nearly 16% of the hereditary breast cancer cases (Peto, Collins et al. 1999).

BRCA1 was first identified in the King laboratory through genetic linkage analysis of families with early-onset breast cancer (Hall, Lee et al. 1990); the gene was later cloned by researchers from the University of Utah and Myriad Genetics (Miki, Swensen et al. 1994), while a collaboration headed by the Institute of Cancer Research led to the localisation and cloning of *BRCA2* (Wooster, Neuhausen et al. 1994, Wooster, Bignell et al. 1995).

Table 1.3 Susceptibility genes linked to hereditary breast cancer.

Breast cancer risk	Gene	Reference
High: 10- to 20-fold relative risk	*BRCA1*	Miki et al. 1994
	BRCA2	Wooster et al. 1994
	TP53	Li et al. 1988
Intermediate: 2- to 4-fold relative risk	*CHEK2*	Meijers-Heijboer et al. 2002
	ATM	Renwick et al. 2006
	CDH1	Masciari et al. 2007
	PTEN	Liaw et al. 1997
	BRIP/FANCJ	Seal et al. 2006
	PALB2/FANCN	Tischkowitz et al. 2007
Low: <2-fold relative risk	*CASP8*	Cox et al. 2007
	FGFR2	Easton et al. 2007, Hunter et al. 2007
	TNRC9/TOX3	Easton et al. 2007
	MAP3K1	Easton et al. 2007
	LSP1	Easton et al. 2007

Both BRCA genes encode for very large proteins which have an essential role in the repair of double-strand DNA breaks (Gudmundsdottir and Ashworth 2006); mutations in these genes can be quite heterogeneous and show very high penetrance: the carriers have an 80% life-time risk of developing breast cancer and 20-40% risk of ovarian cancer (Narod and Foulkes 2004).

Susceptibility genes with moderate penetrance include the cell-cycle checkpoint kinases *CHEK2* (Meijers-Heijboer, van den Ouweland et al. 2002) and *ATM* (Renwick, Thompson et al. 2006), the cell surface glycoprotein *CDH1* (Masciari, Larsson et al. 2007) and two Fanconi anaemia genes (Seal, Thompson et al. 2006, Tischkowitz, Xia et al. 2007); moreover, inherited mutations in *TP53* and *PTEN* cause multiple cancer syndromes (Li–Fraumeni and Cowden respectively) that are associated with a high risk of familial breast cancer (Li, Fraumeni et al. 1988, Liaw, Marsh et al. 1997).

Overall, the susceptibility genes listed so far can explain approximately 20% of the hereditary risk of this malignancy (Thompson and Easton 2004): despite the multiple attempts to find a third high-penetrance breast cancer gene, no ‘‘BRCA3’’ has been identified so far, most likely because no single gene is responsible for the familial breast cancer cases that are not associated with *BRCA1* or *BRCA2* mutations (Narod and Foulkes 2004).

The remaining 80% of hereditary risk can probably be explained by common low-penetrance alleles, which confer smaller increases in risk but have a much higher population frequency (Stratton and Rahman 2008). Genome-wide association studies have so far identified single-nucleotide polymorphisms in five such genes and many more are likely to be discovered in future studies (Cox, Dunning et al. 2007, Easton, Pooley et al. 2007, Hunter, Kraft et al. 2007).

1.3.2.2 Classification criteria

Breast cancer is a very heterogeneous disease that can be classified according to its histological features, receptor status and molecular signature.

At the histological level, grade and type are the two main classification criteria: the grade reflects the aggressiveness of the tumour by measuring its degree of differentiation and proliferation rate, while the type depends on the tumour growth pattern (reviewed in Weigelt, Geyer et al. 2010).

The main distinction lies between *in situ* and invasive breast carcinomas, but pathologists have identified as many as 18 different histological types (Figure 1.12); the most common, which account for up to 75% of cases, is the invasive ductal carcinoma not otherwise specified (IDC-NOS), also called invasive ductal carcinoma of no special type (IDC-NST). The so-called “special types” are rarer and include invasive lobular, mucinous, ductal/lobular, tubular, papillary and medullary carcinomas (reviewed in Malhotra, Zhao et al. 2010, Weigelt, Geyer et al. 2010).

From a clinical perspective, however, the most important classification is based on the receptor status of the tumour: the malignant cells may or may not express oestrogen, progesterone and human epidermal growth factor receptors (ERα, PR and HER2), which, once bound to their ligands, transduce a mitogenic signalling to the nucleus and activate cell proliferation (Langlands, Horgan et al. 2013). As discussed in more detail in chapter 1.3.2.3, the status of these receptors helps determine which treatment option is the most beneficial for the patient.

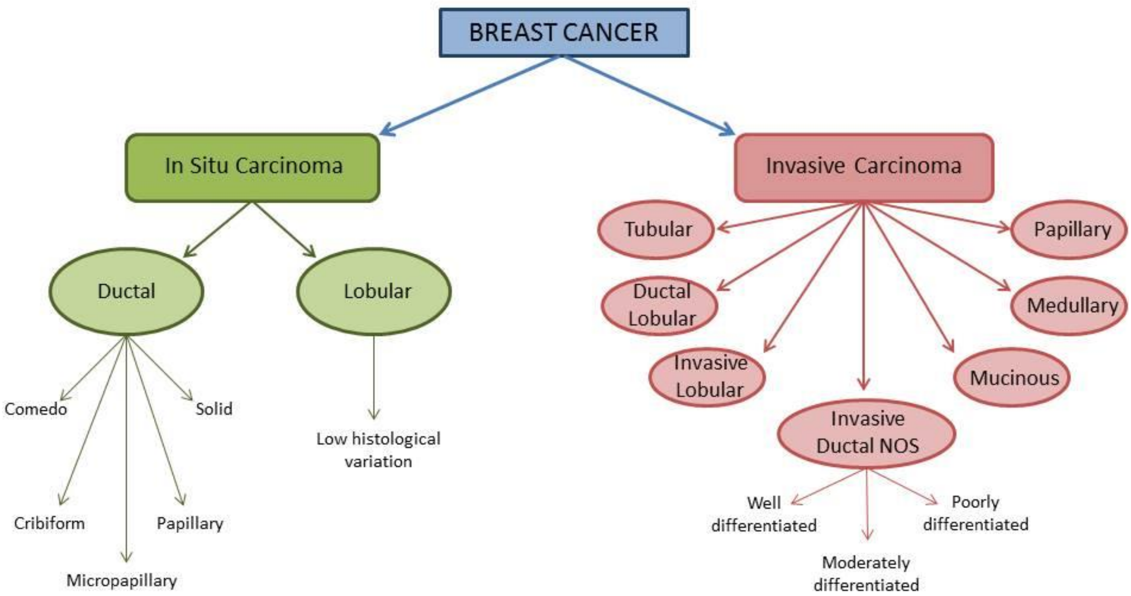

Figure 1.12 Histological classification of breast cancer.

In the past decade the field of breast cancer research was revolutionised by a series of microarray studies showing that gene expression profiling can classify breast carcinomas in different molecular subtypes (Perou, Sorlie et al. 2000, Sorlie, Perou et al. 2001, Sorlie, Tibshirani et al. 2003). Their work conclusively demonstrated that breast cancer cannot be considered as a single disease and identified five molecular subtypes, with a sixth one being added more recently (Herschkowitz, Simin et al. 2007, Prat, Parker et al. 2010).

As shown in Figure 1.13, hierarchical clustering analysis revealed that the main dichotomy is between ER-positive and ER-negative tumours. The former are called luminal because they express genes that are usually found in normal luminal epithelial cells, like cytokeratins 8 and 18; these tumours can be further divided in luminal A and luminal B: the two groups seems to be characterised by different histological grade and proliferation rates, however this distinction remains controversial and some authors prefer considering the luminal tumours as a continuum (reviewed in Malhotra, Zhao et al. 2010, Weigelt, Geyer et al. 2010, Colombo, Milanezi et al. 2011).

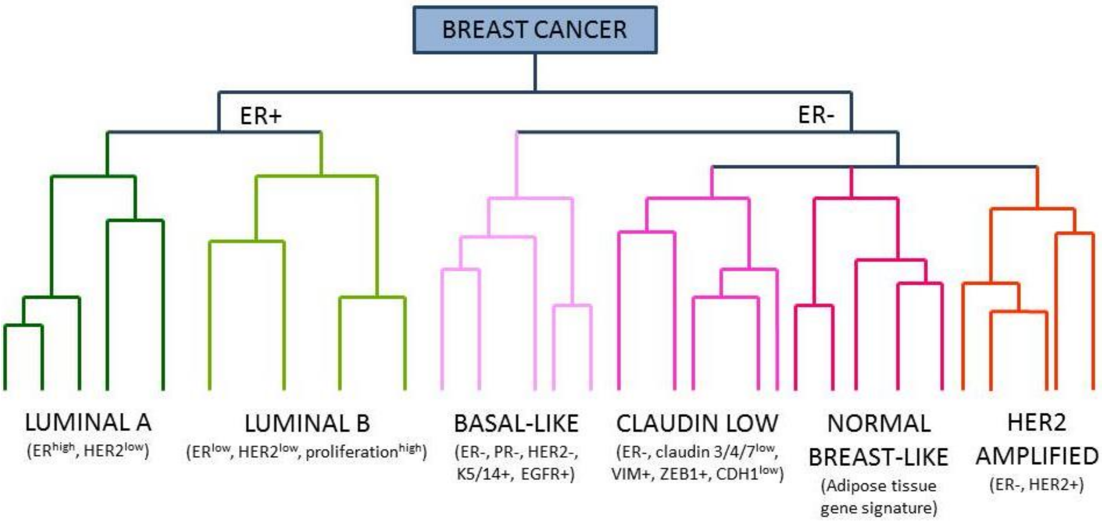

Figure 1.13 Molecular classification of breast cancer.

The ER-negative branch originally included the HER2-overexpressing tumours, the poorly characterised normal breast-like cancers and the basal-like subtype; the latter shows a gene signature usually associated with normal basal/myoepithelial cells, with high levels of cytokeratins 5 and 17, caveolins 1 and 2, EGFR, CD44, P-cadherin and nestin. Recently a fourth, claudin-low group has been identified: these tumours have been described as being enriched for EMT markers and cancer stem cell-like features (reviewed in Colombo et al. 2011, Malhotra et al. 2010, Weigelt at al. 2010).

1.3.2.3 Treatment options

Breast cancer management is based on several histological and clinical factors, such as tumour stage, size and type, axillary status, age of the patient and presence of lymphovascular invasion or metastasis.

The traditional approach used to rely exclusively on local treatment of the tumour, mainly through surgery (lumpectomy or mastectomy depending on the tumour size), followed by radiotherapy. The last two decades, however, have witnessed the introduction of systemic therapies, which can be administered before (neoadjuvant) or after (adjuvant) the local treatment: these therapies are thought to tackle potential micro-metastasis that would otherwise spread and have so far been proved very beneficial, leading to a 15% drop in mortality (Dixon 2009).

Systemic treatments include chemotherapy, monoclonal antibodies and endocrine therapy, which are selected according to the receptor status of the tumour. ER+/PR+ patients are usually given ER modulators like tamoxifen or aromatase inhibitors, which prevent the conversion of androgens to oestrogens, while HER2 overexpressing cancers are treated with trastuzumab, a humanised monoclonal antibody against the external domain of this receptor (reviewed in Tessari, Palmieri et al. 2013, Charehbili, Fontein et al. 2014).

Until recently, chemotherapy was the only option available to treat triple negative tumours, which lack the expression of ER/PR/HER2 and mainly display basal-like features. Around 30% of triple negative breast cancers are associated with BRCA1/2 mutations (Greenup, Buchanan et al. 2013) and this specific subgroup of tumours seems to respond well to PARP-inhibitors, as shown by several phase III clinical trials (Davar, Beumer et al. 2012).

This new class of drugs, first described by the Ashworth group (Farmer, McCabe et al. 2005), blocks the repair of DNA single-strand breaks, which become double-strand breaks after replication: this type of lesions would usually be repaired by homologous recombination, but this pathway is defective in BRCA-mutated cells and therefore the tumour cells die due to mitotic catastrophe (reviewed in Dedes, Wilkerson et al. 2011, Polyak and Garber 2011).

All in all, substantial progress has been made in the treatment of breast cancer, however, many questions are still unanswered, especially regarding the mechanisms through which cancer cells can develop drug resistance and the strategies that could be used to overcome this resistance.

1.4 Current knowledge on the role of WT1 in the mammary gland and in breast cancer

Very little is known on WT1 in the context of healthy mammary cells and so far only two papers have reported WT1 expression in the normal gland (Silberstein et al. 1997, 2002).

In these studies, immunohistochemistry on human specimens showed that all the myoepithelial cells stain heavily with WT1 antibodies, whereas the luminal cells display a more scattered staining and can be divided into two populations based on chromatin morphology and nuclear density. Cells characterised by diffuse chromatin and rounded nuclei, which the authors consider as potential stem cells, are mostly WT1 positive, while the more differentiated cells, with condensed chromatin and polygonal nuclei, can be either positive or negative for WT1 staining (Silberstein et al. 1997).

At the current state of research, however, no functional or knockout studies have been published and the role of *WT1* in the mammary gland remains unknown.

Also *WT1* function in breast cancer is still unclear, despite the fact that a considerable body of data has been accumulated in the last fifteen years.

Several groups have reported *WT1* expression in this type of malignancy and the percentage of WT1-positive tumours varies from 23 to 87%, probably due to differences in the detection method, antibody specificity and histological subtype (Table 1.4).

Table 1.4 Studies on WT1 expression in breast cancer.

Author	Cohort size	WT1 positive	Detection method	Histological subtype
Silberstein et al. 1997	21	28.6%	IHC (C19 Santa Cruz, rabbit polyclonal)	Not described
Cheng et al. 2001	81	23%	RT-PCR	IDC
Loeb et al. 2001	31	87%	WB (C19 Santa Cruz, rabbit polyclonal)	Not described
Miyoshi et al. 2002	99	36%	RT-PCR	97 IDC, 2 ILC
Silberstein et al. 2002	39	65.7%	IHC (C19 Santa Cruz, rabbit polyclonal)	Not described
Gillmore et al. 2006	37	89.2%	RT-PCR	Not described
Nakatsuka et al. 2006	30	80%	IHC (C19 Santa Cruz, rabbit polyclonal)	IDC
		56.5%	IHC (6F-H2 Dako, mouse monoclonal)	

Abbreviations: RT-PCR, Real-Time Polymerase Chain Reaction; IHC, Immunohistochemistry; WB, Western Blot; IDC, Invasive Ductal Carcinoma; ILC, Invasive Lobular Carcinoma

In the first of these studies, Silberstein reported reduced WT1 staining in most breast cancer samples if compared to the normal gland and suggested that the loss of *WT1* expression may somehow be related to mammary carcinogenesis (Silberstein et al. 1997).

The finding that the *WT1* promoter is aberrantly methylated in breast cancer further supported this hypothesis (Huang, Laux et al. 1997, Laux, Curran et al. 1999, Cheng, Wu et al. 2001); moreover, the exogenous expression of *WT1* in the MDA-MB-231 breast cancer cell line was shown to suppress the clonal growth of these cells in soft agar assays and to inhibit tumour formation in nude mice (Zhang, Yu et al. 2003). Subsequently, WT1 was also found to halt the proliferation of neoplastigenic mammary epithelial cells both *in vitro* and *in vivo* (Wang & Wang 2008).

According to all these observations, *WT1* would behave as a tumour suppressor gene in breast cancer, however, there are as many findings suggesting that it may instead be an oncogene.

Firstly, Loeb and colleagues analysed *WT1* expression in normal and malignant mammary cells using RT-PCR: only one out of the 20 healthy samples seemed to express *WT1*, while the vast majority of tumours (27 out of 31) were WT1-positive (Loeb et al. 2001).

Secondly, high *WT1* expression is associated with poor long-term survival in breast cancer patients, indicating that the mRNA levels of *WT1* can be used as a significant prognostic factor (Miyoshi et al. 2002); lastly, down-regulation of *WT1* through antisense oligonucleotides has been shown to lead to growth inhibition in several breast cancer cell lines (Zapata-Benavides, Tuna et al. 2002).

All these contradictory findings seem hard to reconcile, but they may be explained, at least in part, by the complexity of the WT1 protein: Burwell and colleagues have in fact reported that the ectopic expression of different WT1 isoforms has opposite effects on the mammary epithelial cell line H16N-2.

In their study, the +Exon 5/+KTS variant displays oncogenic features such as induction of EMT and redistribution of CDH1 from the cell membrane to the cytoplasm; in contrast, overexpression of the –Exon 5/-KTS isoform decreases proliferation by causing a cell cycle arrest in G2 and up-regulating p21 (Burwell, McCarty et al. 2006).

Of particular importance is also the fact that the ratio between + and – KTS splice variants is different between breast cancer cell lines and the developing kidney, where WT1 acts as a tumour suppressor (Haber, Sohn et al. 1991, Caldon, Lee et al. 2008): the ratio is of 5:1 and 14:1 respectively, which could indicate that the higher relative levels of the +KTS isoforms observed in breast cancer may push towards an oncogenic function.

Additional evidence is however required to validate this hypothesis, as well as to unveil the exact role played by WT1 in both mammary gland development and breast cancer progression.

1.5 Conclusion and aim of the project

The Wilms' Tumour Suppressor gene 1, *WT1*, encodes for a complex protein which plays a crucial role in the regulation of the epithelial-mesenchymal balance during development, whereas in the adult it is involved in the maintenance of tissue homeostasis.

WT1 expression has been reported in both healthy mammary glands and breast cancer samples, however its function in this context is not well understood and the evidence gathered so far is extremely contradictory.

This project aims to clarify the role of WT1 in normal and malignant mammary cells by answering the following questions:

• Which specific cell types express WT1 in the mammary gland?

• Does WT1 expression change throughout the different phases of mammary gland remodeling?

• Is WT1 an essential gene for the post-natal development of the mammary gland?

• Is WT1 expression associated with a specific molecular subtype of breast cancer?

• How does WT1 loss affect breast cancer cells both *in vivo* and *in vitro*?

• Is WT1 loss associated with any phenotypic change linked to a disrupted epithelial-mesenchymal balance?

The original research topic chosen for this PhD was the role of WT1 in breast cancer. However, the results section will start by describing the experiments performed to study WT1 in the normal gland. Since this part was only added during the last year of the PhD, this work is still at an early stage, but will provide a clear picture of WT1 in the healthy mammary tissue and serve as an introduction to and framework for the breast cancer study.

Chapter 2: Studying WT1 role in the mammary gland

2.1 Introduction

Considerable evidence supports the existence of an epithelial hierarchy within the mammary gland: mammary stem cells (MaSCs), which are usually found in the basal layer, have the ability to self-renew and to differentiate into committed progenitor cells, which ultimately give rise to the mature myoepithelial and luminal cells (Figure 2.1) (reviewed in Prat and Perou 2009, Visvader 2009).

The identification of cell-surface molecular markers, which are specific for the different populations, was a major breakthrough in mammary gland biology and, similarly to what happened with the study of haematopoietic lineages, it is now possible to isolate the different cell types through fluorescence-activated cell sorting (FACS) (reviewed in Regan and Smalley 2007).

As mentioned in chapter 1.4, very little is known on WT1 in the context of healthy mammary cells and there are conflicting reports comparing its expression in normal and neoplastic mammary tissue: the breast cancer samples are described to be overexpressing WT1 (Loeb et al. 2001), but also to be characterised by reduced staining (Silberstein et al. 1997).

Immunohistochemistry performed on human specimens has showed that all the myoepithelial cells stain heavily for WT1, while the luminal compartment displays a more scattered staining: based on the position and morphology of the stained cells, the authors suggest that the WT1-positive luminal cells may be potential stem cells (Silberstein et al. 1997).

However, since uncertainty remains over the exact lineage of the WT1-positive cells, it would be interesting to assess *Wt1* expression levels in the different populations isolated through FACS.

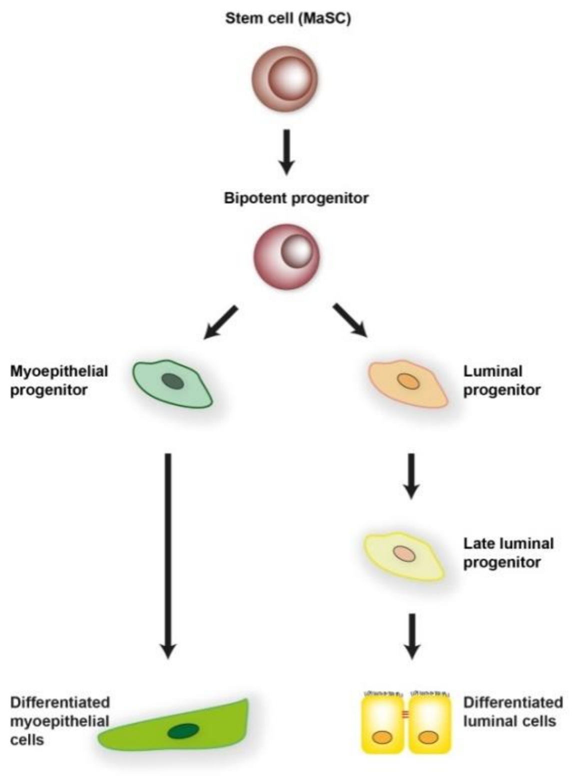

Figure 2.1 Model of the differentiation hierarchy in the mammary epithelium.
Mammary stem cells give rise to bi-potent progenitors, which will then commit to the myoepithelial or luminal lineage.

Moreover, several established WT1 target genes are known to play important roles in the mammary gland: *Areg* is an essential paracrine mediator of the mitogenic stimulus triggered by oestrogen during puberty (Ciarloni, Mallepell et al. 2007), *Wnt4* mediates progesterone signalling and is necessary for the side-branching which occurs at the early stages of pregnancy (Brisken, Heineman et al. 2000), *Snai1* and *Snai2* are also involved in the epithelial branching morphogenesis (Kouros-Mehr and Werb 2006, Lee, Gjorevski et al. 2011).

All in all, it is not clear if *WT1* has any role in the mammary gland, but at the current state of research there is enough circumstantial evidence to make the investigation worthwhile.

2.2 Aim

The aims of the experiments described in this chapter were:

• to identify which specific mammary gland cell types express *Wt1*

• to determine if *Wt1* expression changes throughout the different phases of mammary gland remodeling

• to develop mammary-specific *Wt1* conditional knockout and knockin models

• to analyse the consequences of *Wt1* loss and overexpression in these models, paying particular attention to the mammary branching morphogenesis which occurs during pregnancy.

2.3 WT1 expression in the mammary gland

In order to determine the spatial and temporal distribution of WT1 in the healthy gland, human and murine samples were examined through different techniques.

Firstly, RT-PCR of FACS-purified populations and immunohistochemistry were performed on the glands of 10-week-old virgin female FVB mice; secondly, an *in silico* analysis was carried out to determine if *Wt1* expression levels change throughout the different phases of mammary remodeling.

Lastly, RT-PCR was performed on samples obtained from breast cancer patients and healthy donors, to verify if WT1 expression is higher in the healthy or the neoplastic mammary tissue.

Unfortunately, no reliable antibody for Western blot was available during my PhD, therefore the WT1 protein levels could not be assessed.

2.3.1 *Wt1* expression in the murine gland

In order to identify which specific cell types express *Wt1*, RT-PCR was performed on different mammary gland populations isolated through FACS.

The isolation was carried out in the Smalley laboratory (European Cancer Stem Cell Research Institute, Cardiff), while the retrotranscription was performed by our collaborator Dr. Sproul (MRC HGU, The University of Edinburgh).

In brief, single cells were prepared from the fourth mammary fat pads of 10-week-old virgin female FVB mice, incubated with the antibodies for the cell-surface markers and sorted by flow cytometry according to the following molecular profiles (Regan, Sourisseau et al. 2013):

• Mammary Stem Cells = $CD45^{-}$ $CD24^{+/Low}$ Sca-1^{-} $CD49f^{High}$ c-Kit^{-}

• Myoepithelial = $CD45^{-}$ $CD24^{+/Low}$ Sca-1^{-} $CD49f^{Low}$ c-Kit^{-}

• Luminal ER- progenitor = $CD45^{-}$ $CD24^{+/High}$ Sca-1^{-} c-Kit^{+}

• Luminal ER+ differentiated = $CD45^{-}$ $CD24^{+/High}$ Sca-1^{+} c-Kit^{-}

RT-PCR was performed using primers that target the zinc-finger domain and can therefore amplify all the known isoforms: as shown in Figure 2.2, *Wt1* is expressed in the MaSCs and, at lower levels, in the myoepithelial compartment, but cannot be detected in the luminal cells, independently of their differentiation status.

The myopithelial expression of WT1 was also confirmed through immunohistochemistry using the C19 polyclonal antibody from Santa Cruz, which recognises the last 19 residues of the fourth Zinc finger.

Consistently with what observed for the human gland (Silberstein et al. 1997), the myoepithelial cells stain heavily for WT1, while the luminal compartment is characterised by fainter and less frequent signal; intense staining can also be observed in the endothelial cells, which were not analysed in the original paper (Figure 2.3).

Since the MaSCs are usually found in the basal layer, they could not be distinguished from the myoepithelial cells and a WT1/CD49f double staining should be performed to identify the WT1-positive stem cells.

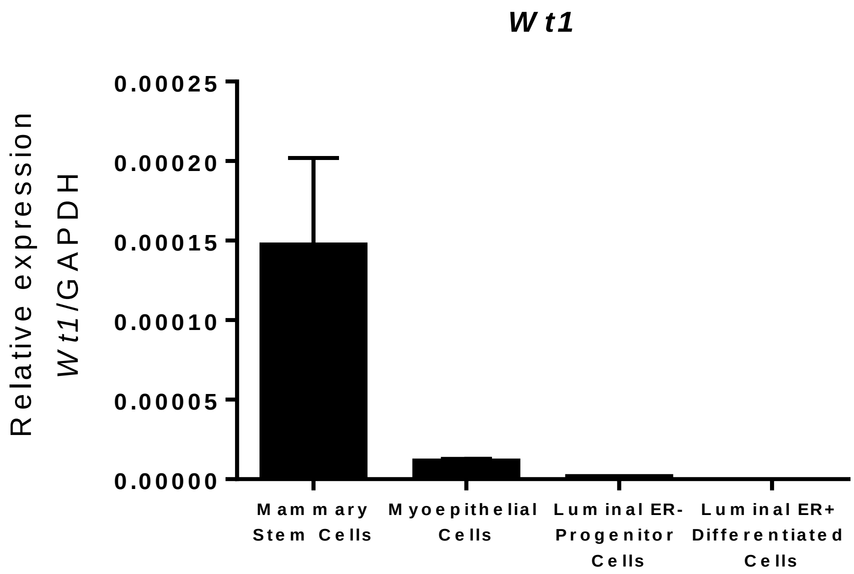

Figure 2.2 Quantitative RT-PCR for *Wt1* mRNA expression in different mammary cell populations.

Quantitative RT-PCR for *Wt1* mRNA expression using primers binding to the transcripts of exon 7 and 8; the different mammary cell populations of 10-week-old virgin FVB mice were isolated through FACS by the Smalley lab. Data points represent the relative expression of *Wt1*, error bars represent the standard deviation of three technical replicates.

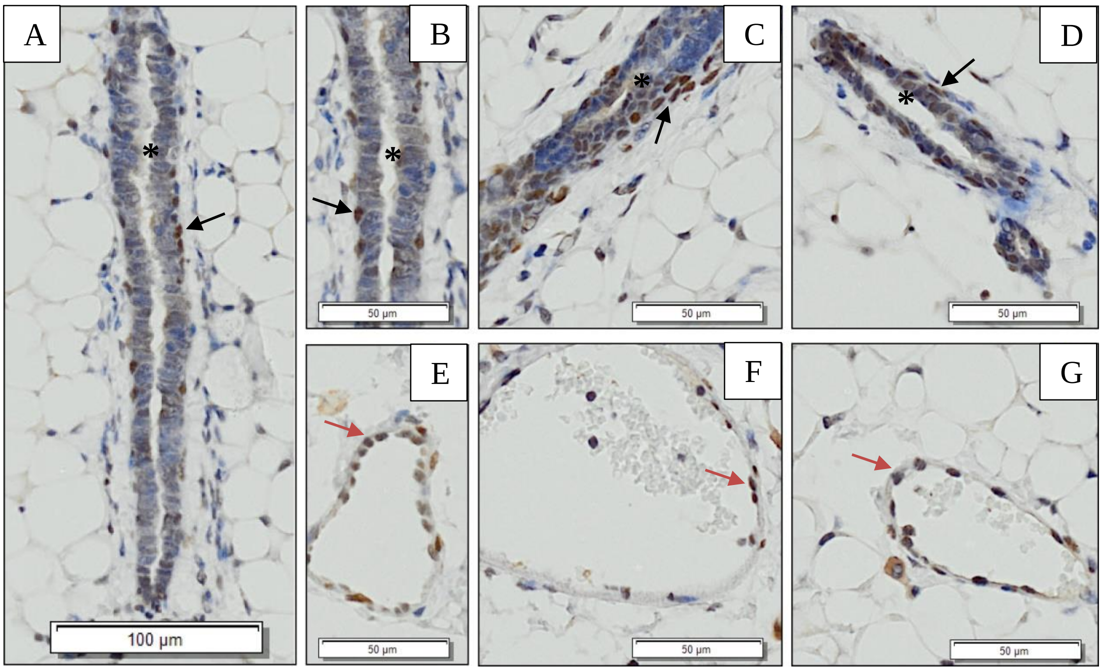

Figure 2.3 WT1 immunohistochemistry of mammary glands in virgin FVB mice.

The mammary glands of 10-week-old virgin female FVB mice were stained using the C19 polyclonal antibody from Santa Cruz, which recognises the last 19 residues of the fourth Zinc finger. Positive staining can be observed in both the myoepithelial and luminal layers (black arrows and asterisks respectively, A-D) as well as in the endothelial cells (red arrows, E-G).

2.3.2 Bioinformatics analysis of *Wt1* expression in the mouse mammary gland

The expression profile of the mammary gland changes extensively throughout life and the genes required for a specific stage usually undergo the most dramatic modulation (Stute, Sielker et al. 2012).

In order to determine whether *Wt1* expression levels change throughout the different phases of mammary gland remodeling, I analysed the publicly available microarray data published by the Watson group (Clarkson, Wayland et al. 2004).

Their work investigated the transcriptional changes which occur during the mouse pregnancy cycle using an Affymetrix MGU74ver2a chip and included a total of 12 time-points (8-week-old virgin; day 5, 10 and 15 of gestation; day 0, 5 and 10 of lactation; hour 12, 24, 48, 72 and 96 of involution).

The expression profile based on the microarray data shows that *Wt1* mRNA in the mammary gland peaks at the beginning of involution, while slightly lower levels can be observed at gestation day 5 and lactation day 5 (Figure 2.4).

However, the graph becomes more informative if the expression profile of *Wt1* is plotted next to some of its potential targets: from this comparison, it becomes evident that the *Wt1* RNA levels are constant throughout the different phases, unlike *Areg* and *Snai2* which are drastically overexpressed at 8 weeks and late gestation respectively; also, *Wt1* expression profile seems to correlate quite closely to that of *Snai1*.

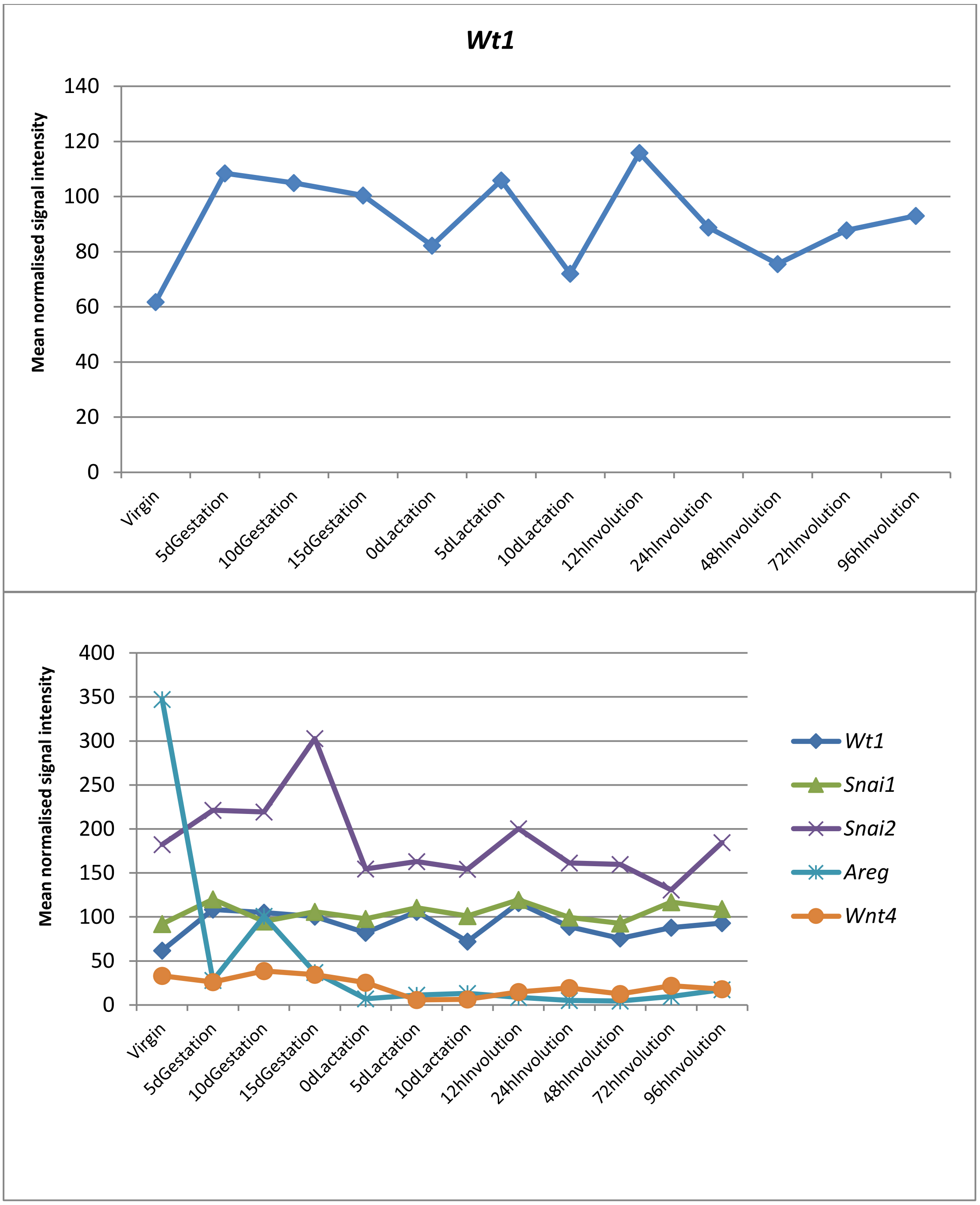

Figure 2.4 Expression profiles relative to the different phases of mammary gland remodelling. The graphs show the analysis of *Wt1* expression (top) as well as some of its potential target genes (bottom) based on publicly available microarray data (Clarkson et al. 2003).

2.3.3 Comparing *WT1* expression in healthy and neoplastic mammary tissues

An RNA sample of human adult mammary gland was purchased from AMSBIO and retrotranscribed; the specimen consisted of a pool from 5 healthy donors of different age (36, 57, 76, 78 and 83 years old).

In parallel, 50 fresh frozen breast cancer samples were obtained through a collaboration with Dr. Katz (see chapter 3 for their molecular classification) and compared to the normal gland through RT-PCR.

As shown in Figure 2.5, WT1 mRNA was more abundant in the healthy tissue, which had higher expression levels than any of the tumour samples (Figure 2.5).

This finding is in line with what observed by Silberstein (Silberstein et al. 1997), however, it must be noted that the pool of healthy donors is clearly skewed towards post-menopause subjects; since the expression profile of the mammary gland changes dramatically throughout life stages (Stute et al. 2012), this imbalance may represent a confounding factor.

In order to verify the biological relevance of this result, *WT1* expression should be analysed in matched normal/neoplastic tissues of younger donors.

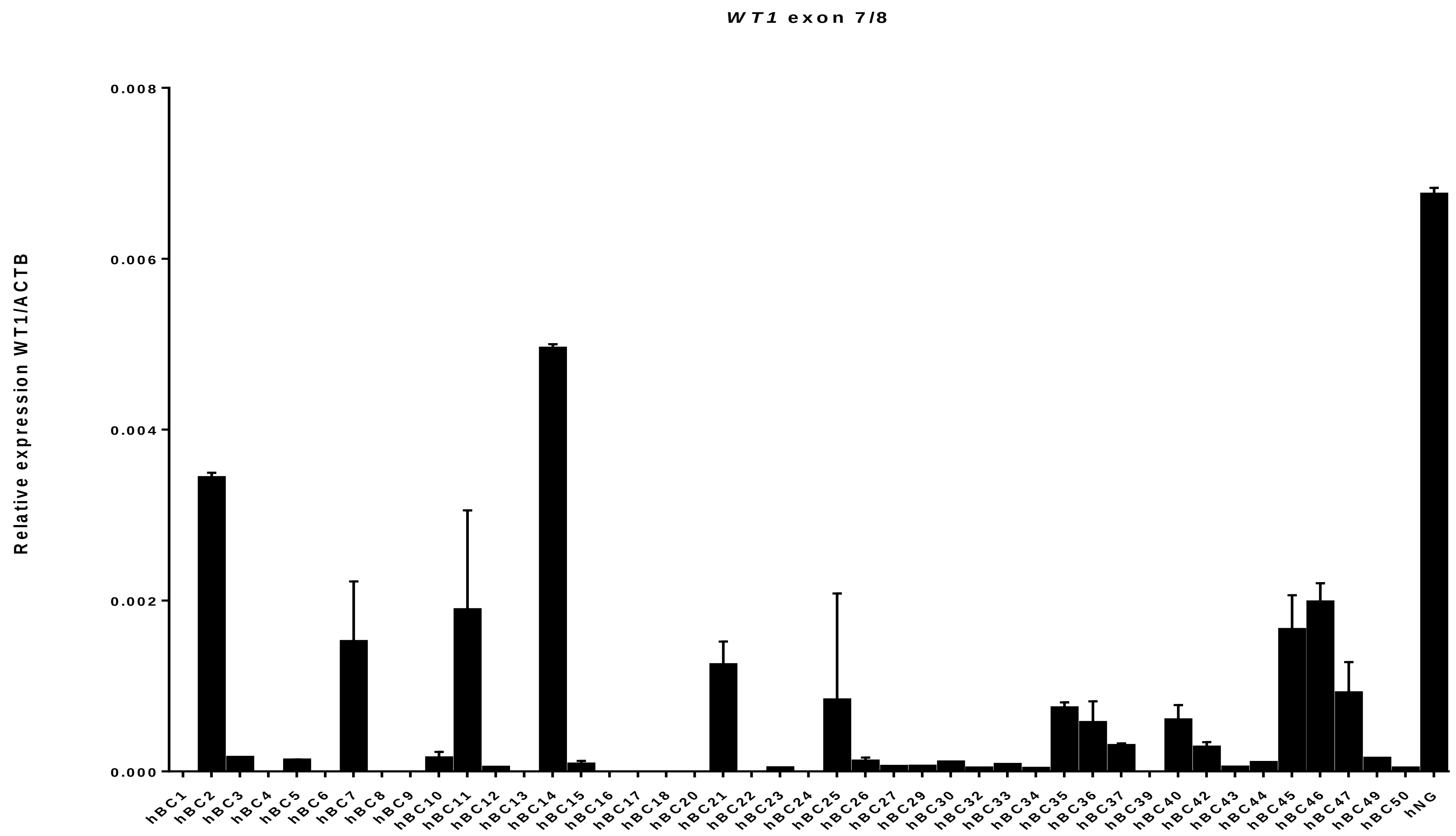
WT1 exon 7/8
Relative expression WT1/ACTB
0.008
0.006
0.004
0.002
0.000
hBC1
hBC2
hBC3
hBC4
hBC5
hBC6
hBC7
hBC8
hBC9
hBC10
hBC11
hBC12
hBC13
hBC14
hBC15
hBC16
hBC17
hBC18
hBC20
hBC21
hBC22
hBC23
hBC24
hBC25
hBC26
hBC27
hBC29
hBC30
hBC32
hBC33
hBC34
hBC35
hBC36
hBC37
hBC39
hBC40
hBC42
hBC43
hBC44
hBC45
hBC46
hBC47
hBC49
hBC50
hNG

Figure 2.5 Quantitative RT-PCR for *WT1* mRNA expression.

The graph compares the *WT1* levels in the normal mammary gland (hNG) and breast cancer samples (hBC). Data points represent the relative expression of *WT1*, error bars represent the standard deviation of three technical replicates.

2.4 Generation of a mammary-specific *Wt1* conditional knockout

In order to characterise WT1 role in the mammary gland, we chose to study the effects of its loss in a mammary-specific conditional knockout model.

Our group had already generated a *Wt1* conditional mouse, in which Exon 1 is flanked by LoxP sites and can therefore be deleted through Cre-mediated recombination (Martinez-Estrada et al. 2010).

In this study, the conditional *Wt1* knockout mice were separately crossed with two different Cre lines, the *MMTV-Cre* and a C3(1)-driven doxycycline-inducible Cre, creating the *MMTV-Co* and *C3-Co* lines respectively.

Given the increasing number of reports on the off-target and toxic effects of Cre recombinase (Schmidt, Taylor et al. 2000, Loonstra, Vooijs et al. 2001, Semprini, Troup et al. 2007, Huh, Mysorekar et al. 2010), we also included a Cre control group; as a whole, three groups of experimental animals were generated for each Cre line and they will be addressed with the following terminology:

CONTROL – Cre-negative $Wt1^{co/co}$

KNOCKOUT – Cre-positive $Wt1^{co/co}$

Cre CONTROL – Cre-positive $Wt1^{+/+}$

2.4.1 MMTV-Cre line

In this line (a kind gift from Dr. Brunton, CRUK, The University of Edinburgh), Cre recombinase is under the transcriptional control of the mouse mammary tumour virus long terminal repeat (MMTV-LTR), which is predominantly active in secretory cell types (Wagner, McAllister et al. 2001).

The MMTV-Cre line is extensively used in mammary gland biology because high levels of recombination are observed in both epithelial and myoepithelial cells throughout all the different stages from puberty to involution (Wagner et al. 2001).

2.4.1.1 Characterisation of the MMTV-driven *Wt1* knockout

Control, knockout and Cre control animals were culled at different stages of the pregnancy cycle (virgin, day 8.5 and 16.5 of gestation, hour 24 and 48 of involution) and the mammary tissue was harvested as follows: the fourth gland was fixed in 4% PFA, the fifth and tenth were preserved in RNAlater, the ninth was fixed in Carnoys solution for wholemount analysis.

Unfortunately, difficulties were encountered during RNA extraction, most likely due to the limited compatibility of RNAlater with fatty tissues; additional samples have been collected and snap frozen, but not yet processed.

Since no good quality RNA was available for RT-PCR, the efficiency of the *Wt1* knockout could not be verified; nonetheless, we proceeded with the analysis of the samples, which showed no significant differences in the gland morphology of virgin mice (data not shown).

The animals of all three experimental groups would develop, breed and nurse their pups normally, however, during pregnancy, the putative knockout glands showed a significant increase in the number of ductular branches if compared to both control and Cre control samples.

The branching analysis was performed by Dr. Del Pozo and Dr. Morrison (The Royal School of Veterinary Studies, The University of Edinburgh) and revealed that the increase is limited to the primary branches at GD 8.5 and the secondary branches at GD 15.5 (Figure 2.6).

As mentioned above, all the females seemed able to lactate normally, and this observation was confirmed by the weight of the pups: as shown in Figure 2.7, the pups of three different litters per experimental group were weighed when three-week-old (right before weaning) and no statistically significant difference was observed between knockout and control animals.

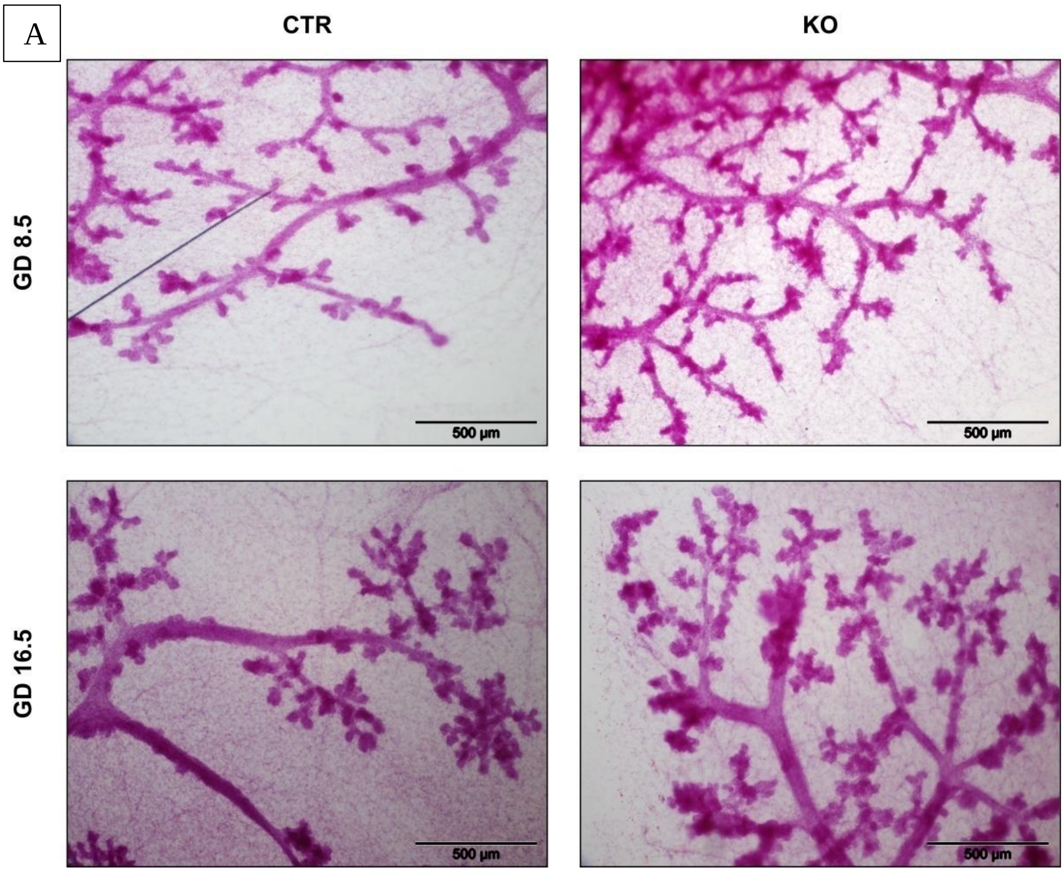
A
CTR
KO
GD 8.5
GD 16.5
500 µm

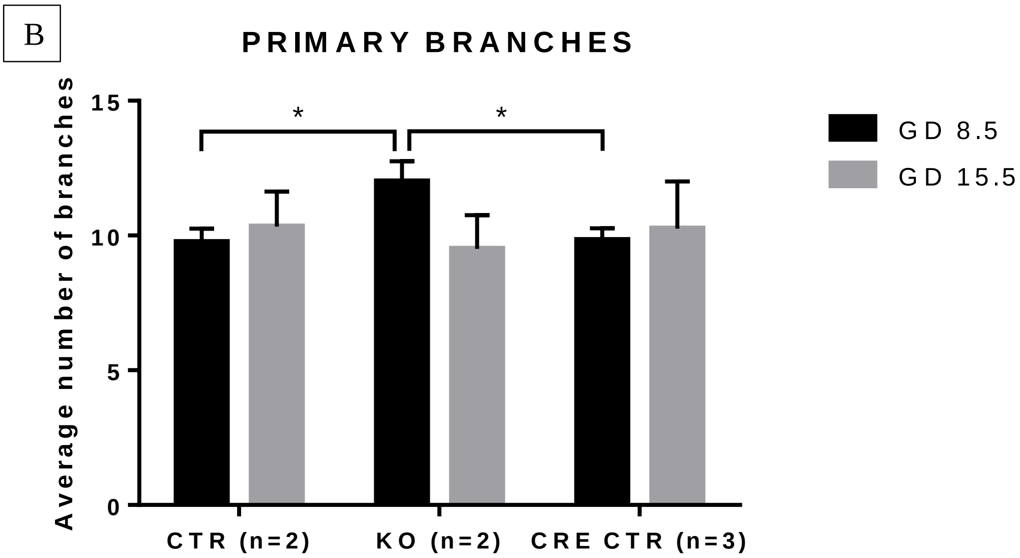
B
PRIMARY BRANCHES
Average number of branches
15
10
5
0
*
*
GD 8.5
GD 15.5
CTR (n=2)
KO (n=2)
CRE CTR (n=3)

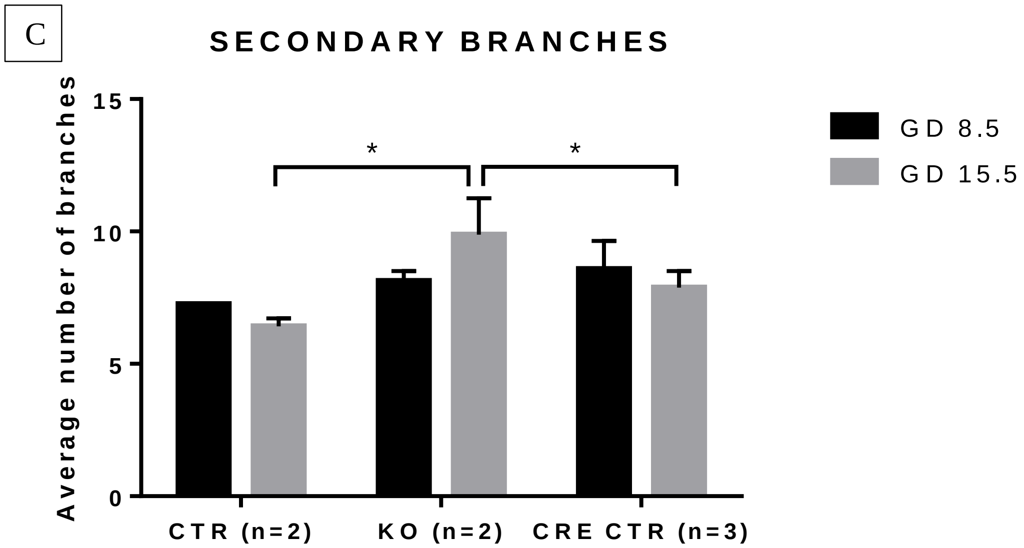

Figure 2.6 Branching analysis of the MMTV-driven *Wt1* knockout mammary glands.

Representative images of mammary gland wholemounts of MMTV-Cre and MMTV-Co mice at GD 8.5 and 16.5 (A), quantification and statistical analysis of the primary branches (B), quantification and statistical analysis of the secondary branches (C) (* $p<0.05$).

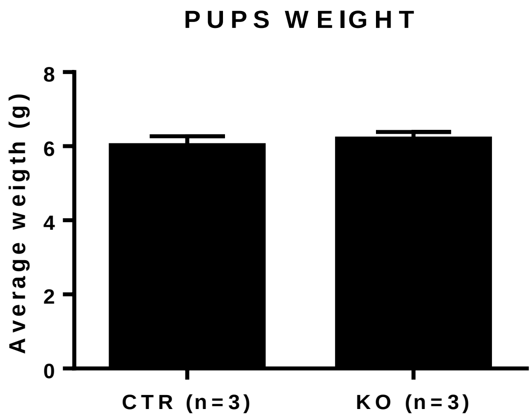

Figure 2.7 Average pup weight in the litters of MMTV-Cre and MMTV-Co mice.

The pups of three different litters per experimental group were weighed when three-week-old and no statistically significant difference was observed between knockout and control animals.

The analysis of the samples collected at the involution stage is still ongoing and has mainly been focused on the size of the glands at 24 and 48 hours after lactation is halted.

As mentioned earlier, involution is characterised by extracellular matrix remodeling and extensive apoptosis of the secretory epithelial cells, which bring the mammary tissue back to its pre-gestation state: if *Wt1* loss affects involution, either by causing an acceleration or a delay of the whole process, the size of the knockout glands would differ significantly from the controls.

However, a very preliminary analysis has revealed that the size of the gland is characterised by high inter-individual variability, which complicates the comparison between the different experimental groups (data not shown).

2.4.2 C3(1)-Cre line

This inducible Cre (a kind gift from Dr. Els Robanus, LUMC, Leiden, The Netherlands) allows temporal and cell-type specific control of DNA recombination by combining the advantages of tetracycline-mediated transcriptional activation and the Cre-LoxP system.

Tetracycline-controlled gene expression is a tool that relies on the antibiotic tetracycline (or its semisynthetic derivative doxycyline) to selectively activate or inhibit the transcription of a specific gene (Gossen and Bujard 1992).

In a Tet-On system like the one used in this project, Cre expression is activated by the rtTA protein, which can successfully bind to the rtTA-responsive promoter “TetO” only in the presence of doxycycline (Figure 2.8).

The *C3(1)-Cre* line, originally designed by Dr. Hohenstein, is based on a construct which integrates both the rtTA and “TetO”-Cre cassettes in a single transgene (Utomo, Nikitin et al. 1999) and was obtained by cloning the C3(1) promoter in the *EcoRI* site of the core construct developed by Utomo.

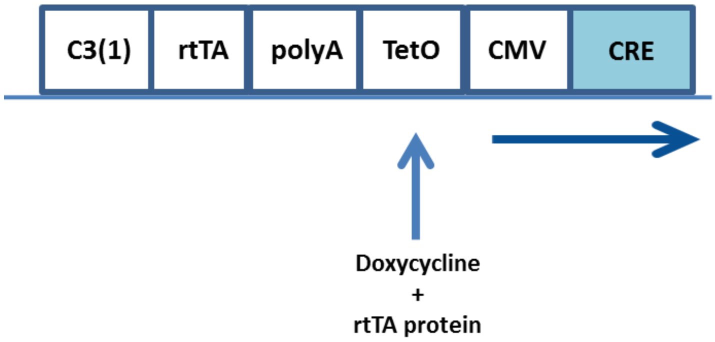

Figure 2.8 Scheme of the C3(1)-Cre transgene.

The *C3(1)-Cre* line is based on a construct which integrates both the rtTA and "TetO"-Cre cassettes in a single transgene regulated by the C3(1) promoter.

2.4.2.1 C3(1)-Cre reporter study

In this line, the expression of Cre recombinase is under the control of the C3(1) promoter, which is active in the epithelium of both prostate and mammary glands (Maroulakou, Anver et al. 1994).

In order to fully characterise this line, *C3(1)-Cre* animals were crossed with a reporter strain where a LoxP-flanked stop sequence and the EYFP cDNA had been targeted into the *Rosa26* locus (*Rosa26R*$^{YFP/YFP}$) (Srinivas, Watanabe et al. 2001); upon Cre-mediated DNA recombination, the stop sequence is excised and EYFP becomes permanently expressed.

The experimental animals were dosed with doxycycline for 5 consecutive weeks (from the third to the eight after birth) and culled at ten weeks of age: once harvested, the mammary tissue was frozen for cryosectioning and then analysed for EYFP expression.

The fluorescent signal appears to be localised to the ductal epithelium and can be detected in approximately half of the luminal cells, while no significant expression is observed in the basal compartment (Figure 2.9).

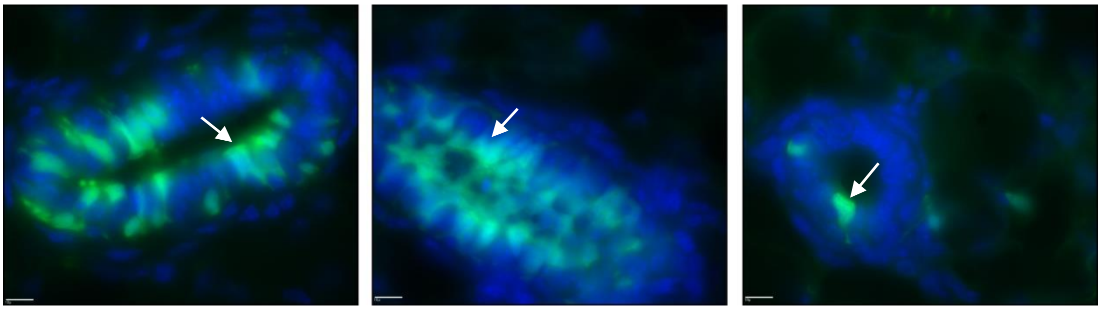

Figure 2.9 C3(1)-Cre-mediated EYFP expression in the mammary gland.
C3(1)-Cre animals crossed with a EYFP reporter strain were dosed with doxycycline from the third to the eight week after birth and culled at ten weeks of age: the representative images of mammary tissue show that the fluorescent signal is localised to the ductal epithelium (white arrows) and can be detected in approximately half of the luminal cells (Scale bars represent 10µm).

2.4.2.2 Characterisation of the C3(1)-driven *Wt1* knockout

The experimental animals were dosed with doxycycline for 5 consecutive weeks (from the third to the eight after birth) and either mated or culled at ten weeks of age; the pregnant mice were sacrificed at gestation day 8.5 and harvested for tissue as previously described.

Good quality RNA could be extracted from snap-frozen samples and used to assess the efficiency of the knockout through RT-PCR: as shown in Figure 2.10, up to 80% reduction of *Wt1* expression was achieved in the knockout glands.

Similarly to what observed for the MMTV-driven knockout, the loss of *Wt1* did not affect gland morphology in virgin mice (data not shown), but led to increased ductular branching during pregnancy.

The knockout glands show higher numbers of primary and secondary branches if compared to the control samples (the Cre control wholemounts have not yet been analysed); the increase, however, is statistically significant only for the secondary branches (Figure 2.11).

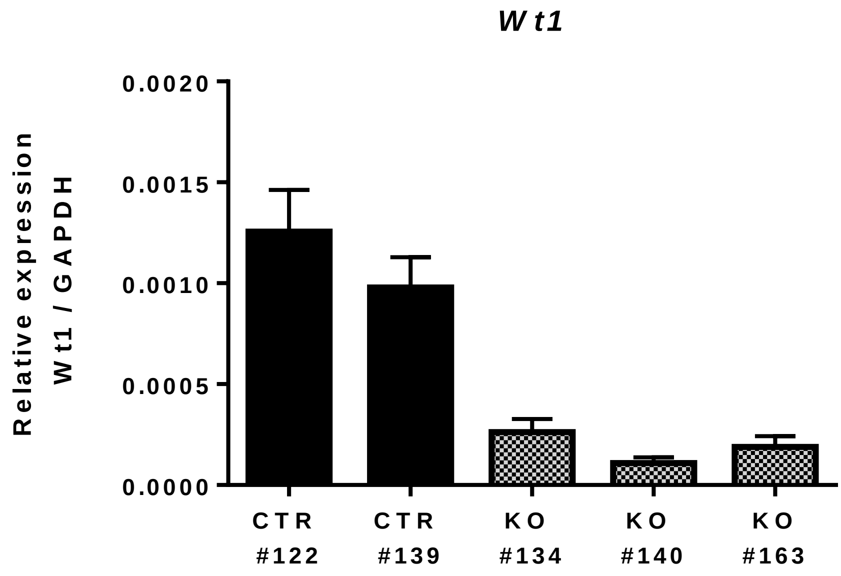

Figure 2.10 Quantitative RT-PCR for *Wt1* mRNA expression in the mammary glands of C3(1)-Cre and C3-Co mice.

Quantitative RT-PCR for *Wt1* mRNA expression using primers binding to the transcripts of exon 7 and 8; data points represent the relative expression, error bars represent the standard deviation of three technical replicates.

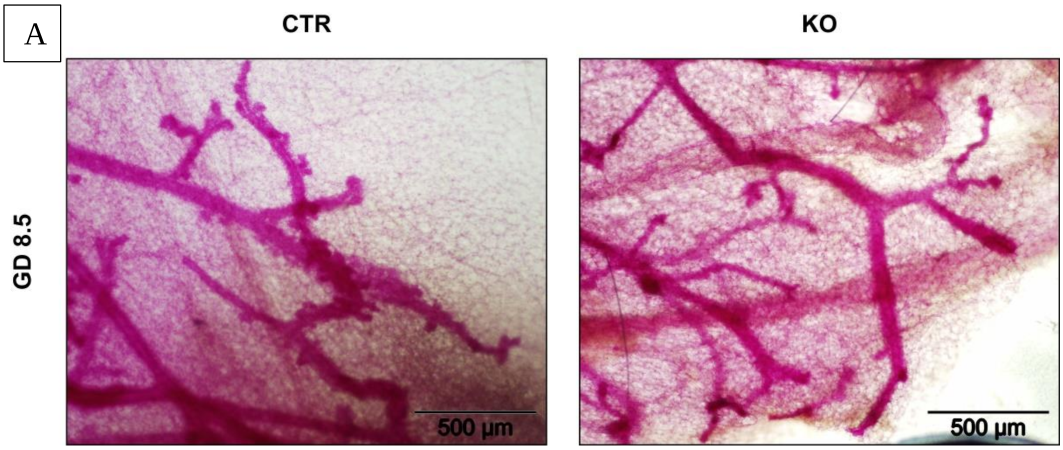

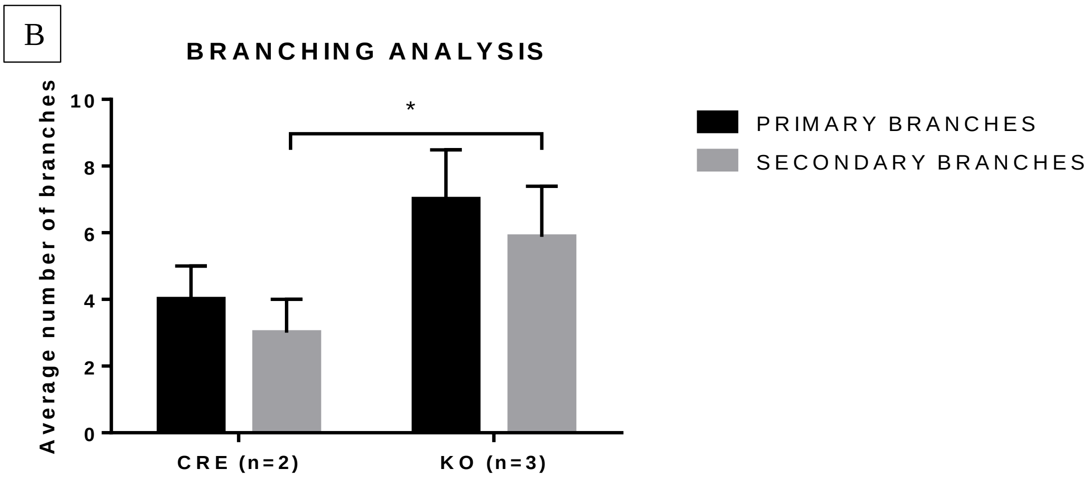

Figure 2.11 Branching analysis of the C3(1)-driven *Wt1* knockout mammary glands at GD 8.5. Representative images of mammary gland wholemounts of C3(1)-Cre and C3(1)-Co mice at GD 8.5 (A), quantification and statistical analysis of the primary and secondary branches (B) (* $p<0.05$).

2.5 Multiple gestations and ectopic *Wt1* expression

The results obtained so far indicate that *Wt1* may be involved in the side branching which occurs during pregnancy and two additional experiments have been performed to further study this potential role.

Firstly, *MMTV-Co* mice were allowed to complete one full pregnancy cycle (from fertilisation to involution) and were culled at gestation day 8.5 or 15.5 during their second pregnancy.

The "multiple pregnancies" strategy is often used in mammary gland biology because it can either rescue or exacerbate a knockout phenotype, depending on whether compensative mechanisms can be activated (Liu, Gallego et al. 1998, Wagner, Krempler et al. 2004, Atabai, Fernandez et al. 2005, Choi, Chakrabarti et al. 2009).

Secondly, *C3(1)-Cre* mice were crossed with a *Wt1* knockin model where the -KTS isoforms are ectopically overexpressed (Bandiera, Vidal et al. 2013).

This line was generated by targeting the *Wt1*-KTS cDNA to the Rosa26 locus (Figure 2.12): upon Cre-mediated excision of the STOP cassette, the *Wt1*-KTS cDNA is linked to the first exon of the Rosa26 locus and transcripted in a chimeric mRNA, but, since the endogenous Rosa26 sequences are not translated into protein, only the WT1-KTS peptide is synthesised (Hohenstein, Slight et al. 2008).

Figure 2.12 Scheme of the Wt1-KTS knockin construct targeted to the Rosa26 locus.
In the presence of Cre recombinase, the *Wt1*-KTS cDNA targeted to the Rosa26 locus is linked to the first exon of the Rosa26 locus and transcripted in a chimeric mRNA.

C3-Rosa26:Wt1-KTS mice were continuously kept on doxycycline to activate *Wt1* overexpression, mated and culled and different stages of gestation.

At the time of writing, the samples obtained from both experiments had been processed and branching analysis was being performed by Dr. Del Pozo and Dr. Morrison.

2.6 Discussion

The experiments described in this chapter identify the stem cell and myoepithelial compartments as the main sites of WT1 expression in the mammary gland, providing the first molecular evidence for what had been hypothesised almost two decades ago (Silberstein et al. 1997).

The finding that WT1 is expressed in MaSCs is intriguing, especially since this gene is required for the differentiation of renal and hematopoietic progenitor cells (Kreidberg et al. 1993, Chau et al. 2011). Gene expressed in MaSCs are ususally important regulators of mammary cell fate and their knockout affects the expansion and differentiation of the stem cell compartment (Chakrabarti, Wei et al. 2012, Chen, Li et al. 2014); to determine if this is the case for WT1, FACS analysis should be performed to compare the abundance of the different mammary populations in knockout and control glands.

Based on the immunohistochemistry staining, WT1 seems to be expressed also in some cells of the luminal layer, however, the RT-PCR performed on the luminal ER- progenitor and ER+ differentiated populations gave negative results. This discrepancy may be explained by the presence of a third luminal cell type, the ER+ progenitor cells, which are characterised by a Sca-1^{+} c-Kit^{+} phenotype (Regan, Kendrick et al. 2012); in order to verify if these are indeed the WT1-positive luminal cells observed through immunohistochemistry, RT-PCR should be performed on a FACS-isolated sample of this population.

Despite being at an early stage, the characterisation of the mammary *Wt1* knockouts has obtained encouraging results and revealed a branching phenotype in both models analysed (even though *Wt1* expression levels in the *MMTV-Co* line remain to be assessed).

At both GD 8.5 and 15.5, the *Wt1* knockout glands display a higher number of branches and the difference is statistically significant despite the small population size analysed so far ($n \leq 3$ for each experimental group), which would suggest that higher significance could be achieved with the analysis of the outstanding samples.

The potential involvement of *Wt1* in the regulation of mammary branching may be related to its role as a regulator of the epithelial-mesenchymal balance: partial EMT has been detected at the tips of growing branches and has been hypothesised to be necessary for their invasion into the extracellular matrix (Micalizzi, Farabaugh et al. 2010, Nistico, Bissell et al. 2012).

In this scenario, the loss of *Wt1* may push the mammary cells towards a more mesenchymal phenotype, facilitating the EMT process at the tips of the branches and therefore causing increased branching.

In terms of potential mechanisms through which *Wt1* may act, several hypotheses can be made: as previously mentioned, important branching regulators such as *Wnt4* and *Snai1* are *Wt1* targets at least in the heart and kidneys (Essafi et al. 2011, Martinez-Estrada et al. 2009) and ChIP experiments could verify if they are in the mammary tissue as well.

Moreover, the RNA-sequencing described in chapter 4.4.1 has revealed that, upon *WT1* knockdown, the human breast cancer line MDA-MB-157 shows significant upregulation of the protein disulfide isomerase *AGR2*, suggesting that this gene may be negatively regulated by WT1. Since the *in vivo* overexpression of *Agr2* produces a branching phenotype similar to the one observed in the *Wt1* knockout (Verma, Salmans et al. 2012), *Agr2* may lie downstream of *Wt1* in a branching regulatory pathway.

All in all the experiments described in this chapter identified for the first time a potential role for *Wt1* in the mammary gland. Further work is however required: firstly, lineage tracing experiments should be performed to determine which cell lineage originates from the WT1-expressing MaSCs; secondly, the *Wt1* knockout glands need to be analysed for the expression of epithelial and mesenchymal markers to assess if the partial EMT occurring at the branching sites is somewhat increased.

Lastly, ChIP should be performed in order to identify the exact mechanism through which *Wt1* may regulate the mammary branching.

Chapter 3: *WT1* expression in breast cancer

3.1 Introduction

Several groups have described *WT1* expression in breast cancer (Silberstein et al. 1997, Cheng et al. 2001, Loeb et al. 2001, Miyoshi et al. 2002a, Silberstein et al. 2002, Gillmore et al. 2006, Nakatsuka et al. 2006), however, their data on the frequency of *WT1*-positive tumours are not in agreement.

As mentioned in chapter 1, the percentage of *WT1*-expressing tumours varies from 23% (Cheng et al. 2001) to 87% (Loeb et al. 2001), most likely as a result of differences in detection techniques and antibody specificity: four out of the seven publications relied on RT-PCR and used primers targeting the Zinc finger region, that would therefore detect all the different *WT1* isoforms (Cheng et al. 2001, Miyoshi et al. 2002a, Gillmore et al. 2006); only one group performed Western Blot (Loeb et al. 2001), while the remaining three resorted to IHC (Silberstein et al. 1997, Silberstein et al. 2002, Nakatsuka et al. 2006).

Interestingly, one study performed IHC using two different antibodies (the rabbit polyclonal C19 from Santa Cruz and the mouse monoclonal 6F-H2 from Dako) showing that the sensitivity differs greatly between the two, which respectively stained 80% and 56.5% of the breast cancer samples (Nakatsuka et al. 2006). Since the C19 recognises the last 19 residues of the forth Zinc finger, while the 6F-H2 is targeted against the N-terminus, the authors speculate that the difference in immuno-reactivity may be caused by the presence of WT1 isoforms with an altered/truncated N-terminus that would not be detected by the 6F-H2 antibody (Nakatsuka et al. 2006).

Such WT1 isoforms have indeed been described and derive from a maternally-imprinted alternative exon 1 (exon 1A, Dallosso et al. 2004), a cryptic promoter in intron 5 (Dechsukhum et al. 2000) and two alternative translation start sites (Bruening et al. 1996, Scharnhorst et al. 1999), however, very little is known about these variants, especially in relation to breast cancer: most of the literature is focused on the four major WT1 configurations described in Chapter 1 (+/- KTS and +/- Exon 5), as does the only *in vitro* study that assessed the expression of different WT1 isoforms in a panel of breast cancer cell lines (Caldon et al. 2008).

Besides the differences in detection methods and antibody specificity, it should be pointed out that only three of the above-mentioned publications specified the histological subtype of the tumours they analysed (mainly IDC, Cheng et al. 2001, Miyoshi et al. 2002a, Nakatsuka et al. 2006), while none reported the molecular subtype: given the extreme heterogeneity of breast cancer, this may represent an additional confounding factor and it is possible that different subtypes of the disease express different levels of WT1.

In this regard, the only study that examined the relationship between WT1 expression and molecular subgroups claims that WT1 correlates with ER-negative, basal-like and HER2 breast cancers (Qi, Zhang et al. 2012); however, the analysis was conducted on just one microarray dataset and requires further validation.

In particular, a possible link between WT1 and the ER/PR status of the tumour should be thoroughly investigated; several papers have in fact implicated WT1 in steroid hormone pathways: both estradiol and progesterone are known regulators of WT1 expression in breast cancer cells (Zapata-Benavides et al. 2002, Caldon et al. 2008), WT1 co-immunoprecipitates with ERα in MCF7 cells (Reizner, Maor et al. 2005) and conflicting reports have shown that it can either activate or repress ERα (Han, Yang et al. 2008, Kang, Wang et al. 2011).

Overall, considering the discrepancies found in the literature, it seems worthwhile performing a more detailed and comprehensive analysis of *WT1* expression in breast cancer as well as examining in more depth the role of the less studied isoforms.

3.1.1 Aim

The aims of the experiments described in this chapter were:

• to characterise *WT1* expression in breast cancer through different approaches (*in vitro*, *in vivo* and *in silico*)

• to verify whether *WT1* is indeed associated with any specific histological or molecular subtype of breast cancer

• to determine if two of the least studied isoform of *WT1* (“exon 1A” and “intron 5”) are expressed in this malignancy.

3.2 Expression of *WT1* in a panel of breast cancer cell lines

In the last decades, breast cancer cell lines have been extensively used to investigate the biological mechanisms underlying this disease as well as to test the efficacy of potential drugs. Despite its many limitations, this *in vitro* system has been shown to mirror several aspects of the primary tumours, including their genomic and molecular heterogeneity (Neve, Chin et al. 2006).

For this study, a panel of thirteen different breast cancer cell lines was chosen to represent the variability of the disease, while the pancreatic cancer cell line Panc1, known to express high levels of *WT1* (Takahara, Koido et al. 2011), was used as a positive control.

Quantitative RT-PCR was first performed using primers targeting exon 7/8 of *WT1*, so that the assay would amplify all the known isoforms (Figure 3.1A): seven cell lines were found to express detectable levels of *WT1*, with the highest expression occurring in the basal triple-negative lines HBL100 and MDA-MB-157 and in the luminal ER+ line ZR75.

Additional assays were designed to specifically amplify exon 1A (Figure 3.1B) and the portion of intron 5 which is transcribed in the truncated variant described by Dechsukhum (Dechsukhum et al. 2000) (Figure 3.1C). Only the basal triple–negative lines BT20 and MDA-MB-231 expressed detectable levels of the intron 5 isoform, while exon 1A was expressed only by the BT20 cells.

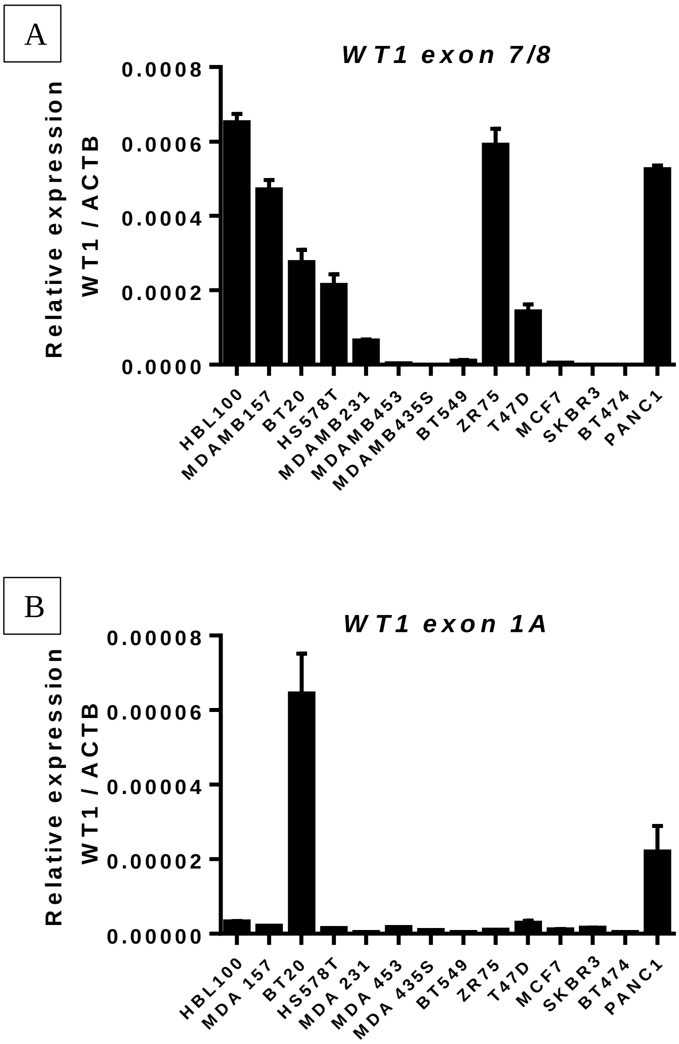

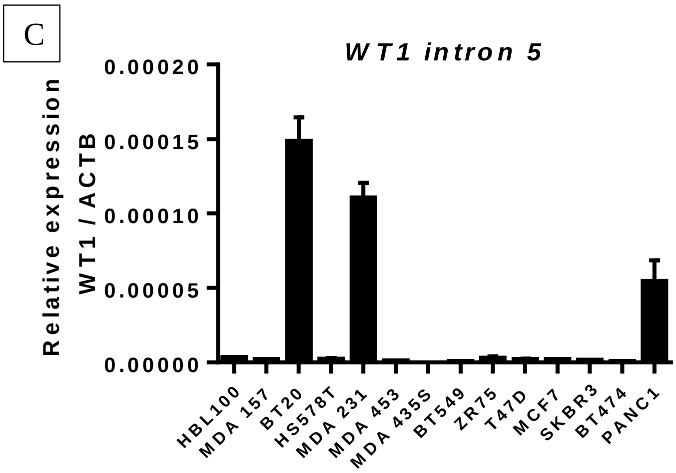

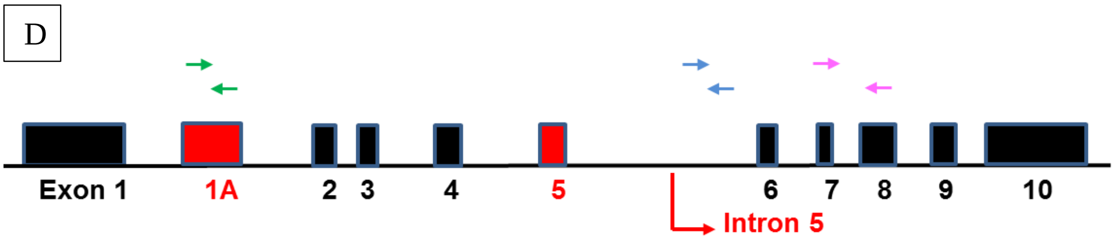

Figure 3.1 Quantitative RT-PCR for *WT1* mRNA expression in different breast cancer cell lines. Data points represent the relative expression of the respective isoform (A, exon 7/8; B, exon 1A; C, intron 5), error bars represent the standard deviation of three biological replicates. The schematic in D represents the position of the primers for each assay (exon 1A in green, intron 5 in blue, exon 7/8 in pink).

These results are in agreement with previous experiments carried out during my MSc, which detected the truncated isoform in SW480, Panc1 and MDA-MB-231 cells; moreover, neither exon 1 nor exon 1A were found in MDA-MB-231 cells, suggesting that intron 5 may be the only *WT1* isoform present in this breast cancer line (Artibani 2010).

A comparative analysis was then carried out on all the studies that assessed *WT1* expression in the same cell lines used in this project (Table 3.1).

Similarly to what observed for the primary tumours, conflicting results were reported and the discrepancies could once again be due to differences in detection techniques (RT-PCR, WB, NB) and antibody specificity (C19 vs 6F-H2). In this case, however, we should also consider the typical pitfalls of *in vitro* work: the cell lines from different laboratories may in fact have been maintained in different culture conditions, contaminated with other cell lines, or they may simply have accumulated genomic instability due to long-term-culture, all of which could affect gene expression and therefore *WT1* mRNA/protein levels (Osborne, Hobbs et al. 1987, van Staveren, Solis et al. 2009).

In this context, my RT-PCR data fit quite well with the most recent and complete publication (Caldon et al. 2008), with the only exception of BT20 and MDA-MB-231 cells, which have been found *WT1*-positive in this study but negative by Caldon.

Unfortunately, doubts remain over the WT1 protein levels expressed by the breast cancer cells: several Western blots performed during my PhD gave negative results (data not shown), suggesting that WT1 expression in these lines is very low.

However, the fact that extremely faint bands were observed for the M15 positive control (data not shown) and that other groups have obtained positive results (Zapata-Benavides et al. 2002, Han et al. 2004, Tuna et al. 2005, Reizner et al. 2005, Caldon et al. 2008), would indicate an antibody problem and additional antibodies are currently being tested.

Table 3.1 Comparison of in vitro WT1 expression with previous reports.

	Laux et al. 1999 (NB)	Oji et al. 1999 (RT-PCR)	Loeb et al. 2001 (NB)	Zapata-Benavides et al. 2002 (WB – 6F-H2)	Han et al. 2004 (WB – C19)	Tuna et al. 2005 (WB – 6F-H2)	Reizner et al. 2005 (WB – F-6)	Caldon et al. 2008 (WB – C19, RT-PCR)	This study (RT-PCR)
HBL100	-	-	-	-	-	-	-	-	√
MDA-MB-157	-	-	**X**	-	-	-	-	√	√
BT20	-	-	**X**	-	-	-	-	**X**	√
HS578T	√	-	√	√	-	-	-	√	√
MDA-MB-231	**X**	√	**X**	√	-	√	-	**X**	√
MDA-MB453	-	-	-	√	-	√	-	X	X
MDA-MB-435s	-	-	-	-	-	-	-	-	X
BT549	-	-	-	-	-	-	-	X	X
ZR75	-	-	-	-	-	-	-	√	√
T47D	√	**X**	√	√	-	-	-	√	√
MCF7	X	-	X	√	√	√	√	X	X
SKBR3	-	-	X	√	-	√	-	X	X
BT474	-	-	-	√	-	√	-	X	X

Abbreviations and symbols: RT-PCR, Real-Time Polymerase Chain Reaction; NB, Northern Blot; WB, Western Blot; -, data not available; √, positive for WT1 expression; X, negative for WT1 expression. The discrepancies between my study and previous reports are emphasised in red.

3.3 Expression of *WT1* in human breast cancer samples

For the *in vivo* part of the study, two different sets of human breast cancer samples were examined for *WT1* expression:

• the first set was obtained through a collaboration with Dr. Katz and consisted of 50 fresh frozen breast cancer samples of unknown molecular and histological subtype; to better characterise these tumours, their ER, PR and HER2 status was assessed through both IHC and RT-PCR

• the second set was obtained from the Tissue Bank in collaboration with Dr. McGregor and Dr. Kendall; it consisted of 60 ductal carcinomas NST of known grade, ER and HER2 status.

3.3.1 First set of tumour samples

In clinical practice, strict guidelines regulate the IHC protocol which is used to assess the ER/PR/HER2 status of breast carcinomas (Hammond, Hayes et al. 2010, Hammond, Hayes et al. 2011). Since some of these criteria could not be met (eg. the samples should be formalin-fixed and paraffin-embedded), validated RT-PCR assays were performed to complement and verify the IHC results (de Cremoux, Tran-Perennou et al. 2002, de Cremoux, Tran-Perennou et al. 2003).

For the RT-PCR experiments, the threshold for positivity was set at a relative expression of 0.05, while the stainings were examined under the guidance of Dr. Thomas (Figure 3.2): ER and PR were scored using the Allred method, which combines the percentage of positive cells and the intensity of the staining (Harvey, Clark et al. 1999, Gown 2008), HER2 overexpression was determined according to the HercepTest guidelines (http://www.dako.com/38602_19feb10_herceptest_scoring_guidelines- breast_ihc.pdf).

As shown in Figure 3.2A, the histological quality of the samples was extremely poor; nonetheless, both ER and PR stainings were informative and correlated with the RT-

PCR results in 82% and 78% of the samples respectively (Figure 3.2B, 3.2C, Table 3.2).

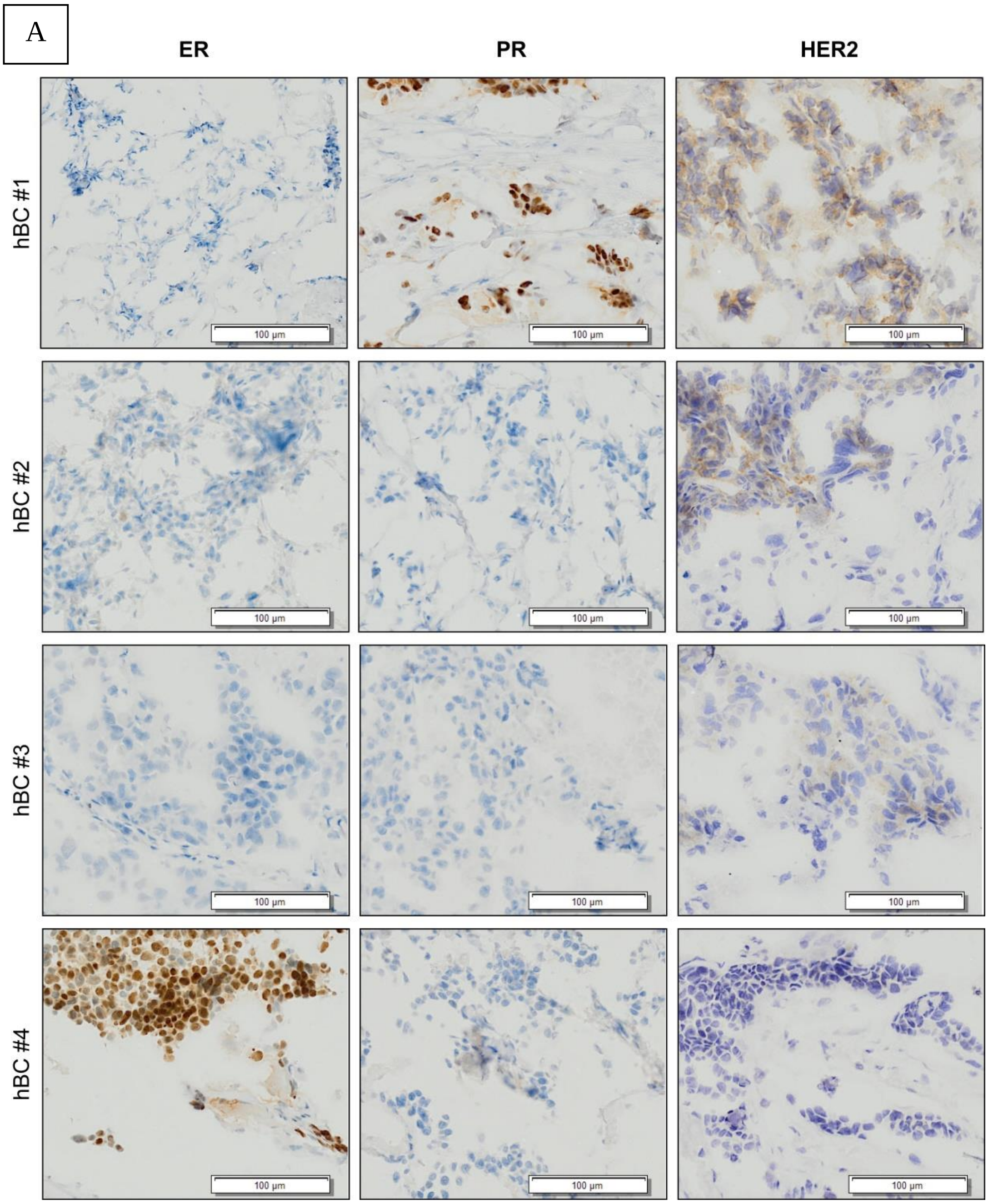

B

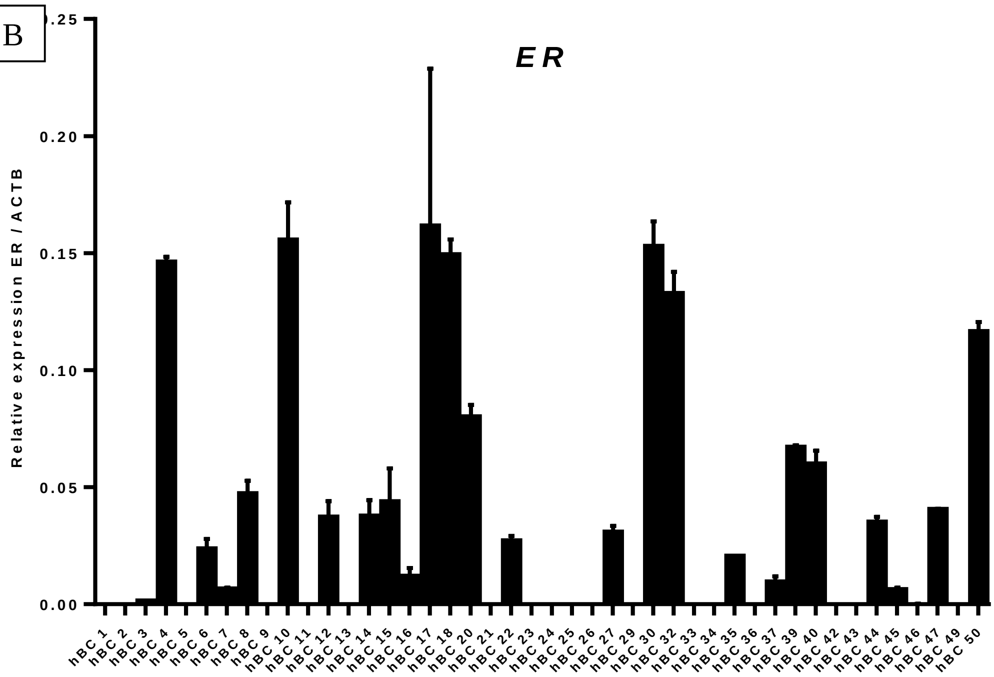
ER
Relative expression ER / ACTB
0.25
0.20
0.15
0.10
0.05
0.00
hBC 1
hBC 2
hBC 3
hBC 4
hBC 5
hBC 6
hBC 7
hBC 8
hBC 9
hBC 10
hBC 11
hBC 12
hBC 13
hBC 14
hBC 15
hBC 16
hBC 17
hBC 18
hBC 20
hBC 21
hBC 22
hBC 23
hBC 24
hBC 25
hBC 26
hBC 27
hBC 29
hBC 30
hBC 32
hBC 33
hBC 34
hBC 35
hBC 36
hBC 37
hBC 39
hBC 40
hBC 42
hBC 43
hBC 44
hBC 45
hBC 46
hBC 47
hBC 49
hBC 50

C

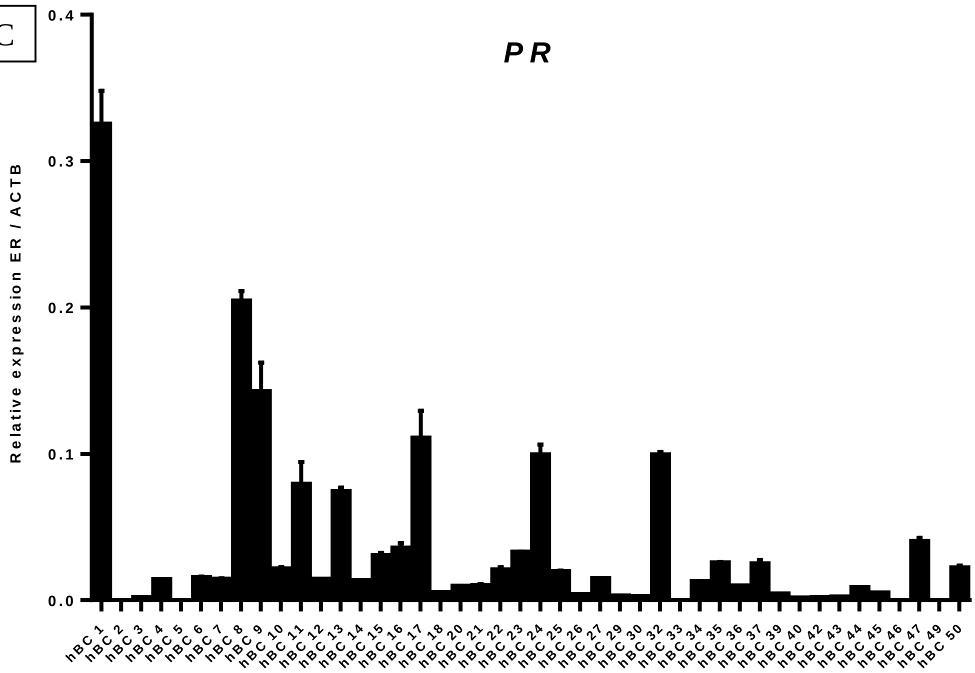
PR
Relative expression ER / ACTB
0.4
0.3
0.2
0.1
0.0
hBC 1
hBC 2
hBC 3
hBC 4
hBC 5
hBC 6
hBC 7
hBC 8
hBC 9
hBC 10
hBC 11
hBC 12
hBC 13
hBC 14
hBC 15
hBC 16
hBC 17
hBC 18
hBC 20
hBC 21
hBC 22
hBC 23
hBC 24
hBC 25
hBC 26
hBC 27
hBC 29
hBC 30
hBC 32
hBC 33
hBC 34
hBC 35
hBC 36
hBC 37
hBC 39
hBC 40
hBC 42
hBC 43
hBC 44
hBC 45
hBC 46
hBC 47
hBC 49
hBC 50

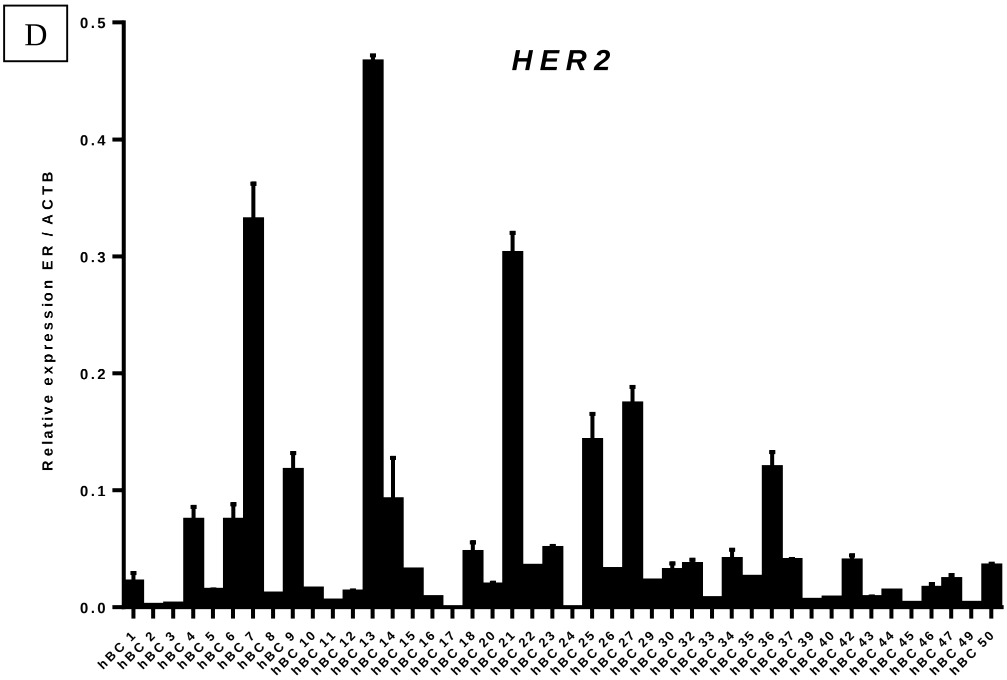

Figure 3.2 Testing the ER, PR and HER2 status of the first set of tumours.

A) IHC of representative samples. B) Quantitative RT-PCR for *ER* mRNA expression. C) Quantitative RT-PCR for *PR* mRNA expression. D) Quantitative RT-PCR for *HER2* mRNA expression. Data points represent the relative expression of the target gene, error bars represent the standard deviation of three technical replicates. Samples with a relative expression > 0.05 were considered positive.

Unfortunately, difficulties were encountered with the HER2 antibody, which failed to show the characteristic membrane staining pattern (Dr. Thomas, personal communication). In the clinical practice, the specimens with equivocal IHC results are usually analysed with FISH (Fluorescence In Situ Hybridisation) to detect gene amplification (Gown 2008); in this case, however, the poor quality of the samples precluded this option and the HER2 status was determined through RT-PCR (Figure 3.2D).

All the breast cancer samples were then analysed for *WT1* mRNA expression using the same assays described for the *in vitro* experiments (Figure 3.3A, B, C).

Variable levels of expression were detected within the tumour set and applying an arbitrary cut-off at 0.001, only 7 samples resulted positive for exon 7/8; similar results were obtained with the other two assays but, as shown in Table 3.2, some inconsistencies were observed: six samples expressed exon 1A and the truncated isoform starting from intron 5 but resulted negative for exon 7/8, which is unexpected, since both variants are known to include the Zinc-finger region comprised in exon 6/10 (Dallosso et al. 2004, Dechsukhum et al. 2000). This unusual result could be either due to false positive RT-PCR data or to the existence of C-terminal truncated isoforms which have not yet been documented in the literature.

Chi-squared tests were then performed to determine whether the expression of the different *WT1* isoforms associates with a specific status of the ER/PR and HER2 markers (Table 3.3): the analysis did not give statistically significant results, even when the tests were repeated without applying any cut-off (which raised the number of *WT1* positive samples to 23, data not shown).

To compare the expression levels of the different isoforms between healthy and neoplastic tissue, we analysed the sample of human adult mammary gland described in the previous chapter. The normal tissue, which consisted of a pool from 5 different healthy donors, expressed higher *WT1* levels than any of the tumour samples (Figure 3.3A), but lacked both exon 1A (Figure 3.3B) and intron 5 (Figure 3.3C) isoforms.

A

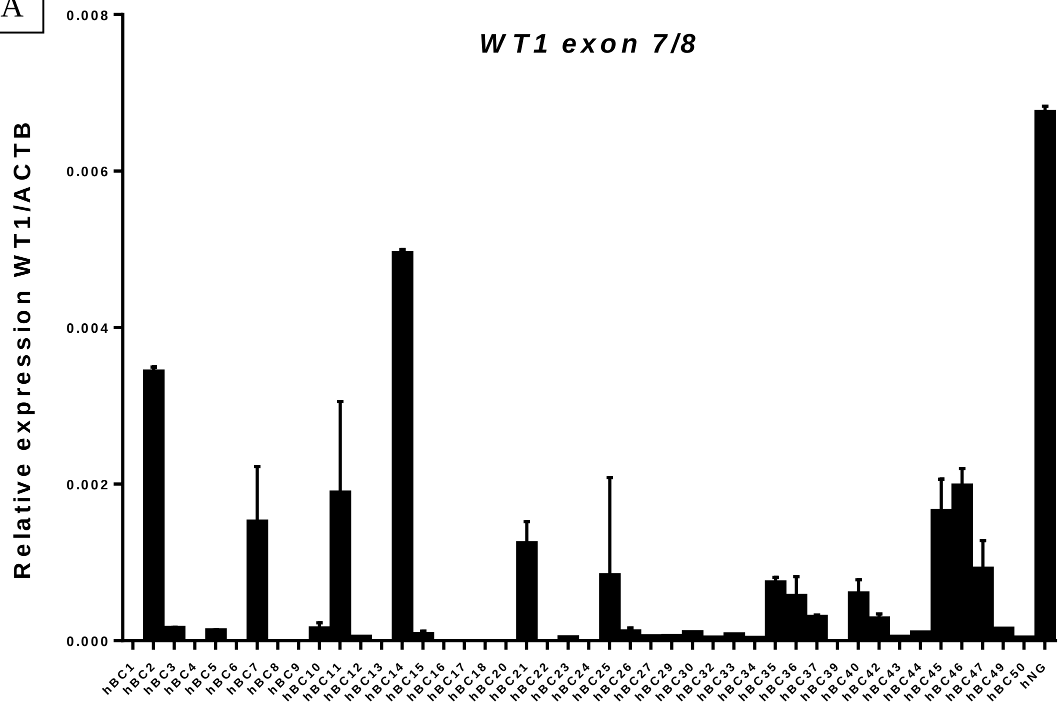
WT1 exon 7/8
Relative expression WT1/ACTB
0.008
0.006
0.004
0.002
0.000
hBC1 hBC2 hBC3 hBC4 hBC5 hBC6 hBC7 hBC8 hBC9 hBC10 hBC11 hBC12 hBC13 hBC14 hBC15 hBC16 hBC17 hBC18 hBC20 hBC21 hBC22 hBC23 hBC24 hBC25 hBC26 hBC27 hBC29 hBC30 hBC32 hBC33 hBC34 hBC35 hBC36 hBC37 hBC39 hBC40 hBC42 hBC43 hBC44 hBC45 hBC46 hBC47 hBC49 hBC50 hNG

B

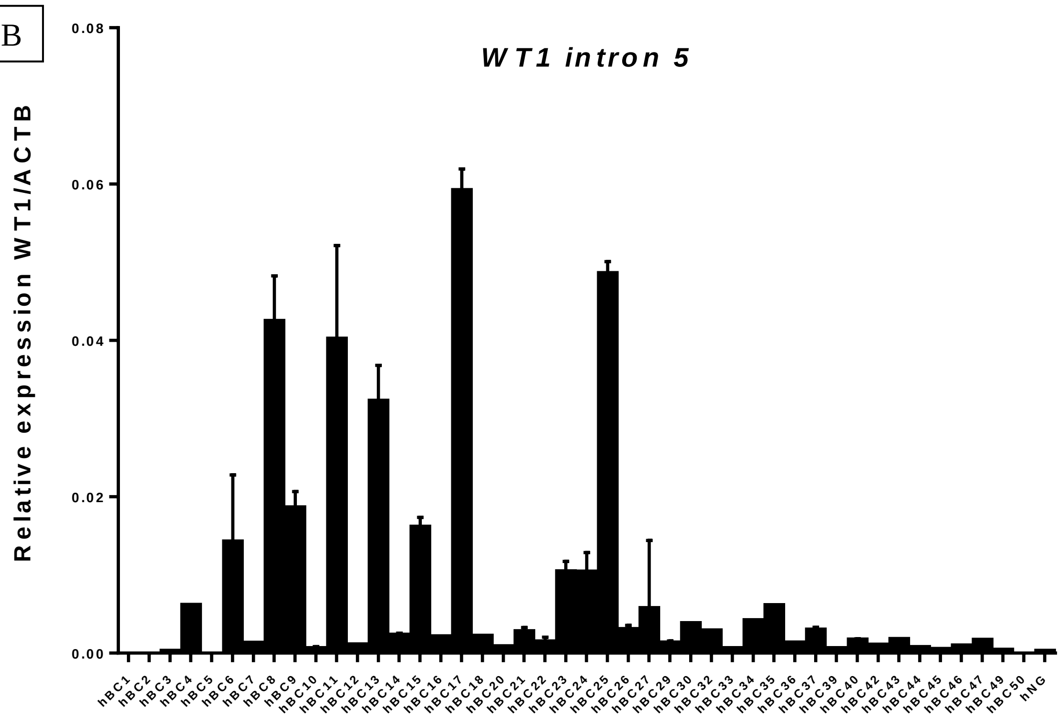
WT1 intron 5
Relative expression WT1/ACTB
0.08
0.06
0.04
0.02
0.00
hBC1 hBC2 hBC3 hBC4 hBC5 hBC6 hBC7 hBC8 hBC9 hBC10 hBC11 hBC12 hBC13 hBC14 hBC15 hBC16 hBC17 hBC18 hBC20 hBC21 hBC22 hBC23 hBC24 hBC25 hBC26 hBC27 hBC29 hBC30 hBC32 hBC33 hBC34 hBC35 hBC36 hBC37 hBC39 hBC40 hBC42 hBC43 hBC44 hBC45 hBC46 hBC47 hBC49 hBC50 hNG

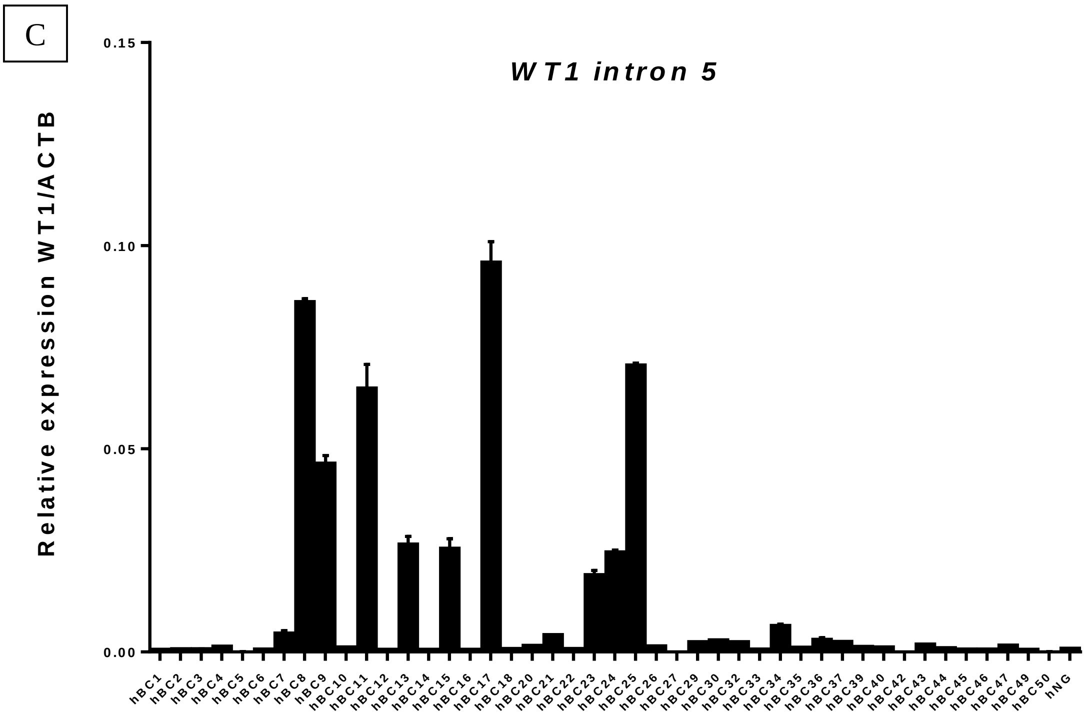

Figure 3.3 Assessing *WT1* expression in the first set of tumours.

A) Quantitative RT-PCR for *WT1* mRNA expression (exon 7/8); samples with a relative expression > 0.001 were considered positive. B) Quantitative RT-PCR for *WT1* mRNA expression (exon 1A); samples with a relative expression > 0.01 were considered positive. C) Quantitative RT-PCR for *WT1* mRNA expression (intron 5); samples with a relative expression > 0.02 were considered positive. Data points represent the relative expression of the respective isoform, error bars represent the standard deviation of three technical replicates.

Table 3.2 Summary of ER, PR, HER2 and WT1 expression in the first set of tumour samples.

hBC #	ER		PR		HER2		WT1		
	IHC	RT-PCR	IHC	RT-PCR	IHC	RT-PCR	ex7/8	ex1A	int5
1	red	red	green	green	-	red	red	red	red
2	red	red	red	red	-	red	green	red	red
3	red	red	red	red	-	red	red	red	red
4	green	green	red	red	-	green	red	red	red
5	red	red	red	red	-	red	red	red	red
6	green *	red *	red	red	-	green	red	red	red
7	red	red	red	red	-	green	red	red	red
8	red	red	red *	green *	-	red	red *	green *	green *
9	red	red	red *	green *	-	green	red *	green *	green *
10	green	green	green *	red *	-	red	red	red	red
11	red	red	red *	green *	-	red	green	green	green
12	red	red	red	red	-	red	red	red	red
13	red	red	red *	green *	-	green	red *	green *	green *
14	green *	red *	green *	red *	-	green	green	red	red
15	green	green	red	red	-	red	red *	green *	green *
16	green *	red *	green *	red *	-	red	red	red	red
17	green	green	red *	green *	-	red	red *	green *	green *
18	green	green	red	red	-	red	red	red	red
19	red	-	red	-	-	-	-	-	-
20	green	green	red	red	-	red	red	red	red
21	red	red	red	-	-	green	green	red	red
22	red	red	green *	red *	-	red	red	red	red
23	red	red	red	red	-	red	red *	green *	green *
24	green *	red *	green	green	-	red	red *	green *	green *
25	red	red	red	red	-	green	green	red	green
26	red	red	red	red	-	red	red	red	red
27	green *	red *	red	red	-	green	red	red	red
28	red	-	red	-	-	-	-	-	-
29	red	red	red	red	-	red	red	red	red
30	green	green	red	red	-	red	red	red	red
31	red	-	red	-	-	-	-	-	-
32	green	green	green	green	-	red	red	red	red
33	red	red	red	red	-	red	red	red	red
34	red	red	red	red	-	red	red	red	red
35	green *	red *	red	red	-	red	red	red	red
36	red	red	red	red	-	green	red	red	red
37	red	red	red	red	-	red	red	red	red
38	green	-	red	-	-	-	-	-	-
39	green	green	red	red	-	red	red	red	red
40	green	green	red	red	-	red	red	red	red
41	red	-	red	-	-	-	-	-	-
42	red	red	red	red	-	red	red	red	red
43	red	red	red	red	-	red	red	red	red
44	green *	red *	green *	red *	-	red	red	red	red
45	green *	red *	red	red	-	red	green	red	red
46	red	red	red	red	-	red	green	red	red
47	green *	red *	green *	red *	-	red	red	red	red
48	red	-	red	-	-	-	-	-	-
49	red	red	red	red	-	red	red	red	red
50	green	green	green *	red *	-	red	red	red	red

Abbreviations and symbols: IHC, immunohistochemistry; RT-PCR, Real-Time Polymerase Chain Reaction; -, data not available; green, positive; red, negative. The inconsistencies between RT-PCR/IHC data and among the WT1 isoforms are emphasised with asterisks.

Table 3.3 Chi-square tests performed on the distribution of the *WT1* isoforms in the first set of tumour samples.

	Exon 7/8	**Exon 1A**	**Intron 5**
ER/PR status	p value = 0.977	p value = 0.992	p value = 0.986
HER2 overexpression	p value = 0.629	p value = 0.961	p value = 0.800

3.3.2 Second set of tumour samples

The second set of breast cancer samples was obtained from the Tissue Bank and consisted of 60 ductal carcinomas NST of known grade, ER and HER2 status.

So far, WT1 immunofluorescence has been performed on half of the specimens by Dr. McGregor, who has also scored the number of WT1 positive cells for each tumour by counting the stained cells in five different regions of the slide, each one covering an area of 200 μm^2.

All the samples showed some degree of staining, therefore, I grouped them according to their grade, ER and HER status and then plotted the average number of WT1 positive cells for each group (Figure 3.4).

A one-way Anova conducted to compare the average number of WT1-expressing cells in grade 1, grade 2 and grade 3 tumours revealed no statistically significant difference among the groups (Figure 3.4A, p value of 0.161); similar results were obtained for the ER and HER2 markers (Figure 3.4B and C, p value of 0.075 and 0.194 respectively), even though the analysis cannot be considered conclusive due to the limited numbers of ER negative (n=3) and HER2 positive (n=5) tumours taken into consideration.

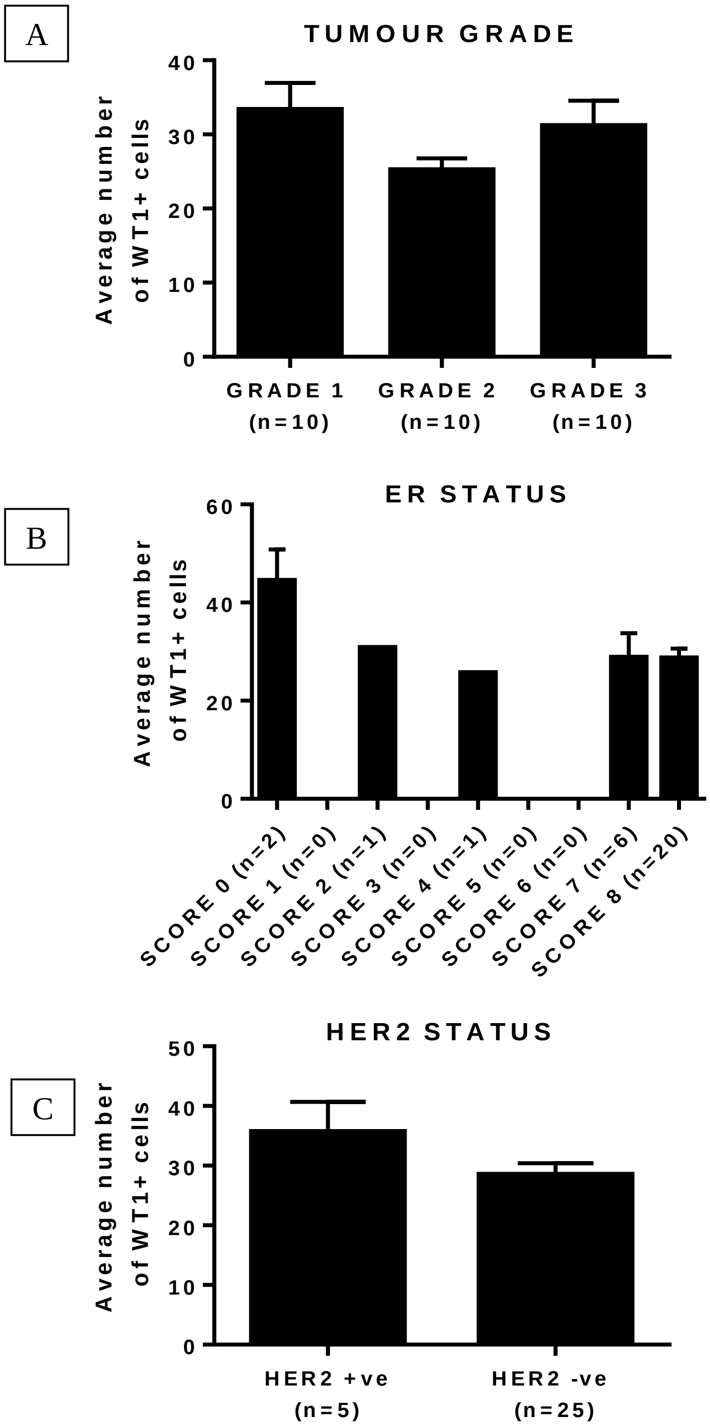

Figure 3.4 *WT1* expression in the second set of human breast cancer samples.

WT1 immunofluorescence was performed on 30 tumours, the number of WT1 positive cells was calculated by counting the stained cells in five different regions of the slide, each one covering an area of 200 μm^2. The average number of WT1 positive cells was plotted against the tumour grade (A), the Allred score for the ER status (B) and the HER2 status (C). Error bars = +/- SEM. No statistically significant difference was observed among the groups.

3.4 *In silico* analysis of *WT1* gene expression in published breast cancer datasets

Publicly available gene expression data were analysed by our collaborator Dr. Sims in order to complement the *in vitro* and *in vivo* work described in the previous paragraphs and overcome their sample size limitations.

WT1 expression was first assessed in three microarray datasets (E-TABM-194, GSE10890, GSE12777), each representing a panel of breast cancer cell lines analysed on traditional 3’ Affymetrix GeneChips, with probes targeting the 3’ end of the mRNA sequence (Git et al. 2008, Hoeflich et al. 2009, Stinson et al. 2011). *WT1* was detected in 40 out of the 173 lines (Figure 3.5A) and, as observed in the *in vitro* experiments, the expression level was not significantly associated with the luminal, basal or claudin-low cell line subtypes (Mann-Whitney U test $p>0.05$) (Figure 3.5B).

Given the extraordinary complexity of the *WT1* locus, we also analysed a dataset representing a panel of 41 breast cancer cell lines using Affymetrix exon GeneChips (GSE16732, Riaz et al. 2009). Exon microarrays are designed with up to four probes targeting each exonic region and therefore can provide more information on alternative splicing and isoform variation.

The exon array data resulted in agreement with my RT-PCR experiments, showing high levels of *WT1* expression for ZR75, MDA-MB-157, HS578T and T47D cell lines (Figure 3.5C); moreover, *WT1* expression in MDA-MB-231 cells seemed to be restricted to exons 6 to 10, which supports the hypothesis that this cell line may only express the truncated intron 5 isoform.

In parallel, *WT1* expression was analysed in 17 datasets of primary human breast cancer (Moleirinho, Chang et al. 2013) (Figure 3.6A): the transcript could only be reliably detected in 11% of the tumours (329 out of the total 2999) and showed the highest expression levels in the luminal and HER2 amplified subtypes (Figure 3.6B). Furthermore, amongst the samples in which it was detected, *WT1* expression was significantly higher in ER-positive than in ER-negative tumours (Figure 3.6C, p value of 1e-5).

Since *WT1* is a known regulator of the epithelial/mesenchymal balance during development and may play a similar role in cancer, we went on to assess whether *WT1* expression was associated with EMT-related transcripts (*CDH1*, *CDH3*, *SNAI1*, *SNAI2*, *VIM*, *TWIST1*, *CLDN7*) (Figure 3.6A). Statistically significant differences were only observed for the mesenchymal markers *VIM* and *SNAI1* (p value of 0.001 and 0.05 respectively); both genes showed higher expression in the *WT1*-negative samples (Figure 3.7), suggesting that the lack of WT1 may be associated to a more mesenchymal phenotype.

Next, significance analysis of microarray (SAM) was performed in order to identify differentially expressed genes between *WT1*-high and *WT1*-low breast tumours.

Out of 500 modulated transcripts (listed in appendix A), only 5 showed a negative correlation with *WT1* expression, being up-regulated in the *WT1*-low tumours and down-regulated in the *WT1*-high; this group includes one gene involved in Fas-mediated apoptosis (*MUDENG*) and two regulators of vescicular trafficking (*STX4, VPS37B*) (Bennett, Garcia-Arraras et al. 1993, Stuchell, Garrus et al. 2004, Lee, Shin et al. 2008).

The rest of the modulated genes correlated with *WT1* expression, displaying up-regulation in the *WT1*-high tumours and down-regulation in the *WT1*-low. The differentially expressed transcripts include several enzymes of the cytochrome P450 as well as different types of metalloproteases (both MMPs and members of the ADAM gene family).

Gene Ontology analysis revealed that the GO terms significantly enriched in this group ranged from neuroactive ligand-receptor interaction to calcium signalling pathway. Drug and xenobiotics metabolisms were also observed, along with unexpected terms related to heart conditions such as dilated and hypertrophic cardiomyopathy (Table 3.4).

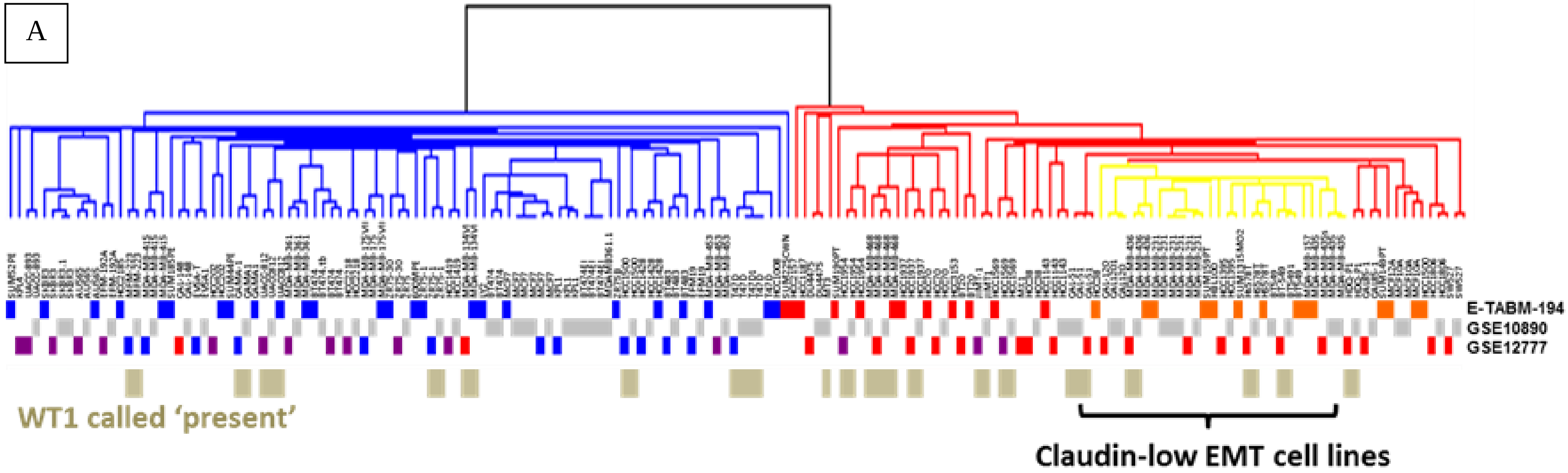
A
E-TABM-194
GSE10890
GSE12777
WT1 called ‘present’
Claudin-low EMT cell lines

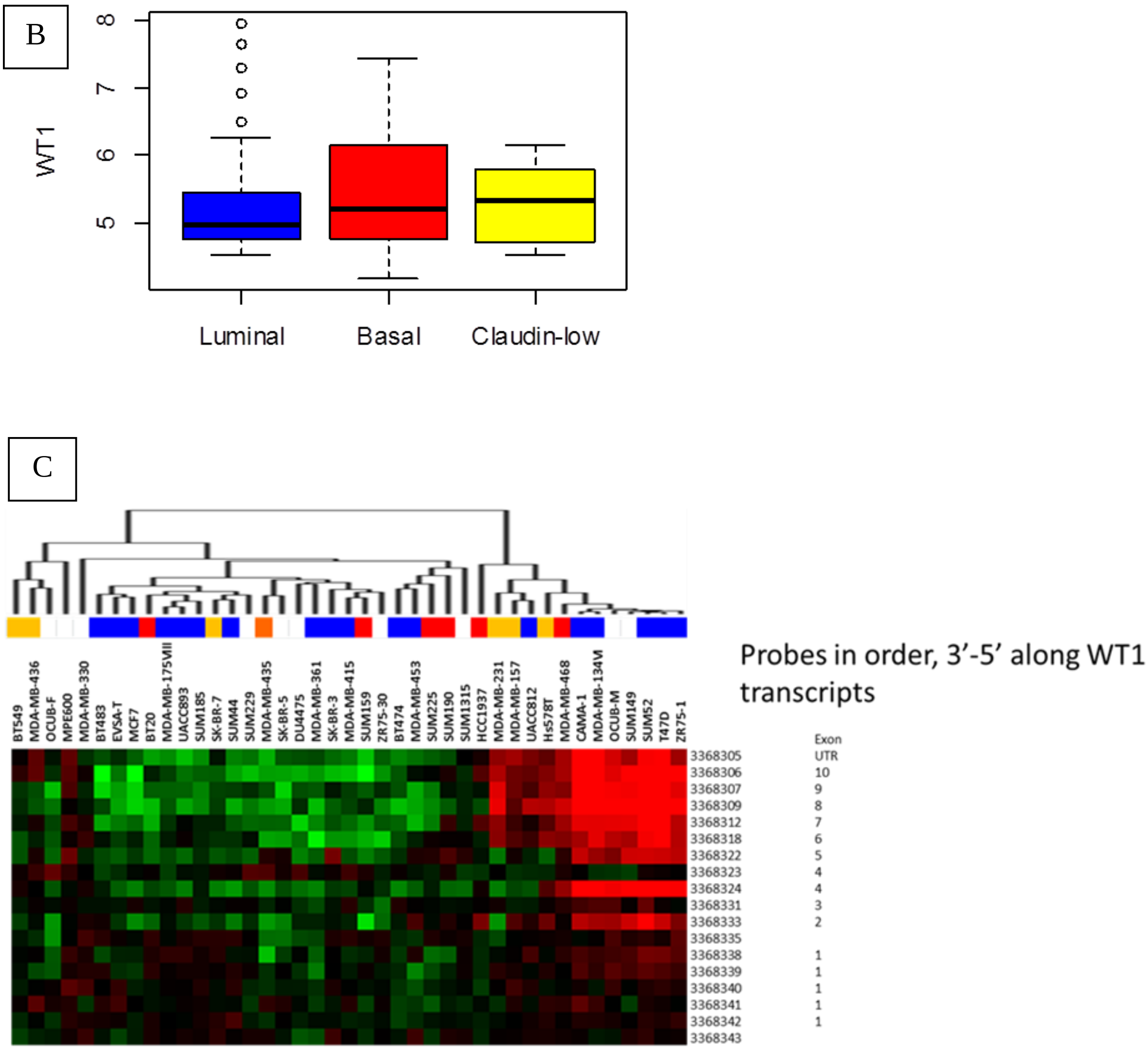

Figure 3.5 *WT1* transcript expression in published breast cancer cell line datasets.

A) Gene expression analysis data from 3 combined microarray datasets (E-TABM-194, GSE10890, GSE12777, n = 173 cell lines). The bars under each cell line indicate their original dataset, shown on the right. The hierarchical clustering resulted from the 500 most variable genes, demonstrating that the same cell lines from different studies cluster together after batch correction. B) Boxplot of *WT1* expression in the different subtypes of breast cancer cell lines represented in the 3 datasets, log2 expression values. C) Heatmap visualization of the relative expression of probes representing each *WT1* exon across a panel of breast cancer cell lines in a published dataset (GSE16732). The different colours indicate the cell line subtype (red = basal, orange = basal B / mesenchymal, purple = HER2 amplified, blue = luminal, yellow = claudin-low). (The bioinformatics analysis represented in this figure was entirely conducted by Dr. Sims.)

A

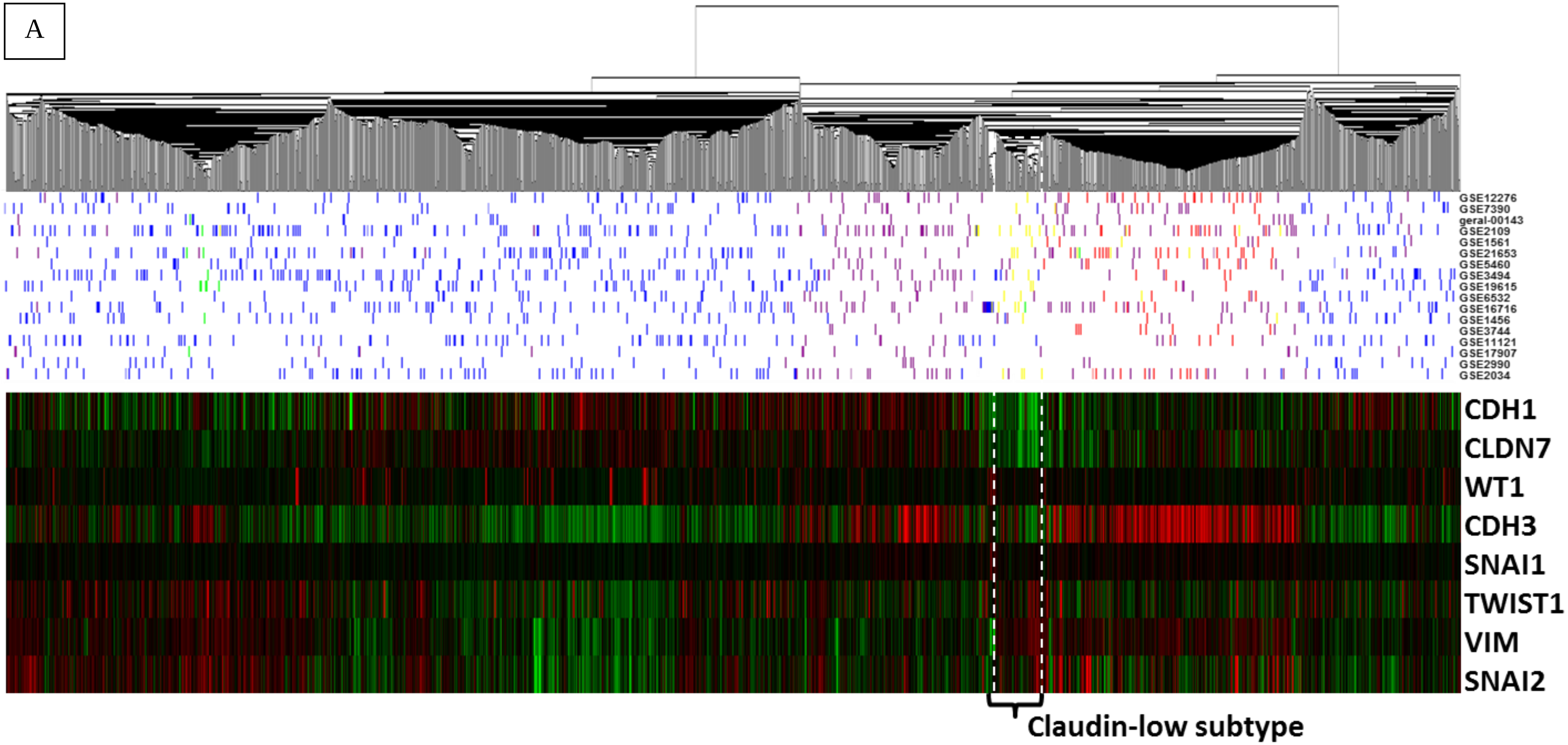
GSE12276
GSE7390
geral-00143
GSE2109
GSE1561
GSE21653
GSE5460
GSE3494
GSE19615
GSE6532
GSE16716
GSE1456
GSE3744
GSE11121
GSE17907
GSE2990
GSE2034
CDH1
CLDN7
WT1
CDH3
SNAI1
TWIST1
VIM
SNAI2
Claudin-low subtype

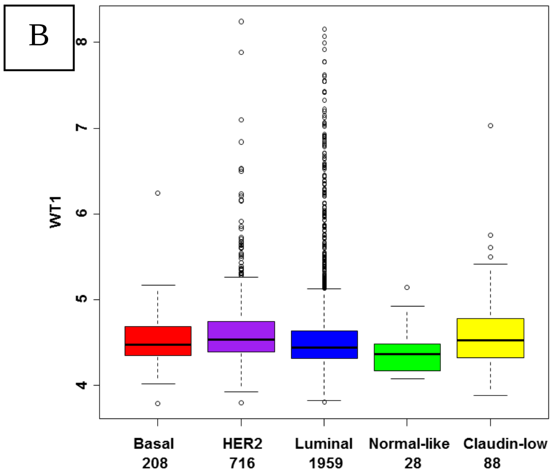

Mann-Whitney 2 independent sample	p-val
Basal v HER2	**0.004**
Basal v Luminal	0.077
Basal v Claudin-low	0.45
Basal v Normal-like	**0.003**
HER2 v Luminal	**<0.001**
HER2 v Claudin-low	0.332
HER2 v Normal-like	**<0.001**
Luminal v Claudin-low	0.081
Luminal v Normal-like	**0.017**
Claudin-low v Normal-like	**0.005**

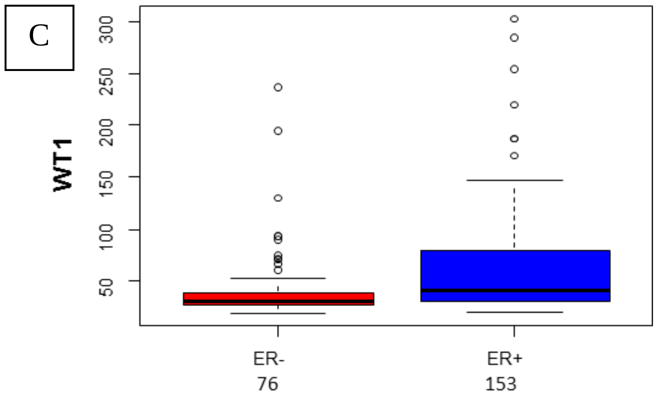

Figure 3.6 Expression of *WT1* and markers of EMT in human primary breast cancer datasets. A) Gene expression analysis data from 17 integrated datasets (n = 2999 tumors). The bars under each tumour sample indicate their original dataset, shown on the right. B) Boxplot of *WT1* expression in the different subtypes and corresponding Mann-Whitney U tests with the significant p-values highlighted in bold, y-axis is log2 values. C) Boxplot of *WT1* expression in ER-positive and ER-negative tumours designated by IHC of ERalpha amongst those tumours with detectable expression of *WT1*. The different colours in A) and B) indicate the tumour subtype (red = basal, purple = HER2 amplified, blue = luminal, green = normal-like, yellow = claudin-low). (The bioinformatics analysis represented in this figure was entirely conducted by Dr. Sims.)

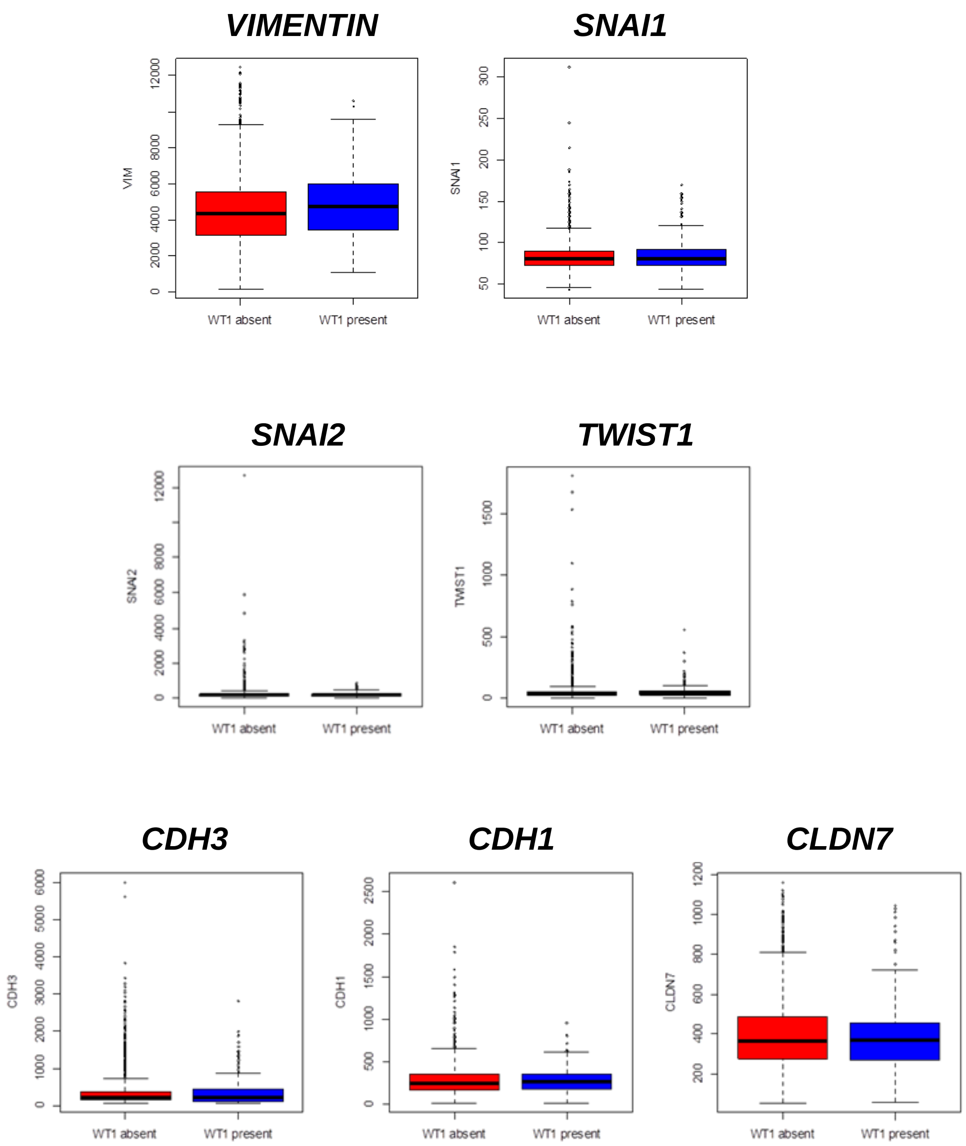

Figure 3.7 Expression of EMT-associated genes in *WT1*-positive vs negative tumours.
Statistically significant differences were observed only for *VIM* and *SNAI1*, which showed higher expression in the *WT1*-negative samples. (The bioinformatics analysis represented in this figure was entirely conducted by Dr. Sims.)

Table 3.4 GO terms from SAM analysis of *WT1*-high vs *WT1*-low tumours.

Term	**p-value**	**Genes**
Neuroactive ligand-receptor interaction	3E-11	MCHR1, TACR3, THRB, GABRB2, TACR2, DRD2, GRIK3, OPRK1, DRD5, TRHR, TSHB, HTR1B, HTR1A, P2RY4, GALR3, CNR2, MC5R, TAAR5, PRL, TAAR2, HTR1F, HTR1E, GABRD, HTR4, GRIN2A, GABRR2, CHRM5, P2RX6, P2RX1, CHRM2, AVPR1B, P2RX2, MC2R, GRM6, MC4R
Calcium signaling pathway	8E-5	ADCY2, SLC8A2, TACR3, TACR2, PHKG1, DRD5, TRHR, GRIN2A, CHP2, HTR4, CHRM5, P2RX6, P2RX1, CHRM2, AVPR1B, P2RX2, CAMK2B, CACNA1F, CAMK2A
Linoleic acid metabolism	4E-04	CYP3A4, CYP2C19, CYP2C18, CYP2C9, PLA2G6, CYP1A2, PLA2G2E
Retinol metabolism	0.003	CYP3A4, CYP4A11, CYP4A22, CYP2C19, CYP2C18, CYP2C9, CYP2A7, CYP1A2
Arachidonic acid metabolism	0.004	CYP4A11, CYP4A22, CYP2C19, CYP2C18, CYP2C9, PLA2G6, CYP4F2, PLA2G2E
Dilated cardiomyopathy	0.006	ADCY2, MYL3, MYBPC3, CACNB1, CACNG3, CACNG2, ITGB3, CACNB4, CACNA1F, CACNG1
Hypertrophic cardiomyopathy	0.013	MYL3, MYBPC3, CACNB1, CACNG3, CACNG2, ITGB3, CACNB4, CACNA1F, CACNG1
Arrhythmogenic right ventricular cardiomyopathy	0.022	CACNB1, CACNG3, CACNG2, ITGB3, CACNB4, CACNA1F, CACNG1, CTNNA3
Cardiac muscle contraction	0.025	MYL3, ATP1B2, CACNB1, CACNG3, CACNG2, CACNB4, CACNA1F, CACNG1
Caffeine metabolism	0.025	XDH, CYP2A7, CYP1A2
Drug metabolism	0.026	CYP3A4, GSTA3, CYP2C19, CYP2C18, CYP2C9, CYP2A7, CYP1A2
Metabolism of xenobiotics by cytochrome P450	0.070	CYP3A4, GSTA3, CYP2C19, CYP2C18, CYP2C9, CYP1A2
Melanogenesis	0.074	DCT, FZD9, WNT10B, ADCY2, CAMK2B, ASIP, CAMK2A, WNT8B

3.4 Discussion

Our multi-approach analysis showed that *WT1* expression in breast cancer occurs at low frequency (≤ 20%), which is in agreement with some of the earlier studies on the topic (Silberstein et al. 1997, Cheng et al. 2001).

The only inconsistency in our data is represented by the second set of human breast cancer samples, which all stained positive for WT1; since this result could be due to IF artefacts, I am currently in the process of obtaining matched tissue samples on which to perform RT-PCR.

Overall, *WT1* did not show particularly high expression, either *in vivo* or *in vitro*; moreover, the mRNA levels observed in the tumour samples were lower than in the healthy mammary gland. This finding is in keeping with what described by Silberstein, who reported reduced WT1 staining in breast cancer specimens (Silberstein et al. 1997).

In terms of isoform expression pattern, this work led to several results: firstly, all our data corroborate the hypothesis that the truncated transcript starting from intron 5 is a tumour-specific isoform; this short *WT1* variant was first detected in the blood of patients affected by acute leukaemia, then in breast and pancreatic cancer cell lines (Bae et al. 1994, Dechsukhum et al. 2000, Artibani 2010) and we have now shown that it is expressed in human breast cancer biopsies but is absent in the healthy mammary gland.

Secondly, both our *in vitro* and *in silico* experiments seem to demonstrate that the truncated intron 5 is the only *WT1* isoform expressed in MDA-MB-231 cells; if confirmed, any assay targeted against exon 1/5 would give a negative result, which may explain why the reports on *WT1* expression in this cell line are so contradictory (Laux et al. 1999, Oji et al. 1999, Loeb et al. 2001, Zapata-Benavides et al. 2002, Tuna, Chavez-Reyes et al. 2005, Caldon et al. 2008).

Lastly, exon 1A has been detected in few human breast cancer samples and in only one cell line, suggesting that this isoform is unlikely to play any crucial role in breast tumorigenesis.

One of the main goals of this study was to assess whether WT1 is associated with any specific histological or molecular subtype of breast cancer. In this regard, the *in vivo* experiments were inconclusive due to their limited sample size, but the bioinformatics analysis revealed that *WT1* expression correlates with luminal and ER-positive breast cancer.

This finding is in stark contrast with what reported by the only paper published on the subject (Qi et al. 2012), which claims that WT1 is associated with basal and ER-negative tumours. The discrepancy is likely to be caused by the different size of the studies: our analysis was performed on 17 datasets of primary human breast cancer and included also the single dataset used by Qi, which makes the results of this study more robust.

The finding that *WT1* expression is higher in ER-positive tumours is particularly interesting, given that WT1 has been shown to both interact with ERα (Reizner et al. 2005) and modulate its expression *in vitro* (Kang et al. 2011, Han et al. 2008).

The bioinformatics analysis also determined that *WT1*-negative tumours show higher levels of mesenchymal markers than the *WT1*-positive; this observation would suggest that WT1 does not play a pro-EMT role in breast cancer cells, but, on the contrary, its expression is associated with a more epithelial phenotype.

Finally, SAM analysis revealed that the tumours expressing high levels of *WT1* show an up-regulation of several genes belonging to the cytochrome P450 family (CYP).

These oxidizing enzymes play an important and complex role in the metabolism of anti-cancer agents: they participate to the biological activation of many pro-drugs but also to the inactivation of some cytotoxic compounds, two processes that occur predominantly, but not exclusively, in the liver (McFadyen, Melvin et al. 2004). Not surprisingly, polymorphisms and different expression levels of the CYP genes have been shown to influence the outcome of chemotherapeutic treatments (reviewed in Rodriguez-Antona and Ingelman-Sundberg 2006, Seredina, Goreva et al. 2012).

The substrates of one of these up-regulated genes, *CYP3A4*, include drugs routinely used in the management of breast cancer such as tamoxifen, docetaxel, paclixatel, cyclophosphamide and doxorubicin (reviewed in Rodriguez-Antona and Ingelman-Sundberg 2006).

More specifically, CYP3A4 activity in the liver is responsible for the activation of tamoxifen and cyclophosphamide (Crewe, Ellis et al. 1997, Roy, Yu et al. 1999), whereas it transforms docetaxel into inactive hydroxylated derivatives (Engels, Ten Tije et al. 2004); interestingly, high *CYP3A4* levels in breast cancer biopsies can predict a poor therapeutic response to docetaxel, which suggests that also the enzyme within the tumour is involved in the inactivation of this drug (Miyoshi, Ando et al. 2002, Miyoshi, Taguchi et al. 2005).

The association between high *WT1* and *CYP3A4* expression in breast cancer seems intriguing, especially considering the potential repercussions at the clinical level. However, since the *WT1* literature lacks studies on patients treated with docetaxel, any correlation between *WT1* expression and the therapeutic response to this drug remains speculative; further research is needed to investigate whether this association has any molecular basis and if the tumour levels of *WT1* can be used to predict the response of breast cancer patients to docetaxel.

Chapter 4: Studying the effects of *WT1* loss in human breast cancer cell lines

4.1 Introduction

Several studies have tried to determine the role played by WT1 in breast cancer, however, at the current state of research, no conclusive evidence has been provided. Even though high WT1 expression has been shown to predict poor prognosis in breast cancer patients (Miyoshi et al. 2002), WT1 is still at the centre of a debate over potential oncogenic or tumour suppressing functions (as described in detail in chapter 1.4).

In order to avoid any redundancy, this section will only recapitulate what is necessary to contextualise the *in vitro* experiments described in the next paragraphs.

The first, and so far only, *WT1* knockdown in human breast cancer cell lines dates back to 2002, when Zapata-Benavides and colleagues down-regulated *WT1* expression using liposome-incorporated antisense oligonucleotides targeting the translation initiation site in exon 1 (Zapata-Benavides et al. 2002). After a 72-hour incubation, the knockdown cells exhibited significant growth inhibition and cyclin D1 protein level reduction, which suggests that *WT1* is important for the proliferation of breast cancer cells.

Diametrically opposite findings have been reported by the Wang group and describe WT1 as a potent tumour suppressor: in their studies, a *WT1* expression vector containing the –Exon 5/-KTS isoform was transfected in MDA-MB-231 and MCF10A-T3B cells, resulting in suppression of clonal growth in soft agar assays and inhibition of tumour formation in nude mice (Zhang et al. 2003, Wang & Wang 2008).

Particularly significant was the discovery that ectopic expression of different *WT1* isoforms has opposite effects on mammary cells (Burwell et al. 2007). While the +Exon 5/+KTS variant was shown to display oncogenic features such as induction of

EMT and redistribution of CDH1, the –Exon 5/-KTS isoform decreased proliferation by causing a cell cycle arrest in G2 and up-regulating p21.

This study unveiled the mechanism behind the tumour suppressing activity reported by Wang, but the knockdown phenotype observed by Zapata-Benavides remains unexplained: given the structure of the *WT1* locus, in fact, the targeting of exon 1 should result in the equal degradation of both +Exon 5/+KTS and –Exon 5/-KTS isoforms.

Clearly, further research is needed to achieve a complete understanding of the role played by WT1 in breast cancer and, in particular, to comprehend why *WT1* expression correlates with poor survival.

As mentioned in chapter 1.2.3.4, the main hypotheses are related to a potential role of WT1 in angiogenesis, proliferation/apoptosis and EMT/CSCs; while studying blood vessel formation requires an *in vivo* approach, the other two theories can be tested with *in vitro* techniques, as shown in the next paragraphs.

4.1.1 Aim

The aims of the experiments described in this chapter were:

• to develop lentiviral RNAi constructs targeting the zinc finger region of *WT1* (and therefore all its known different isoforms)

• to transduce these constructs in human breast cancer cell lines and achieve stable *WT1* knock-down

• to analyse the consequences of *WT1* loss, paying particular attention to any change in the epithelial/mesenchymal balance.

4.1.2 Experimental approach

An RNAi based gene knockdown strategy was used to investigate the functional role of *WT1* in breast cancer cell lines. Unlike previous studies based on transient transfections, we aimed to achieve stable *WT1* knockdown, which is essential to investigate the long-term effects of *WT1* loss.

To this end, shRNAs targeting the zinc-finger region of the *WT1* transcript were cloned into commercially available lentiviral constructs, creating both a constitutive and an inducible version.

4.2 Cloning RNAi lentiviral vectors for the constitutive and inducible knockdown of *WT1*

The lentiviral RNAi vectors pGIPZ and pTRIPZ were purchased from Thermo Scientific Open Biosystems and used as backbones for the cloning of shRNAs targeting the human *WT1* transcript.

While pGIPZ (Figure 3.1) is constitutively expressed, pTRIPZ (Figure 3.2) is engineered for Tet-controlled expression, so that the shRNA is produced only in the presence of doxycycline.

In previous transient knockdown experiments, the pcDNA6.2-GW/EmGFP-miR vector (Invitrogen, Figure 4.3) had been successfully used to express miRNAs against *WT1* and a reliable miR-lacZ control (Peter Hohenstein, personal communication). Since this pcDNA construct is Gateway-compatible, the already validated shRNA sequences could be cloned into the lentiviral vectors through easy recombination steps using the Gateway Technology.

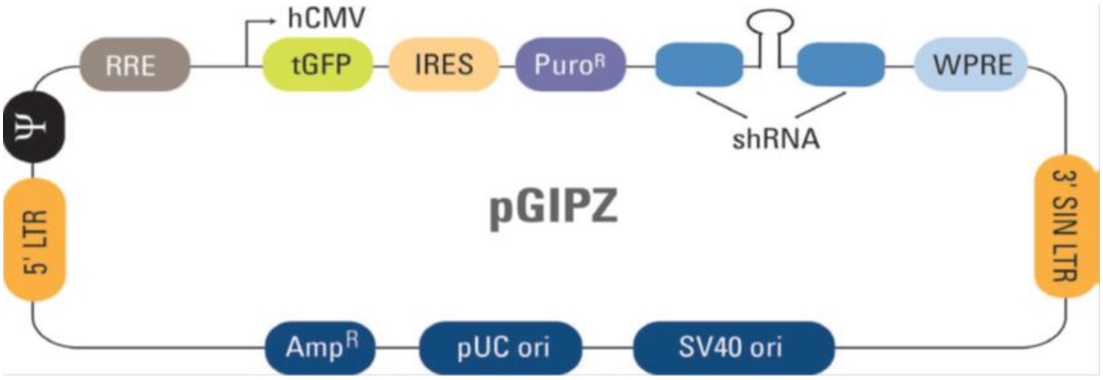

Figure 4.1 Schematic of the pGIPZ lentiviral shRNA vector.

RRE - Rev response element to enhance titer; hCMV - Human cytomegalovirus promoter to drive strong transgene expression; tGFP - TurboGFP reporter for visual tracking of transduction and expression; IRES - Internal ribosomal entry site to allow the expression in a single transcript of TurboGFP and puromycin resistance genes; Puro - Puromycin resistance; shRNA – small hairpin RNA for gene knockdown; WPRE - Woodchuck hepatitis post-transcriptional regulatory element to enhance transgene expression in the target cells; 3' SIN LTR - 3' self-inactivating long terminal repeat to increase lentivirus safety; 5' LTR - 5' long terminal repeat (adapted from the Open Biosystem technical manual).

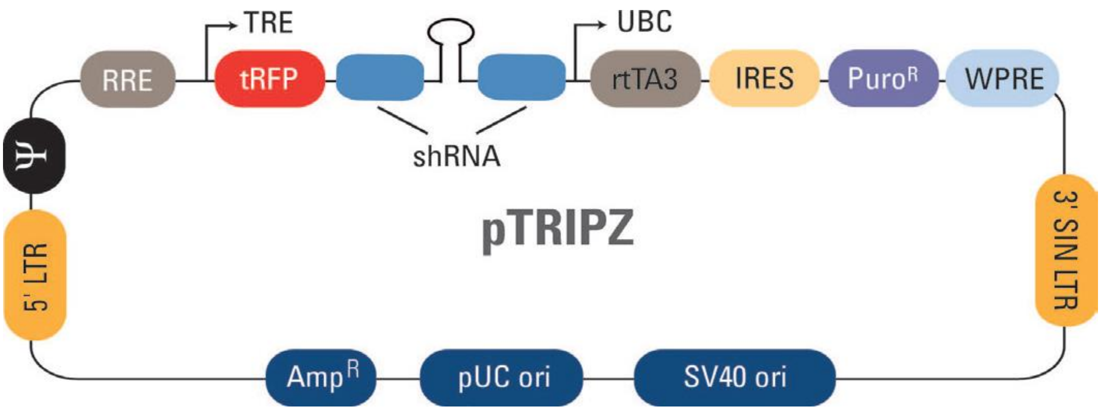

Figure 4.2 Schematic of the pTRIPZ lentiviral shRNA vector.

RRE - Rev response element; IRES - Internal ribosomal entry site to allow the expression in a single transcript of rtTA3 and puromycin resistance genes; Puro - Puromycin resistance; shRNA – small hairpin RNA; WPRE - Woodchuck hepatitis post-transcriptional regulatory element; 3' SIN LTR - 3' self-inactivating long terminal repeat; 5' LTR - 5' long terminal repeat; TRE - Tetracycline-inducible promoter; tRFP - TurboRFP reporter for visual tracking of transduction and shRNA expression; UBC - Human ubiquitin C promoter to constitutively express rtTA3 and puromycin resistance genes; rtTA3 - Reverse tetracycline-transactivator 3 for tetracycline-dependent induction of the TRE promoter (adapted from the Open Biosystem technical manual).

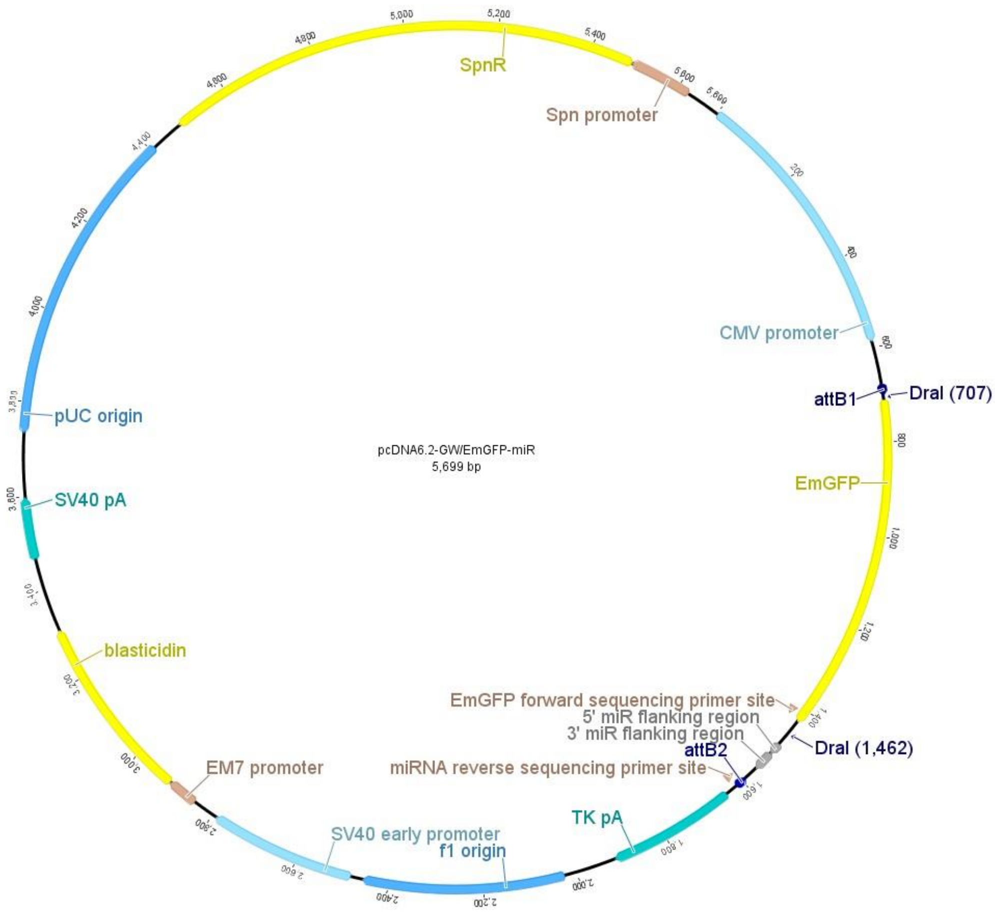

Figure 4.3 Map of the pcDNA6.2-GW/EmGFP-miR vector.

4.2.1 Gateway cloning

The Gateway cloning system provides a rapid and efficient way to transfer DNA fragments by taking advantage of the site-specific recombination properties of bacteriophage lambda (Hartley, Temple et al. 2000).

After infecting E. coli cells, the phage can use the lysogenic pathway to integrate its DNA into the genome of the host (Figure 4.4); in response to certain stimuli, the viral DNA can excise itself from the bacterial chromosome and start a lytic cycle, during which new virions are assembled and then released upon lysis of the host cell.

As shown in Figure 4.4, lambda recombination relies on the activity of several enzymes that bind to specific attachment (*att*) sequences; however, the combination of proteins and *att* sites used in the lysogenic pathway (Int, IHF, attB, attP) is different from that of the lytic pathway (Int, Xis, IHF, attL, attR).

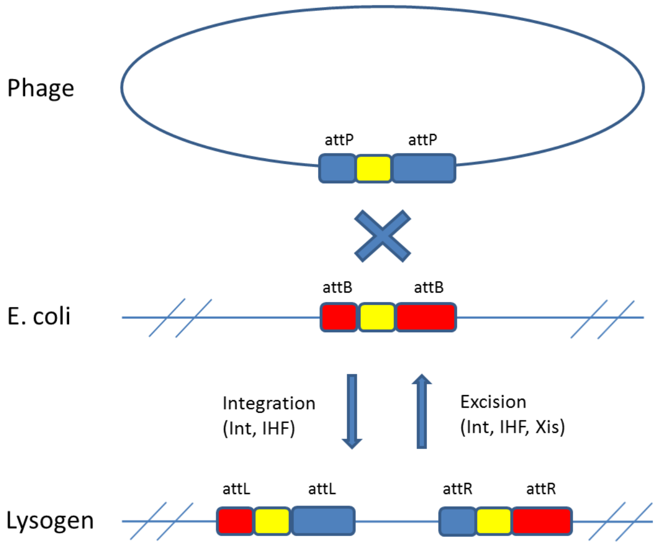

Figure 4.4 The recombination of bacteriophage lambda in E. coli.

The components of this natural system have been adapted by Invitrogen to create the Gateway multisite cloning technology.

The Gateway cloning exploits this natural system to carry out the *in vitro* recombination between attB and attP sites (called BP reaction) and between attL and attR (LR reaction), which can be controlled by providing the necessary combination of enzymes and attachment sequences.

This technology was used to clone the miRNA sequences into the lentiviral vectors in three easy steps (Figure 4.5, see Appendix B for the maps of the constructs created at each step):

1) generation of the new entry clones

2) generation of the destination vectors

3) generation of the expression clones

STEP 1: generating the entry clones

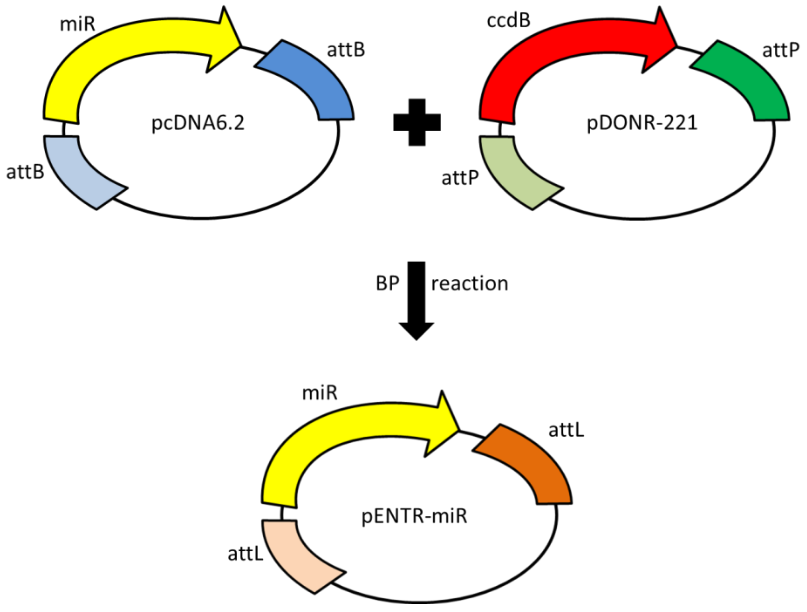

STEP 2: generating the destination vectors

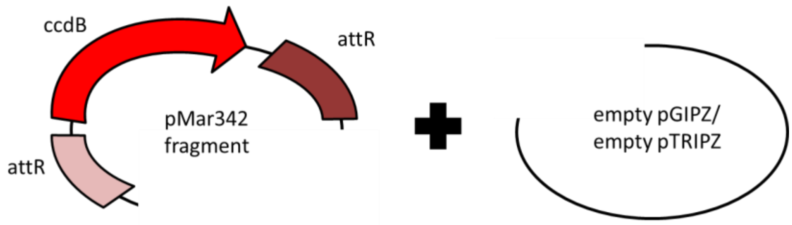

STEP 3: generating the expression clones

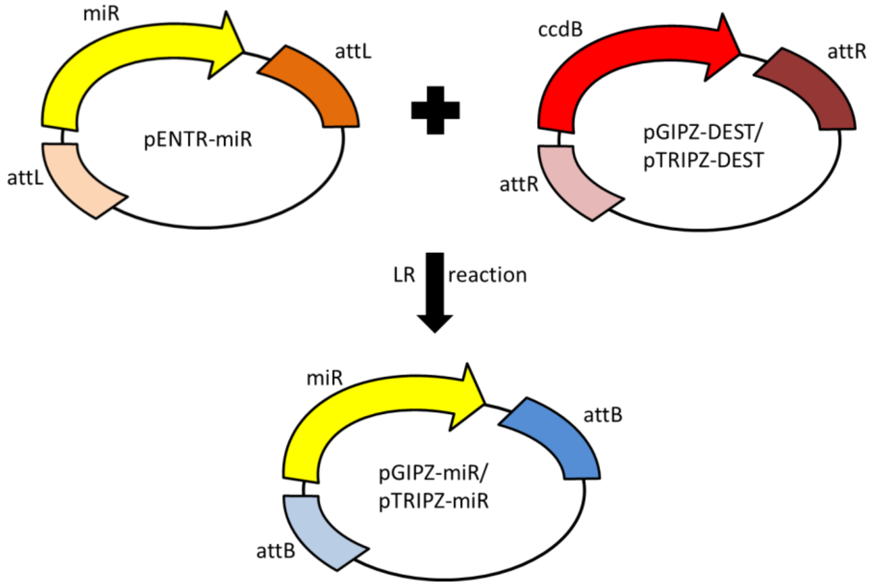

Figure 4.5 Schematic illustrating the steps to generate the pGIPZ-mir and pTRIPZ-mir constructs.

4.2.1.1 Step 1: generating the entry clones

Since the lentiviral vectors already express a fluorescent reporter to identify infected cells (TurboGFP in pGIPZ, TurboRFP in pTRIPZ), all the pcDNA6.2-GW/EmGFP-miR vectors (lacZ control, WT1 knockdown constructs 1407 and 1490) were digested with *DraI* and religated for the removal of their GFP cassette. Following ligation and transformation in DH5α Library Efficient bacteria, a second *DraI* digest was used to confirm the excision of the GFP cassette (data not shown).

A BP reaction was then performed between the resulting vectors and pDONR-221, in order to generate the entry clones (designated pENTR-miR); the reaction mixture was used to transform DH5α Library Efficient bacteria and the correct clones were identified based on the *NruI/BamHI* digest (Figure 4.6).

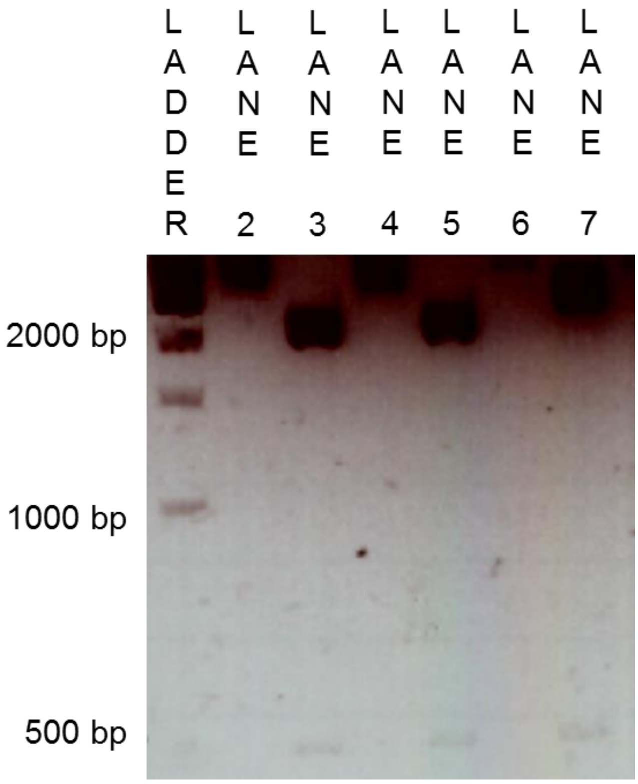

Figure 4.6 Gel image showing the NruI/BamHI digest for the three pENTR-miR vectors.
All the clones were correct, showing a band at 1946 bp and one at 409 bp (lane 1: 1 kb DNA ladder; lane 2: uncut WT1 1407; lane 3: cut WT1 1407; lane 4: uncut WT1 1490; lane 5: cut WT1 1490; lane 6: uncut lacZ; lane 7: cut lacZ).

4.2.1.2 Step 2: generating the destination vectors

In parallel, the destination vector pMar 342 (a kind gift from Dr. M. Reijns) was digested with *EcoRV* and the smaller 1713 bp fragment, which carries a Gateway Entry cassette, was gel purified.

The fragment was then ligated to the backbone of the lentiviral constructs and used to transform ccdB competent DB3.1 bacteria, grown at 30°C: the resulting destination vectors were mini-prepped and the correct clones were identified based on the *EcoRI* digest (for pGIPZ-DEST, Figure 4.7) or the *EcoRI/XbaI* double digest (for pTRIPZ-DEST, Figure 4.8).

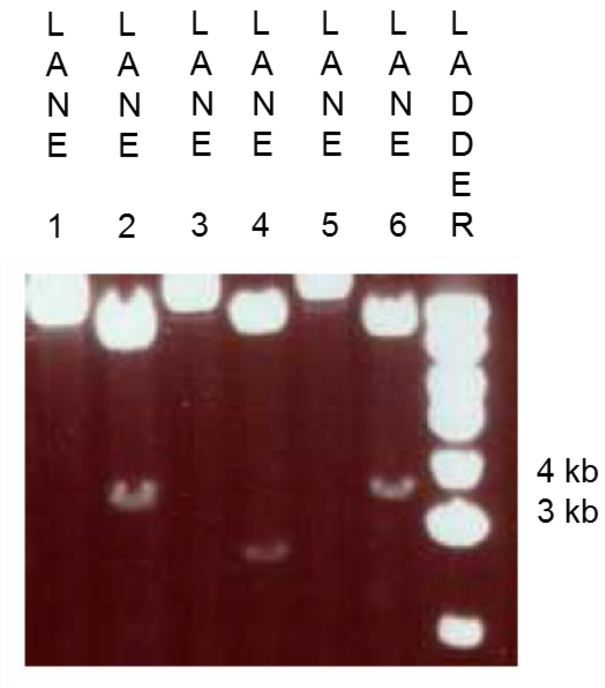

Figure 4.7 Gel image showing the EcoRI digest for the pGIPZ-DEST vector.

Clones number 1 and 3 are correct, as the ligation of GIPZ and pMar342 in the right orientation would give a fragment of 3743 bp (lane 1: uncut clone #1; lane 2: cut clone #1; lane 3: uncut clone# 2; lane 4: cut clone #2; lane 5: uncut clone #3; lane 6: cut clone #3; lane 7: 1 kb DNA ladder).

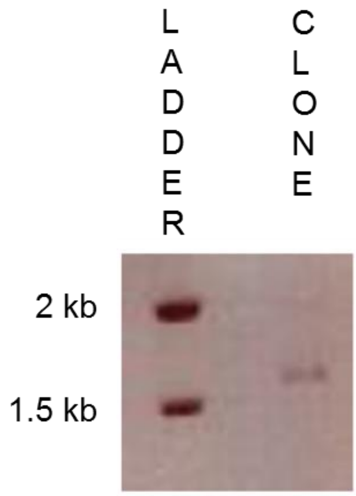

Figure 4.8 Gel image showing the EcoRI/XbaI double digest for the pTRIPZ-DEST vector. The ligation of TRIPZ and pMAR342 in the right orientation should give two fragments of 1553 and 13221 bp, the wrong orientation two fragments of 2356 and 12414 bp. The clone is correct, as shown by the presence of the 1553 bp band (the 13221 bp fragment is too large to be visualised).

4.2.1.3 Step 3: generating the expression clones

Finally, a Gateway LR reaction was performed to subclone the pENTR-miR (LacZ, WT1-1407 and WT1-1490) into the GIPZ-DEST and TRIPZ-DEST vectors.

Following transformation of Stbl2 chemically competent bacteria, grown at 30°C, restriction digests of mini-prepped DNA were used to confirm correct integration. The desired expression clones were identified based on *XbaI* and *HindIII* digests (for pGIPZ-miR, Figure 4.9) or *PvuII* digest (for pTRIPZ-miR, Figure 4.10).

A

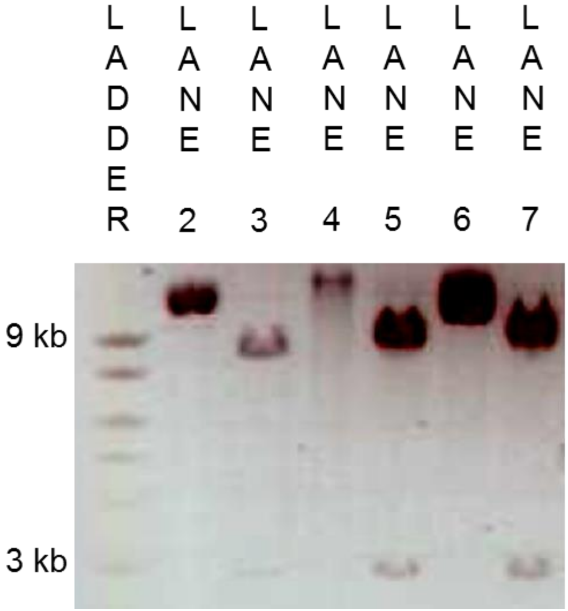
LADDER
LANE 2
LANE 3
LANE 4
LANE 5
LANE 6
LANE 7
9 kb
3 kb

B

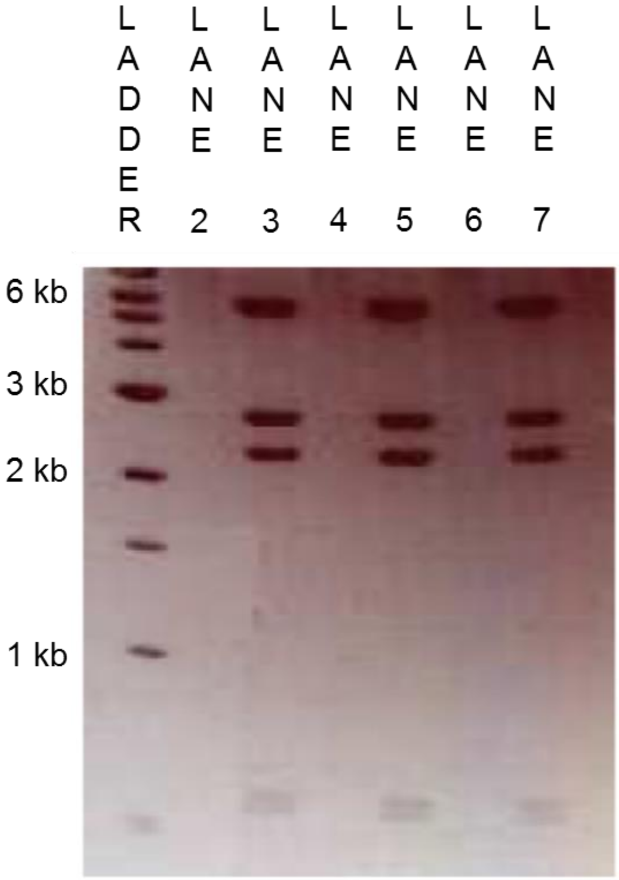
LADDER
LANE 2
LANE 3
LANE 4
LANE 5
LANE 6
LANE 7
6 kb
3 kb
2 kb
1 kb

Figure 4.9 Gel images showing the digests for the final pGIPZ-mir constructs.

All the clones were correct, showing bands at 2840 and 8779 bp for the *XbaI* digest (A), at 5361, 2664, 2110, 588 and 556 bp for *HindIII* (B) (lane 1: 1 kb DNA ladder; lane 2: uncut WT1 1407; lane 3: cut WT1 1407; lane 4: uncut WT1 1490; lane 5: cut WT1 1490; lane 6: uncut lacZ; lane 7: cut lacZ).

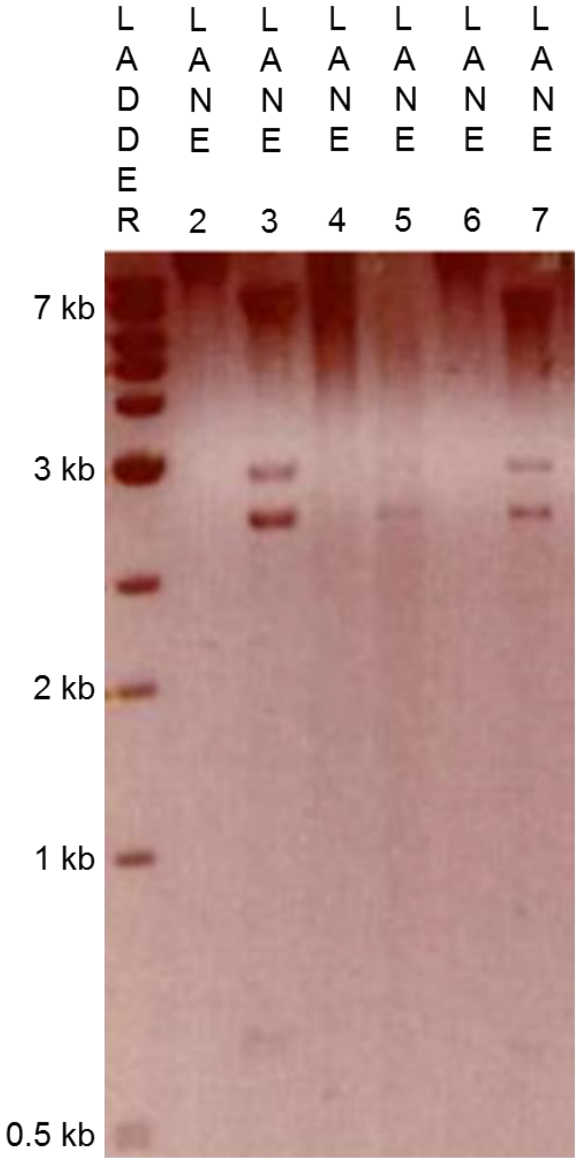

Figure 4.10 Gel image showing the PvuII digest for the final pTRIPZ-miR constructs.
All the clones are correct, showing bands at 626, 2338, 2745 and 7536 bp (lane 1: 1kb DNA ladder; lane 2: uncut lacZ ctr; lane 3: cut lacZ ctr; lane 4: uncut hWT1 1407; lane 5: cut hWT1 1407; lane 6: uncut hWT1 1490; lane 7: cut hWT1 1490).

4.3 Efficient *WT1* knockdown is achieved with the lentiviral system

Lentiviral particles were produced using a trans-lentiviral packaging system developed in the human embryonic kidney cell line SODK3 (Cockrell, Ma et al. 2006). The packaging cells were transfected with the lentiviral vectors described in the previous paragraphs and the resulting viral supernatant was used to transduce four of the human breast cancer cell lines that showed the highest *WT1* expression (MDA-MB-157, HBL100, ZR75, MDA-MB-231).

4.3.1 Constitutive knockdown

Following transduction, the targeted cells were cultured in puromycin selective medium and after one week, they were FACS sorted for GFP: since the fluorescent protein is a surrogate marker of miR expression, sorting the cells with high levels of GFP allowed us to select for maximal miR expression.

The efficiency of the transduction procedure was confirmed by the fact that the vast majority of cells resulted GFP positive (data not shown); from this population, the brightest 15% was sorted and analysed for *WT1* mRNA expression using primers targeting exon 7/8.

Significant down-regulation of the WT1 transcript was achieved by both lentiviral vectors (expressing the 1407 and 1490 targets) in MDA-MB-231 cells, with the best silencing construct showing up to 95% reduction if compared to the virus untreated cells; oddly, only the 1490 vector was successful in MDA-MB-157 and HBL100 cells, leading to 50% and 80% down-regulation respectively (Figure 4.11). Unfortunately, the ZR75 clones were lost due to infection and their transduction could not be repeated within the timeframe of this project.

Ideally, protein levels should also be analysed to confirm the efficacy of the knockdown; however, as discussed earlier, no reliable WT1 antibody was available for Western blot.

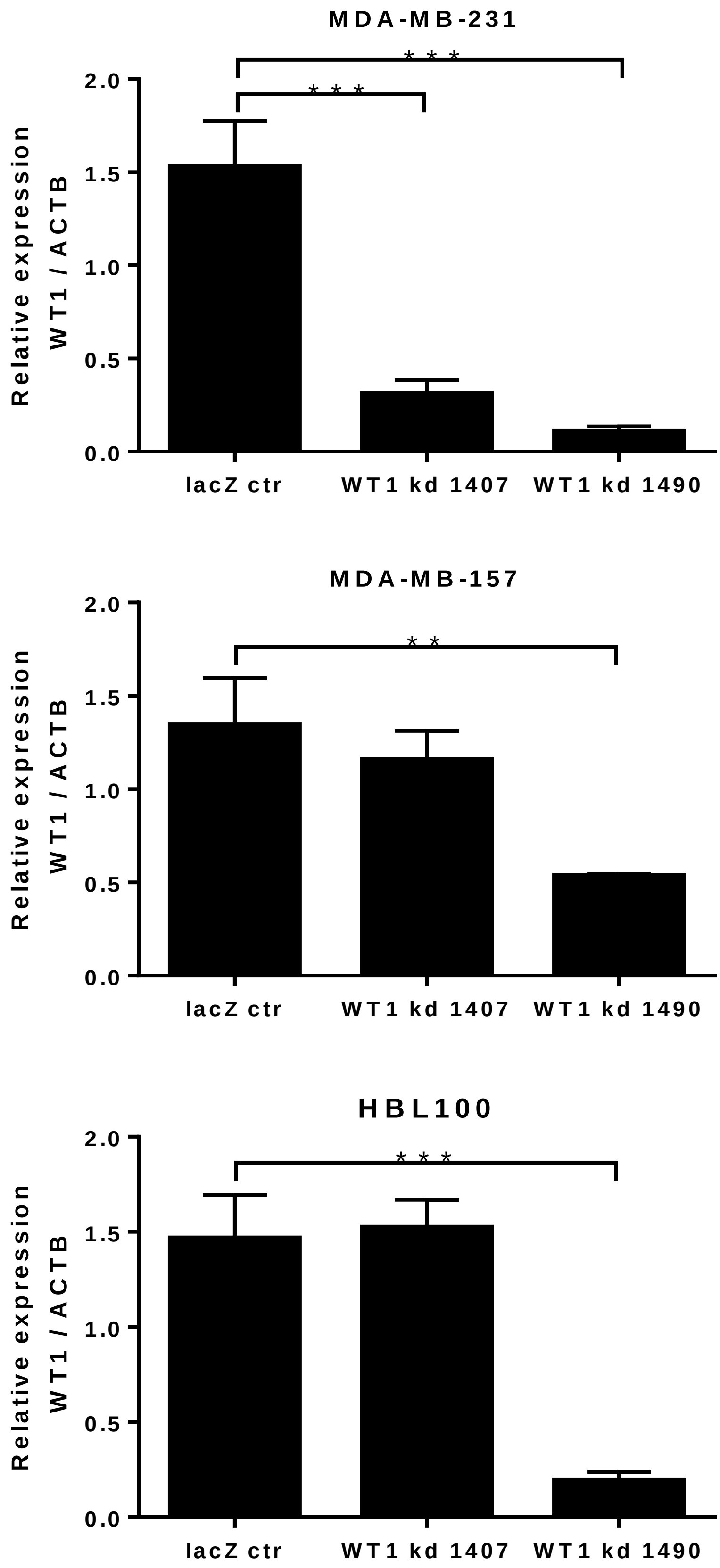
MDA-MB-231
***
***
Relative expression WT1 / ACTB
2.0
1.5
1.0
0.5
0.0
lacZ ctr
WT1 kd 1407
WT1 kd 1490
MDA-MB-157
**
Relative expression WT1 / ACTB
2.0
1.5
1.0
0.5
0.0
lacZ ctr
WT1 kd 1407
WT1 kd 1490
HBL100
***
Relative expression WT1 / ACTB
2.0
1.5
1.0
0.5
0.0
lacZ ctr
WT1 kd 1407
WT1 kd 1490

Figure 4.11 Quantitative RT-PCR for *WT1* mRNA expression in breast cancer cell lines transduced with pGIPZ-miR.

Graph represents fold change of mean expression relative to untransduced cells (given a value of 1); error bars represent the standard deviation of two separate biological replicates. (** $p<0.01$, *** $p<0.001$)

4.3.2 Inducible knockdown

The pTRIPZ construct allows tightly regulatable miR expression that can be induced by doxycycline over a period of 48-72 hours.

At the time of writing, only MDA-MB-157 cells had been transduced with the inducible vectors; following one week of puromycin selection, the cells were exposed to different concentrations of doxycycline (ranging from 0.1 µg/ml to 2 µg/ml, as recommended in the Open Biosystem technical manual) in order to identify the optimal dose.

After a 48-hour incubation, RFP (used to track miR expression) could be detected in the majority of cells, independently of the concentration used (Figure 4.12). RT-PCR, however, showed that maximal *WT1* knockdown was achieved only at the highest dose (2 µg/ml) and in cells transduced with the 1490 vector, while the 1407 did not produce a particularly efficient result (Figure 4.13).

Doxycycline was then administered at the optimal concentration in triplicate for nine consecutive days: in order to monitor *WT1* expression throughout the experiment, RNA samples were collected at different time points before, during and after treatment.

As shown in Figure 4.14, and similarly to what observed in the preliminary study, the 1407 construct was not successful, but significant reduction in *WT1* expression was observed for the cells transduced with the 1490 vector and the efficiency improved with prolonged exposure to doxycycline. Importantly, the *WT1* levels in the 1490 cells went back to normal after the withdrawal of the drug, while in the LacZ control they remained constant throughout the experiment.

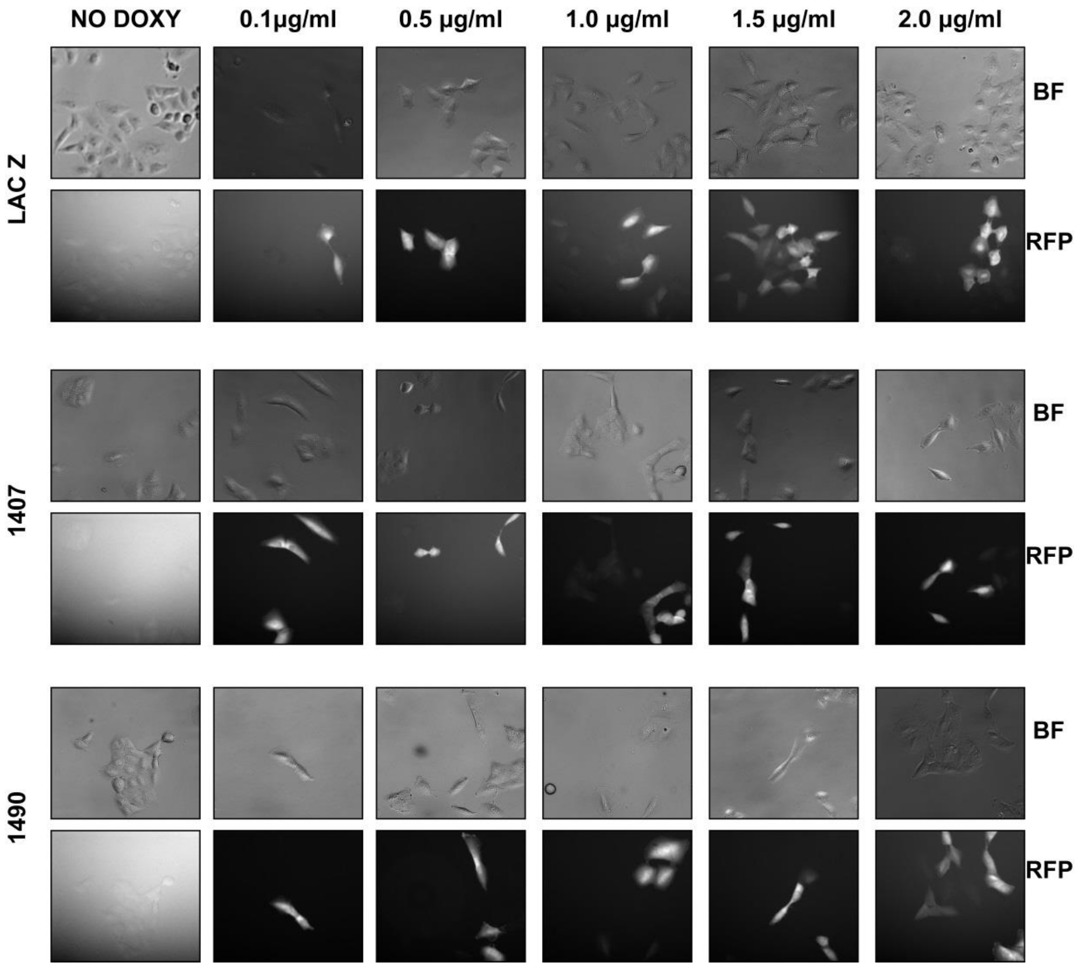

Figure 4.12 Doxycyline-induced expression of RFP in MDA-MB-157 cells transduced with pTRIPZ-miR.

The cells were imaged after a 48-hour incubation with different concentrations of doxycycline. (BF=brightfield, RFP=red fluorescent protein).

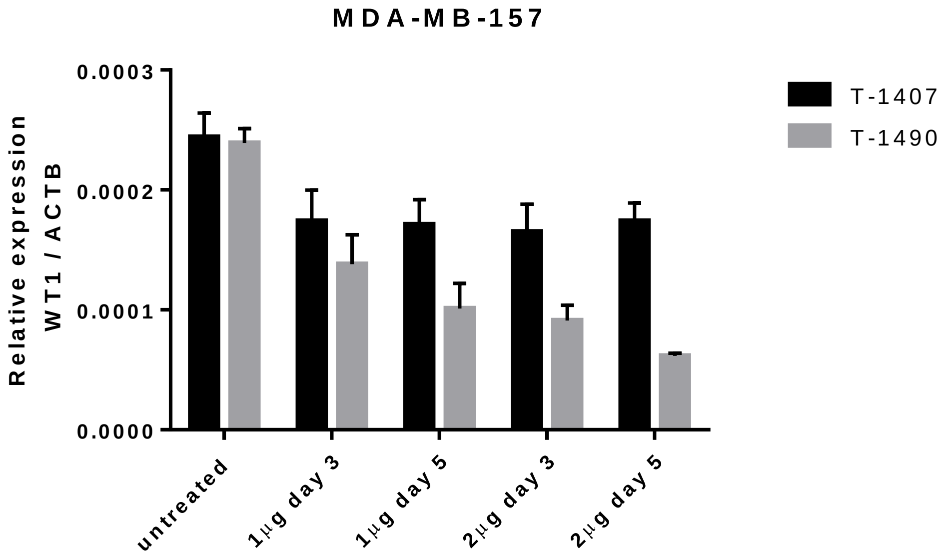

Figure 4.13 Quantitative RT-PCR for *WT1* mRNA expression in MDA-MB-157 cells.

The graph compares the WT1 levels of untreated and pTRIPZ-miR transduced cells exposed to different doses of doxycycline. Data points represent the relative expression of WT1, error bars represent the standard deviation of three technical replicates.

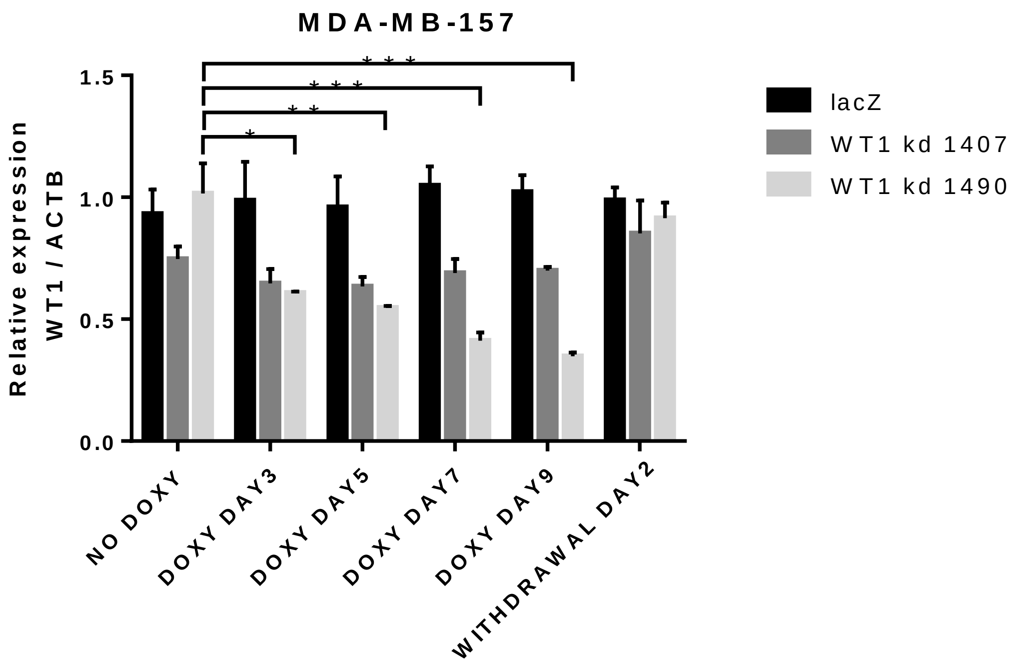

Figure 4.14 Quantitative RT-PCR for *WT1* mRNA expression in MDA-MB-157 cells transduced with pTRIPZ-miR.

The cells were cultured on 2 μg/ml doxycycline. Graph represents fold change of mean expression relative to untransduced cells, error bars represent the standard deviation of three biological replicates. (* $p<0.05$, ** $p<0.01$, *** $p<0.001$)

4.4 Characterisation of the *WT1* knockdown cells

In order to investigate the consequences of *WT1* loss in breast cancer, several experiments were performed on the knockdown cells, including:

- RNA-sequencing
- analysis of EMT and CSCs markers
- studies on proliferation, colony formation and apoptosis.

4.4.1 RNA-sequencing

This technique, based on deep-sequencing technologies, provides extremely precise measurements of transcript levels and has rapidly replaced microarrays in gene profiling experiments (Wang, Gerstein et al. 2009).

In this project, RNA-sequencing was used to compare the transcriptomes of virus-untreated, pGIPZ-miR-lacZ and pGIPZ-miR-WT1kd1490 cells in both MDA-MB-231 and MDA-MB-157 lines.

The data were analysed with two different web-based softwares, the more recently developed GeneProf (Halbritter, Vaidya et al. 2012) and the already established Galaxy analysis suite (Giardine, Riemer et al. 2005); the excel files containing the complete analyses can be found in the attached CD, as well as all the tables for the ToppFun functional enrichment analysis.

4.4.1.1 GeneProf analysis

For each cell line, pair-wise comparisons were performed to analyse the transcriptome of the three samples (untreated, lacZ and WT1 knockdown).

No significantly modulated genes were identified for the MDA-MB-231 dataset, while 165 were found for the MDA-MB-157 line: these transcripts were up or down regulated at least two fold with a p value ≤ 0.05 in both “WT1 kd/lacZ” and “WT1 kd/untreated” comparisons (Figure 4.15).

To rule out any effect due to the transduction procedure itself and identify the genes which were uniquely affected by the knockdown of *WT1*, I removed from this set all the genes which were differentially expressed in the “LacZ/untreated” comparison.

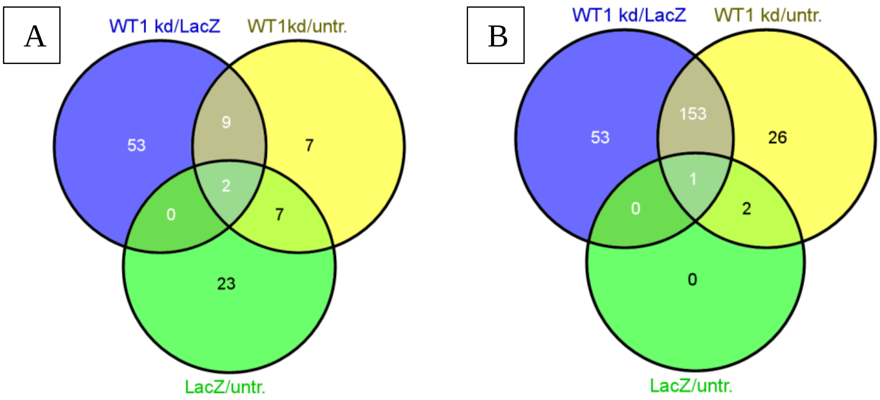

Figure 4.15 Venn analysis of the genes modulated in MDA MB 157 cells.
The distribution of the up-regulated transcripts is shown in A, the down-regulated in B.

The remaining transcripts (9 up-regulated and 153 down-regulated, listed in appendix C) were analysed for gene list functional enrichment using ToppFun Suite (http://toppgene.cchmc.org); through this portal I applied a false rate discovery method (FDR) with a 0.05 cut-off level to correct for multiple comparisons and then grouped the modulated genes according to their Go terms (cellular component, molecular function and biological process).

The analysis of the up-regulated genes could not identify any functional enrichment, most likely because the list is very small and contains heterogeneous genes (*AGR2*, *CNTNAP3B*, *CXCL5*, *C8orf4*, *FLRT3*, *PAPPA*, *PTGS2*, *THSD7A*). The down-regulated group, on the other hand, was enriched for genes expressed in cellular components like the basement membrane, the extracellular matrix and contractile fibers; in terms of biological processes, significant enrichment was found for transcripts involved in cell adhesion and migration, extracellular matrix organization and disassembly, angiogenesis, wound healing and neurogenesis.

4.4.1.2 Galaxy analysis

This analysis was performed by our collaborator Dr. Aitken following the same criteria described in the previous paragraph.

In the MDA-MB-231 dataset, a total of 119 significantly modulated genes were identified (91 up-regulated and 28 down-regulated, listed in appendix D), including several microRNAs (*MIR4763*, *MIRLET7A3*, *MIRLET7B*, *MIRLET7BHG*, *MIR221*, *MIR222*). The ToppFun analysis could not reveal any functional enrichment for the up-regulated transcripts, while the down-regulated were found to be involved in biological processes such as cell adhesion and migration, extracellular matrix organization, apoptosis, vasculature development and response to wounding.

In the MDA-MB-157 dataset, 427 genes were differentially expressed (105 up-regulated and 322 down-regulated, all listed in appendix E). Once again, the ToppFun analysis showed an enrichment in genes related to cell adhesion and migration, extracellular matrix organization and disassembly, angiogenesis, wound healing and neurogenesis.

4.4.1.3 Summary and comparison of results

The newly developed GeneProf software allowed easy and rapid analysis of the RNA-seq data, providing a user-friendly interface and straightforward workflows; however, it did not perform as well as Galaxy in the identification of modulated transcripts: the difference was particularly marked for the MDA-MB-231 dataset, whose differentially expressed genes could only be identified through Galaxy.

As shown by the overlap in Figure 4.16, very few transcripts resulted modulated in both MDA-MB-157 and MDA-MB-231 cells (*COL5A1*, *FAM133A*, *GPR110*, *IL13RA2*, *NOV*, *PLA2G4A*, *TNC*, *WNT5A*).

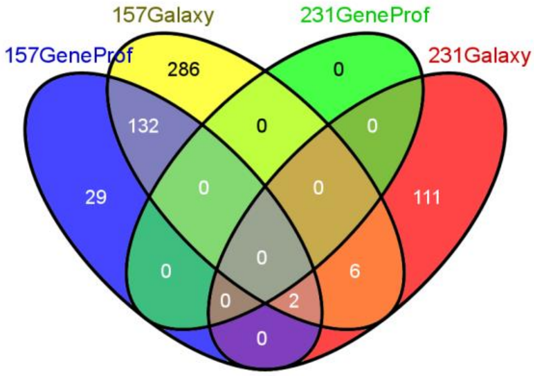

Figure 4.16 Venn analysis of the modulated genes identified by GeneProf and Galaxy.

Nonetheless, the ToppFun analysis detected similar functional enrichment in both datasets and most of the modulated genes seem to be involved in one of the following biological processes:

• cell adhesion (GO terms: biological, cell-matrix and cell-substrate adhesion, positive and negative regulation of cell adhesion)

• cell migration (ameboidal cell migration, cell motility, cell projection morphogenesis and organization, chemotaxis, locomotion, cell migration involved in sprouting angiogenesis)

• cell proliferation (epithelial cell proliferation, negative regulation of epithelial cell proliferation)

• apoptosis (extrinsic apoptotic signaling pathway, regulation of apoptotic process, negative regulation of programmed cell death)

• extracellular matrix organization and disassembly

• angiogenesis (blood vessel development and morphogenesis, vasculature development)

• wound healing (response to wounding)

• neurogenesis (axon development and guidance, axonogenesis, neuron development and differentiation, neuron projection development, guidance and morphogenesis, regulation of neurogenesis).

A potential role for *WT1* in some of these processes has already been hypothesized (apoptosis, proliferation, angiogenesis); others, like cell adhesion and migration, are particularly intriguing given their involvement in metastasis formation.

Functional assays, however, are needed to determine if any of these processes is actually affected by the loss of *WT1* and they will be the subject of the following paragraphs.

4.4.2 Migration assays

The RNA-sequencing data suggest that *WT1* may play a role in the adhesion and migration of breast cancer cells; since the modulated genes include both positive (eg. *MMP2*, *WNT5B*) and negative (eg. *THBS1*, *GSTP1*) regulators of these processes, the effects of *WT1* loss could be either pro- or anti-migratory.

In order to assess if and how *WT1* knockdown affects cell motility, migration assays were performed on MDA-MB-157 cells transduced with the pGIPZ-miR constructs.

In brief, the cancer cells were seeded in both wells of an IBIDI insert, allowing them to attach only in the designated areas; after removing the insert, the closure of the gap was monitored through time-lapse microscopy. Images were collected every 30 minutes for 40 hours (from t=0 to t=80) and then analysed with ImageJ.

A one-way ANOVA conducted to compare the migration capacity of untreated, control and knockdown cells revealed a statistically significant difference among the groups (Figure 4.17, p value of 0.022); post-hoc comparisons using the Tukey test indicated that the mean gap closure percentage for the knockdown cells at t=80 was significantly higher than the other two samples, while untreated and lacZ cells did not differ significantly from each other.

As shown by the representative images in Figure 4.17, the WT1kd1490 cells migrate faster than the controls, suggesting that *WT1* may play a role in the negative regulation of cell motility, at least in MDA-MB-157 cells.

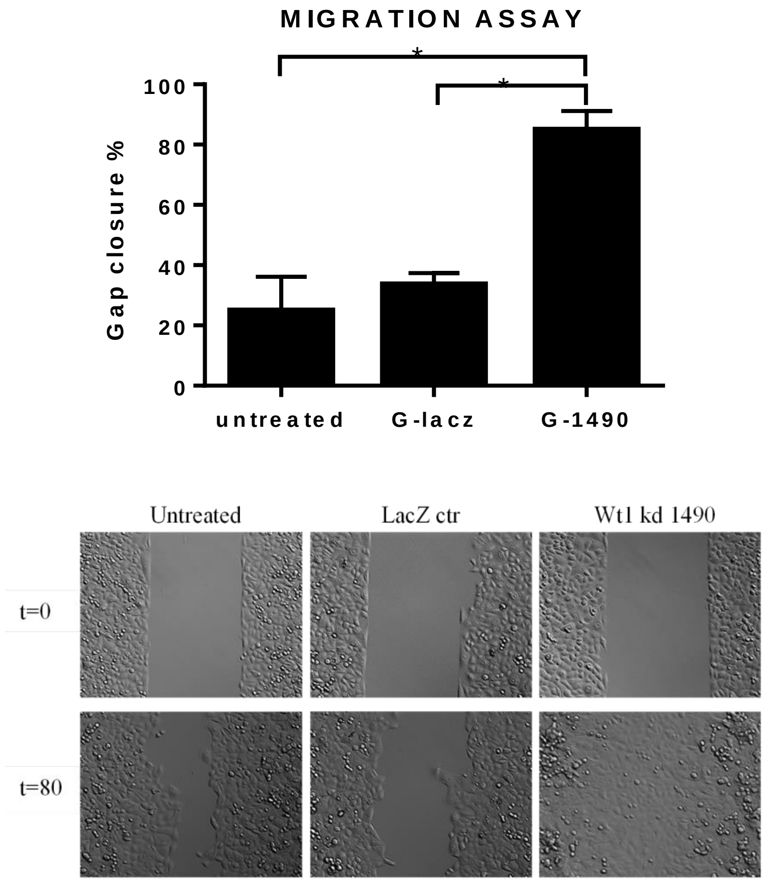

Figure 4.17 Cell migration assay performed on MDA-MB-157 cells transduced with pGIPZ-miR.

Bar diagram representing the mean gap closure percentage of two independent experiments (top); representative images of the assay (bottom). (* p<0.05)

4.4.3 RT-PCR for EMT markers and RNA-seq validation

In order to assess whether the loss of *WT1* affects the epithelial/mesenchymal balance of breast cancer cells, RT-PCR was performed on all the lines transduced with the lentiviral constructs (MDA-MB-157, MDA-MB-231 and HBL100); the RNA levels of several EMT drivers, epithelial and mesenchymal markers were analysed, as well as some of the modulated genes identified through RNA-sequencing (only the statistically significant results are reported below, the complete set of RT-PCR graph can be found in the attached CD).

4.4.3.1 EMT drivers

Significant change in gene expression was observed only in one of the 5 transcripts analysed (*SNAI1*, *SNAI2*, *ZEB1*, *ZEB2*, *TWIST1*).

ZEB2 was up-regulated in MDA-MB-157 cells transduced with the inducible constructs: the mRNA expression was significantly higher after 5 and 7 days of doxycycline treatment, and went back to the untreated levels upon withdrawal of the drug (Figure 4.18).

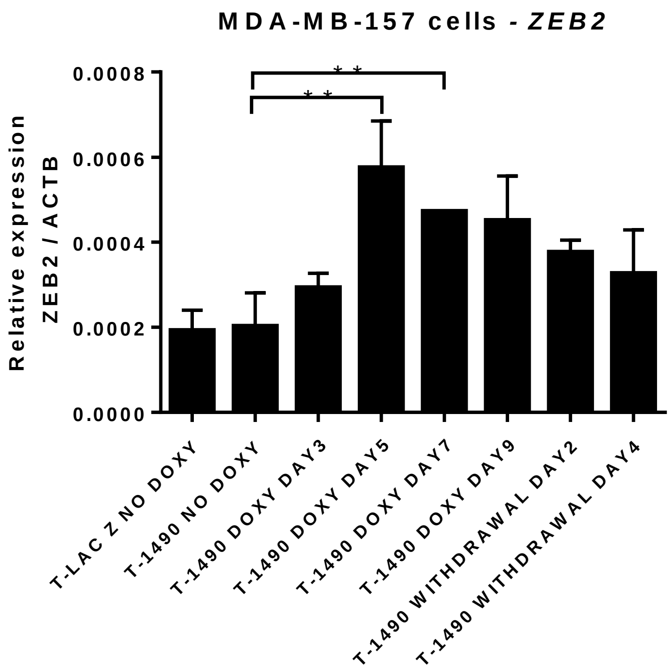

Figure 4.18 Quantitative RT-PCR for *ZEB2* mRNA expression.

Data points represent the relative expression of the gene, error bars represent the standard deviation of three biological replicates. (** p<0.01)

4.4.3.2 Epithelial markers

Among the five genes analysed (*CDH1*, *CTNNA1*, *CTNNA2*, *CTNND1*, *KRT18*), only *CTNNA1* showed a statistically significant difference in expression, being down-regulated in the MDA-MB-157 knockdown cells (Figure 4.19).

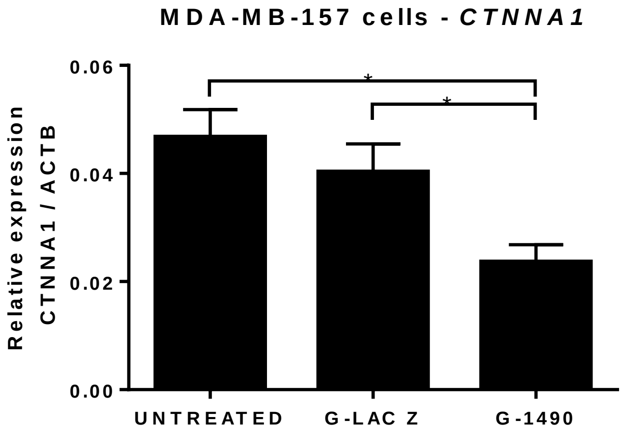

Figure 4.19 Quantitative RT-PCR for *CTNNA1* mRNA expression in MDA-MB-157 cells. Data points represent the relative expression of the gene, error bars represent the standard deviation of two biological replicates. (* $p<0.05$)

Unexpectedly, the *CDH1* transcript could not be detected in any of the samples tested (data not shown): even though its expression is lost in the vast majority of breast carcinomas (De Leuuw et al. 1997), this adhesion molecule has been repeatedly found in several cell lines, including MDA-MB-231 cells (Lombaerts et al. 2006, Tate et al. 2012); hence, this result is likely a false negative due to a defective RT-PCR assay and the analysis should be repeated using a new set of primers.

4.4.3.3 Mesenchymal markers

RT-PCR was performed on ten different mesenchymal markers (*VIM*, *TNC*, *VTN*, *MMP2*, *MMP9*, *TGFB1*, *ACTA2*, *CDH2*, *CXCL1*, *FN1*); statistically significant results were only obtained for *TNC* and *TGFB1*, which displayed higher expression levels in the *WT1* knockdown cells.

TNC was up-regulated in both 1407 and 1490 clones of the MDA-MB-231 line, as well as in MDA-MB-157 cells transduced with both constitutive and inducible constructs (Figure 4.20).

TGFB1 over-expression was only observed in MDA-MB-157 inducible knockdown cells: after 5, 7 and 9 days of doxycycline treatment, the mRNA expression was significantly higher than in the untreated control samples (Figure 4.21).

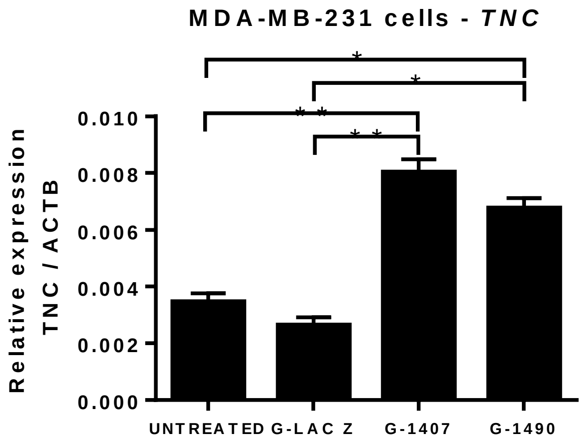
MDA-MB-231 cells - *TNC*
Relative expression
TNC / ACTB
0.010
0.008
0.006
0.004
0.002
0.000
UNTREATED
G-LAC Z
G-1407
G-1490
*
*
* *
* *

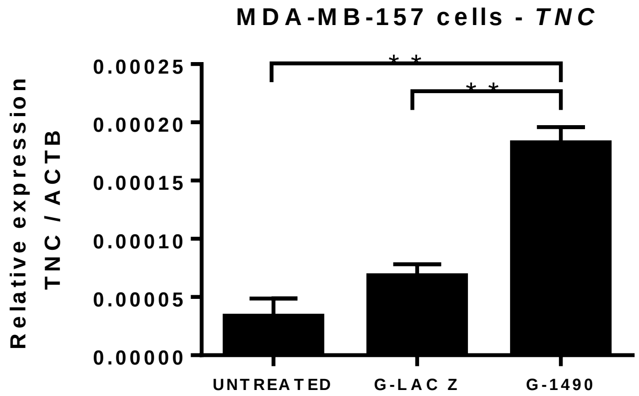
MDA-MB-157 cells - *TNC*
Relative expression
TNC / ACTB
0.00025
0.00020
0.00015
0.00010
0.00005
0.00000
UNTREATED
G-LAC Z
G-1490
* *
* *

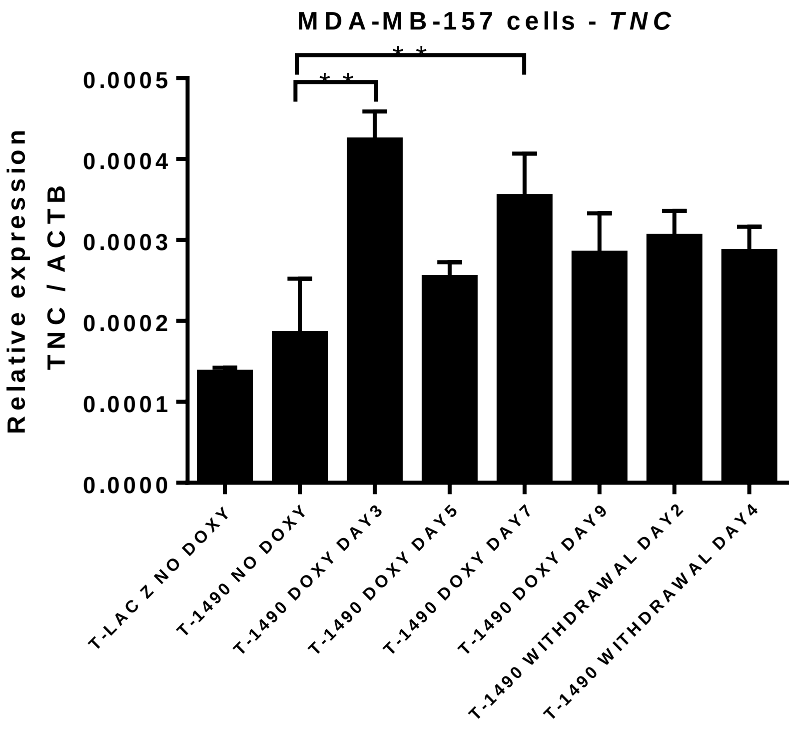
MDA-MB-157 cells - *TNC*
Relative expression
TNC / ACTB
0.0005
0.0004
0.0003
0.0002
0.0001
0.0000
T-LAC Z NO DOXY
T-1490 NO DOXY
T-1490 DOXY DAY3
T-1490 DOXY DAY5
T-1490 DOXY DAY7
T-1490 DOXY DAY9
T-1490 WITHDRAWAL DAY2
T-1490 WITHDRAWAL DAY4
* *
* *

Figure 4.20 Quantitative RT-PCR for *TNC* mRNA expression in MDA-MB-157 and MDA-MB-231 cells.

Data points represent the relative expression of the gene, error bars represent the standard deviation of two (GIPZ clones) or three (TRIPZ clones) biological replicates. (* $p<0.05$, ** $p<0.01$)

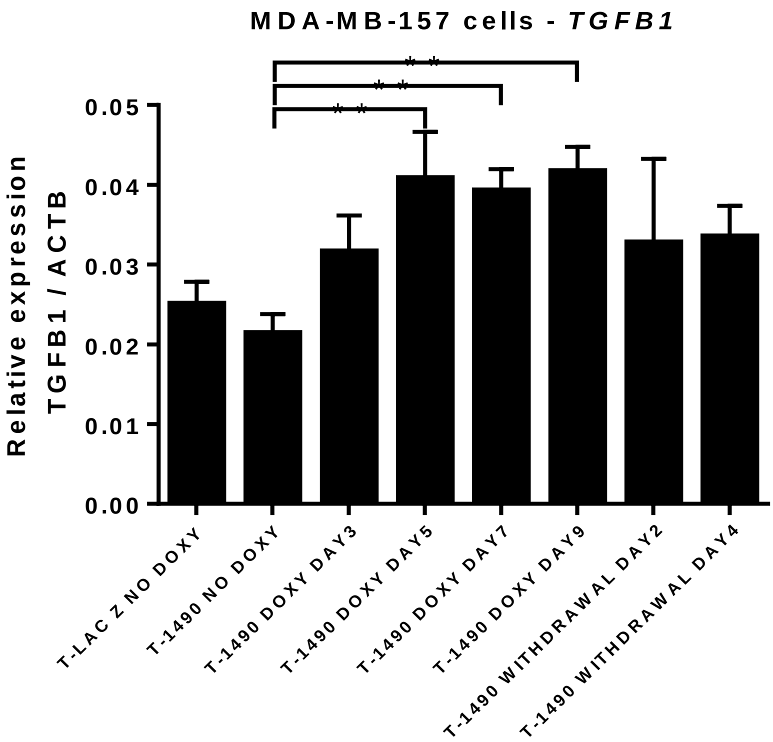

Figure 4.21 Quantitative RT-PCR for *TGFB1* mRNA expression in MDA-MB-157 cells.

Data points represent the relative expression of the gene, error bars represent the standard deviation of three biological replicates. (** $p<0.01$)

4.4.3.4 RNA-seq validation

Five of the modulated genes identified through RNA-sequencing were selected for RT-PCR validation (*TNC*, *MMP2*, *VTN*, *COL3A1*, *SNAI2*).

As previously shown (Figure 4.20), both MDA-MB-231 and MDA-MB-157 knockdown cells showed a significant up-regulation of the mesenchymal marker *TNC*, which is in accordance with the RNA-sequencing results.

No significant change in gene expression was observed for the other four genes (*SNAI2*, *MMP2*, *VTN*, *COL3A1*).

4.4.4 Colony forming assay and stem cell marker analysis

The RT-PCR results revealed that, at least in the MDA-MB-157 line, knocking down *WT1* triggers a partial EMT, characterised by the up-regulation of EMT drivers and mesenchymal markers (*ZEB2*, *TNC*, *TGFB1*) as well as the down-regulation of the epithelial *CTNNA1*.

Since EMT has been linked to the acquisition of cancer stem-cell properties (e.g., an increased ability to form spheres in colony-forming assays, the expression of stem-cell markers) (Morel et al. 2008, Mani et al. 2009), we analysed such stem-cell properties in the WT1 knockdown cells.

In brief, colony forming assays (CFA) were performed in 96-well plates coated with Polyhema in order to prevent cell attachment; semi-solid medium (containing 1% methylcellulose) was used to reduce cell movement and allow the individual cells to develop into colonies. For each clone, 1,000 cells/well were seeded at least in triplicate and incubated for 11 days, after which, the number of colonies > 75 μm in diameter were counted.

As shown in Figure 4.22, the WT1 knockdown cells seem to form fewer spheres than the control in both MDA-MB-157 and HBL100 lines, however, this difference was not statistically significant (p value of the one-way ANOVA > 0.05).

The knockdown cells were then analysed for the expression of cancer stem cell markers. In human breast cancer, the sub-population of $CD44^+/CD24^-$ cells has been reported to be highly enriched in CSCs and can easily be isolated through FACS (Al-Hajj et al. 2003, Mani et al. 2008).

The percentage of $CD44^+/CD24^-$ cells did not change significantly in MDA-MB-157 and HBL100 cells transduced with the GIPZ constructs. In the MDA-MB-231 line, both WT1 knockdown clones showed an increase in the stem cell population if compared to the untreated cells; however, since a similar increase was also observed in the lacZ control, this difference cannot be attributable to the lower expression levels of *WT1* (Figure 4.23).

Finally, no statistically significant difference could be observed in MDA-MB-157 cells transduced with the inducible constructs (Figure 4.24).

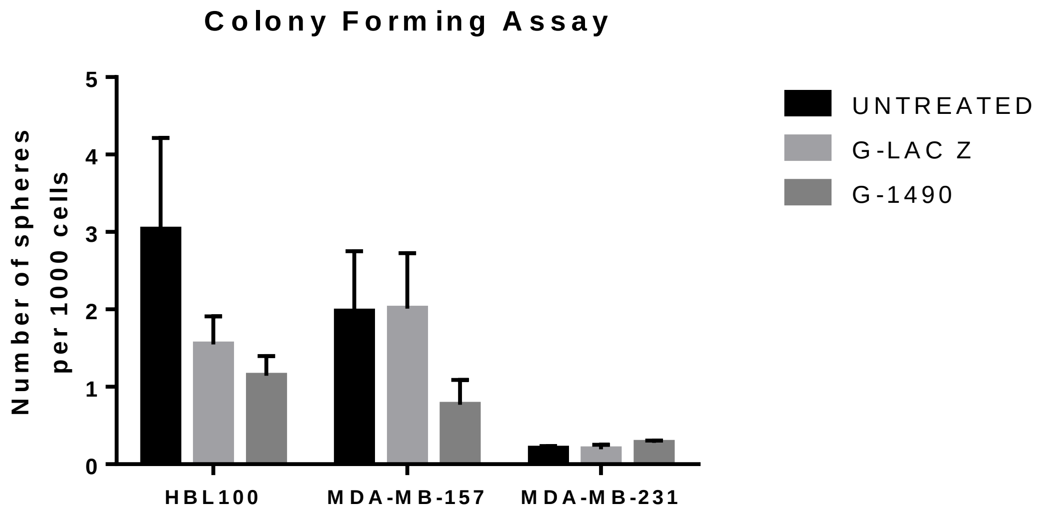

Figure 4.22 Colony forming assay (CFA) of breast cancer cells suspended in semi-solid medium. Data points represent the average number of spheres formed per well, error bars represent the SEM of four biological replicates.

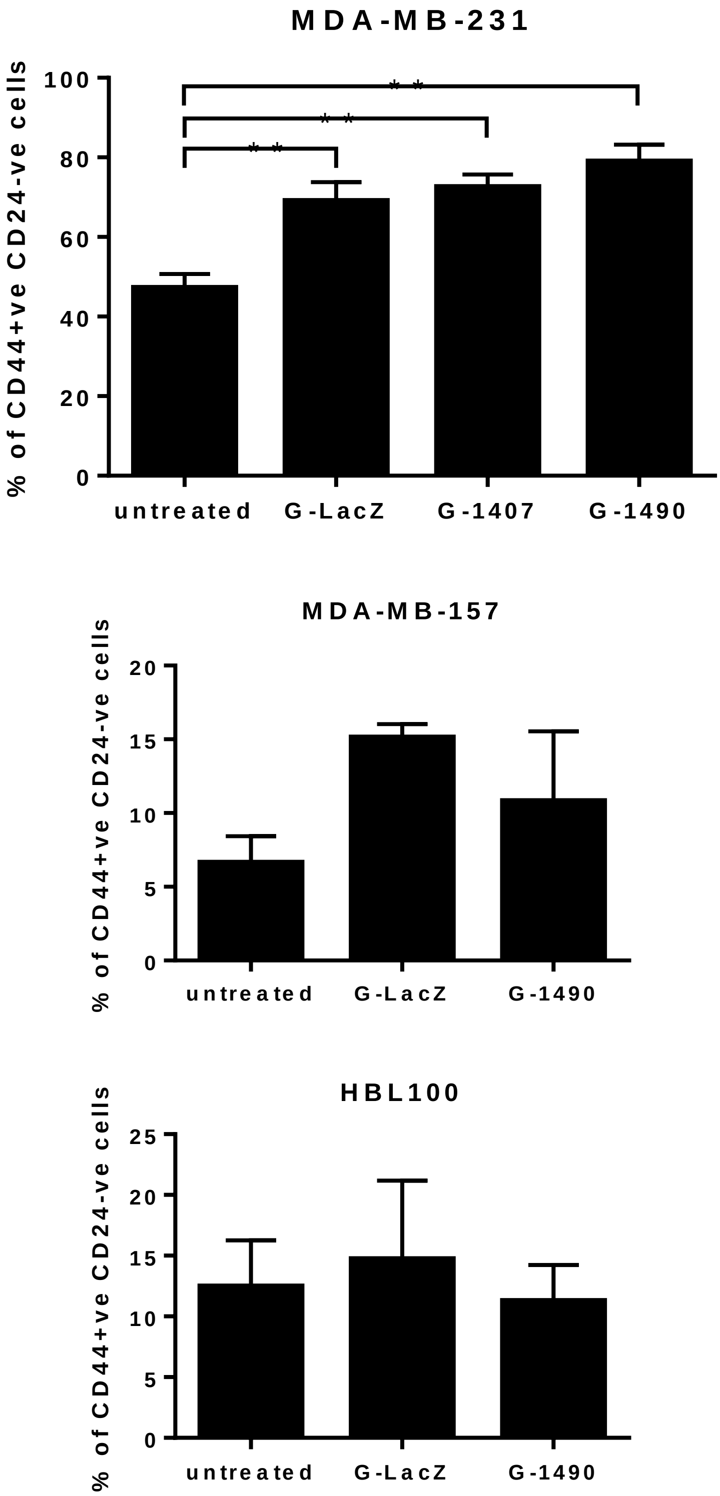

Figure 4.23 FACS analysis of CD24 and CD44 expression in breast cancer cells transduced with the GIPZ constructs.

Bar graphs represent the average percentage of $CD44^{+}/CD24^{-}$ cells in the different clones, error bars represent the SEM of five biological replicates. (** $p<0.01$)

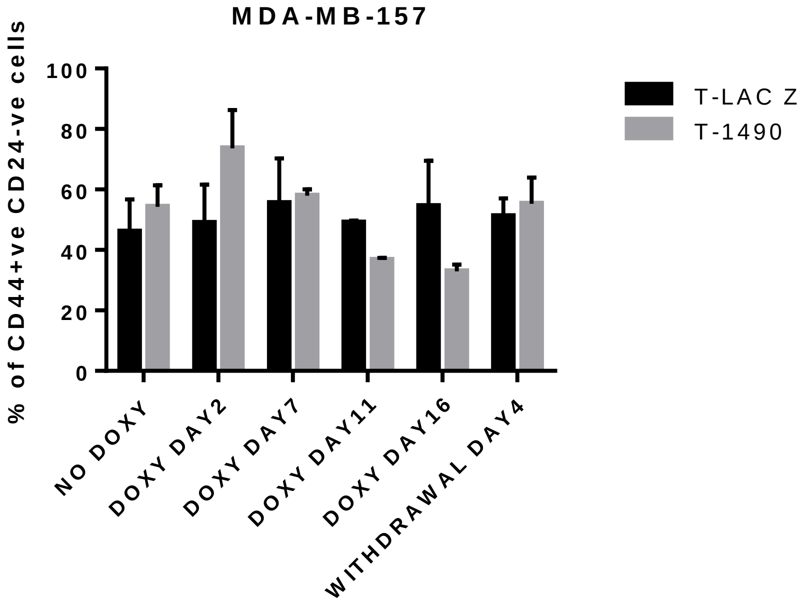

Figure 4.24 FACS analysis of CD24 and CD44 expression in breast cancer cells transduced with the TRIPZ constructs.

Bar graphs represent the average percentage of $CD44^{+}/CD24^{-}$ cells in the different clones, error bars represent the SEM of three biological replicates.

4.4.5 Apoptosis and cell cycle analysis

FACS analysis of Annexin V and DAPI stained cells was performed to investigate apoptosis and cell cycle respectively.

As shown in Figure 4.25 and 4.26, no statistically significant difference could be observed in the percentage of apoptotic cells, independently of the cell line and the knockdown constructs used.

The analysis of cell cycle distribution in MDA-MB-231 cells showed that the WT1 knockdown clone G-1490 has a substantial accumulation of cells in G2/M, compared to both untreated and lacZ control samples (Figure 4.27); no difference was however detected in the other two lines (Figure 4.27, 4.28).

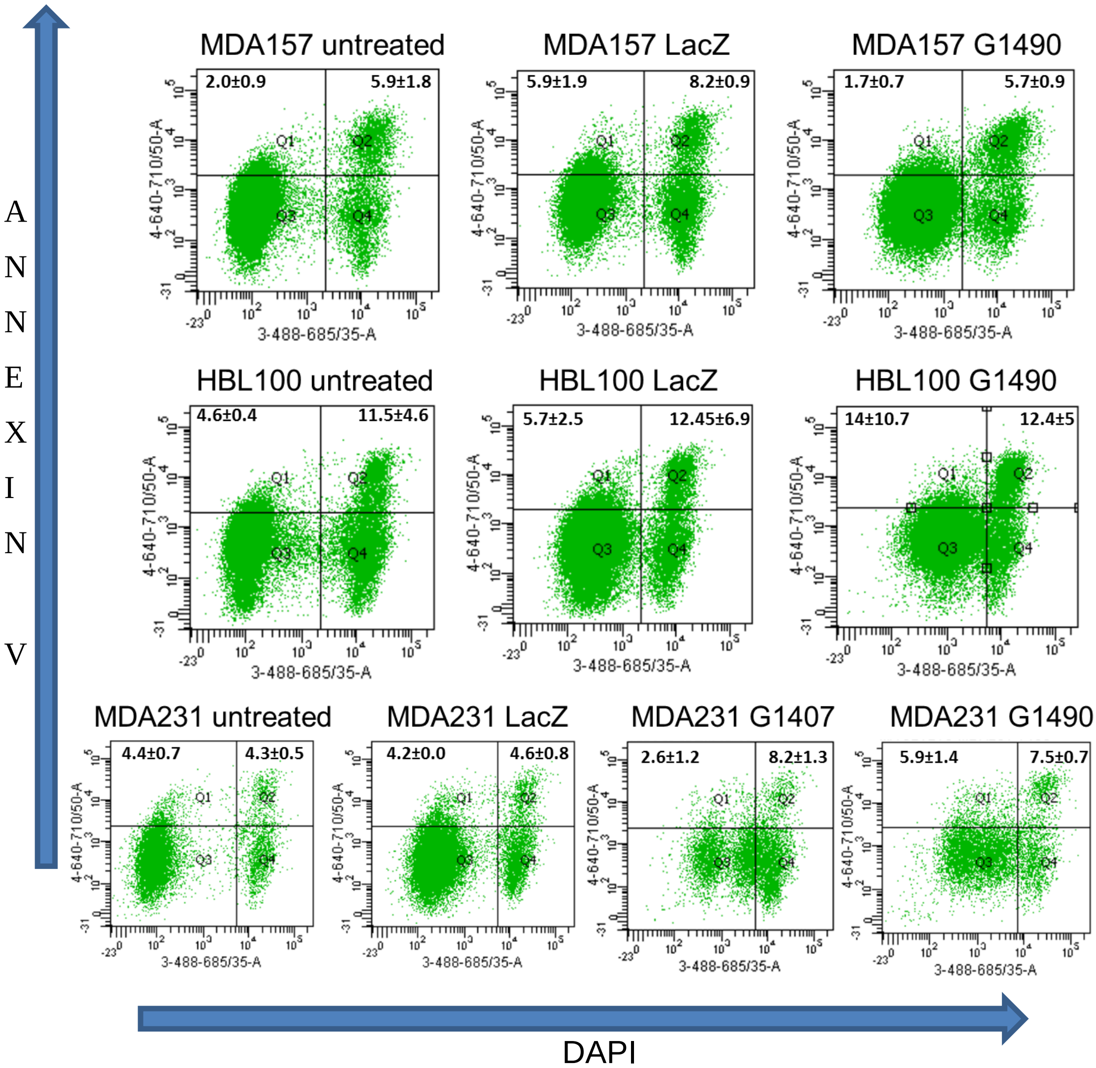

Figure 4.25 FACS analysis of Annexin V-APC in cells transduced with the GIPZ constructs.

The results are presented as mean values ± SEM of three independent experiments.

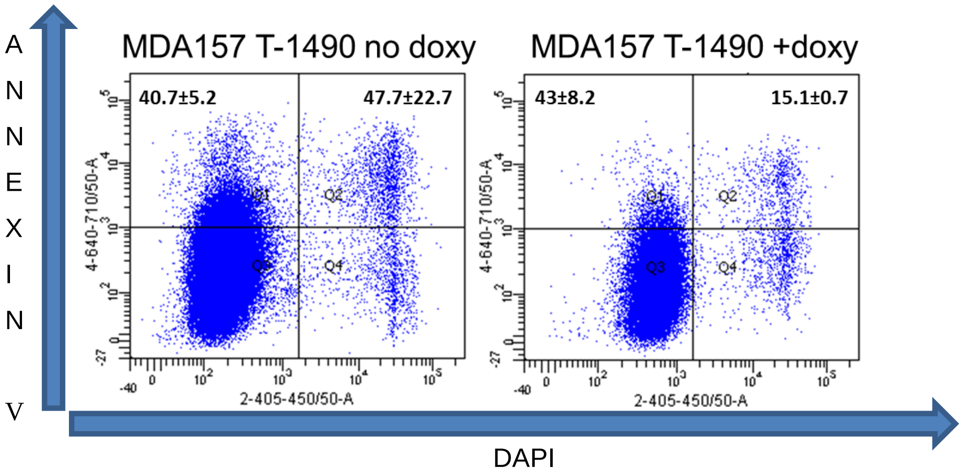

Figure 4.26 FACS analysis of Annexin V-APC stained cells.

The results are presented as mean values ± SEM of two independent experiments.

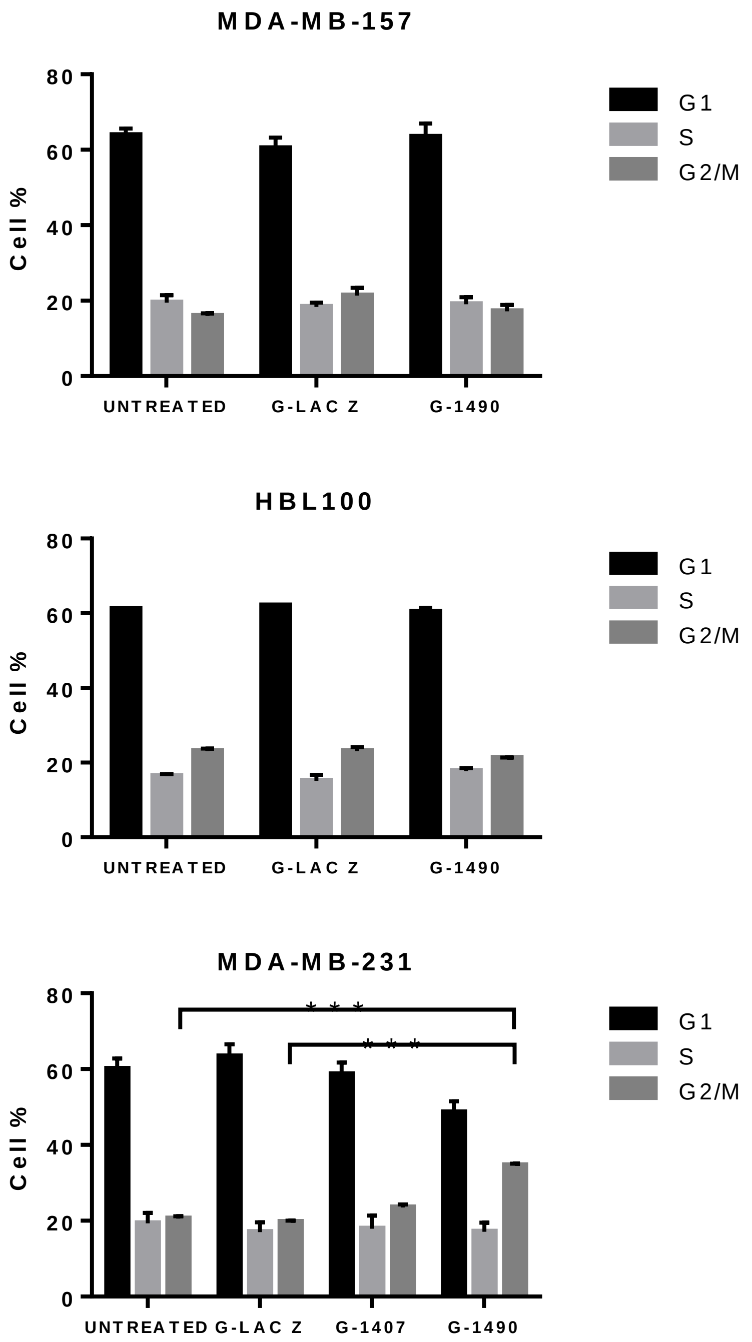

Figure 4.27 FACS analysis of the cell cycle using DAPI staining in cells transduced with the GIPZ constructs.

The results are presented as mean values ± SEM of at least three independent experiments. (*** $p<0.001$, as compared to the relative control samples).

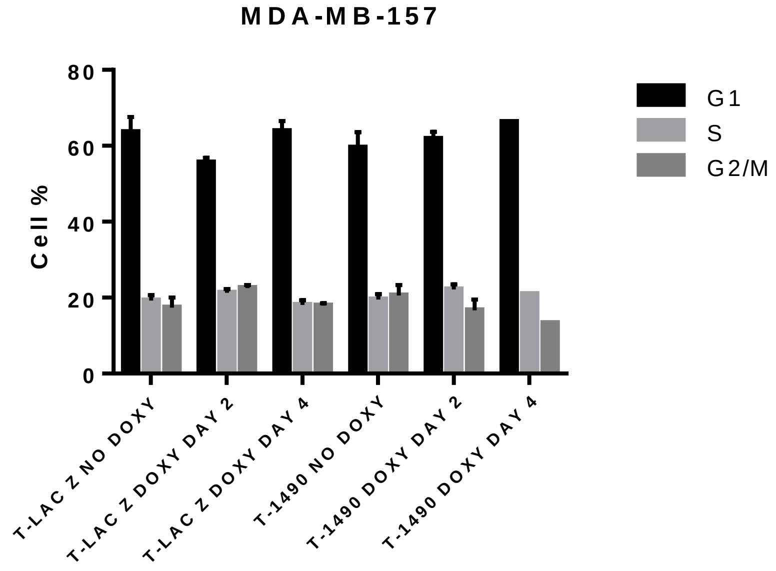

Figure 4.28 FACS analysis of the cell cycle using DAPI staining in cells transduced with the TRIPZ constructs.

The results are presented as mean values ± SEM of two independent experiments.

4.5 Summary of experimental findings

The cloning of RNAi lentiviral vectors was successful and led to the efficient knockdown of *WT1* in three different breast cancer cell lines (MDA-MB-231, MDA-MB-157 and HBL100).

Several experiments were performed to characterise the WT1 knockdown cells and the results can be summarised as follow:

• the RNA-sequencing identified many modulated genes, mainly involved in cell adhesion/migration, extracellular matrix organization/disassembly, angiogenesis, proliferation, apoptosis, wound healing and neurogenesis

• migration assays carried out on the MDA-MB-157 line showed that the WT1 knockdown cells migrate faster than the controls, suggesting that *WT1* may play a role in the negative regulation of cell motility

- the RT-PCR results revealed that, at least in the MDA-MB-157 line, knocking down WT1 triggers a partial EMT, characterised by the up-regulation of EMT drivers and mesenchymal markers (*ZEB2*, *TNC*, *TGFB1*) as well as the down-regulation of the epithelial *CTNNA1*

- the up-regulation of the mesenchymal marker *TNC* in the knockdown cells is observed in two different lines (MDA-MB-231, MDA-MB-157) and through both RNA-sequencing and RT-PCR

- no significant difference was detected in colony forming assay, stem cell marker and apoptosis analyses

- the analysis of cell cycle distribution showed a substantial increase of the G2/M population in MDA-MB-231 knockdown cells.

4.6 Discussion

In this project, an RNAi based gene knock-down strategy was used to investigate the functional role of *WT1* in breast cancer.

A lacZ control and two WT1 knockdown lentiviral vectors were successfully generated through Gateway cloning and then transduced in four different breast cancer cell lines (ZR75, MDA-MB-231, MDA-MB-157, HBL100).

Unfortunately, the clones of the only luminal, ER+ line (ZR75) were lost due to infection; efficient WT1 down-regulation was achieved in the remaining three lines (all belonging to the basal, triple negative subgroup). Despite some similarities, discussed in more details in the following paragraphs, the three cell lines did not show identical responses to the loss of WT1 and these differences may be due to the cell genotypes or to the presence/absence of different WT1 co-factors in each cell line.

4.6.1 *WT1* loss triggers a partial EMT in MDA-MB-157 cells

As shown by RT-PCR and migration assays, the loss of *WT1* affects the epithelial/mesenchymal balance by pushing the cells towards a more mesenchymal and migratory phenotype: the knockdown clones, in fact, migrate faster than the controls and express higher levels of EMT drivers and mesenchymal markers (*ZEB2*, *TNC*, *TGFB1*).

However, while *TNC* is up-regulated in both GIPZ and TRIPZ-transduced cells, the modulation of *ZEB2* and *TGFB1*can only be observed in the inducible knockdown. This inconsistency is probably due to the fact that *ZEB2* and *TGFB1* activation occurs at the very beginning of the EMT process (reviewed in Kalluri and Weinberg 2009).

If, as it seems, *WT1* loss triggers an EMT, the early stages of this induction could not be monitored in a constitutive system, at least not with the protocol used in this project: to achieve an optimal knockdown, the GIPZ-transduced cells were subjected to lengthy selection procedures (puromycin culture, FACS sorting) and several weeks elapsed between the delivery of the lentiviral constructs and the analysis of the clones. This constitutive system is therefore ideal to study the long-term effects of WT1 knockdown on cell proliferation and migration, but the inducible vectors represent a better tool to investigate the immediate response of breast cancer cells.

An additional advantage of the inducible system is the possibility to turn off RNAi production by simply stopping the administration of doxycycline: upon withdrawal of the drug, *WT1* expression has been shown to increase, while the expression levels of *ZEB2*, *TNC* and *TGFB1* go down to the pre-treatment levels, strengthening the correlation between *WT1* and the epithelial/mesenchymal balance of breast cancer cells.

Nevertheless, all the data gathered so far suggest that the EMT triggered in the knockdown clones is only partial: firstly, the changes in gene expression are limited to very few transcripts; secondly, there is no major down-regulation of epithelial markers (which, however, could be due to the mesenchymal nature of the MDA-MB-157 line, whose cells express very low levels of epithelial genes to begin with). Lastly, and more importantly, EMT has been reported to affect several characteristics of cancer cells, including their cancer stem-cell properties, cell proliferation, migration and resistance to apoptosis induction (Mani, Guo et al. 2008, Morel, Lievre et al. 2008, Xie, Ji et al. 2014); since only a migratory phenotype could be observed in the knockdown cells, the loss of *WT1* does not seem sufficient to induce a full-fledged EMT.

Additional experiments, some of which are being performed at the time of writing, will help to better characterise this potential new role of *WT1* as a regulator of the epithelial/mesenchymal balance in breast cancer.

In particular, it would be important to:

• try to rescue the migratory phenotype, by re-expressing *WT1* in the knockdown cells

• perform migration assays on MDA-MB-231 cells, transduce them with the inducible constructs and see if the results obtained with MDA-MB-157 cells are replicated

• knock down *WT1* in more epithelial cell lines (BT20, T47D) and investigate whether a full/partial EMT is induced

• perform tail vein injections in NOD/SCID mice to assess if the metastatic potential of the breast cancer cells is affected by the loss of *WT1*.

4.6.2 *TNC* as a potential WT1 target

In our study, the mesenchymal marker *Tenascin-C* (*TNC*) appears significantly up-regulated in both MDA-MB-157 and MDA-MB-231 knockdown cells.

TNC is an extracellular matrix glycoprotein which is strongly expressed during embryonic development, wound healing and in cancer (reviewed in Jones and Jones 2000). Its expression in breast carcinoma is particularly evident at the invasive front of the tumour, where EMT is supposed to occur, and correlates with more aggressive lung metastasis as well as poorer survival (Jahkola, Toivonen et al. 1996, Jahkola, Toivonen et al. 1998, Oskarsson, Acharyya et al. 2011). Also, breast cancer cells supplemented with TNC have been reported to show EMT-like changes and faster migration (Nagaharu, Zhang et al. 2011).

These findings would suggest that *TNC* up-regulation may be responsible for the phenotype observed in the WT1 knockdown cells. In order to verify this hypothesis, at least two additional experiments should be performed: first, the *TNC* levels need to be analysed through Western blot to confirm protein up-regulation; then, double knockdown cells (for both *WT1* and *TNC*) should be subjected to migration assays, to assess if, and to which extent, the loss of *TNC* can rescue the phenotype.

Since *TNC* upregulation was observed in the knockdown cells of two different lines (MDA-MB-231, MDA-MB-157), through different techniques (RNA-sequencing, RT-PCR) and in both constitutive and inducible systems, there is strong circumstantial evidence suggesting that *WT1* is involved in the regulation of *TNC* expression.

WT1 could regulate *TNC* expression in either a direct or indirect way: in the inducible knockdown cells, significant up-regulation could be detected at the earliest time-point analysed (after only three days of doxycycline treatment), suggesting that *TNC* may be a direct *WT1* target; in order to verify this theory, ChIP analysis should be performed on the breast cancer cells. Alternatively, *WT1* regulation could be indirect and maybe act *via VEGF*; this growth factor is in fact an established *WT1* target (Hanson et al. 2008, McCarty et al. 2011) and is likely upstream of *TNC* (Calvo, Catena et al. 2008).

4.6.3 Possible *WT1* role in the regulation of neuronal genes and nc-RNAs

The RNA-sequencing analysis of WT1 knockdown breast cancer cells has revealed that the modulated genes are unexpectedly enriched in neuronal genes and nc-RNAs.

Several neuronal genes involved in axon guidance have been recently reported to play a role in cancer progression, mainly affecting tumour angiogenesis and cell migration. Among these genes, semaphorins are probably the most important: the SEMA family includes eight different classes of secreted and membrane-bound proteins, some of which can promote tumour progression, while others can inhibit it (reviewed in Tamagnone 2012, Rehman and Tamagnone 2013).

Our RNA-sequencing analysis identified *SEMA3D* and *SEMA5A* as downregulated in the MDA-MB-157 knockdown cells: the former is usually considered as a tumour suppressive semaphorin and is down-regulated in high-grade gliomas (Karayan-Tapon, Wager et al. 2008); the latter has been shown to promote cell migration in pancreatic cancer but to have the opposite effect in gliomas (Sadanandam, Varney et al. 2010, Li, Law et al. 2012).

These two genes may play a role in the phenotype observed in the WT1 knockdown cells, however, before further speculations, RT-PCR should be performed to validate the RNA-sequencing results.

The presence of nc-RNAs among the modulated genes is somewhat less surprising, given that *WT1* is known to play a role in RNA metabolism (reviewed in Hohenstein and Hastie 2006).

The nc-RNAs identified through RNA-sequencing include the microRNA *LET7* and the long nc-RNA *XIST*, respectively up and down-regulated in the WT1 knockdown cells. The *LET7* family members have been reported to negatively regulate *RAS* oncogenes and are therefore considered tumour suppressors (Johnson, Grosshans et al. 2005); *XIST*, on the other hand, is the main mediator of X chromosome inactivation (reviewed in Plath, Mlynarczyk-Evans et al. 2002).

A possible *WT1* role in the regulation of nc-RNAs is in line with the results obtained by other members of our lab: RNA IP experiments have demonstrated that several nc-RNAs interact with the *Wt1* protein and there is strong evidence for a role of WT1 in microRNA processing (Ruthrothaselvi Bharathavikru, personal communication).

In particular, the loss of WT1 in E14 and M15 cells seems to have different effects on *LET7*, depending on the maturity of the transcript: while the pre-miR is upregulated, the expression levels of the mature miR are much lower in the WT1 knockdown than in control cells (Ruthrothaselvi Bharathavikru, personal communication).

Since our RNA-sequencing analysis did not distinguish between pre-miR and mature miR, specific RT-PCR assays should be performed on the breast cancer cells to investigate the expression levels of *LET7* at different stages of processing.

4.6.4 The effect of *WT1* loss on proliferation

In our experiments, knocking down *WT1* did not seem to have a significant impact on cell growth: no major differences were detected in colony forming assays or cell cycle analyses, where only MDA-MB-231 cells transduced with the 1490 construct showed a block in G2/M.

These findings are in sharp contrast with what reported by Zapata-Benavides, who observed significant growth inhibition and cyclin D1 reduction in transient WT1 knockdown cells; this phenotype occurred in the vast majority of the cell lines used in the study, but not in MDA-MB-231 cells (Zapata-Benavides et al. 2002).

This discrepancy can be due to several factors:

• with the exception of MDA-MB-231 cells, the two studies relied on different breast cancer cell lines

• Zapata-Benavides used a transient knockdown and analysed the cells after a 72-hour incubation with antisense oligonucleotides, whereas in our study several weeks elapsed between the delivery of the constitutive constructs and the analysis of the clones; during this time, if the loss of *WT1* did decrease cell growth, the low-expressing *WT1* cells would be disadvantaged and cells characterised by reduced knockdown levels/growth inhibition could be selected. This explanation, however, cannot be applied to the inducible constructs, which represent a closer system to what was used in the older study and yet did not cause any change in proliferation.

• our lentiviral constructs target the zinc finger region of *WT1* (and consequently all its different isoforms), while the antisense oligonucleotides used by Zapata-Benavides are directed against the translation initiation site in exon 1 and therefore cannot knockdown the truncated *WT1* variants.

All in all, uncertainty remains over a potential *WT1* role in the proliferation of breast cancer cells; in order to provide a definitive answer, one crucial experiment could be the sub-cutaneous injection of WT1 knockdown cells in NOD/SCID mice.

4.7 Concluding remarks

The results described in this chapter seem to be more supportive of the tumour-suppressor rather than the oncogene hypothesis: upon *WT1* loss, no major changes are observed in terms of proliferation or apoptosis, however, the knockdown cells undergo a partial EMT, which is usually associated with a more aggressive phenotype.

This finding is in agreement with the *in silico* analysis illustrated in the previous chapter, which suggested that the lack of *WT1* in breast cancer samples may be associated with a more mesenchymal phenotype. On the other hand, these results are in stark contrast with what reported by Miyoshi, who found a correlation between high *WT1* expression and poor prognosis in breast cancer patients (Miyoshi et al. 2002).

The reasons for this divergence are still unclear, but the analysis of larger cohorts of breast cancer patients may help shed some light on the exact *WT1* function in this malignancy.

Chapter 5: Characterisation of a breast cancer mouse model with a mammary-specific *Wt1* conditional knockout

5.1 Introduction

Over the last two decades, genetically engineered mice have been extensively used to study different aspects of breast cancer biology, from tumour initiation to potential therapeutic options.

Several models of this malignancy have been generated, relying on mammary-specific or mammary-selective promoters such as MMTV, WAP and K14; depending on the experimental model, these promoters have been combined with the transgenic overexpression of oncogenes (*Erbb2*, *Myc*, *Ccnd1*) or the targeted ablation of tumour suppressor genes (*Trp53*, *Brca1*, *Pten*) (reviewed in Cardiff, Moghanaki et al. 2000, Borowsky 2011).

Given the extreme heterogeneity of breast cancer and the differences between human and mouse mammary physiology, it would be impossible for the mouse models to recapitulate all the aspects of the human disease: comparative pathology, for example, has shown that the overall histology is quite different and that fibrosis and inflammation are far more common in human tumours than in the mouse counterparts; moreover, the metastases of the murine models are almost exclusively limited to the lungs and do not include sites like liver, bone and brain, which are often affected in breast cancer patients (Cardiff, Anver et al. 2000, reviewed in Vargo-Gogola and Rosen 2007).

Despite these differences, the mouse models can reproduce several aspects of human breast cancer, including the molecular features of specific subtypes (Herschkowitz, Simin et al. 2007), and represent an invaluable tool to investigate this disease.

As mentioned in chapter 1, a considerable amount of data suggests a potential role for WT1 in breast cancer; most of these studies, however, are based on *in vitro* experiments (Zapata-Benavides et al. 2002, Zhang et al. 2003, Burwell et al. 2007, Wang et al. 2008), with the *in vivo* work usually being limited to xenografts or the analysis of WT1 expression in breast cancer patients (Miyoshi et al. 2002, Zhang et al. 2003, Wang et al. 2008).

In order to gain a better understanding on this subject, it would be extremely useful to exploit the potential of breast cancer mouse models, where WT1 could be knocked out and the effects of its loss could be assessed within an *in vivo* context.

5.1.1 Aim

The aims of the experiments described in this chapter were:

• to develop a mouse model of breast cancer with a mammary-specific *Wt1* conditional knockout

• to analyse the consequences of *Wt1* loss in this model, paying particular attention to the size and the epithelial/mesenchymal balance of the tumours.

5.1.2 Experimental approach

Our group had already generated a *Wt1* conditional mouse, in which Exon 1 is flanked by LoxP sites and can therefore be deleted through Cre-mediated recombination (Martinez-Estrada et al. 2010).

In this study, the conditional *Wt1* knockout mice were crossed to the C3(1)/Tag breast cancer model (Maroulakou, Anver et al. 1994) and a C3(1)-driven doxycycline-inducible Cre (the same *C3-Cre* line used for the experiments described in chapter 2) (Figure 5.1).

In the C3(1)/Tag system, tumour formation is induced by the expression of the simian virus 40 large tumour antigen, which binds and inactivates the tumour suppressors p53 and Rb (Holzer, MacDougall et al. 2003).

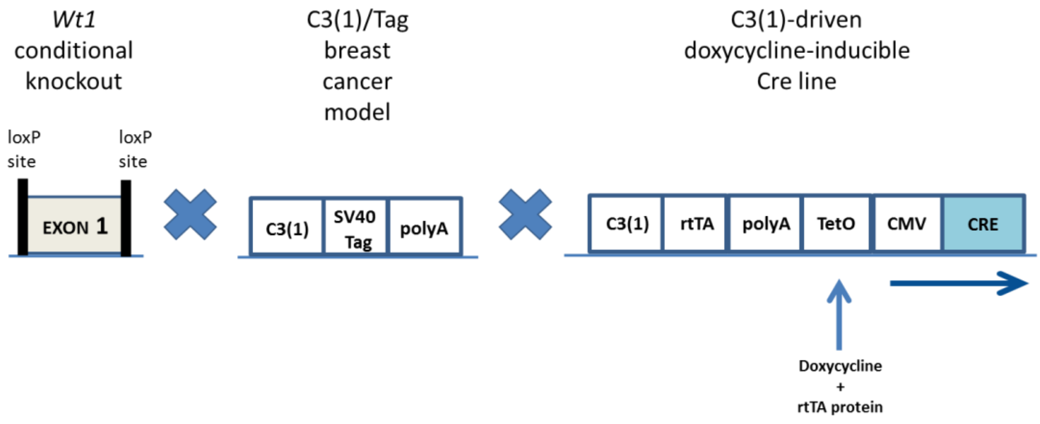

Figure 5.1 Generation of a breast cancer model with a mammary-specific Wt1 conditional knockout.

The conditional *Wt1* knockout mice were crossed to the C3(1)/Tag breast cancer and a C3(1)-driven doxycycline-inducible Cre line.

The C3(1) gene, encoding the C3 subunit of the Prostatic Steroid Binding Protein (PSBP), is expressed in both prostate and mammary glands: since the SV40 Tag is regulated by the C3(1) promoter, its expression is targeted to the epithelium of both organs, driving the development of prostate tumours in male mice and mammary tumours in females (Maroulakou et al. 1994).

Unlike the vast majority of breast cancer models, which rely on the MMTV or WAP promoters, this system does not require hormone treatment or pregnancy to induce tumour formation and is therefore considered a more faithful representation of the human disease (Green, Shibata et al. 2000, Holzer, MacDougall et al. 2003).

From a histological point of view, the lesions observed in this model resemble the human ductal carcinoma *in situ* and evolve quite rapidly: at about 8 weeks of age, the mice show atypia of the mammary ductal epithelium, which soon becomes intraepithelial neoplasia and by 16 weeks of age all the animals have developed an invasive carcinoma (Green et al. 2000).

By crossing this model to the conditional mice and the inducible Cre line, we have obtained a breast cancer model in which *Wt1* deletion can be spatially and temporally regulated through the administration of doxycycline: in this study, the drug was added to the drinking water for 5 consecutive weeks (from the third to the eight after birth) and this timeframe allowed us to knockout *Wt1* in the SV40 Tag-positive population before any cellular transformation takes place.

5.1.3 Breeding scheme

Before the start of my PhD, triple heterozygous mice (Cre$^{+/-}$ *Wt1*$^{co/+}$ Tag$^{+/-}$) were backcrossed for 6 generations to an FVB background, where a more severe and earlier onset mammary phenotype can be achieved (Maroulakou et al. 1994; Peter Hohenstein, personal communication).

In order to facilitate the backcrossing, we used a speed-congenic protocol following 384 polymorphic markers, after which only the regions around *Wt1* and the Cre insertion were still on their original background and the mice could be considered congenics FVB.

After 6 generations, triple heterozygous males and homozygous conditional females, all on congenic FVB background, were inter-crossed to generate experimental animals (Figure 5.2A). From these crosses we obtained Cre+ *Wt1*$^{co/co}$ Tag+ mice (which should develop mammary tumours with Cre-mediated *Wt1* loss) and Cre- *Wt1*$^{co/co}$ Tag+ mice (whose tumours retain *Wt1* expression).

At a later point during the PhD, given the increasing number of reports on the off-target and toxic effects of Cre recombinase (Schmidt et al. 2000, Loonstra et al. 2001, Semprini et al. 2007, Huh et al. 2010), we decided to add a Cre control group to the study; these Cre+ *Wt1*$^{+/+}$ Tag+ mice, which do not carry the conditional allele, were obtained by crossing Cre and Tag double heterozygous mice (Figure 5.2B). As all models were on congenic FVB background, it was possible to directly compare the different crosses.

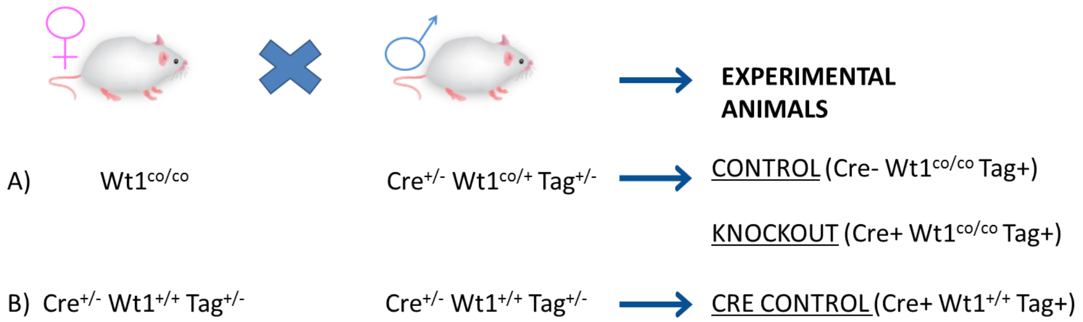

Figure 5.2 Breeding schemes used to obtain the experimental animals.
Triple heterozygous males and homozygous conditional females were inter-crossed to generate control and knockout experimental animals (A); the Cre control group was obtained by crossing Cre and Tag double heterozygous mice (B).

As a whole, three groups of experimental animals were generated and they will be addressed with the following terminology:

CONTROL – Cre-negative $Wt1^{co/co}$ Tag-positive

KNOCKOUT – Cre-positive $Wt1^{co/co}$ Tag-positive

Cre CONTROL – Cre-positive $Wt1^{+/+}$ Tag-positive

5.2 Characterisation of the *Wt1* knockout mammary tumours

As previously mentioned, the three groups of experimental animals were dosed with doxycycline for 5 consecutive weeks (from the third to the eight after birth) to induce the Cre-mediated *Wt1* knockout.

All the mice were examined daily and a record of the tumour onset time was kept for each animal; before the malignancy could cause clear signs of pain or distress, the mice were culled and tumour samples were collected for both immunohistochemistry and gene expression analysis, while the main organs were fixed for metastasis screening.

Full characterisation of the tumour samples was undertaken and included:

• assessment of the *Wt1* knockout through different techniques

• comparison of the tumour onset time in the different groups

• histopathological examination

• RT-PCR and immunohistochemistry analysis of EMT markers.

5.2.1 Assessing *Wt1* knockout

The knockout efficiency was examined at DNA, RNA and protein level through different techniques.

Firstly, a three primer PCR was conducted on the genomic DNA of the tumours: in order to detect the loss of exon 1, the assay was designed with a common forward primer (F2) and two reverse primers (R1, downstream of the 3' loxP site, and R4, in the region between the loxP sites) (Figure 5.3).

Secondly, *Wt1* mRNA levels were assessed through RT-PCR, using primers that target the zinc-finger domain (exon 7/8) and can therefore amplify all the known isoforms; lastly, immunohistochemistry was performed on tumour sections using the

C19 polyclonal antibody from Santa Cruz, which recognises the last 19 residues of the forth Zinc finger.

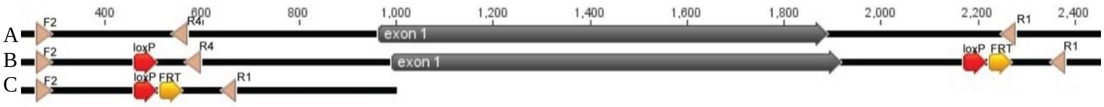

Figure 5.3 Scheme of the three primer PCR used to assess the Cre-mediated loss of *Wt1* exon 1. A) Wildtype Wt1 allele B) Conditional *Wt1* allele C) Recombined conditional *Wt1* allele. (The FRT site is a remainder of the neo selectable marker used for targeting and removed by Flp expression, see Martinez-Estrada et al. 2010).

On a completely wild type allele, the three primer PCR assay can only give a 300 nt F2/R4 fragment, since a hypothetical F2/R1 product would be 2000 nt and therefore too large to amplify under the assay conditions. Similarly, the conditional allele before recombination will only give a 327 nt F2/R4 fragment, as the F2/R1 combination would be 2110 nt long; upon Cre-mediated loss of exon 1, the binding sequence for primer R4 is lost, but primer R1 becomes close enough to F2 to give an amplification product of 420 nt.

As expected, the control tumours only show the conditional band at 327 nt, while all the knockout tumours display the recombined band at 420 nt; however, the shorter 327 fragment can also be observed in some of the knockout samples, suggesting that the Cre is not active in all the tumour cells (a representative gel is shown in Figure 5.4).

The presence of both conditional and recombined bands is most likely due to the fact that this model relies on an epithelial Cre: as described in chapter 2, *Wt1* expression in the mammary gland occurs in different cell types, including myoepithelial, endothelial and luminal epithelial cells; upon doxycycline administration, Cre-mediated recombination takes place in the epithelial compartment, but not in the myoepithelial and endothelial cells, which have un-recombined conditional alleles and therefore produce the short 327 nt fragment.

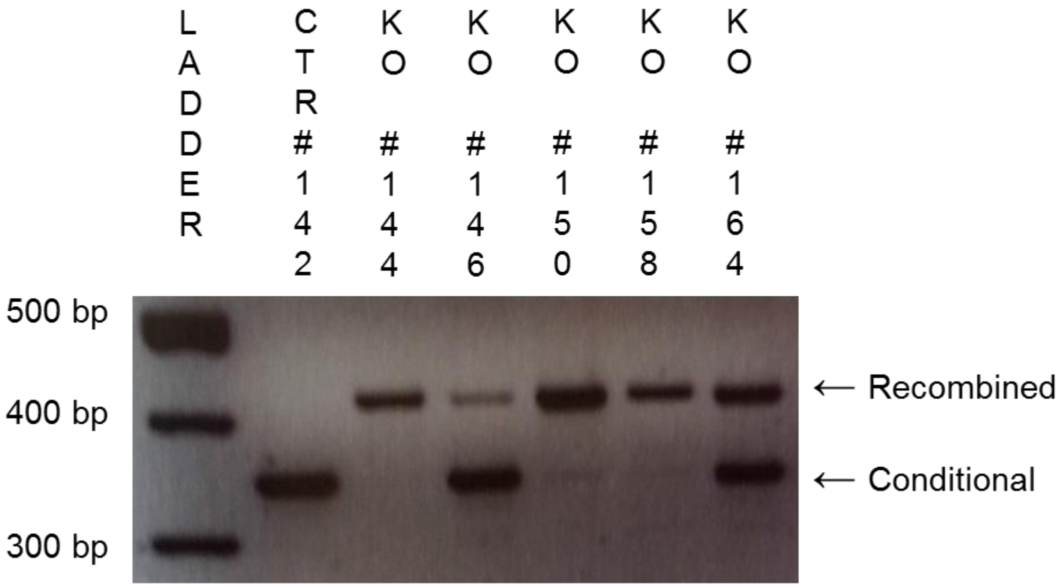

Figure 5.4 Representative gel image showing the products of the three primer PCR assay in control and knockout tumours.

The RT-PCR revealed that *Wt1* mRNA expression is quite low and extremely variable, with just four out of ten control tumours showing relatively high *Wt1* levels (indicated by the red stars in Figure 5.5); moreover, within the knockout group, only eight samples have lower *Wt1* expression than the controls (indicated by the black stars).

The fact that some knockout tumours have expression levels comparable to the high-*Wt1* controls may be due to the presence of "escapee cells": these tumours may in fact arise from cells in which the Cre is not completely active and if the expression of *Wt1* confers an advantage, this subpopulation could then outgrow the low-*Wt1* expressing cells.

The immunohistochemistry performed on the tumour sections revealed that most myoepithelial and endothelial cells stain heavily for WT1 in both control and knockout samples, while the epithelial cells that form the bulk of the tumour show less intense staining (Figure 5.6); even though immunohistochemistry cannot be considered as a quantitative method, no major difference could be observed in the frequency of *Wt1*-positive epithelial cells between control and knockout tumours.

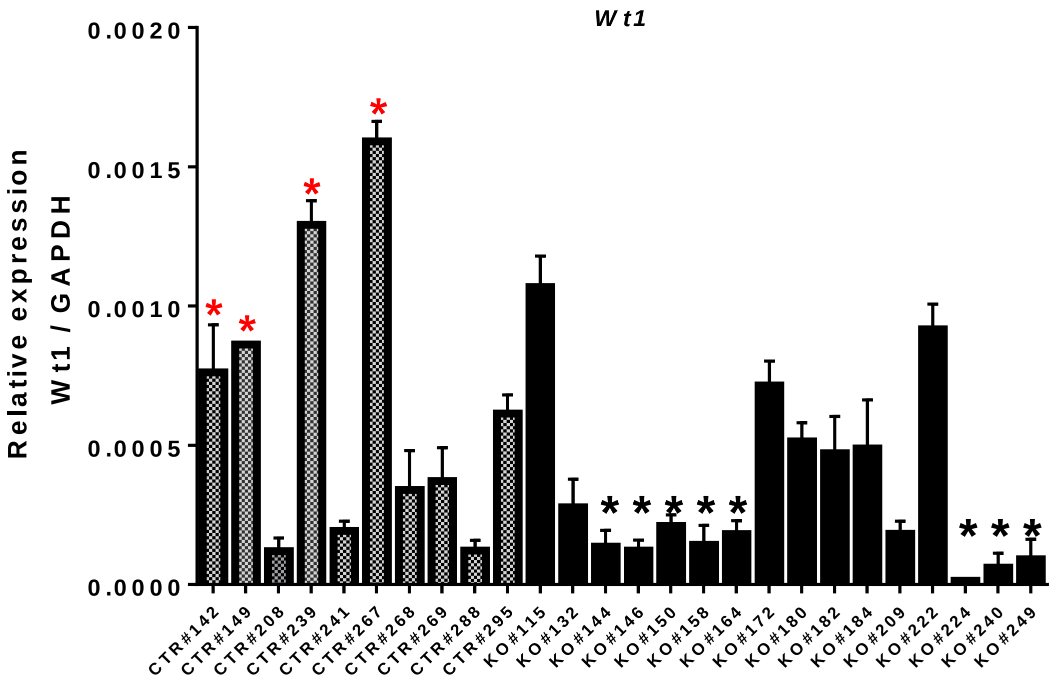

Figure 5.5 Quantitative RT-PCR for *Wt1* mRNA expression (exon 7/8) in the C3(1)Cre Tag tumours.

Data points represent the relative expression, error bars represent the standard deviation of three technical replicates. Red stars indicate the high-*Wt1* expressing controls, black stars indicate the low-*Wt1* expressing knockouts.

Overall, there is no conclusive evidence demonstrating the loss of *Wt1* in the knockout tumours and the lack of a reliable antibody for Western blot further complicates the investigation.

Nonetheless, all the samples were thoroughly examined and the comparison between the controls and the putative knockouts was performed in two different ways: first considering all the samples (n=10 CTR, n=16 KO), then narrowing down the groups according to the RT-PCR results and including only the high-*Wt1* expressing controls (n=4) and the low-*Wt1* expressing knockouts (n=8).

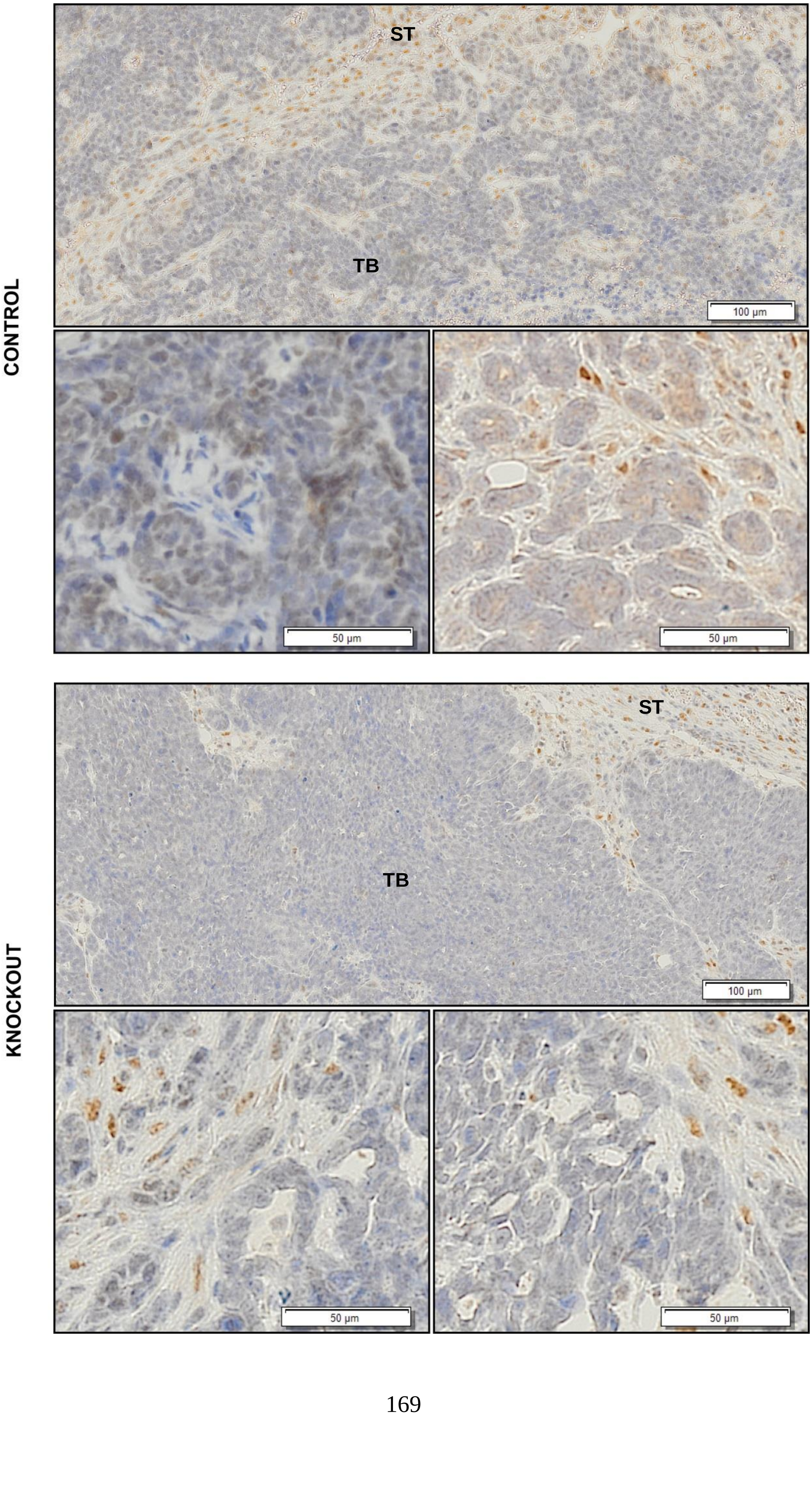
CONTROL
ST
TB
100 µm
50 µm
50 µm
KNOCKOUT
ST
TB
100 µm
50 µm
50 µm

Figure 5.6 WT1 immunohistochemistry of C3(1)Cre Tag tumours.

Images of representative control and knockout samples are shown: the tumour stroma (ST), myoepithelial and endothelial cells stain heavily for WT1 in both control and knockout samples, while the epithelial cells that form the tumour bulk (TB) show less intense staining.

No major difference is observed in the frequency of *Wt1*-positive epithelial cells between control and knockout tumours.

5.2.2 Comparing the tumour onset time

In order to keep a precise record of the tumour onset time, all C3(1)Cre Tag mice were examined and palpated daily to detect the presence of mammary tumors.

Kaplan-Meier curves were calculated by plotting the percentage of tumour-free animals as a function of time for each of the three experimental groups: the tumor latency in the putative knockout animals did not differ significantly from either the control or the Cre control mice and similar results were obtained when the analysis was repeated including only the high-*Wt1* expressing controls and the low-*Wt1* expressing knockouts (Figure 5.7).

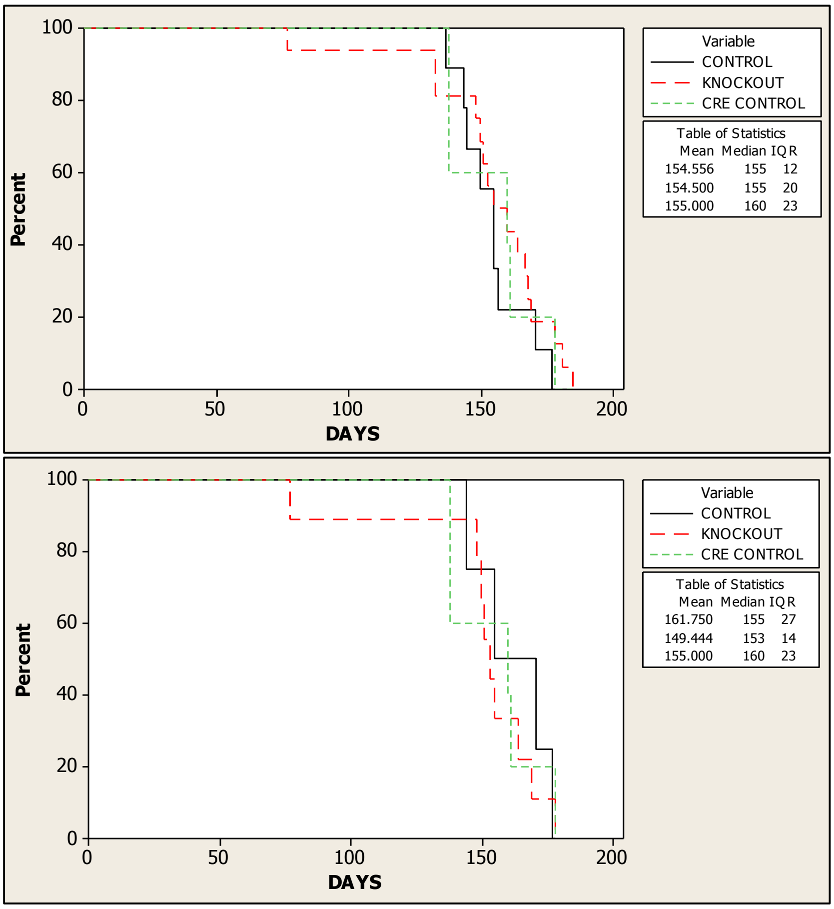

Figure 5.7 Kaplan-Meier curves relative to the C3(1)Cre Tag animals.

The curves plot the percentage of tumour-free animals as a function of time, with time zero indicating the time each mouse was born; the analysis includes all the C3(1)Cre Tag tumours (top) or only the selection based on the RT-PCR results (bottom).

5.2.3 Histopathological analysis

All the samples were analysed by J. Bailey, Specialist in European Veterinary Pathology, and Dr. M. Diaz (Queen's Medical Research Institute, The University of Edinburgh), following the recommendations resulting from the Annapolis meeting on the mammary pathology of genetically engineered mice (Cardiff et al. 2000).

The histopathological study compared the tumour number, size, grade and cell morphology of the three experimental groups: when the statistical analysis was performed on all the samples (n=10 CTR, n=16 KO), the only significant difference was observed in the size of the malignances; the knockout tumours resulted smaller than the controls, but there was no statistically significant difference between the knockouts and the Cre controls, suggesting that this phenotype may not be due to the loss of *Wt1* but to the expression of Cre (Figure 5.8).

When the analysis was repeated including only the high-*Wt1* expressing controls and the low-*Wt1* expressing knockouts, the difference in tumour size lost its significance, but the knockout tumours showed a significant decrease in spindaloid cells; unfortunately, the cell morphology of the Cre controls has not yet been examined (Figure 5.8).

In terms of metastasis screening, only one knockout and one control animal presented secondary tumours, respectively to the lung and the mammary lymph nodes; given the very low metastatic potential showed by this model, it is impossible to determine whether the loss of *Wt1* has any effect on the dissemination of cancer cells to secondary sites.

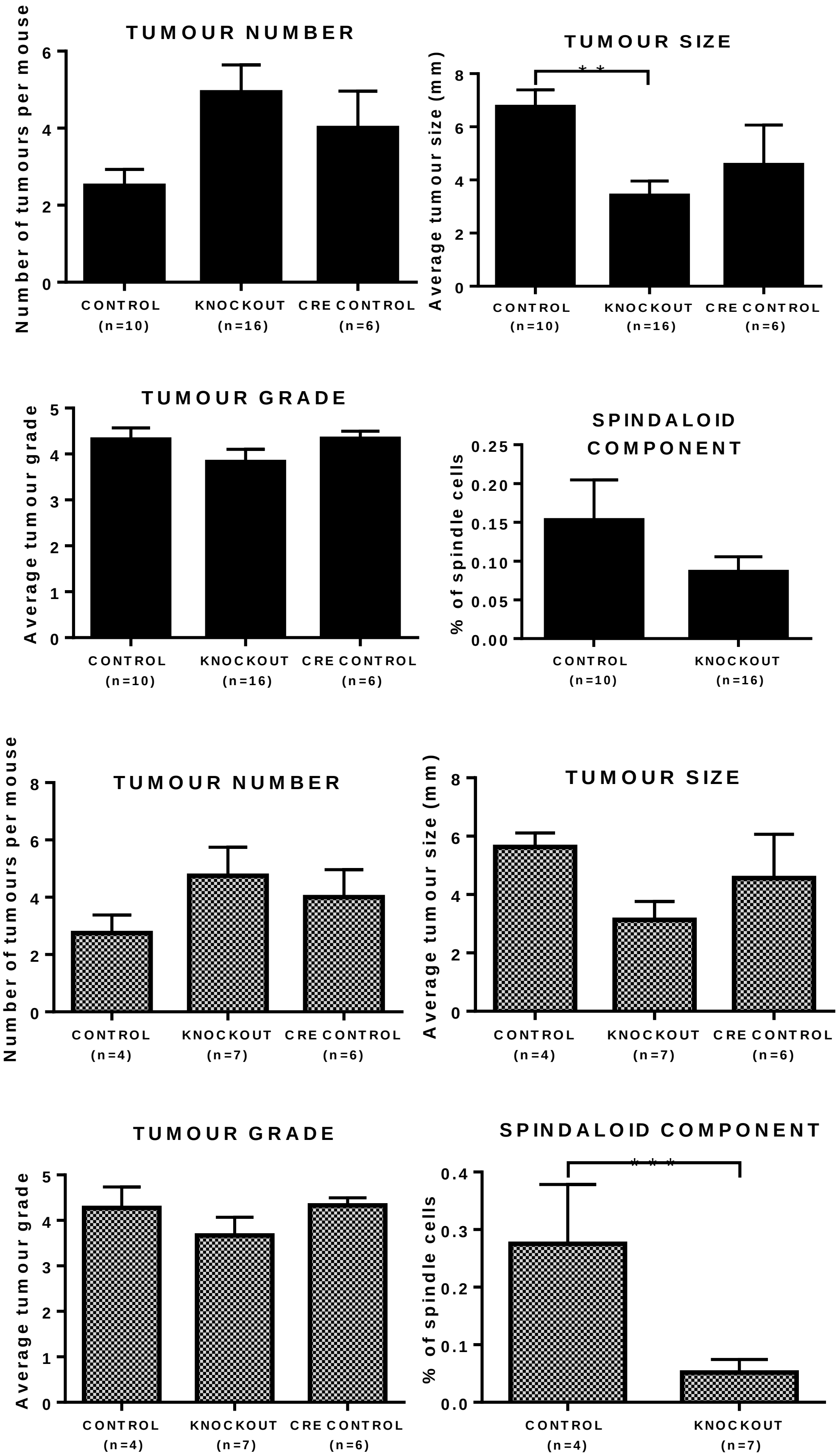
TUMOUR NUMBER
Number of tumours per mouse
0
2
4
6
CONTROL (n=10)
KNOCKOUT (n=16)
CRE CONTROL (n=6)
TUMOUR SIZE
Average tumour size (mm)
0
2
4
6
8
**
CONTROL (n=10)
KNOCKOUT (n=16)
CRE CONTROL (n=6)
TUMOUR GRADE
Average tumour grade
0
1
2
3
4
5
CONTROL (n=10)
KNOCKOUT (n=16)
CRE CONTROL (n=6)
SPINDALOID COMPONENT
% of spindle cells
0.00
0.05
0.10
0.15
0.20
0.25
CONTROL (n=10)
KNOCKOUT (n=16)
TUMOUR NUMBER
Number of tumours per mouse
0
2
4
6
8
CONTROL (n=4)
KNOCKOUT (n=7)
CRE CONTROL (n=6)
TUMOUR SIZE
Average tumour size (mm)
0
2
4
6
8
CONTROL (n=4)
KNOCKOUT (n=7)
CRE CONTROL (n=6)
TUMOUR GRADE
Average tumour grade
0
1
2
3
4
5
CONTROL (n=4)
KNOCKOUT (n=7)
CRE CONTROL (n=6)
SPINDALOID COMPONENT
% of spindle cells
0.0
0.1
0.2
0.3
0.4
***
CONTROL (n=4)
KNOCKOUT (n=7)

Figure 5.8 Graph summary of the histopathological analysis carried out on the C3(1)Cre Tag tumours.

The analysis included all the samples (top) or a selection based on the RT-PCR results (bottom) (** $p<0.01$, *** $p<0.001$).

5.2.4 EMT markers analysis

As mentioned in chapter 1, there is some evidence suggesting that WT1 may play a role in the induction of cancer-related EMT, while the experiments described in the previous chapter show that the *WT1* knockdown cells undergo a partial EMT.

In order to investigate whether the epithelial/mesenchymal balance of the tumours is somehow affected by the loss of *Wt1*, the expression of several markers was examined through RT-PCR and immunohistochemistry.

The mRNA levels of EMT drivers (*Snai1*, *Snai2*, *Zeb1*, *Zeb2*, *Twist1*), epithelial (*Cdh1*, *Ctnna1*, *Ctnnd1*) and mesenchymal markers (*Cdh2*, *Fn1*, *Vim*) were analysed in the high-*Wt1* controls and the low-*Wt1* knockouts: the RT-PCR results showed that the expression levels in the tumours are quite variable and no statistically significant difference could be observed between the two experimental groups (Figure 5.9, 5.10, 5.11).

Similarly, the immunohistochemistry performed with antibodies against SNAIL, TWIST1, ZEB2 and VIMENTIN did not detect any major difference between the staining pattern of control and knockout samples (Figure 5.12).

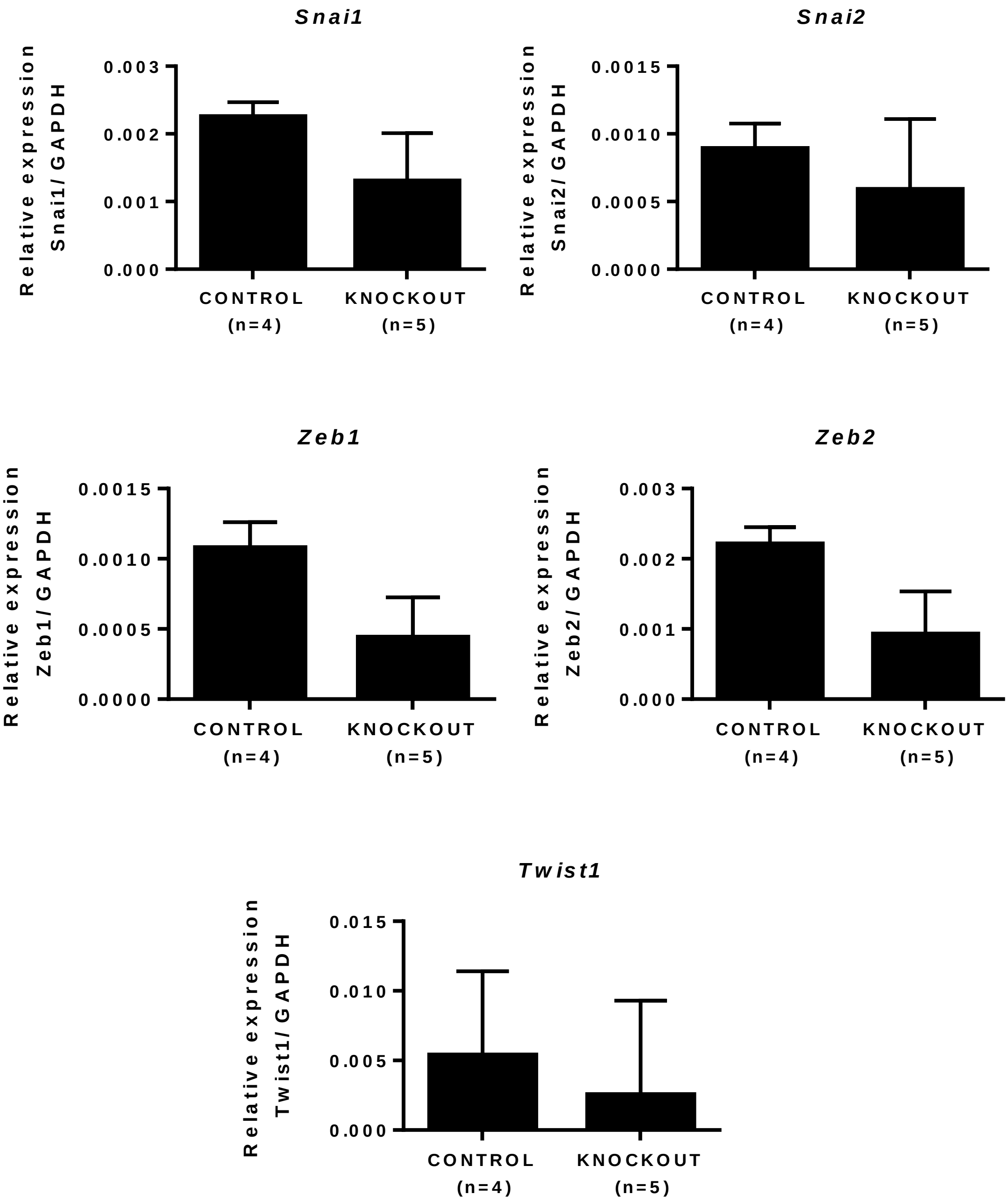

Figure 5.9 Quantitative RT-PCR of EMT drivers in the C3(1)Cre Tag tumours.

Data points represent the relative expression of the gene, error bars represent the standard deviation of the biological replicates indicated in brackets.

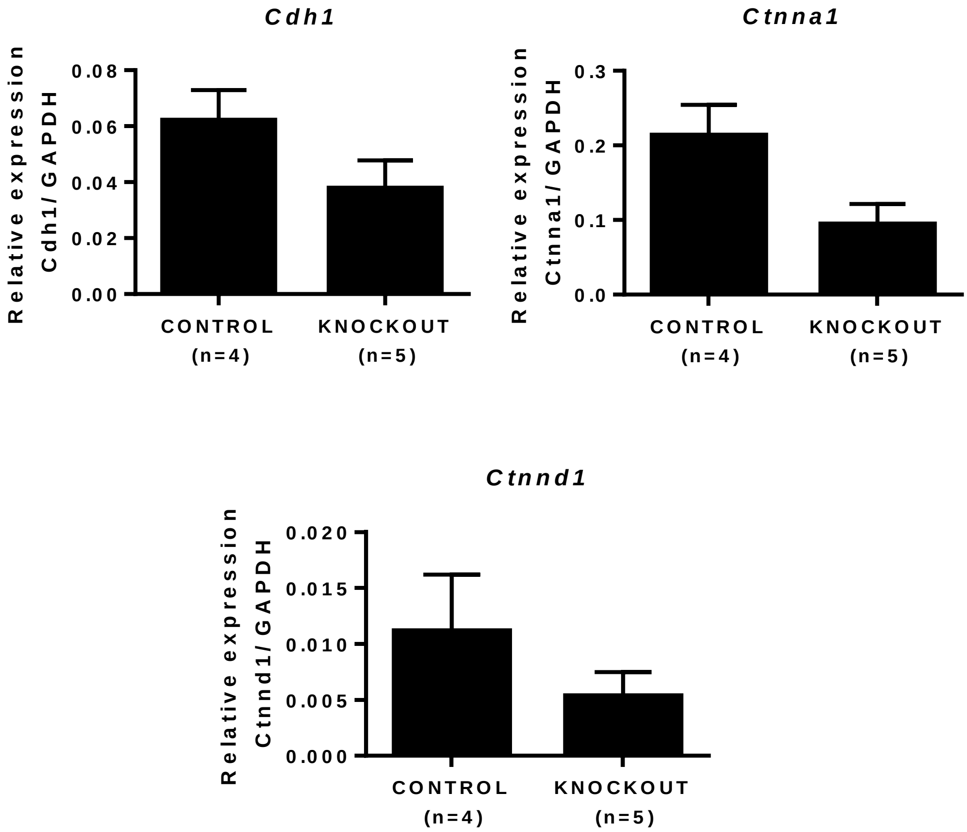

Figure 5.10 Quantitative RT-PCR of epithelial markers in the C3(1)Cre Tag tumours.
Data points represent the relative expression of the gene, error bars represent the standard deviation of the biological replicates indicated in brackets.

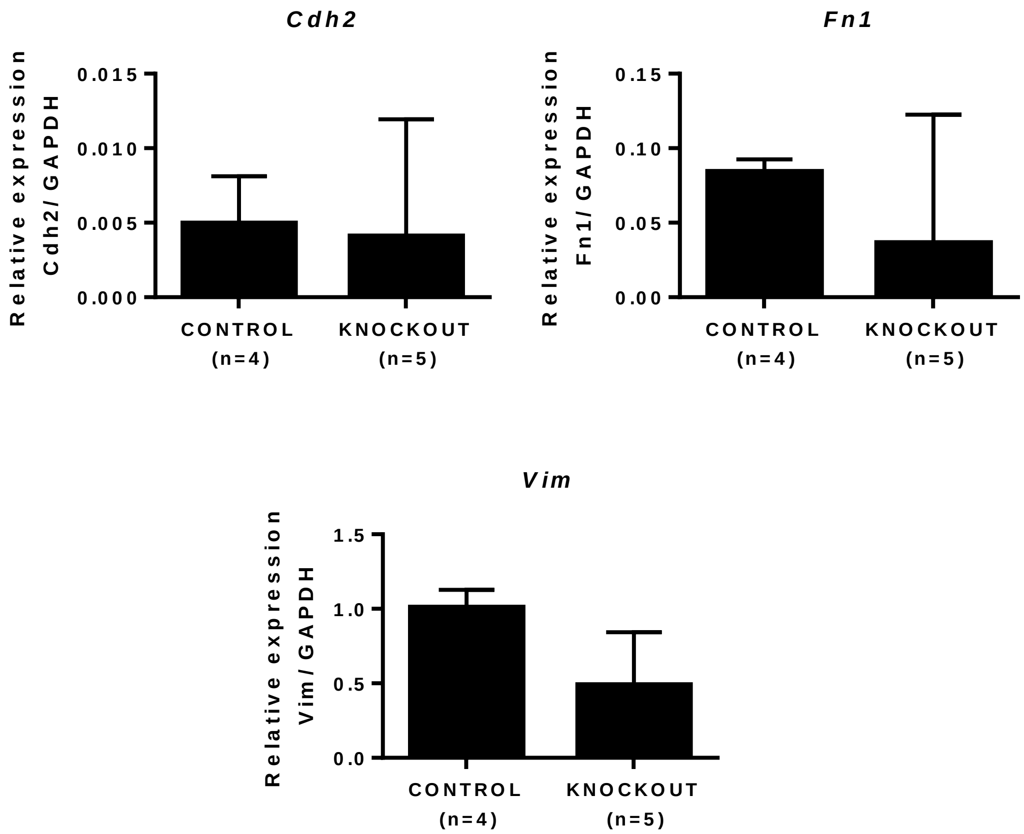

Figure 5.11 Quantitative RT-PCR of mesenchymal markers in the C3(1)Cre Tag tumours. Data points represent the relative expression of the gene, error bars represent the standard deviation of the biological replicates indicated in brackets.

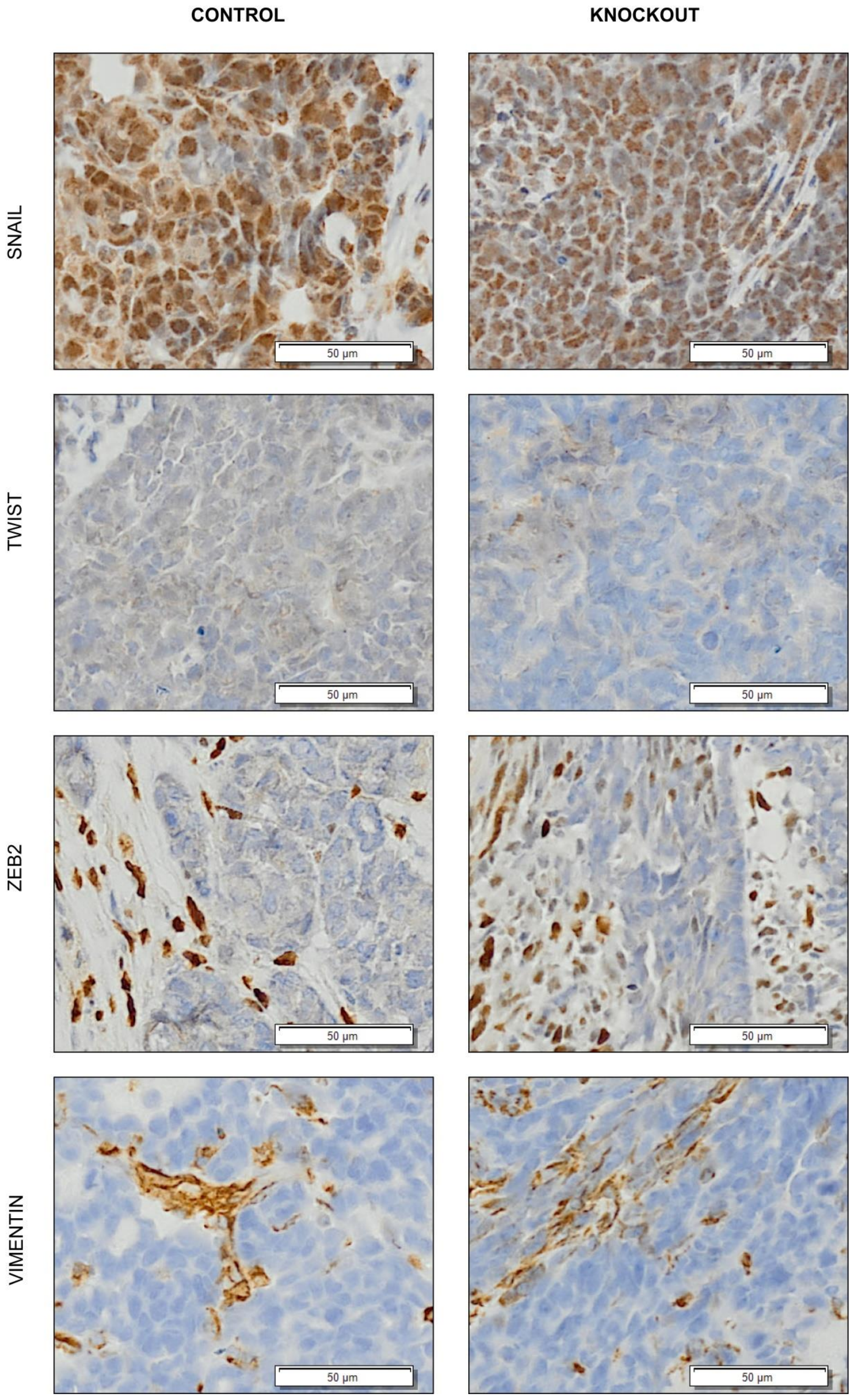
CONTROL
KNOCKOUT
SNAIL
TWIST
ZEB2
VIMENTIN
50 µm

Figure 5.12 Immunohistochemistry of EMT markers in C3(1)Cre Tag tumours.

Images of representative control and knockout samples are shown; no significant differences are observed in the staining pattern of SNAIL, TWIST, ZEB2 and VIMENTIN.

5.2.5 Additional experiments

As mentioned in paragraph 5.2.1, the fact that some knockout tumours have relatively high *Wt1* levels may be due to the presence of escapee cells and two different strategies have been adopted to address this issue.

Firstly, primary cultures were established from control and knockout tumours developed in mice which had not received any doxycycline treatment; after one week of cell propagation, doxycycline was added daily to the culture media at a concentration of 2µg/ml, in the hope that a direct *in vitro* sub-ministration would give rise to a more homogeneous population of *Wt1* knockout cells.

RT-PCR showed that only three of the five primary cultures analysed were positive for *Wt1* and when detectable, the expression levels were extremely low (with relative expression values < $3x10^{-5}$). The administration of doxycycline to the knockout tumours seemed to reduce *Wt1* mRNA in sample #362 and increase it in #371 (Figure 5.13), but the expression levels were so low that the results cannot be considered reliable and the only conclusion that can be drawn from this experiment is that *Wt1* expression in the primary cultures is almost undetectable.

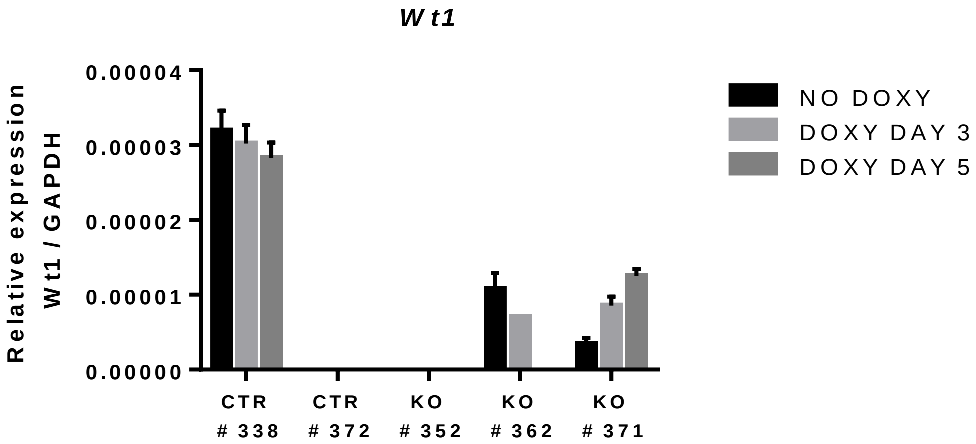

Figure 5.13 Quantitative RT-PCR for *Wt1* mRNA expression (exon7/8) in the primary cultures of C3(1)Cre Tag tumours.

Data points represent the relative expression, error bars represent the standard deviation of three technical replicates.

Secondly, we aimed to cross the conditional *Wt1* knockout mice to the *MMTV-NIC* breast cancer model, where tumour formation is driven by an activated version of Her2 (Neu) under the control of the mouse mammary tumour virus promoter (Schade, Rao et al. 2009).

As shown in Figure 5.14, the presence of an internal ribosome entry sequence between the cDNA of Her2 and Cre ensures that they are both expressed within the same mammary epithelial cell; using this model would prevent the formation of escapee cells because every tumour cell will express similar levels of Cre recombinase, leading to a more homogeneous knockout of *Wt1*.

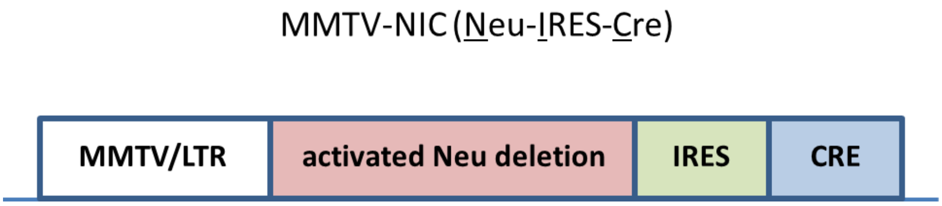

Figure 5.14 Scheme of the *MMTV-NIC* mouse model of breast cancer.
In the *MMTV-NIC* breast cancer model, tumour formation is driven by an activated version of Her2 (Neu) under the control of the mouse mammary tumour virus promoter; the presence of an internal ribosome entry sequence between the cDNA of Her2 and Cre ensures that they are both expressed within the same mammary epithelial cell.

Before crossing this model to the conditional *Wt1* knockout mice, RT-PCR was performed on two different *MMTV-NIC* tumours to assess the *Wt1* mRNA levels; unfortunately, both samples resulted negative for *Wt1* expression (data not shown) and the experiments were not pursued any further.

5.3 Discussion

The experiments described in this chapter were not particularly successful, in that a breast cancer model with a *Wt1* conditional knockout was generated, but we could not unequivocally demonstrate that the knockout was efficient.

Additional experiments may help in this respect (eg. WT1 immunofluorescence, Western Blot with a reliable antibody), however, it is probably not worthwhile investigating this model any further.

Even if definitive evidence of *Wt1* loss was to be gathered, no major differences have been observed between the control and knockout tumours: the size reduction may in fact be caused by the expression of Cre recombinase and the decrease of spindle cells, while interesting, is unlikely to reflect any real shift in the epithelial/mesenchymal balance of the tumours, since both RT-PCR and immunohistochemistry have shown no difference in the EMT markers.

The main limitation of this work lies in the use of an epithelial Cre when, at least in the C3(1)Tag animals, *Wt1* is mainly expressed in the myoepithelial and endothelial compartments. This expression pattern was first observed through immunohistochemistry and later confirmed by the extremely low *Wt1* levels of the primary cultures, where the myoepithelial and endothelial cells are not propagated as efficiently as the epithelial cancer cells.

The fact that the epithelial cells of C3(1)Tag tumours have very low levels of *Wt1* and that no expression whatsoever was found in the MMTV-NIC model would suggest that *Wt1* is unlikely to play any major role in breast cancer.

However, microarray studies have detected significant *Wt1* expression in different breast cancer models, such as WAP-*Int3*, WAP-*Myc*, MMTV-*Wnt1* and DMBA-induced (Herschkowitz et al. 2007).

Future studies may be planned to cross these models with the *Wt1* conditional mice, but preliminary experiments are required to determine if the truncated transcript we have detected in several human breast cancer lines (see chapter 3) is also present in the mouse mammary tumours; should this be the case, the current conditional (in which exon 1 is flanked by LoxP sites) would not be able to target the intron 5 isoform and a new one should be generated.

Wt1 expression in the myoepithelial compartment is particularly fascinating because these cells have been shown to exhibit many anti-tumorigenic properties (reviewed in Adriance, Inman et al. 2005); a study on PABC, an extremely aggressive form of breast cancer which is associated with pregnancy, has revealed that the myoepithelial expression of *Wt1* is drastically reduced in these tumours, suggesting that it may be important for the tumour-suppressing activity of the myoepithelial cells (Xu, Wang et al. 2009).

Future projects should consider the generation of endothelial- and myoepithelial-specific knockout models, in order to investigate the exact role played by *Wt1* in these two cell types.

All in all, this part of the project was not very informative, but it helped in the identification of new experiments which could improve our understanding of *Wt1* role in breast cancer.

Chapter 6: General discussion

6.1 Summary of results

The major findings described in this thesis can be summarised as follows:

• WT1 expression in the mammary gland is mainly restricted to MaSCs, myoepithelial and endothelial cells

• *Wt1* knockout glands form a higher number of side branches during pregnancy, which could be due to an alteration of the epithelial-mesenchymal balance at the branching sites

• *WT1* expression in breast cancer is not particularly high, neither *in vivo* nor *in vitro*, and is lower than in the healthy mammary tissue

• bioinformatics analysis showed that the *WT1*-positive tumours mainly belong to the luminal/ER-positive subtypes and express lower levels of mesenchymal markers than the *WT1*-negative tumours

• the truncated transcript starting from intron 5 is likely to be a tumour-specific *WT1* isoform

• knocking down *WT1* in breast cancer cells triggers a partial EMT and an increase in cell motility.

6.2 A new perspective on WT1 role in normal and neoplastic mammary cells

At the start of this PhD, WT1 role in breast cancer was still unclear and had been described as oncogenic by some authors (Loeb et al. 2001, Miyoshi et al. 2002, Zapata-Benavides et al. 2002), as tumour suppressing by others (Huang et al. 1997, Laux et al. 1999, Cheng et al. 2001, Zhang et al. 2003, Wang & Wang 2008).

Based on the analysis of *WT1* knockdown breast cancer cells, this work seems to rule out a potential oncogenic function and be more in line with the tumour suppressor hypothesis: upon *WT1* loss, in fact, the knockdown cells undergo a partial EMT, which is usually associated with a more aggressive phenotype characterised by increased tumour invasion and metastasis (Trimboli et al. 2008, Brabletz et al. 2005, Prall 2007, Micalizzi et al. 2010, Iwatsuki et al. 2010).

However, since no major changes are observed in terms of proliferation or apoptosis, the label of tumour suppressor is probably not the most appropriate in this context. As pointed out by Huff, applying this whole oncogene/tumour suppressor terminology to WT1 can be quite misleading: these categories are usually used for genes such as receptor tyrosine kinases or p53, which have a direct role in the regulation of cell proliferation, cell cycle and apoptosis, while WT1 effect on these pathways, when detectable, is mainly indirect (Huff 2011).

At the current state of research, the WT1 role supported by the strongest experimental evidence is that of regulator of the epithelial-mesenchymal balance during embryonic development (reviewed in Hohenstein and Hastie 2006).

Several of our findings would indicate a similar function for WT1 in the adult mammary gland, in both healthy and neoplastic cells: firstly, the increased number of pregnancy-associated side branches observed in the *Wt1* knockout glands may be due to an alteration of the epithelial-mesenchymal balance at the branching sites. Secondly, *WT1*-negative breast cancer show higher levels of mesenchymal markers than the *WT1*-positive and, lastly, the loss of *WT1* induces a partial EMT in breast cancer cells.

Taken together, these results depict a scenario where WT1 expression is important to maintain the epithelial state of the mammary cells: with its loss, there is a shift towards a more mesenchymal phenotype, which leads to increased branching in the healthy gland and increased motility in the cancer cells.

Further investigation is still required to validate this theory, in particular to verify any alteration of the epithelial-mesenchymal balance at the branching sites of the *Wt1* knockout glands and to assess if the mesenchymal/migratory phenotype observed in the knockdown cells is translated in increased tumour invasion and metastasis *in vivo*.

However, if confirmed by the additional experiments, this theory would provide a brand new perspective on WT1 role in the mammary tissue as well as identify a potential therapeutic target to tackle the migration of breast cancer cells.

6.3 Future work

As mentioned in the discussion sections of the respective chapters, several experiments have already been planned to address the outstanding questions emerging form this thesis, first and foremost how does the loss of WT1 cause the *in vivo* and *in vitro* phenotypes just described?

6.3.1 Further investigation on WT1 contribution to mammary gland development

One of the most interesting findings in this thesis was the observation that *Wt1* is expressed in the MaSCs, however, there was insufficient time to establish which cell lineage originates from the WT1-positive stem cells.

This question will be addressed using a lineage-tracing approach similar to the one adopted by Van Keymeulen, who first determined the fate of the K14- and K8-

expressing progenitor cells in the mammary gland (Van Keymeulen, Rocha et al. 2011).

The first step is to generate an inducible Cre line under the transcriptional regulation of the *Wt1* promoter, by using either a CreERT2 (already available in our laboratory) or a TetO-Cre (Van Keymeulen et al. 2011), and then cross it with the *Rosa26R*$^{YFP/YFP}$ reporter strain.

Depending on the Cre line adopted, tamoxifen injections or doxycycline administration can be used to follow the fate of the WT1-expressing stem cells throughout the different phases of the mammary cycle.

Given the similarities between MaSCs and embryonic mammary cells (Wansbury, Mackay et al. 2011), future experiments should also assess if WT1 is expressed in the mammary structures of the embryo.

Considering some key features of the developing gland, a positive result would not be totally unexpected: both the mammary primordial epithelium and the associated mesenchyme have been shown to express EMT-associated genes (Wansbury et al. 2011), while the Wnt/β-catenin signalling pathway, which is essential for the embryonic gland (reviewed in Incassati, Chandramouli et al. 2010), is negatively regulated by *Wt1* in the developing testis (Chang, Gao et al. 2008).

6.3.2 Further investigation on the branching phenotype

One of the main outstanding questions concerns the molecular mechanisms behind the branching phenotype observed in the knockout gland.

At least two different hypotheses could be formulated to explain the increased number of branches: if WT1 expression in the mammary gland is indeed important to keep the cells in an epithelial state, for example by repressing *Snai1*, its loss may shift the cell towards a mesenchymal phenotype, which is more permissive for branching formation (Micalizzi et al. 2010, Nisticò et al. 2012, Kouros-Mehr & Werb 2006, Lee et al. 2011). Alternatively, WT1 may directly repress the expression of important branching promoters such as *Wnt4* and *Agr2* (Brisken et al. 2000, Verma et al. 2012); with the deletion of *Wt1*, both genes would be upregulated, leading to the formation of more branches.

Significantly, *Wnt4* and *Snai1* are established *Wt1* targets in the developing heart and kidney (Essafi et al. 2011, Martinez-Estrada et al. 2009), and our RNA-sequencing experiment has identified *Agr2* as a potential WT1 target in breast cancer cells.

ChIP will be required to verify if WT1 directly regulates the transcription of these genes in the mammary tissue or if alternative mechanisms should be investigated.

6.3.3 Further investigation on the role of WT1 in breast cancer

A major disappointment during this project was the failure to generate a robust *Wt1* knockout mouse model of breast cancer.

Our *C3(1)Tag* animals developed mammary tumours with low and extremely variable levels of *Wt1* mRNA and, since the protein expression could not be assessed due to the lack of a reliable WT1 antibody for Western blot, we could not demonstrate the efficiency of the knockout.

The main limitation of this work, however, lies in the use of an epithelial Cre when, at least in the *C3(1)Tag* tumours, *Wt1* is mainly expressed in the myoepithelial and endothelial compartments.

Since an *in vivo* approach remains the best option to investigate WT1 role in breast cancer, future work should aim at the generation of a new knockout model and take into account the issues encountered in this project: firstly, by choosing a breast cancer model where significant *Wt1* expression has already been observed, such as WAP-*Int3*, WAP-*Myc* and MMTV-*Wnt1* (Herschkowitz et al. 2007); secondly, by using either a Cre line that can target both the epithelial and myoepithelial populations (eg. MMTV-Cre, Wagner et al. 2001) or endothelial-specific lines such as VE-Cadherin and Tie-1 Cre (Gustafsson, Brakebusch et al. 2001, Alva, Zovein et al. 2006).

Besides the generation of the new knockout model, additional experiments should also be performed to further investigate the results obtained from the *in vitro* work.

The analysis of breast cancer cells transduced with lentiviral RNAi constructs has revealed that the loss of *WT1* triggers a partial EMT: the knockdown cells migrate faster than the controls and express higher levels of mesenchymal markers and EMT drivers (*TNC*, *ZEB2*, *TGFB1*), suggesting that WT1 may negatively regulate these transcripts.

Interestingly, WT1 has already been shown to repress *TGFB1* expression in kidney cells (Dey et al. 1994), while breast cancer cells supplemented with TNC display EMT-like changes and faster migration (Nagaharu et al. 2011).

ChIP experiments will determine if WT1 directly regulates these genes in breast cancer or if, alternatively, the overexpression observed in the knockdown cells is due to downstream indirect effects.

Independently of the molecular mechanism causing this partial EMT, it needs to be established if the mesenchymal/migratory phenotype observed in vitro is somehow translated in vivo: in this optic, tail vein injections in NOD/SCID mice are currently being performed to assess if the metastatic potential of the knockdown cells is affected by the loss of WT1.

6.4 Concluding remarks

Using a conditional knockout model, this study has established that *Wt1* is not necessary for the post-natal development of the mammary gland, but may have a role in the regulation of the side branching that occurs during pregnancy: the *Wt1* knockout glands form a higher number of branches, which could be due to an alteration of the epithelial-mesenchymal balance.

Moreover, *in silico* and *in vitro* analyses have showed that the loss of *WT1* pushes breast cancer cells towards a more mesenchymal and migratory phenotype.

As a whole, the results of this thesis suggest that WT1 expression may be important to maintain the epithelial state of the mammary tissue, identifying WT1 as a potential regulator of the epithelial-mesenchymal balance in both normal and neoplastic mammary cells.

Chapter 7: Materials and methods

7.1 Cell culture

7.1.1 Tumour cell lines

All the cancer cell lines used in this study were cultured in the appropriate medium (Table 7.1) supplemented with 10% FCS, glutamine, penicillin/streptomycin and maintained at standard cell culture conditions (37°C, 5% CO_2 in humidified incubator).

Tet System Approved FBS (Clontech 631106) was used in the culture media of TRIPZ-transduced cells, to ensure that the inducible regulation of the system was not altered by the presence tetracycline-derived contaminants.

7.1.2 Primary cultures from *C3TCo* mammary tumours

The tumours were minced with a McIlwain Tissue Chopper (kindly provided by Dr. Patel) and then transferred to a digestion mix consisting of 5ml serum-free DMEM (Sigma D567) supplemented with 20mg Collagenase B (Roche 11088815001), 20 mg Dispase (Gibco 17105-041) and 2mg Hyaluronidase (Sigma H3884).

This was incubated for 2 hours at 37^{o}C in a shaking incubator and then centrifuged for 5 minutes at 1200 rpm; after discarding the supernatant, 5 ml trypsin were added to the pelleted cells and incubated for 5 minutes at 37 ^{o}C while shaking.

Trypsin was inactivated by washing the cells in 10 ml PBS/ 2% FCS; the pellet was then resuspended in 2 ml PBS/2% FCS containing 5µl DNase (Ambion AM1907) and incubate at room temperature for 2 minutes. After dissociating the pellet with a p1000 pipette, the cells were washed in 10 ml PBS/2% FCS, passed through a 70 µm strainer and counted.

Table 7.1 List of cancer cell lines used in the project.

CELL LINE	MEDIUM	CELL TYPE
MDA MB 231	DMEM (Sigma D5796)	Breast cancer cells (ER-, PR-, HER2-)
MDA MB 157 (a kind gift from D. Sproul)	DMEM (Sigma D5796)	Breast cancer cells (ER-, PR-, HER2-)
MDA MB 435S	DMEM (Sigma D5796)	Breast cancer cells (ER-, PR-, HER2-)
MDA MB 453	DMEM (Sigma D5796)	Breast cancer cells (ER-, PR-, HER2-)
HBL100	DMEM (Sigma D5796)	Breast cancer cells (ER-, PR-, HER2-)
MCF7	DMEM (Sigma D5796)	Breast cancer cells (ER+, PR+, HER2-)
BT549 (a kind gift from D. Sproul)	RPMI (Sigma R0883)	Breast cancer cells (ER-, PR-, HER2-)
BT474	RPMI (Sigma R0883)	Breast cancer cells (ER+, PR+ , HER2+)
BT20	DMEM (Sigma D5796)	Breast cancer cells (ER-, PR-, HER2-)
SKBR3	DMEM (Sigma D5796)	Breast cancer cells (ER-, PR-, HER2+)
T47D	DMEM (Sigma D5796)	Breast cancer cells (ER+, PR+, HER2-)
ZR75	DMEM (Sigma D5796)	Breast cancer cells (ER+, PR-, HER2-)
HS578T	DMEM (Sigma D5796)	Breast cancer cells (ER-, PR-, HER2-)
PANC1	DMEM (Sigma D5796)	Pancreatic cancer cells

The cells were cultured in DMEM/10% FCS supplemented with 1% penicillin/streptomycin and maintained at standard cell culture conditions (37°C, 5% CO_2 in humidified incubator).

Cre recombinase was induced by the addiction of Doxycycline Hyclate (Sigma D9891) to the culture medium. Doxycycline was added to PBS, filter sterilised and kept in the dark at 4 °C until use; the appropriate volume was added daily to the culture media to obtain a final concentration of 2 µg/ml.

7.1.3 Cell migration assay

Migration assays were performed on 24well plates containing culture inserts made of biocompatible silicone material (Ibidi 80209).

For each experiment, cells were washed with PBS, trypsinised and resuspended in culture medium to obtain a concentration of 5 x 10^5 cells/ml; 70 µl of this cell suspension were applied to each well of the insert and incubated under normal conditions for 24 hours to allow cell attachment.

The next day, the inserts were removed using sterile tweezers and 2ml of medium were added to each well; the plate was then placed in the incubation chamber of a Nikon TiE (Perfect Focus System) microscope and three areas per well were randomly identified.

Time-lapse photography was carried out by taking serial images across each area every 30 minutes, over 40 hours.

Quantification of cell migration was performed using ImageJ.

7.1.4 Colony-forming assay

Sphere formation was induced by culturing the cancer cells in suspension in serum-free medium (DMEM-F12 + GlutaMAX-I, Life Technologies 10565-018) supplemented with B27 (1:50, Life Technologies 12587-010), 20 ng/mL EGF (R&D

236-EG-01M), 0.4% bovine serum albumin (Sigma A9576-50ML), 4 μg/mL insulin (Sigma I3536-100MG) (Yu et al. 2007).

To quantify colony formation, cells were plated at a density of 1,000 cells per well in 96-well plates coated with poly(2-hydroxyethyl metacrylate) to prevent cell attachment to the surface (Sigma P3932-10G); cells were diluted in supplemented serum-free media containing 1% methylcellulose (Sigma M0512-100G) and the number of colonies > 75 μm in diameter was counted after 11 days (Wellner et al. 2009).

7.1.5 FACS analysis

Flow cytometer analysis and sorting were performed by Dr. Freyer, MRC HGU Core Technical Services, using a FACSAriaII Flow Cytometer (Becton Dickinson) equipped with violet (404 nm), blue (488 nm), green (532 nm), yellow (561 nm) and red (635 nm) lasers. Data were analysed using FlowJo software.

7.1.5.1 Sorting of GFP-positive cells

Cells were washed with PBS, trypsinised and resuspended in 1ml PBS/0.5% FCS; for all the experiments, GFP-negative control cells were used to set the parameters for the FACS gating.

Cells were sorted either in RNAlater (for RNA extraction) or FCS (for further expansion in culture).

7.1.5.2 Cancer stem cell markers analysis

For each sample, $1x10^6$ cells were resuspended in 100μl PBS/5% FCS and incubated in the antibody dilution shown in Table 7.2.

The GIPZ-transduced cells were incubated with CD44-APC and CD24-PE antibodies, the TRIPZ-transduced cells with CD44-APC and CD24-FITC (the RFP of the TRIPZ vectors would have overlapped with the signal of the PE-conjugated antibody).

After a 15 minute incubation on ice, the cells were washed twice in PBS, resuspended in 100µl PBS/5% FCS and analysed.

Table 7.2 Antibodies used for CSCs analysis

Antibody (clone)	Species	Source (Cat. no.)	Dilution
CD44-APC (G44-26)	Mouse	BD Pharmingen (559942)	2.5 µl/100 µl
CD24-PE (ML5)	Mouse	BD Pharmingen (555428)	10 µl/100 µl
CD24-FITC (ML5)	Mouse	BD Pharmingen (555427)	1.25 µl/100 µl

7.1.5.3 Apoptosis and cell cycle analysis

The Annexin V Apoptosis Detection Kit APC (eBioscience 88-8007) was used according to the manufacturer’s instructions: cells were washed once and resuspended at a concentration of $1x10^6$ cells/ml in the binding buffer provided with the kit; 5 µl of the APC-conjugated antibody were added to 100 µl of cell suspension and incubated for 15 minutes at room temperature.

After one wash, cells were resupended in 200 µl of binding buffer and 1 µg/ml DAPI (Sigma D9542) was added immediately before the analysis.

For cell cycle analysis, cells were trypsinised and resuspended in 1.2 ml PBS; 3ml ice cold 95% ethanol were then added dropwise while vortexing, to obtain a final 70% ethanol solution where the cells were incubated for 30 minutes.

After two washes in PBS, cells were pelleted and counted; $1x10^6$ cells were resuspended in 1ml DAPI stain solution (0.1% Triton-X, 1 µg/ml DAPI in PBS) and incubated on ice for 30 minutes prior to analysis.

7.2 RNA interference

7.2.1 Lentiviral packaging

A trans-lentiviral packaging system was used to transduce the micro-RNA constructs shown in Table 7.3.

Table 7.3 Sequence of the miRNAs used in the knockdown study.

miR	Sequence
LacZ/TOP	tgctgaaatcgctgatttggtagtcgttttggccactgactgacgactacacatcagcgattt
LacZ/BOTTOM	cctgaaatcgctgatgtgtagtcgtcagtcagtggccaaaacgactacacaaatcagcgatttc
WT1-1407/TOP	tgctgttacctgtatgagtcctggtggttttggccactgactgaccaccaggacatacaggtaa
WT1-1407/BOTTOM	cctgttacctgtatgtcctggtggtcagtcagtggccaaaaccaccaggactcatacaggtaac
WT1-1490/TOP	tgctgtgtgatggcggactaattcatgttttggccactgactgacatgaattaccgccatcaca
WT1-1490/BOTTOM	cctgtgtgatggcggtaattcatgtcagtcagtggccaaaacatgaattagtccgccatcacac

The system was developed in the human embryonic kidney cell line SODK3 (Cockrell et al. 2006), which expresses GFP and all trans-lentivirus packaging proteins from a Tet-Off system. The cells were cultured in DMEM-HIGH (Sigma 51435C) supplemented with 10% FCS, glutamine, penicillin / streptomycin, 1μg/ml puromycin, 600μg/ml neomycin and 1 μg/ml doxycycline (which was used to inhibit the expression of the lentiviral proteins and prevent toxic effects).

To activate the packaging system, the cells were washed twice with PBS, split 1:3 and grown for 3 days without doxycycline; on the fourth day the cells were FACS sorted for GFP expression and the brightest 15% was plated on a 0.001% poly-L-Lysine coated plate and grown overnight without doxycycline.

The following day, the SODK3 cells were transfected with the lentiviral vectors using FuGene6 (Roche 11815091001) as per manufacturer's instructions; the medium, containing 5mM sodium butyrate (Sigma B5887) but no doxycycline, was changed at 12 and 36 hours post-tranfection. 72 hours after the last medium change, the virus-containing supernatants were harvested and centrifuged for 20 minutes at 4°C to pellet cell debris. Virus stocks were aliquoted and stored at -80° C.

7.2.2 Transduction of target cells

The human breast cancer cells were plated in full medium in 6-well plates (3 x 10^5 cells per well) and cultured overnight; the following day the medium was removed, the cells incubated with 0.5 ml viral supernatant + 0.5 ml OPTIMEM (Life Technologies 31985062) + 4µg/ml polybrene (Sigma 107689) and after 6 hours 1 ml of full medium was added to each well.

From day 2 post-transduction cells were maintained on selective media, using 1µg/ml puromycin concentration (established though a kill curve).

7.3 Mouse lines

7.3.1 MMTV-Co & MMTV-Cre

Our group had already generated a *Wt1* conditional mouse (referred to as *Wt1*$^{co/co}$), in which the exon 1 is flanked by LoxP sites and can therefore be deleted through Cre-mediated recombination (Martinez-Estrada et al. 2010). Crossbreeding with the *MMTV-Cre* mouse (a kind gift from Dr. Brunton, CRUK, The University of Edinburgh) generated the *MMTV-Co* line; in order to check for the off-target and toxic effects of Cre recombinase, *MMTV-Cre* mice were used in the Cre control group.

7.3.2 *C3-Co* & *C3-Cre*

Wt1$^{co/co}$ mice were crossed with a C3(1)-driven doxycycline-inducible Cre (a kind gift from Dr. Els Robanus, LUMC, Leiden, The Netherlands), creating the *C3-Co* line, while C3-Cre mice provided the respective Cre control.

7.3.3 ***C3-CreR26R***$^{YFP/YFP}$

The C3-Cre mouse was crossed with a *Rosa26*$^{YFP/YFP}$ reporter to obtain YFP expression at the sites of Cre-mediated DNA recombination.

7.3.4 ***C3-Rosa26:Wt1-KTS***

The C3(1)-driven doxycycline-inducible Cre was crossed with a *Wt1*-KTS knockin (a kind gift from Dr. Schedl), which requires Cre activity to trigger the ectopic overexpression of *Wt1*.

7.3.5 *C3TCo* & *C3TCre*

Wt1$^{co/co}$ mice were crossed with the C3(1)/Tag breast cancer model (Maroulakou et al. 1994) and the C3(1)-driven doxycycline-inducible Cre, creating the *C3TCo* line. The Cre control group (*C3TCre*) was generated by crossing the *Wt1*$^{co/co}$ mice only to the C3(1)/Tag line.

7.3.6 MMTV-NIC

This additional model of breast cancer was a kind gift from Dr. Brunton (CRUK, The University of Edinburgh); *MMTV-NIC* mice were only used for the analysis of *Wt1* expression.

7.4 Animal experiments

7.4.1 Animal husbandry

The *MMTV-Co*, *MMTV-Cre*, *C3-Rosa26:Wt1-KTS* and *MMTV-NIC* mice were housed in the Biomedical Research Facility (BRF, University of Edinburgh), while the *C3-Co*, *C3-Cre*, *C3-CreR26R*$^{YFP/YFP}$, *C3TCo* and *C3TCre* lines were in the Transgenic Unit (TGU, MRC Human Genetics Unit).

In both facilities, the animals were housed with food and water *ad libitum*, in a 12h light/12h dark cycle and at constant temperature (21°C) and humidity (53%).

Animal care, plug-checking and culling of the experimental animals were performed by TGU & BRF staff, while matings set-up and earclipping were carried out by our technician Anna Thornburn.

The females used in the gestation studies were checked every morning for the presence of vaginal plugs and, if positive, were staged at 0.5dpc (days post-coital).

7.4.2 Doxycycline administration

Doxycycline Hyclate (Sigma D9891) was dissolved in the drinking water at a concentration of 2 mg/ml; the bottles were wrapped in foil and sealed with black tape to keep the doxycyline solution in the dark.

7.4.3 Tissue harvesting

The experimental animals were usually culled by cervical dislocation; CO_2 inhalation had to be used for few mice which had developed big mammary tumours in proximity to the neck.

The mammary glands were dissected by performing a midline inverted Y incision into the skin, pulling away the skin flaps from the peritoneum and then gently excising the mammary tissue. The glands to be used for histological analysis were fixed in 4% PFA, those for RNA extraction were either stored in RNAlater (Ambion AM7021) or snap frozen, the glands for wholemount analysis were spread out on a microscope slide and fixed in Carnoy's solution (24ml ethanol, 12ml chloroform, 4ml acetic acid, made up fresh each time).

The mammary tumours, liver, brain and lungs were either fixed in 4% PFA, stored in RNAlater (Ambion AM7021) or snap frozen, depending on their further application.

7.4.4 FACS analysis of mammary cells

Mammary cell suspensions were prepared in the Smalley laboratory (European Cancer Stem Cell Research Institute, Cardiff) from the fourth mammary fat pad of 10-week-old virgin female FVB mice.

After removing the intra-mammary lymph nodes, the fat pads were minced with a McIlwain Tissue Chopper and transferred to a digestion mix of serum free Leibowitz L15 medium (Gibco 11415-049) supplemented with 3 mg/ml collagenase A (Roche 11 088 793 001) and 1.5 mg/ml trypsin.

The tissue was incubated for 1 hour at 37^{o}C in a shaking incubator, washed in Leibowitz L15/10% FCS and then incubated with red blood cell lysis buffer (Sigma R7757) for 5 minutes. After a second wash in Leibowitz L15/10% FCS, the cells were plated in DMEM/10% FCS for 1 hour at 37^{o}C, to allow the contaminating fibroblasts to attach to the tissue culture plastic; the epithelial cells were then removed, washed in Versene and incubated for 15 minutes in Joklik's Modification of Minimal Essential Medium (Sigma M8028) to obtain a single cell suspension.

After a 2 minute-incubation at 37 ^{o}C in 2 ml trypsin, 1 μg/ml DNase I (Sigma 9003-98-9) was added to the cells and a p1000 pipette was used to gently break up any clumps; trypsin was deactivated by incubating the samples for 5 minutes at 37^{o}C in an equal volume of Leibowitz L15/10% FCS.

After filtrating the cell suspension through a 40 µm strainer, the resulting single cells were resuspended in fresh Leibowitz L15/10% FCS and counted.

Mammary cell suspensions at 10^6 cells/ml were incubated at 4°C with the antibodies listed in Table 7.4; after 45 minutes, the samples were washed in L15/10% FCS and resuspended in L15/10% FCS/0.01% DAPI.

Table 7.4 Antibodies used for the sorting of mammary cells.

ANTIBODY (clone)	SPECIES	MANUFACTURER (Cat. #)	DILUTION
CD24-FITC (M1/69)	Rat	BD Biosicences (553261)	1.25 µl/ml
CD45-PE-Cy7 (30-F11)	Rat	BD Biosciences (552848)	5.0 µl/ml
CD49f-PE-Cy5 (GoH3)	Rat	BD Biosciences (551129)	5.0 µl/ml
c-Kit-PE (2B8)	Rat	BD Biosciences (553355)	5.0 µl/ml
Sca-1-APC (D7)	Rat	Insight Biotechnology (108112)	5.0 µl/ml

Cells were sorted on a FACSAria (Becton Dickenson) equipped with violet (404 nm), blue (488 nm), green (532 nm), yellow (561 nm) and red (635 nm) lasers. The analysis was performed with the FACSDiva software using single stained samples as compensation controls and excluding both dead cells (DAPI bright) and leukocytes ($CD45^+$).

7.5 Microbiology and cloning

7.5.1 Culture methods

Aseptic technique was used to carry out all the microbiology work, including the preparation of agar plates and glycerol stocks, the set-up of liquid and dry cultures and the picking and growing of single colonies.

Agar plates for bacterial selection were prepared by melting agar at low power in the microwave, cooling to 55°C and adding the appropriate antibiotics (kanamycin 50 μg/ml, ampicillin 50 μg/ml, spectinomycin 100 μg/ml, chloramphenicol 12.5 μg/ml).

Liquid cultures were grown in LB broth with antibiotic selection and vigorous shaking (220rpm), while dry cultures grown on Agar plates were incubated overnight in inverted position. The bacterial cultures of Library Efficiency DH5α competent cells (Life Technologies 18263-012) were grown at 37˚C, MAX Efficiency Stbl2 competent cells (Life Technologies 10268-019) and One Shot ccdB survival cells (Life Technologies 11828-029) at 30˚C.

Plasmid mini-prep were obtained by inoculating a single colony in 5ml LB containing the appropriate antibiotic; the starter culture was then incubated overnight with vigorous shaking.

For plasmid maxi-prep, 500 µl of an overnight starter culture were added to 400ml LB and grown for 16-20hours with the appropriate antibiotic selection and vigorous shaking.

7.5.2 Bacterial transformation

Bacterial cells were transformed using heat shock as per the supplier's recommendations.

After thawing the bacteria on ice, 1-10ng DNA was added to the cells; following a 30 minute incubation on ice, the vial was heat-shocked at 42°C for 45 seconds and then immediately placed on ice for 2 minutes.

After adding 250µl warmed SOC media, the cells were incubated at 30ºC for one hour, then plated on agar plates and grown overnight at 30ºC with the appropriate antibiotic selection.

7.5.3 Reagents prepared by the MRC HGU Core Scientific Services

LB (Luria-Bertani) Broth:

- 10g Tryptone
- 5g yeast extract
- 10g NaCl
- 1g Glucose
- Made up to 1000ml in dH20 and autoclaved

Agar:

- 1l LB broth
- 15g Agar
- Autoclaved

7.5.4 Gateway cloning

All Gateway reactions were performed as described in the Gateway Manual (Life Technologies).

In each BP reaction, 150ng of pDONR-221 were combined with 150ng of the pcDNA6.2 vectors containing the lacZ or WT1 miR; after adding 2 µl BP clonase (Life Technologies 11789-020) and TE to a total volume of 8 µl, the reaction was left overnight at room temperature.

In the LR reactions, 150ng of the destination vector (pGIPZ-DEST or pTRIPZ-DEST) were combined with 150ng of the entry clone (lacZ, WT1-1407 or WT1-1490); after adding 2 µl LR clonase (Life Technologies 11791-043) and TE to a total volume of 8 µl, the reaction was left overnight at room temperature.

7.6 DNA

7.6.1 Isolation of genomic DNA for genotyping of experimental animals

Ear clips were collected at weaning for both identification and genotyping purposes. After adding 75µl of 25mM NaOH, 0.2mM EDTA to each sample and incubating at 95˚C for 30 minutes, the solution was neutralized with 75µl of 40mM Tris.HCl, vortexed and stored at -20˚C.

7.6.2 Isolation of genomic DNA from mammary tumours preserved in RNAlater

The DNA extraction from tissues stored in RNAlater was performed following the manufacturer's recommendations.

The tumours were finely minced and placed in a 2ml tube containing 1.5 ml digestion buffer (60 mM Tris pH 8.0, 100 mM EDTA, 0.5% SDS, 500µg/ml proteinase K).

After a 24 hour incubation at 55°C, each sample was divided in two aliquots and equal volumes of 50:50 phenol/chloroform (Sigma P2069) were added; following 2 minutes of mixing by inversion, the samples were centrifuged for 10 minutes, then the resulting upper phase was aspirated with a wide-bore pipette tip and moved to a new tube.

The phenol/chloroform extraction was performed other 2 times, followed by a final choloroform extraction; after adding 1/10 volume 3M sodium acetate (pH 5.2) and 1 volume 95% ethanol, the samples were mixed by inversion and centrifuged for ten minutes.

The resulting DNA pellet was washed in 70% ethanol for 10 minutes, air-dried and then resuspended overnight in TE at 4°C.

7.6.3 Isolation of plasmid DNA

The DNA from plasmid mini- and maxi-prep was extracted using the Plasmid Mini Kit (Qiagen 27106) and the Plasmid MaxiKit (Qiagen 12163) respectively, as per manufacturer's instructions.

7.6.4 Measuring DNA concentration

DNA concentration was measured using a Nanodrop 2000 Spectrophotometer (Thermo Scientific).

7.6.5 Digestion with restriction enzymes

The digestion of DNA with restriction enzymes was performed according to the supplier's recommendations; both single and double digests were carried out using the most suitable buffer and the appropriate incubation temperature (Table 7.5).

Table 7.5 Restriction digests

RESTRICTION ENZYME	BUFFER	INCUBATION TEMPERATURE	MANUFACTURER
DraI	SuRE/Cut M	37°C	Roche
EcoRV	SuRE/Cut B	37°C	Roche
EcoRI	SuRE/Cut H	37°C	Roche
*Xba*I	SuRE/Cut H	37°C	Roche
HindIII	SuRE/Cut B	37°C	Roche
PvuII	2	37°C	Neb
EcoRI/XbaI	SuRE/Cut H	37°C	Roche
NruI/BamHI	SuRE/Cut B	37°C	Roche

7.6.6 DNA ligation, purification and precipitation

DNA ligation was performed by combining appropriate quantities of DNA with T4 DNA ligase (Roche 0716359001), the supplied buffer and dH_2O for a total reaction volume of 30 µl; the ligation mix was left at 16°C overnight.

DNA was gel purified using QIAquick Gel Extraction Kit (Qiagen 28704).

DNA precipitation was carried out mixing 1 volume of DNA with 1/10 volume 3M Sodium Acetate and 2.5 volumes cold 100% ethanol; after overnight incubation at -20°C, the samples were centrifuged for 15 minutes at 4°C and the resulting DNA pellet was washed in 70% ethanol. After air-drying the pellet, DNA was resuspended in the appropriate volume of TE.

7.6.7 PCR

Polymerase chain reactions were performed using 0.2mM dNTPs (Life Technologies 10297-018), 0.25 µM primers, Taq DNA Polymerase and the supplied buffer (Life Technologies 10342-053), 2.5 mM Mg^{2+} (Life Technologies), template DNA and dH_20 for a total reaction volume of 20 µl.

The primers, listed in Table 7.6, were designed with either Geneious Pro software or Primer 3 Programme (http://primer3.sourceforge.net/)

Table 7.6 Primers used for genotyping

GENOTYPING	FORWARD PRIMER	REVERSE PRIMER	PCR
Wt1	tgggttccaaccgtaccaaaga	gggcttatctcctcccatgt	Geno58
Cre	gcattaccggtcgagcaacgagtgatgag	gagtgaacgaacctggtcgaaatcagtgcg	Geno58
Fabpi (internal control)	tggacaggactggacctctgctttcctaga	tagagctttgccacatcacaggtcattcag	Geno58
Rosa26	ggcttaaaggctaacctgatgtg	ggagcgggagaaatggatatg	MTRosa
Tag	caaatgttgcttgtctggtg	gtcagtcgagtgcacagttt	Geno58

PCR Program - Geno58

Temperature (°C)	Incubation Time
94	2 min
94	15 sec
58	30 sec (35 cycles)
72	1 min
72	5 min
4	10 min

PCR Program - MTRosa

Temperature (°C)	Incubation Time
94	4 min
94	1 min
60	45 sec (30 cycles)
72	1 min
72	10 sec
4	10 min

7.6.8 Gel electrophoresis

DNA fragments were separated by size using agarose gel electrophoresis. Depending on the size of the fragments to be separated, different percentages of agarose (weight/volume) were used for each gel; the required amount of agarose was dissolved in TBE and melted in a microwave.

After cooling, ethidium bromide (BDH) was added to obtain a final concentration of 50μg/100ml; the agarose was then poured into a tray and left to set.

The DNA samples were mixed with loading Buffer (3ml Glycerol, 6ml dH_2O, 1ml 10X TBE, bromophenol blue [Sigma B0126]) and loaded onto the gel with either a 1kb (Neb N3232L) or a 100bp (Neb N3231L) DNA ladder; after filling the electrophoresis tank with 1X TBE, electrophoresis was run 70-150V.

Gels were visualized under UV illumination and photographed with a BioDocit (UVP) imaging system.

7.7 RNA

RNA work was carried out taking all the necessary precautions to avoid contamination with RNases: surfaces and equipment were cleaned with 70% ethanol and the RNsase-inactivating agent RNAZap (Ambion AM9782), filter tips and RNase-free reagents were reserved solely for RNA work, all samples were kept on ice during the experiments to minimise the activity of endogenous RNases and stored at -80˚C.

7.7.1 RNA isolation

RNA was extracted with the following Qiagen kits as per manufacturer's instructions: the RNeasy Mini Kit (Qiagen 74104) was used for cell lines, mouse mammary tumours and human breast cancer samples, the RNeasy Lipid Tissue Mini Kit (Qiagen 74804) for the healthy mouse mammary glands.

Before the extraction, glands and tumours were finely minced, added to a 2ml tube containing 1ml Qiazol Lysis Reagent + two stainless steel beads (Qiagen 69989) and homogenized for 10 minutes using a Tissue Lyser LT (Qiagen 85600).

DNAse digestion was performed during the extraction (Qiagen 79254), RNA was eluted in 30µl RNase-free water and its concentration measured using a Nanodrop 2000 Spectrophotometer (Thermo Scientific).

7.7.2 Retrotranscription

cDNA was synthesized from 2 µg total RNA using AMV reverse transcriptase (Roche 11495062001) and oligo d(T) priming.

For each reaction, the appropriate volume of RNA (made up to 12.5µl with RNAse free water) was added to a mix containing 4µl AMV Reverse Transcriptase 5x Reaction Buffer, 0.25µl RNAse inhibitor (Promega N2611), 1µl oligo d(T), 1.25µl RNase free dNTPs and 1µl AMV reverse transcriptase.

The samples were incubated at 48°C for 2 hours, then, the resulting cDNA was diluted in TE to a final concentration of 10ng/µl.

2µl of diluted cDNA was used per Real Time PCR reaction.

7.7.3 Real Time PCR

All the quantitative Real Time PCR experiments were performed on the Roche Lightcycler 480 system.

Universal Probe Library probes and primers, shown in Table 7.7 and 7.9, were designed with the Universal Probe Library Assay Design Centre (Roche) and ordered from Roche and Sigma respectively. The assays used for *ER*, *PR* and *HER2* (Table 7.8) were based on previous publications (de Cremoux et al. 2002, 2003) and were supplied by IDT.

All primers were shipped as lyophilized powders, rehydrated in TE to obtain a stock solution of 100µM and diluted to 20µM working solutions.

Each reaction was carried out following the manufacturers' instructions and using 0.2µl forward primer (target gene), 0.2µl reverse primer (target gene), 0.2µl target probe, 0.2µl forward and reverse primers (reference gene), 0.2µl reference probe, 2 µl RNAse free dH2O, 5µl Lightcycler Master Mix (Roche 04887301001) and 2µl cDNA.

Relative expression for each target gene was quantified using a reference gene (GAPDH for mouse [Roche 05046211001], ACTB for human [Roche 05046165001]). All the experiments were performed and analysed in triplicate using the ΔΔCT method.

Table 7.7 Primers and UPL probes used for the human transcripts.

TRANSCRIPT	FORWARD PRIMER	REVERSE PRIMER	UPL PROBE #
WT1 exon 7/exon 8	agctgtcccacttacagatgc	ccttgaagtcacactggtatgg	4
WT1 exon 1A	agggctctgaggattgtgc	agggctctgaggattgtgc	37
WT1 intron 5	caacttgccgaggatgaaac	acggtctaggtctcgctcag	59
CDH1	tggaggaattcttgctttgc	cgctctcctccgaagaaac	84
CTNNA1	agacgatgcctcacagcac	aagctcaaggggtccacaat	25
CTNNA2	ggtgaaacttaactatgtagcagcaa	ccatctcatcccgacagtg	17
CTNND1	ccctcattttcattgttcagg	ggcaaacacagttctctacaagc	29
VIM	aaagtgtggctgccaagaac	agcctcagagaggtcagcaa	16
FN1	caccacagccatctcacatt	cttccaacggcctacagaat	39
CDH2	gcacagtggccacctaca	tgaaaggtttttatctctatcagacct	29
ZEB1	gcggcatatggtgacaca	ttgccacactctgtgcattt	68
ZEB2	caagaggcgcaaacaagc	aacctgtgtccactacattgtca	79
SNAI1	gctgcaggactctaatccaga	atctccggaggtgggatg	11
SNAI2	acagcgaactggacacacat	gatggggctgtatgctcct	73
TWIST1	gggccggagacctagatg	tttccaagaaaatctttggcata	50
VTN	accttaccctttgccagctc	ctttctccggtgggaacc	23
ACTA2	gcctgagggaaggtcctaac	ctggagctgcttcacaggat	36
CXCL1	catcgaaaagatgctgaacagt	cttcaggaacagccaccagt	69
TNC	gaaggtggaggggtacagtg	gaaggatctgccattgtggt	62
KRT18	cctgctgtccgtgtccat	ggaccggtagttggtgga	39
MMP2	cggaaaagattgatgcggta	tgctggctgagtagatccag	63
MMP9	tcttccctggagacctgaga	gccacccgagtgtaaccata	53
TGFB1	cacgtggagctgtaccagaa	cagccggttgctgaggta	72

Table 7.8 Primers and non-UPL probes used for the human transcripts.

TRANSCRIPT	FORWARD PRIMER	REVERSE PRIMER	PROBE
ER	agcacccagtgaagctact	tgaggcacacaaactcct	6FAM - tggctacatcatcggttccgca-BHQ-2
PR	gaaccagatgtgatctatgcagga	cgaaaacctggcaatgatttagac	6FAM - acctgacacctccagttctttgctgacaag-BHQ-2
HER2	caaccaagtgaggcaggtcc	cgtgatcaagacccctccttt	6FAM - agaggctgcggattgtgcga-BHQ-2

Table 7.9 Primers and UPL probes used for the mouse transcripts.

TRANSCRIPT	FORWARD PRIMER	REVERSE PRIMER	UPL PROBE #
Wt1 exon 7/exon 8	caccaaaggagacacacagg	gggaaaactttcgctgacaa	47
Cdh1	atcctcgccctgctgatt	accaccgttctcctccgta	18
Ctnna1	ggaccatcgcagaccatt	gcgatgcgctgaaggtag	62
Ctnnd1	ctcaacggaccccaggat	tcctcggtgtaggtttccac	92
Vim	ccaaccttttcttccctgaa	tgagtgggtgtcaaccagag	109
Fn1	gatgccgatcagaagtttgg	ggttgtgcagatctcctcgt	46
Cdh2	gccatcatcgctatccttct	ccgtttcatccataccacaaa	18
Zeb1	gccagcagtcatgatgaaaa	tatcacaatacgggcaggtg	48
Zeb2	caagaggcgcaaacaagc	tgcgtccactacgttgtcat	79
Snai1	atccttggggcgtgtaagt	tgaaccactgtgatccttgg	6
Snai2	gtaaggtgtgcggcaagg	tgcagtgagaacaggtataggg	1
Twist1	gctcagctacgccttctcc	tccttctctggaaacaatgaca	88

7.7.4 RNA-sequencing

Total RNA was isolated and sent to GATC Biotech (Germany) for library preparation and sequencing on the Illumina HiSeq 2000 platform.

The raw data were analysed using Galaxy (https://usegalaxy.org/) and Geneprof (http://www.geneprof.org/GeneProf/).

7.8 Histology

7.8.1 Paraffin embedding

Tissue harvesting was performed as described in paragraph 7.4.3; the mammary tumours, mammary glands, liver, brain and lungs were fixed in 4% PFA (Sigma 158127-500G) overnight at 4°C.

The next day, the samples were washed twice in PBS, taken through serial dilutions of ethanol (15minutes 25% ethanol, 15mins 50% ethanol, 15mins 75% ethanol) and then stored at 4°C in ethanol 70%.

An automated TissueTekVIP 5 Jr machine was used to embed the samples in paraffin; the blocks were then sectioned with a microtome at 4μm and dried at 50ºC before staining.

7.8.2 OCT media embedding

The mammary glands of *C3-CreR26R*$^{YFP/YFP}$mice were fixed in 4% PFA overnight at 4°C. The next day, the samples were washed twice in PBS, dehydrated in PBS/5% sucrose for 45 minutes and then in PBS/20% sucrose until the gland sank.

Tissue samples were placed in a cryomold, submerged in OCT media (Tissue-Tek 25608-930) and stored at -80ºC. Sections were cut at 10μm using a cryostat.

7.8.3 Mammary gland wholemounts

Tissue harvesting was performed as described in paragraph 7.4.3; the ninth mammary gland was spread out on a microscope slide and fixed for 4 hours in Carnoy's solution (24ml ethanol, 12ml chloroform, 4ml acetic acid, made up fresh each time).

Samples were taken through decreasing ethanol solutions (15minutes 70% ethanol, 15mins 50% ethanol, 15mins 25% ethanol), washed once in dH_2O for 5 minutes and then incubated overnight in carmine alum (StemCell Technologies 07070) at room temperature.

The following day, the glands were dehydrated with sequential 15 minute washes in 70, 95 and 100% ethanol, left to defat in xylene for at least 48 hours and then mounted under a cover slip.

7.8.4 Staining

All immunohistochemistry and immunofluorescence stainings were performed by Ruth Hamblin and Nancy Evans (SuRF, QMRI, The University of Edinburgh), using a Leica BOND machine and the antibodies listed in table 7.10.

Table 7.10 Antibodies used for IHC and IF

ANTIBODY	SPECIES	MANUFACTURER (Cat. #)	DILUTION	PROTOCOL
WT1-C19	Rabbit	Santa Cruz (sc-192)	IHC 1:5000 IF 1:10000	IHC Rabbit refine IF Tyramide
ER	Mouse	Abcam (ab9269)	1:100	Impress MoM
PR	Rabbit	Santa Cruz (sc-0538)	1:500	Rabbit refine
HER2	Rabbit	Dako (A0485)	1:1000	Rabbit refine
SNAIL	Goat	Abcam (ab53519)	1:250	Impress anti goat
TWIST	Rabbit	Abcam (ab49254)	1:200	Rabbit refine
ZEB2	Rabbit	Sigma (HPA027524)	1:250	Rabbit refine
VIMENTIN	Rabbit	Cell Signalling (5741)	1:500	Rabbit refine

Rabbit refine protocol:

- Peroxide block (5mins)
- Primary Ab (120mins)
- Polymer (15mins)

- Dab (5mins)
- Haematoxylin (5mins)

Tyramide protocol:

- H_2O_2 (1:10, 10mins)
- Serum block (neat, 10mins)
- Primary Ab (120mins)
- HRP 2ndary (1:500, 30 mins)
- Tyramide Amplification (1:50, 10mins)
- DAPI counter stain (1:1000, 10mins)

Impress MoM protocol:

- Peroxide Block (5mins)
- Rodent Block (30mins) (Abcam Mouse on Mouse polymer IHC kit ab127055/GR84050-2)
- Primary Ab (120mins)
- HRP Polymer (30mins) (Abcam Mouse on Mouse polymer IHC kit ab127055/GR84050-2)
- Dab (5mins)
- Haematoxylin (5mins)

Impress anti goat protocol:

- Peroxide Block (5mins)
- Normal horse serum block (20mins) (Vector ImmPRESS MP-7405)
- Primary Ab (120mins)
- HRP Polymer (30mins) (Vector ImmPRESS MP-7405)
- Dab (5mins)
- Haematoxylin (5mins)

7.9 Microscopy

Slides were visualized using an Olympus Dotslide microscope (for brightfield) or a Zeiss Axioplan 2 microscope (for fluorescence).

7.9.1 Quantification of mammary branching

The analysis of the mammary branching was performed by Dr. Morrison and Dr. Del Pozo using ImageJ.

For each wholemount, four different quadrants were randomly selected using the lymph node as a reference; the number of primary and secondary ductular branches were counted for each of the four quadrants.

7.9.2 Staining score

The ER and PR status of the first set of human breast cancer samples was determined using the Allred method, which combines the percentage of positive cells and the intensity of the staining (Harvey et al. 1999, Gown 2008).

7.10 Bioinformatics

Frequently used websites include the UPL Assay Design Centre (http://lifescience.roche.com/shop/CategoryDisplay?catalogId=10001&tab=Assay+Design+Center&identifier=Universal+Probe+Library&langId=-1, used to design probes and primers for Real Time PCR experiments), the genome browser Ensembl (http://www.ensembl.org/index.html), the NCBI (http://www.ncbi.nlm.nih.gov/, mainly used to search for articles on PubMed), Galaxy (https://usegalaxy.org/) and Geneprof (http://www.geneprof.org/GeneProf/) for the analysis of the RNA-sequencing data.

7.11 Statistical methods

Statistical analyses were performed using Excel and MiniTab.

Unless stated otherwise, data are represented as mean value ± standard error of the mean (SEM); ANOVA and Student's t test were carried out to compare the values obtained for the different experimental groups. Only p values < 0.05 were considered as statistically significant.

7.12 Solutions prepared by the MRC HGU Core scientific services

Phosphate Buffered Saline (PBS):

- NaCl 8g
- KCl 0.2g
- Na2HPO4 1.44g
- KH2PO4 0.24g
- Dissolve in 800ml dH_20
- Adjust pH to 7.4

- Bring final volume to 1000ml with dH_20

Tris HCL:

- Dissolve Tris (hydroxymethyl) aminomethane in sterile water
- Adjust pH with HCl

EDTA:

- Dissolve ethyldiaminetetraacetic acid di-sodium salt in sterile water
- Add solid NaOH to adjust pH to 8.0

TE Buffer:

- 10mM Tris.HCl (pH 7.5)
- 1mM EDTA

TBE Buffer (20x Stock):

- Tris (hydroxymethyl) aminomethane 242g
- Glacial acetic acid 57.1ml
- 0.5M EDTA 100ml
- Bring volume to 1000ml with dH_2O

Trypsin:

- Tryspin 1:250 2g

- Phenol Red 5ml
- Penicillin 0.06g
- Streptomycin 0.13g
- Make up to 1000ml in PBS
- Adjust pH to 7.3 using $NaHCO_3$

Versene:

- Dulbeccos Tablets 10
- Sodium EDTA 0.4g
- 0.2% Phenol Red 5ml
- Make up to 1000ml with dH_2O

Appendix A

List of the differentially expressed genes between *WT1*-high and *WT1*-low breast tumours (*in silico* analysis conducted by Dr Sims, chapter 3.4).

GENE ID		FOLD CHANGE
ENSG00000184937	WT1	3.2627606
ENSG00000166426	CRABP1	2.7068319
ENSG00000170367	CST5	2.1108505
ENSG00000198077	CYP2A7	1.8083495
ENSG00000142973	cyp4b1	1.7070984
ENSG00000198251	NA	1.6062471
ENSG00000172379	ARNT2	1.5676866
ENSG00000130707	ASS1	1.5491251
ENSG00000183242	WIT1	1.4143376
ENSG00000102466	FGF14	1.2896552
ENSG00000196090	PTPRT	1.2555033
ENSG00000158089	Galnt14	1.2441012
ENSG00000109424	UCP1	1.1480072
ENSG00000019505	Syt13	1.1262895
ENSG00000092421	SEMA6A	1.0752181
ENSG00000091831	Esr1	1.0664327
ENSG00000091129	nrcam	1.0528864
ENSG00000165973	Nell1	1.0384021
ENSG00000187097	Entpd5	1.0375941
ENSG00000106571	Gli3	1.0083115
ENSG00000168502	KIAA0802	0.9821728
ENSG00000152953	STK32B	0.978741
ENSG00000204421	LY6G6C	0.9410021
ENSG00000185652	NTF3	0.9143917
ENSG00000120262	C6orf97	0.8868726
ENSG00000130558	OLFM1	0.8800146
ENSG00000173599	Pc	0.865724
ENSG00000171444	MCC	0.8565602
ENSG00000134873	CLDN10	0.8024998
ENSG00000168032	entpd3	0.7836371
ENSG00000006071	ABCC8	0.7770491
ENSG00000158125	XDH	0.775519
ENSG00000151090	thrB	0.7641556
ENSG00000108852	MPP2	0.7602601
ENSG00000197993	KEL	0.7476327
ENSG00000140600	Furin	0.7404536
ENSG00000151789	ZNF385D	0.7380647
ENSG00000115844	Dlx2	0.7352178
ENSG00000154645	CHODL	0.7317931
ENSG00000004776	hspb6	0.7201727
ENSG00000153802	TMPRSS11D	0.7096169
ENSG00000204539	CDSN	0.7075104
ENSG00000214313	NA	0.7041051
ENSG00000198183	PLUNC	0.7028216
ENSG00000163218	PGLYRP4	0.7023318
ENSG00000162365	CYP4A22	0.7015143
ENSG00000144681	Stac	0.7003124

GENE ID		FOLD CHANGE
ENSG00000118160	SLC8A2	0.6988419
ENSG00000111181	SLC6A12	0.6890078
ENSG00000182575	NXPH3	0.6875476
ENSG00000148702	habp2	0.6858277
ENSG00000140835	SH3GL3	0.6838867
ENSG00000167531	LALBA	0.6823775
ENSG00000124564	SLC17A3	0.675671
ENSG00000140564	ST8SIA2	0.6716713
ENSG00000005073	HOXA11	0.6711294
ENSG00000115850	Lct	0.6701857
ENSG00000180999	C1orf105	0.6677879
ENSG00000198910	L1cam	0.6631864
ENSG00000130988	rgn	0.6621441
ENSG00000171847	FAM90A1	0.6502502
ENSG00000187045	TMPRSS6	0.649691
ENSG00000085465	Ovgp1	0.6493229
ENSG00000169469	Sprr1b	0.6418517
ENSG00000128310	GALR3	0.6403372
ENSG00000118298	CA14	0.6402423
ENSG00000111291	GPRC5D	0.639007
ENSG00000139292	LGR5	0.6385381
ENSG00000115194	SLC30A3	0.6378245
ENSG00000172867	KRT2	0.6355214
ENSG00000137440	FGFBP1	0.6344793
ENSG00000187908	DMBT1	0.6324247
ENSG00000073670	ADAM11	0.625735
ENSG00000125462	C1orf61	0.6245103
ENSG00000162631	Ntng1	0.621992
ENSG00000118271	TTR	0.6206785
ENSG00000187048	CYP4A11	0.6203746
ENSG00000064309	cdon	0.6191863
ENSG00000113262	GRM6	0.6141273
ENSG00000100665	SERPINA4	0.6093785
ENSG00000151655	ITIH2	0.6090731
ENSG00000116218	NPHS2	0.608211
ENSG00000122126	OCRL	0.6045666
ENSG00000018236	Cntn1	0.6030904
ENSG00000165061	ZMAT4	0.6023889
ENSG00000139985	ADAM21P1	0.5983589
ENSG00000006432	MAP3K9	0.5974899
ENSG00000158485	CD1B	0.5966805
ENSG00000176009	ASCL3	0.5933009
ENSG00000163209	Sprr3	0.5928909
ENSG00000120903	CHRNA2	0.5927368
ENSG00000144671	SLC22A14	0.5917461
ENSG00000105467	SYNGR4	0.5894936
ENSG00000179097	HTR1F	0.5865926
ENSG00000104833	Tubb4	0.5864432

ENSG00000130055	Gdpd2	0.5847233
ENSG00000135454	B4GALNT1	0.5843271
ENSG00000104499	Gml	0.5809121
ENSG00000135222	CSN2	0.5791323
ENSG00000135406	prpH	0.5728184
ENSG00000132429	POPDC3	0.5714618
ENSG00000112078	KCTD20	0.5705174
ENSG00000104044	OCA2	0.56873
ENSG00000166391	MOGAT2	0.5672148
ENSG00000183150	GPR19	0.5650472
ENSG00000113196	HAND1	0.5637788
ENSG00000171936	OR10H3	0.5623491
ENSG00000184029	DSCR4	0.5584929
ENSG00000087237	cetp	0.5584765
ENSG00000105219	CNTD2	0.5557165
ENSG00000169903	TM4SF4	0.5554724
ENSG00000171532	NEUROD2	0.5543291
ENSG00000130226	Dpp6	0.5540548
ENSG00000186704	PMS2L11	0.5519221
ENSG00000107187	lhx3	0.5511107
ENSG00000132563	reep2	0.5500818
ENSG00000169213	RAB3B	0.5479504
ENSG00000143858	Syt2	0.5464042
ENSG00000160808	Myl3	0.545696
ENSG00000147596	PRDM14	0.5438953
ENSG00000169676	DRD5	0.5381932
ENSG00000204248	Col11a2	0.5381378
ENSG00000168830	HTR1E	0.5357975
ENSG00000215904	NA	0.5335831
ENSG00000196220	SRGAP3	0.5333425
ENSG00000188822	Cnr2	0.5314116
ENSG00000213988	ZNF253	0.5289593
ENSG00000162188	GNG3	0.5286025
ENSG00000127529	OR7C2	0.5281672
ENSG00000168530	MYL1	0.5279375
ENSG00000005206	SPPL2B	0.5261692
ENSG00000187021	PNLIPRP1	0.5255608
ENSG00000170290	Sln	0.5215829
ENSG00000015592	stmn4	0.520911
ENSG00000175175	PPM1E	0.5205844
ENSG00000130948	HSD17B3	0.5189425
ENSG00000034971	MYOC	0.5184033
ENSG00000167780	Soat2	0.5175625
ENSG00000204542	C6orf15	0.516592
ENSG00000079393	DUSP13	0.5156491
ENSG00000168124	OR1F1	0.5137901
ENSG00000141013	chst4	0.5137043
ENSG00000162706	CADM3	0.5133538
ENSG00000112619	PRPH2	0.5124375
ENSG00000080561	Mid2	0.5114128
ENSG00000149054	ZNF215	0.5110592
ENSG00000102001	Cacna1f	0.5108228
ENSG00000163975	mfi2	0.5104852
ENSG00000163207	IVL	0.5099288
ENSG00000103313	MEFV	0.509625
ENSG00000102904	TSNAXIP1	0.5091238
ENSG00000147869	Cer1	0.5086131
ENSG00000203492		0.5085052
ENSG00000205250	e2f4	0.5033823
ENSG00000102891	MT4	0.5027977
ENSG00000175189	INHBC	0.5024616
ENSG00000155886	SLC24A2	0.5016286
ENSG00000186912	P2RY4	0.5013635
ENSG00000151224	mat1a	0.4990712
ENSG00000166863	TAC3	0.4984578
ENSG00000138109	CYP2C9	0.4979917
ENSG00000189108	IL1RAPL2	0.4970828
ENSG00000135622	SEMA4F	0.4950161
ENSG00000033627	ATP6V0A1	0.4948015
ENSG00000006659	LGALS14	0.4947493
ENSG00000156925	ZIC3	0.4942947
ENSG00000169474	Sprr1a	0.4937908
ENSG00000182389	CACNB4	0.4920932
ENSG00000102021	Luzp4	0.4919696
ENSG00000100350	FOXRED2	0.4914017
ENSG00000125965	GDF5	0.4905979
ENSG00000143171	RXRG	0.4902254
ENSG00000171097	CCBL1	0.4888681
ENSG00000164458	t	0.487567
ENSG00000146013	GFRA3	0.4873821
ENSG00000151014	CCRN4L	0.4872194
ENSG00000128285	MCHR1	0.4869873
ENSG00000113303	BTNL8	0.4868108
ENSG00000058404	Camk2b	0.4864793
ENSG00000196188	CTSE	0.4857468
ENSG00000183454	GRIN2A	0.4852238
ENSG00000111886	GABRR2	0.4851845
ENSG00000135312	HTR1B	0.4850555
ENSG00000187730	Gabrd	0.4829325
ENSG00000184381	pla2g6	0.4824674
ENSG00000101280	Angpt4	0.4823877
ENSG00000156282	cldn17	0.4822584
ENSG00000116726	PRAMEF12	0.4821422
ENSG00000155087	ODF1	0.4818998
ENSG00000189433	GJB4	0.4777173
ENSG00000169955	ZNF747	0.4775547
ENSG00000184933	OR6A2	0.4768006
ENSG00000087903	rfx2	0.4764647
ENSG00000172367	PDZD3	0.4758359
ENSG00000171462	DLK2	0.4753419
ENSG00000177143	cetn1	0.4738809
ENSG00000158516	Cpa2	0.4729744
ENSG00000010379	SLC6A13	0.4721155
ENSG00000131080	EDA2R	0.4716156
ENSG00000134007	ADAM20	0.4704574
ENSG00000169884	wnt10b	0.4703993
ENSG00000185823	C15orf2	0.4698561
ENSG00000172179	PRL	0.4689865
ENSG00000112462	OR5V1	0.4679678
ENSG00000132016	C19orf57	0.4679112
ENSG00000108947	Efnb3	0.4646418
ENSG00000105642	KCNN1	0.4638032
ENSG00000186115	CYP4F2	0.4619074
ENSG00000183813	ccr4	0.4617819
ENSG00000108753	HNF1B	0.4613426
ENSG00000198049	AVPR1B	0.4613318

ENSG00000108878	CACNG1	0.4612877
ENSG00000126500	FLRT1	0.4610802
ENSG00000170454	Krt75	0.4605806
ENSG00000062096	ARSF	0.4602484
ENSG00000181418	DDN	0.4602249
ENSG00000152595	MEPE	0.4602186
ENSG00000105723	GSK3A	0.4597491
ENSG00000056345	ITGB3	0.4583277
ENSG00000105810	Cdk6	0.4580759
ENSG00000039987	BEST2	0.4580435
ENSG00000143839	REN	0.4575807
ENSG00000105641	Slc5a5	0.4561921
ENSG00000204956	PCDHGA1	0.4560402
ENSG00000154917	rab6b	0.4557763
ENSG00000164776	phkg1	0.4554574
ENSG00000116176	TPSG1	0.4552406
ENSG00000019485	PRDM11	0.4547918
ENSG00000143627	PKLR	0.4546033
ENSG00000197273	GUCA2A	0.4529973
ENSG00000138784	FLJ20184	0.4528865
ENSG00000109132	Phox2b	0.4528522
ENSG00000140522	Cyp1a2	0.4527531
ENSG00000182257	C22orf26	0.4526219
ENSG00000184984	Chrm5	0.4516589
ENSG00000183230	CTNNA3	0.4505777
ENSG00000106328	FSCN3	0.4505311
ENSG00000171403	KRT9	0.4500175
ENSG00000166930	Ms4a5	0.4494258
ENSG00000152254	G6PC2	0.4492261
ENSG00000070808	Camk2a	0.4486853
ENSG00000172987	Hpse2	0.4478929
ENSG00000103375	AQP8	0.4474493
ENSG00000163884	klf15	0.4474369
ENSG00000204444	APOM	0.4446222
ENSG00000112499	slc22a2	0.4445184
ENSG00000136531	SCN2A	0.4444786
ENSG00000155980	Kif5a	0.4443835
ENSG00000145692	bhmT	0.444374
ENSG00000169777	TAS2R1	0.4443352
ENSG00000096088	PGC	0.4435527
ENSG00000183668	PSG9	0.4426178
ENSG00000196184	OR10J1	0.4411586
ENSG00000158571	pfkfb1	0.4405098
ENSG00000163283	ALPP	0.4396378
ENSG00000104888	slc17a7	0.4395806
ENSG00000166313	APBB1	0.4393657
ENSG00000120500	Arr3	0.4393023
ENSG00000101440	Asip	0.4374516
ENSG00000156269	NAA11	0.4370985
ENSG00000169397	RNASE3	0.4370191
ENSG00000144834	TAGLN3	0.4363283
ENSG00000130287	NCAN	0.4362788
ENSG00000105198	LGALS13	0.4357608
ENSG00000178607	ERN1	0.4338798
ENSG00000185069	KRT76	0.4338384
ENSG00000080166	dct	0.4337677
ENSG00000145864	GABRB2	0.4336275
ENSG00000165970	SLC6A5	0.4335491
ENSG00000181072	CHRM2	0.4333702
ENSG00000170925	TEX13B	0.4332786
ENSG00000131737	KRT34	0.4332197
ENSG00000168484	SFTPC	0.4315164
ENSG00000174156	GSTA3	0.4313968
ENSG00000008226	DLEC1	0.4313711
ENSG00000137080	IFNA21	0.4313375
ENSG00000118557	PMFBP1	0.4309121
ENSG00000173517	SGK269	0.4305675
ENSG00000166869	chp2	0.4303418
ENSG00000072080	spp2	0.4302633
ENSG00000147113	CXorf36	0.4299574
ENSG00000187516	CXorf27	0.4298952
ENSG00000111046	MYF6	0.4293299
ENSG00000120055	C10orf95	0.4292851
ENSG00000131480	Aoc2	0.4286803
ENSG00000008118	Camk1g	0.4273697
ENSG00000140505	Adam21	0.426976
ENSG00000130561	SAG	0.4269603
ENSG00000133874	RNF122	0.4268767
ENSG00000186723	OR10H1	0.4266471
ENSG00000111145	ELK3	0.4263969
ENSG00000189013	KIR2DL4	0.4244034
ENSG00000163206	Smcp	0.4243736
ENSG00000124134	KCNS1	0.4239395
ENSG00000187010	RHD	0.4238045
ENSG00000204538	PSORS1C2	0.4234329
ENSG00000185800	DMWD	0.4233641
ENSG00000198844	ARHGEF15	0.423218
ENSG00000080618	CPB2	0.4226427
ENSG00000135409	AMHR2	0.4224075
ENSG00000173406	dab1	0.4220541
ENSG00000134200	Tshb	0.4216173
ENSG00000154165	GPR15	0.4214909
ENSG00000104537	Anxa13	0.4201347
ENSG00000142784	WDTC1	0.4197645
ENSG00000099957	P2RX6	0.4189903
ENSG00000068976	PYGM	0.4185931
ENSG00000159248	Gjd2	0.4182148
ENSG00000061938	TNK2	0.4176788
ENSG00000163464	Cxcr1	0.4173818
ENSG00000168038	Ulk4	0.417083
ENSG00000162139	Neu3	0.4170207
ENSG00000188763	FZD9	0.4162886
ENSG00000091536	MYO15A	0.4153879
ENSG00000174417	TRHR	0.414013
ENSG00000125815	Cst8	0.4138338
ENSG00000105650	PDE4C	0.4136546
ENSG00000101327	Pdyn	0.4133892
ENSG00000167346	MMP26	0.4124655
ENSG00000197584	KCNMB2	0.4123594
ENSG00000184156	KCNQ3	0.412281
ENSG00000126767	elk1	0.4121938
ENSG00000204290	BTNL2	0.4120363
ENSG00000146378	Taar2	0.4118536
ENSG00000130940	CASZ1	0.4118239
ENSG00000142609	KIAA1751	0.4110397
ENSG00000105428	Znrf4	0.4109898

ENSG00000166736	HTR3A	0.4104677	ENSG00000123454	DBH	0.3870875
ENSG00000176383	B3GNT4	0.4102418	ENSG00000110881	ACCN2	0.3864553
ENSG00000075290	wnt8b	0.4101921	ENSG00000104804	TULP2	0.3861663
ENSG00000120328	PCDHB12	0.4100875	ENSG00000096996	IL12RB1	0.3842836
ENSG00000171360	KRT38	0.4100363	ENSG00000196475	Gk2	0.383927
ENSG00000127362	TAS2R3	0.4090366	ENSG00000099866	MADCAM1	0.3831429
ENSG00000180720	NA	0.4088639	ENSG00000130385	BMP15	0.3830996
ENSG00000168748	CA7	0.408859	ENSG00000116983	HPCAL4	0.3829261
ENSG00000070748	chat	0.4087487	ENSG00000129535	Nrl	0.3822551
ENSG00000176136	Mc5r	0.4083293	ENSG00000178522	AMBN	0.3821295
ENSG00000149124	Glyat	0.408111	ENSG00000151388	ADAMTS12	0.3809926
ENSG00000183434	TFDP3	0.4080805	ENSG00000125618	PAX8	0.3808582
ENSG00000108405	P2RX1	0.407558	ENSG00000165841	CYP2C19	0.3802325
ENSG00000109047	Rcvrn	0.4067586	ENSG00000137634	FAM55D	0.3798088
ENSG00000137561	ttpa	0.4061951	ENSG00000134940	Acrv1	0.37969
ENSG00000153012	lgi2	0.4040055	ENSG00000156575	Prg3	0.3791942
ENSG00000131899	Llgl1	0.4032065	ENSG00000102385	DRP2	0.37841
ENSG00000148795	CYP17A1	0.4027695	ENSG00000078295	ADCY2	0.3782568
ENSG00000197479	PCDHB11	0.4027176	ENSG00000124140	SLC12A5	0.3779007
ENSG00000144596	GRIP2	0.4023646	ENSG00000073536	NLE1	0.3771268
ENSG00000198854	C1orf68	0.4022644	ENSG00000168158	OR2C1	0.3763339
ENSG00000167034	NKX3-1	0.4012097	ENSG00000149305	HTR3B	0.3761535
ENSG00000187266	EPOR	0.4005779	ENSG00000131398	Kcnc3	0.3751786
ENSG00000115665	SLC5A7	0.3996199	ENSG00000128254	C22orf24	0.3751768
ENSG00000105549	THEG	0.3994963	ENSG00000104361	NIPAL2	0.3746246
ENSG00000167994	RAB3IL1	0.3991495	ENSG00000168903	BTNL3	0.3744093
ENSG00000172819	rarg	0.3985539	ENSG00000082556	oprk1	0.3739701
ENSG00000135569	Taar5	0.3982276	ENSG00000075073	TACR2	0.3734025
ENSG00000185527	Pde6g	0.3978273	ENSG00000184895	SRY	0.3715192
ENSG00000184566	NA	0.397718	ENSG00000166603	MC4R	0.3700897
ENSG00000126231	PROZ	0.3971376	ENSG00000143340	Fam163a	0.3696579
ENSG00000146039	SLC17A4	0.3965438	ENSG00000169548	ZNF280A	0.369349
ENSG00000164076	CAMKV	0.396409	ENSG00000134376	Crb1	0.3684604
ENSG00000160282	ftcD	0.3960544	ENSG00000180245	RRH	0.3682381
ENSG00000116183	PAPPA2	0.3958086	ENSG00000132703	Apcs	0.368163
ENSG00000105321	CCDC9	0.3953248	ENSG00000184166	OR1D2	0.3679829
ENSG00000112333	nr2e1	0.3947202	ENSG00000180509	KCNE1	0.3675812
ENSG00000163497	Fev	0.3943335	ENSG00000161572	LYZL6	0.3669826
ENSG00000161573	CCL16	0.3940819	ENSG00000134249	Adam30	0.3661856
ENSG00000163873	Grik3	0.3940596	ENSG00000163352	Lenep	0.3661724
ENSG00000169894	MUC3B	0.3930184	ENSG00000112232	khdrbs2	0.3659111
ENSG00000182533	CAV3	0.3929687	ENSG00000198339	HIST2H4B	0.3655837
ENSG00000168263	KCNV2	0.3928466	ENSG00000006377	DLX6	0.3652651
ENSG00000170322	Nfrkb	0.3928128	ENSG00000134571	MYBPC3	0.3652194
ENSG00000130377	acsbg2	0.3922678	ENSG00000105261	LOC728361	0.3646877
ENSG00000149295	DRD2	0.3916209	ENSG00000178394	HTR1A	0.3637261
ENSG00000185313	Scn10a	0.39119	ENSG00000148200	Nr6a1	0.3633277
ENSG00000125861	GFRA4	0.3909068	ENSG00000100249	C22orf31	0.3630733
ENSG00000124701	APOBEC2	0.3902581	ENSG00000143536	CRNN	0.3620211
ENSG00000112212	Tspo2	0.3899292	ENSG00000118113	MMP8	0.3614806
ENSG00000131864	usp29	0.3895764	ENSG00000197852	c1orf183	0.3606969
ENSG00000172146	OR1A1	0.389537	ENSG00000151615	POU4F2	0.3606859
ENSG00000205073	c1orf222	0.3894993	ENSG00000188784	pla2g2e	0.3600528
ENSG00000163217	Bmp10	0.389487	ENSG00000169836	TACR3	0.3598443
ENSG00000166402	TUB	0.3894465	ENSG00000167580	AQP2	0.3593991
ENSG00000177791	myoz1	0.3889347	ENSG00000006116	CACNG3	0.359335
ENSG00000166862	CACNG2	0.3883932	ENSG00000167419	LPO	0.3584167
ENSG00000186842	NA	0.387269	ENSG00000160868	CYP3A4	0.3583202

ENSG00000145826	Lect2	0.3579107	ENSG00000140557	Rlbp1	0.3329264
ENSG00000016082	Isl1	0.3576786	ENSG00000120211	INSL4	0.3326295
ENSG00000149922	tbx6	0.3575435	ENSG00000172150	OR1A2	0.332537
ENSG00000155966	AFF2	0.3566581	ENSG00000065609	SNAP91	0.3321786
ENSG00000130032	PRRG3	0.3556359	ENSG00000126016	amot	0.3308822
ENSG00000106341	C7orf16	0.3537939	ENSG00000122121	XPNPEP2	0.3304179
ENSG00000187848	P2RX2	0.3537733	ENSG00000138030	Khk	0.3302165
ENSG00000173862	FLJ20712	0.3529881	ENSG00000158486	DNAH3	0.3296735
ENSG00000129244	Atp1b2	0.3520614	ENSG00000177301	KCNA2	0.3292115
ENSG00000168594	ADAM29	0.3503074	ENSG00000164270	HTR4	0.3279244
ENSG00000165495	pknox2	0.3492189	ENSG00000204688	OR2H1	0.3232672
ENSG00000142163	GAS8	0.3491661	ENSG00000189430	Ncr1	0.3200652
ENSG00000096264	NCR2	0.346509	ENSG00000151704	KCNJ1	0.3189544
ENSG00000119121	TRPM6	0.3462056	ENSG00000184194	gpr173	0.3186719
ENSG00000147432	CHRNB3	0.346169	ENSG00000150394	CDH8	0.3183765
ENSG00000182674	Kcnb2	0.3450224	ENSG00000067191	CACNB1	0.3178703
ENSG00000100024	UPB1	0.3438957	ENSG00000212128	Tas2r13	0.314547
ENSG00000136750	GAD2	0.3435718	ENSG00000124440	HIF3A	0.3144289
ENSG00000105507	CABP5	0.3417005	ENSG00000101446	Spint3	0.3056903
ENSG00000171587	dscam	0.3416663	ENSG00000117400	mpl	0.3025792
ENSG00000108242	CYP2C18	0.341074	ENSG00000171408	Pde7b	0.2945992
ENSG00000179148	Aloxe3	0.3408911	ENSG00000154646	PRSS7	0.2912065
ENSG00000123307	NEUROD4	0.3401013	ENSG00000036828	Casr	0.280495
ENSG00000138669	PRKG2	0.3397503	ENSG00000112077	RHAG	0.2725781
ENSG00000136695	IL1F5	0.33888	ENSG00000103496	STX4	-0.710558
ENSG00000135443	Krt85	0.3357302	ENSG00000053770	mudeng	-0.7783777
ENSG00000185231	MC2R	0.3354115	ENSG00000139722	vps37b	-0.8385161
ENSG00000196115	ADAM5P	0.3345217	ENSG00000151881	C5orf28	-0.9725618
ENSG00000197410	DCHS2	0.3344258	9ENSG00000143514	tp53bp2	-1.3019142

Appendix B

Maps of the intermediate constructs (pENTR-miR, pMAR342, GIPZ-DEST, TRIPZ-DEST) and final lentiviral vectors (GIPZ-miR, TRIPZ-miR) generated through Gateway cloning (chapter 4.2).

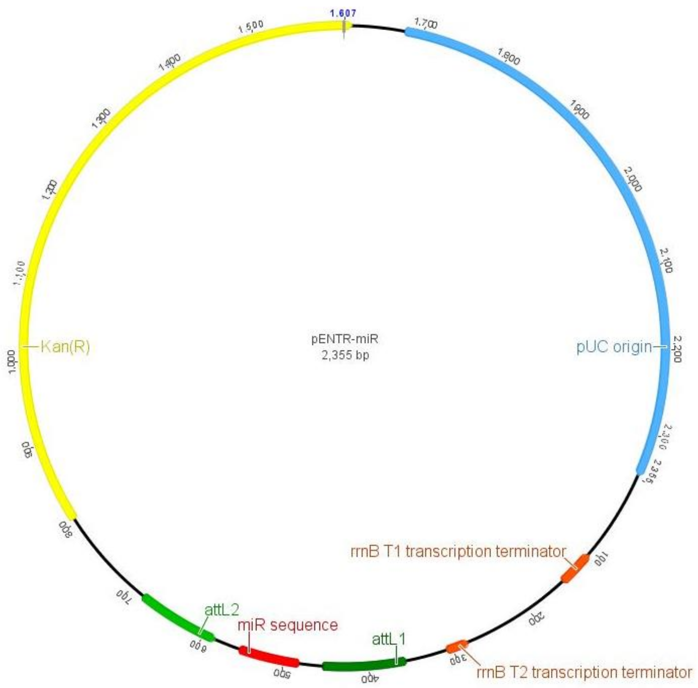

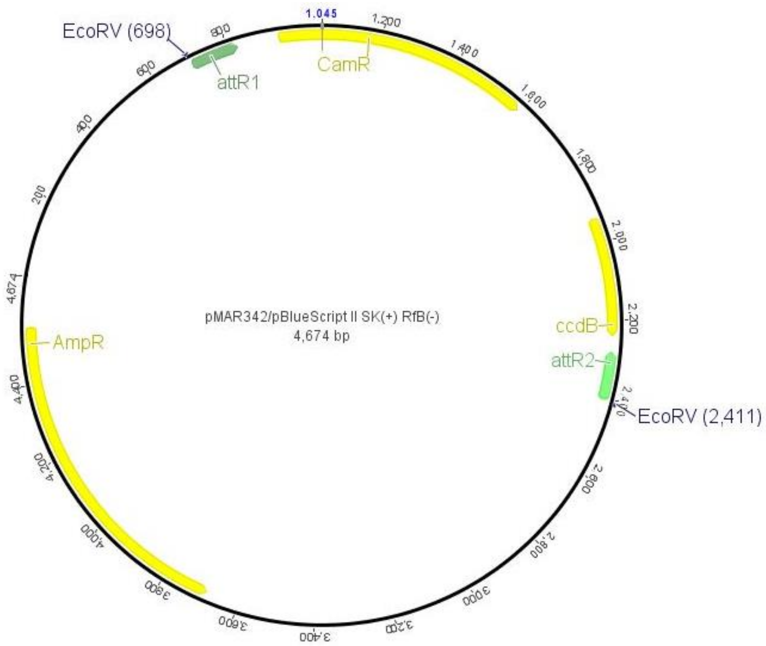

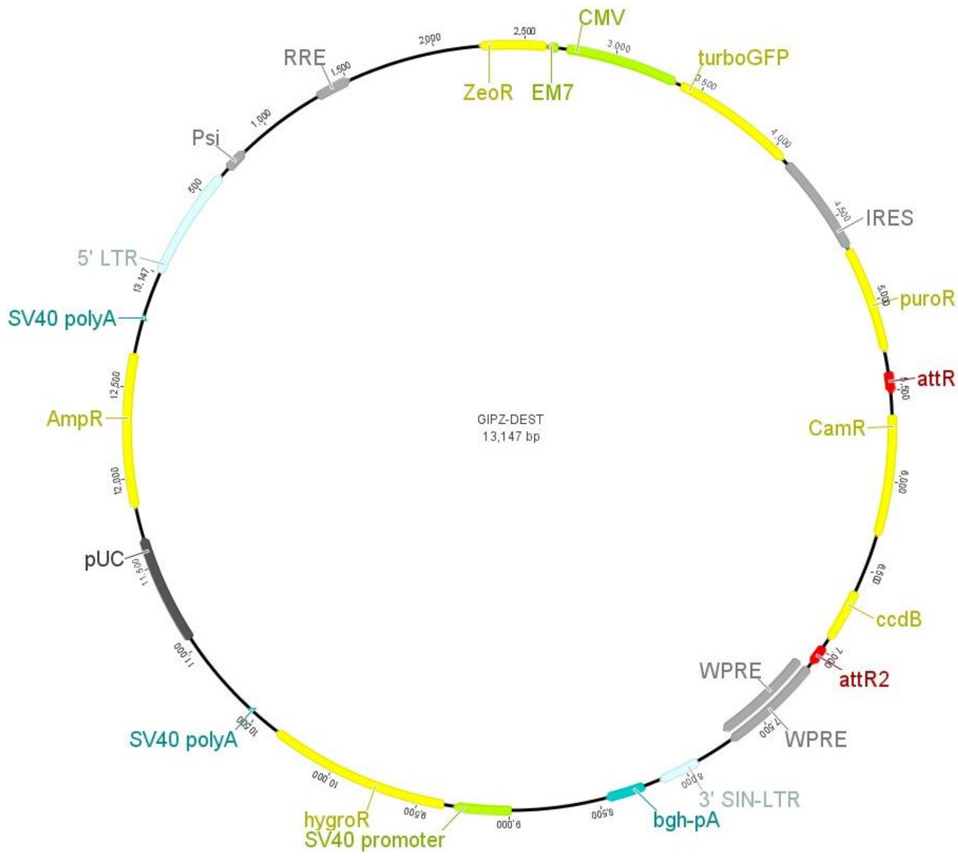
GIPZ-DEST
13,147 bp
CMV
turboGFP
IRES
puroR
attR1
CamR
ccdB
attR2
WPRE
WPRE
3' SIN-LTR
bgh-pA
SV40 promoter
hygroR
SV40 polyA
pUC
AmpR
SV40 polyA
5' LTR
Psi
RRE
ZeoR
EM7

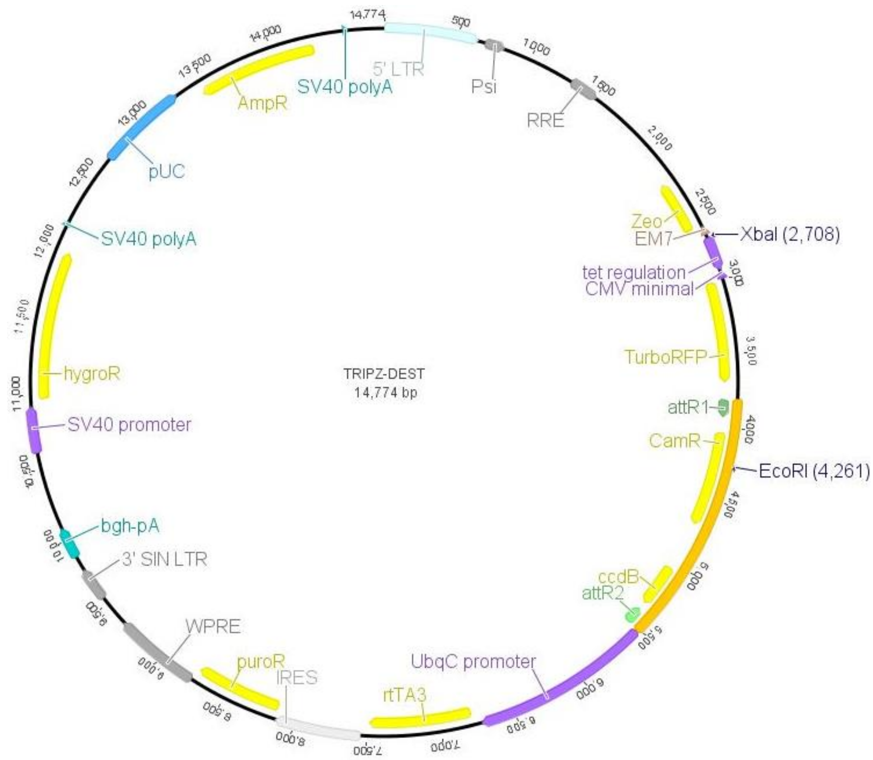
TRIPZ-DEST
14,774 bp
5' LTR
Psi
RRE
SV40 polyA
AmpR
pUC
SV40 polyA
hygroR
SV40 promoter
bgh-pA
3' SIN LTR
WPRE
puroR
IRES
rtTA3
UbqC promoter
attR2
ccdB
CamR
EcoRI (4,261)
attR1
TurboRFP
tet regulation
CMV minimal
Zeo
EM7
XbaI (2,708)

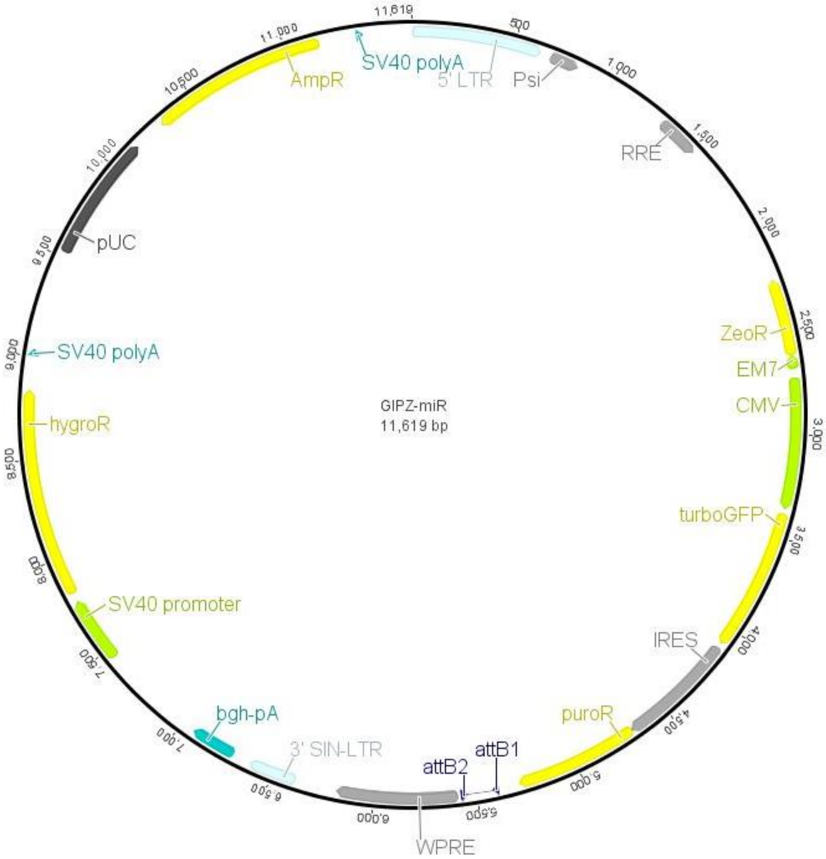

GIPZ-miR
11,619 bp
SV40 polyA
5' LTR
Psi
RRE
ZeoR
EM7
CMV
turboGFP
IRES
puroR
attB1
attB2
WPRE
3' SIN-LTR
bgh-pA
SV40 promoter
hygroR
SV40 polyA
pUC
AmpR

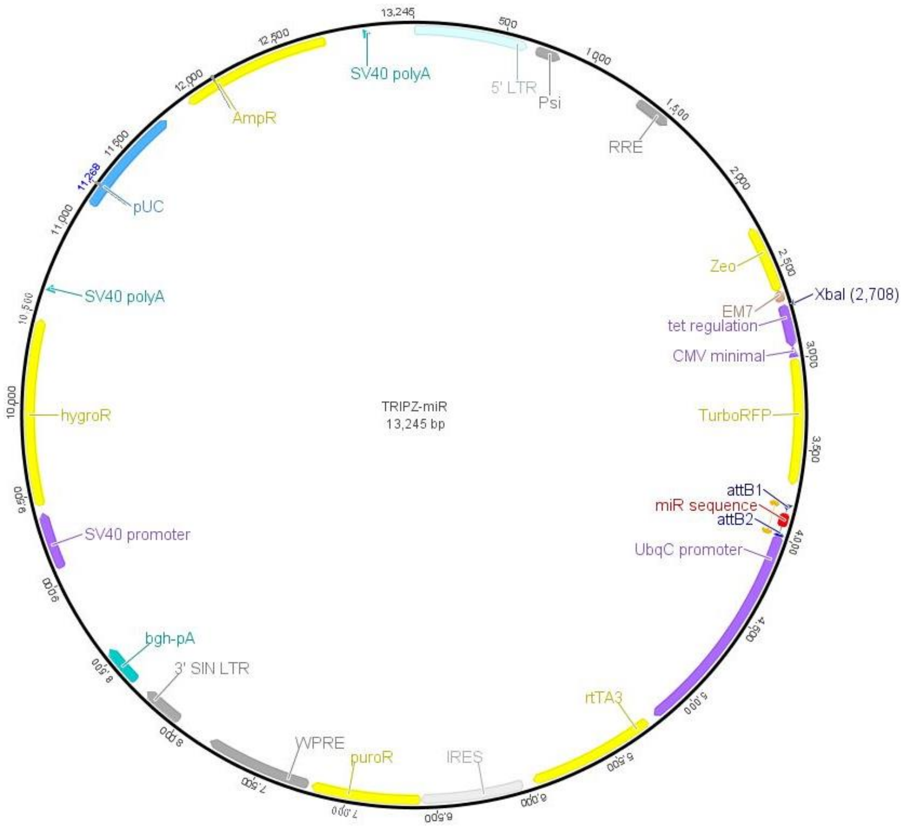

TRIPZ-miR
13,245 bp
SV40 polyA
5' LTR
Psi
RRE
Zeo
XbaI (2,708)
EM7
tet regulation
CMV minimal
TurboRFP
attB1
miR sequence
attB2
UbqC promoter
rtTA3
IRES
puroR
WPRE
3' SIN LTR
bgh-pA
SV40 promoter
hygroR
SV40 polyA
pUC
AmpR

Appendix C

GeneProf analysis of the RNA-seq data: significantly modulated genes in the MDA-MB-157 dataset (fold change relative to WT1 kd vs lacZ).

GENE	FOLD CHANGE	GENE	FOLD CHANGE
AGR2	3.340328	CNTNAP3B	3.006891
CXCL5	2.549697	C8orf4	2.675672
FLRT3	5.084235	PAPPA	2.479477
PTGS2	5.995349	THSD7A	3.696566
AB019438.55	0.007443	ABI3BP	0.034932
AC004696.1	0.014718	AC007879.7	0.019264
AC022409.1	0.023116	AC104135.3	0.015594
AC104135.4	0.014555	ADAMTS2	0.017123
AFF3	0.029771	AIM1	0.157894
AJAP1	0.017702	ALS2CR11	0.016374
ANPEP	0.244917	ARMCX1	0.035404
ATCAY	0.009924	ATP2B2	0.012842
B3GALNT1	0.016581	BGN	0.006506
C21orf56	0.035087	C9orf109	0.039102
C9orf110	0.045963	CACNA1C	0.04517
CAMK4	0.065497	CCNA1	0.021832
CDH6	0.041366	CDKN2A	0.006318
CDKN2B	0.005	COL1A1	0.04004
COL23A1	0.017702	COL5A3	0.010141
COL3A1	0.005484	COL6A1	0.218063
COL6A2	0.179608	COL6A3	0.035791
COL8A2	0.026916	COL9A2	0.059542
COLEC12	0.012397	CPA4	0.099534
CPXM1	0.011908	CRISPLD1	0.044404
CRISPLD2	0.082529	CTB-36O1.5	0.16307
CTHRC1	0.095929	CXCL12	0.014238
CYP1B1	0.24449	CYP27A1	0.037074
DCHS1	0.033138	DDR2	0.022781
DLX1	0.192759	DLX2	0.043401
DMD	0.059542	DNAJC15	0.061212
EFNB2	0.214272	EGFLAM	0.034472
ELAVL2	0.027636	ELAVL3	0.035087
EMILIN2	0.233364	ENG	0.074549
FAM101A	0.008911	FAM133A	0.02413
FBLN2	0.023846	FLNC	0.098863
GAS1	0.021128	GLI3	0.022945
GNAO1	0.018194	GPR1	0.08618
GYPC	0.007528	HLA-B	0.162063
IFITM3	0.2399	IL7R	0.022848
INHBA	0.011491	KCNE4	0.029437
KIAA1644	0.138932	KIF26B	0.020153
KIT	0.007518	L1CAM	0.182542
LAMA4	0.018581	LAMC2	0.281636
LUM	0.003342	LY6K	0.107176
LZTS1	0.054018	MAFB	0.011491
MAGEA3	0.007557	MAGEC2	0.003046
MAN1A1	0.04517	MATK	0.009632
MCAM	0.312072	METRNL	0.177358
MME	0.009492	MMP16	0.016624
MMP2	0.176415	MT-ATP8	0.00933

MXRA5	0.004781	MXRA8	0.189681
MYL9	0.138228	MYO7B	0.011627
NDN	0.018713	NFIX	0.213752
NLGN4X	0.016794	NMNAT2	0.169345
NPTX2	0.016374	ODZ2	0.043664
OLFML2B	0.084722	OXCT1	0.096686
PARP10	0.111221	PCDH7	0.047634
PCOLCE	0.204851	PDGFRB	0.008329
PFTK2	0.017012	PRLR	0.077055
PRMT6	0.015782	PRSS23	0.105397
PTX3	0.088368	QPRT	0.174658
RAMP1	0.016374	RBP7	0.042631
RCAN2	0.007891	RIPK4	0.214238
RP11-414K1.3	0.012129	RP4-788L13.1	0.019264
RSPO4	0.012596	SDC2	0.015748
SECTM1	0.096319	SEMA3D	0.02911
SEMA5A	0.007005	SHE	0.049619
SIM1	0.013099	SLC1A3	0.008931
SLC2A10	0.031189	SLCO2A1	0.006238
SNAI2	0.054258	SORBS2	0.067176
SPARC	0.017949	SV2A	0.032061
TDRD12	0.017654	THNSL2	0.011101
TIAM1	0.16172	TIMP3	0.103476
TMEM200A	0.007043	TMEM46	0.019264
TMTC1	0.012329	TNC	0.090205
TRPS1	0.006009	VGF	0.140787
WNT5B	0.132118	XIST	0.007104
ZNF100	0.017702	ZNF257	0.013099
ZNF439	0.027871	ZNF440	0.015411
ZNF700	0.055742	ZNF793	0.060227
ZNF804A	0.004517	ZNF812	0.022585
ZNF844	0.024716		

Appendix D

Galaxy analysis of the RNA-seq data: significantly modulated genes in the MDA-MB-231 dataset (fold change relative to WT1 kd vs lacZ).

GENE	FOLD CHANGE	GENE	FOLD CHANGE
ADAM23	2.511692762	IGFN1	6.96368044
ADAMTS1	1.686152473	IGSF3	4.119759159
AIF1L	2.456833348	IL13RA2	4.400477255
AMPH	3.362210381	IL18	1.759904324
ARMCX2	3.335308015	KIAA1211	2.848672953
B3GNT7	4.014721745	KIAA1462	3.179213712
BHG	231.3318338	KRT81	1.877086326
BMP2	2.942862222	LAMA1	3.221293245
CA8	3.371311653	LCP1	3.785647288
CALCR	4.516577612	LINC00261	2.085538579
CD24	2.872864601	LMO2	2.733785406
chr14:97744396 – 97745322	5.289055081	LRRN1	6.10783039
chr15:56365586 – 56365765	4.029749054	MIR4763	231.3318338
chr17:38278139 – 38278488	3.190229029	MIRLET7A3	231.3318338
chr2:151086211 – 151086448	4.04483261	MIRLET7B	231.3318338
chr2:235819436 – 235819635	3.785647288	MIRLET7	231.3318338
chr2:51559914 – 51577291	9.066024123	MMP1	5.685668556
chr2:75145080 – 75170865	2.511118306	MSI2	2.680811908
chr3:152593079 – 152593567	3.722108214	NOV	2.322582752
chr3:152593629 – 152594223	3.105832444	NRG2	3.834185136
chr3:152691773 – 152692289	2.784754216	OLFML3	3.304014458
chr3:154327061 – 154327580	2.662774025	PELI2	2.41288641
chr3:17797074 – 17797481	2.540777426	PIK3AP1	3.20572351
chr4:126630409 – 126631173	2.609114034	PKIB	3.105832444
chr4:98054359 – 98056135	2.670685326	PLA2G4A	2.321922791
chr5:92389310 – 92389681	2.872864601	PLCB1	2.998310928
chr5:92389766 – 92390286	3.017533944	PPARGC1A	4.039369158
chr5:97384044 – 97384667	3.190229029	PROS1	1.996134593
chr6:113667099 – 113667513	3.381304635	PTGFR	5.087510969
chr6:113667593 – 113667933	3.722108214	RAB27B	2.564326565
chr6:34231052 – 34231519	5.093650596	SALL2	2.462954541
chr6:72113343 – 72113457	4.349320426	SEL1L3	2.462357097
chr7:93695904 – 93696621	7.723688602	SLC16A2	4.068705897
chr9:84969780 – 84969996	4.108096297	SLC1A1	2.774715779
CHRNA1	5.42261972	SLC4A4	2.523821714
CPEB1	8.201512545	SLC9A2	2.811694794
CREB5	2.373325535	SNTB1	1.958985881
ENPP5	7.370129658	SOX4	2.677283657
ESM1	6.641273902	SPANXA2	4.108096297
FAM133A	4.354689938	STOX2	5.991511489
FAM49A	4.668017598	TFPI2	2.144914291
FOXQ1	1.797330847	TMEM98	3.44117199
GNPTAB	1.674532063	TNC	1.932390948
GPNMB	4.735051116	WNT5A	2.859791564
GPR137B	2.169481073	WTAPP1	5.614994798
HS6ST3	2.944392497		
AFAP1L2	0.512003295	MIR221	0.30450546
AKT2	0.545414893	MIR222	0.30450546
chr2:12246697 – 12271707	0.150272195	MUSK	0.219962577

chr22:20399807 – 20401615	0.369393401	PLCB4	0.319589076
chr7:142494046 – 142500772	0.475847105	PTGS1	0.281672378
chr7:22896548 – 22899240	0.259354984	RSAD2	0.240964079
chrX:45624166 – 45629581	0.211646715	S100A2	0.547708054
COL5A1	0.529931209	SERPINB9	0.551853794
CST6	0.242737683	STMN3	0.502417284
DAPK1	0.387540771	THBS1	0.495140547
EHD1	0.595828897	TNXA	0.240964079
EPHB3	0.206791673	TNXB	0.211646715
GPR110	0.252875645	UCA1	0.313066273
GSTP1	0.547857653	WT1	0.270974688

Appendix E

Galaxy analysis of the RNA-seq data: significantly modulated genes in the MDA-MB-157 dataset (fold change relative to WT1 kd vs lacZ).

GENE	FOLD CHANGE	GENE	FOLD CHANGE
ABCC3	2.087896215	HLA-DMB	4.3472709
AGR2	3.250068218	HS3ST6	10.91726824
ALDH3A2	1.870413179	IGFBP4	2.237131405
APOC1	3.563660742	INSL4	6.174918092
ARSE	2.88457745	ITGB5	2.675984946
ASB4	2.777005434	JUP	2.866339494
BCAS1	6.663499302	KRT4	8.064192065
BCL3	2.701891984	LIMD1	2.034832441
BLVRB	2.101777573	LITAF	2.431691145
C3	2.090068173	LOC100505817	2.082144219
C8orf4	2.328385599	LRP5	2.432955613
CA11	8.489208212	LRRK2	2.87033674
CA12	1.791834014	LSAMP	3.570583854
CACNG6	6.151848607	MALAT1	2.446535132
CACNG7	6.028044219	MEGF9	1.793395894
CDH1	2.638997529	MID1IP1	2.043666803
CDR1	8.955599429	MMD	3.784886401
CELSR2	2.411949999	MTUS1	2.837558233
chr1:201978910 – 201979569	3.753561185	NCMAP	6.348650684
chr10:43839191 – 43839950	11.07427233	NR0B1	2.017054408
chr21:16189782 – 16191179	7.047248074	NR4A1	3.406003695
chr21:16191248 – 16192059	6.443211713	NUP210	1.777533808
chr7:128109116 – 128110111	12.30472065	NUPR1	6.901500205
chr9:39796149 – 39817619	7.096609882	PADI2	11.13376784
CNNM1	2.024842929	PALM3	4.712818104
CNTN1	2.341868389	PAPPA	2.438814451
CNTNAP3	3.068705077	PCDH9	2.046757242
CNTNAP3B	3.321212423	PCSK9	3.434690253
CPLX2	3.531497316	PDK4	3.086817094
CSDC2	7.282430358	PGD	2.56112914
CXCL5	2.33392791	PIFO	7.434573596
CYB5B	3.533921517	PLA2G4A	4.533860493
CYP24A1	2.227646017	PLEKHG2	1.902778989
CYP2S1	2.374609032	PON3	2.469707181
CYSTM1	1.830443192	PPFIBP2	2.109366817
DLL4	20.96803846	PTGS2	5.424837791
DPEP1	7.835145141	RAB26	5.585320234
DUSP5	2.827486233	RAB37	4.946746605
EFCAB12	5.728669072	RASGEF1A	2.827505832
ELF3	3.073835586	SCD	4.716478202
ELMO1	3.036501328	SLC12A2	2.40423847
FGA	8.023546136	SOX2	3.766618714
FGB	4.897583196	SREBF1	3.332257756
FGL1	3.235704814	STEAP1	2.569700104
FKBP10	1.836035559	SULT2B1	8.086749935
FLRT3	4.563750748	SUSD2	8.817563131
FZD8	2.352948917	SYT12	3.468952293
GDF15	2.756676548	THSD7A	3.651759036
GLI1	5.016391686	TMEM2	2.070041943
GPCPD1	2.257068181	TNNC1	9.24280022

GPR20	20.96803846	TSKU	2.380970919
GPRIN3	2.818270325	VTN	4.986854118
HEATR5A	2.387052009		
AARD	0.083956742	LINC00460	0.142841788
ABI3BP	0.043504848	LINC00552	0.045710519
ACHE	0.134351096	LINC00565	0.063864588
ADAM12	0.36472222	LOC100128252	0.007427488
ADAMTS2	0.017677524	LOC100134259	0.152803554
ADAMTS3	0.074816485	LOC100505806	0.057755414
ADRB2	0.140419967	LOC339166	0.057777837
AFP	0.069187729	LOC339535	0.145827024
AIM1	0.162799526	LOC339975	0.010544248
AJAP1	0.014536059	LRCH2	0.220860909
ALS2CR11	0.009449838	LUM	0.002964922
ANPEP	0.275115628	LY6K	0.110131571
ARC	0.103249736	LYPD6	0.231302057
ARHGAP29	0.443501227	LZTS1	0.048459388
ARMCX1	0.035066081	MAFB	0.012999951
ARMCX4	0.182636877	MAGEA3	0.009132085
ATCAY	0.103476137	MAGEC2	0.001546186
ATP2B2	0.017512028	MAL2	0.087259741
B3GALNT1	0.021143822	MAMDC2	0.111316549
BEX1	0.007373737	MAN1A1	0.042999092
BGN	0.007468031	MATK	0.011726908
BHLHE41	0.23943401	MCAM	0.345903136
BNC1	0.094462138	METRNL	0.218120912
C5orf58	0.010678849	METTL7A	0.201434123
CAMK4	0.089128461	MFAP2	0.083810221
CD248	0.0145279	MIR3606	0.006111321
CD34	0.065268921	MME	0.006619876
CDH6	0.032699446	MMP16	0.020518513
CDK15	0.024425468	MMP2	0.194199313
CDKN2A	0.008647147	MXRA5	0.004774515
CDKN2B	0.006160338	MXRA8	0.186442155
CHPF	0.499231198	MYBL1	0.263870139
chr10:5636836 – 5638428	0.167206171	MYL9	0.151168557
chr13:41958149 – 41958436	0.050931076	MYO7B	0.010031701
chr13:41958605 – 41958839	0.067243098	NAP1L3	0.176890687
chr14:106825766 – 106854876	0.016870423	NDC80	0.466898222
chr14:106856142 – 107131115	0.037990434	NDN	0.020589035
chr14:50504528 – 50507288	0.124928973	NFIX	0.259381951
chr15:101624496 – 101626648	0.020518513	NID1	0.417908787
chr17:61506209 – 61509453	0.057755414	NLGN4X	0.016930519
chr18:14969325 – 14970440	0.114966863	NMNAT2	0.159678281
chr2:208104168 – 208111511	0.024750131	NOV	0.268138447
chr2:75145007 – 75170621	0.018644449	NPTX2	0.017440074
chr2:96190805 – 96192490	0.201350366	NR2E1	0.024095708
chr20:57203068 – 57210876	0.025552885	OLFML2B	0.091735249
chr21:43188227 – 43189538	0.03728709	OXCT1	0.090116807
chr21:43194207 – 43198404	0.039937006	PAG1	0.246990935
chr3:197205853 – 197206504	0.01677911	PARP10	0.143843307
chr4:119991134 – 119991452	0.154564403	PCDH18	0.06711644
chr5:13986064 – 13987434	0.128794242	PCDH7	0.048296753
chr5:42951009 – 42955759	0.245233844	PCDHB14	0.100159419
chr6:45631241 – 45632621	0.119318529	PCDHB3	0.127221993
chr7:55840864 – 55841459	0.017666867	PCDHB4	0.190481131
chr8:49293258 – 49297732	0.069209313	PCDHB7	0.147401182
chr8:60032480 – 60033396	0.099289158	PCLO	0.151693377
chr9:137514718 – 137516870	0.029181139	PCOLCE	0.182991685

CLDN11	0.153997624	PDGFRB	0.008272735
COL12A1	0.328071005	PDLIM3	0.184200643
COL15A1	0.082190189	PEA15	0.454757709
COL1A1	0.048813364	PEG3	0.002057787
COL21A1	0.267961939	PITPNC1	0.399373358
COL23A1	0.030542247	PLA2G7	0.080845988
COL3A1	0.006111321	PLAC8	0.152069212
COL5A1	0.493468534	PRKCDBP	0.126210164
COL5A3	0.012029246	PRMT6	0.016870423
COL6A1	0.262962685	PRR16	0.045710519
COL6A2	0.217434082	PRRX1	0.044090755
COL6A3	0.040967964	PRSS35	0.103214674
COL8A2	0.031137135	PTH2R	0.083636703
COL9A2	0.083636703	PTX3	0.086458403
COLEC12	0.010678849	PXDN	0.537244234
COX7B2	0.029181139	QPRT	0.210860388
CPA4	0.103200367	RAB20	0.207312642
CPXM1	0.038489	RAMP1	0.02078577
CRABP1	0.093034524	RASSF8	0.389628199
CRISPLD1	0.038992217	RBP7	0.040653405
CRISPLD2	0.091988671	RCAN2	0.00918239
CRLF1	0.134660628	RIPK4	0.247061138
CSF1R	0.105638674	RORB	0.003519387
CTHRC1	0.08431248	SALL3	0.016726971
CTNNAL1	0.36187416	SAMD9L	0.263093954
CXCL12	0.017456402	SDC2	0.0145279
CXCR7	0.18557445	SDC4	0.453306892
CYP1B1	0.235501801	SDR16C	0.233952897
CYP27A1	0.050738687	SECTM1	0.111619423
DACT1	0.18992214	SEMA5A	0.015934969
DCHS1	0.04105495	SERTAD2	0.432034971
DDR2	0.026610511	SH2B3	0.430098797
DLL1	0.117876661	SHE	0.062946065
DLX1	0.208007867	SHISA2	0.032203471
DLX2	0.053439488	SHISA3	0.107085867
DMD	0.075699102	SHROOM2	0.351603174
DNAJC15	0.058350547	SIX	0.108707245
DPF3	0.165630469	SLC12A8	0.115470001
EDIL3	0.058141012	SLC1A3	0.008072493
EFNB2	0.211838982	SLC2A10	0.022435078
EGFLAM	0.020710411	SLC6A10P	0.072594799
ELAVL2	0.020877605	SLCO2A1	0.006445916
ELAVL3	0.041106775	SLFN12	0.065403425
ELFN1	0.193884584	SNAI2	0.050010679
EMILIN2	0.310167622	SNCA	0.067240767
EMP1	0.414849514	SORBS2	0.054519646
ENG	0.06763904	SPARC	0.01744491
ENPP2	0.065445146	SPATC1L	0.042589157
EPHA4	0.28813164	SPOCK1	0.480970395
ETS1	0.409257284	SSTR2	0.161999358
FAM133A	0.021825825	ST8SIA6-AS1	0.013365615
FAM225A	0.045774565	SV2A	0.03150883
FAM225B	0.060598252	TDRD12	0.022618076
FAM43A	0.279687949	TENM2	0.037089124
FAM90A1	0.065454219	THNSL2	0.090116807
FAP	0.049157999	TIAM1	0.166580335
FBLL1	0.095991469	TIMP3	0.100525959
FBLN2	0.030132413	TMEM200A	0.009449838
FBXL7	0.303468778	TMEM255A	0.114852168

FLI1	0.012471856	TMEM63C	0.229258956
FLNC	0.110694849	TMPRSS3	0.103432394
FOSL1	0.230975222	TMTC1	0.017547752
FOXC2	0.123315837	TNC	0.089349905
FRMD6	0.296743843	TNFRSF9	0.119690454
G0S2	0.102951018	TOX	0.129809691
GAS1	0.024710705	TRIB2	0.096910715
GBP1	0.167155184	TRIM58	0.056235307
GBP4	0.155524093	TRPS1	0.007373737
GIPC3	0.182085759	TUBB2A	0.46323302
GLI3	0.022296638	TXNIP	0.184888834
GLIS1	0.0363271	UGT3A2	0.119690454
GNAO1	0.031807262	VGF	0.189242758
GPR1	0.104992632	VIT	0.135415989
GPR110	0.053540707	WNT3A	0.086603552
GUSBP5	0.044702831	WNT5A	0.127064243
GYPC	0.009096573	WNT5B	0.131805556
HEY1	0.196623818	XAF1	0.100523868
HEY2	0.102047306	XIST	0.010209033
HK2	0.312942607	ZIC1	0.127221993
HLA-B	0.254018674	ZIM2	0.002057787
HLA-C	0.254018674	ZNF100	0.066021055
HOXC12	0.010565025	ZNF253	0.066020597
ID4	0.195894663	ZNF257	0.021621494
IFI44	0.160512772	ZNF320	0.154572974
IFITM3	0.359312243	ZNF347	0.241278288
IL11	0.382144455	ZNF429	0.122102107
IL13RA2	0.0187727	ZNF440	0.03918214
IL6	0.120426099	ZNF471	0.122730864
IL7R	0.038489	ZNF486	0.085083902
ITGA4	0.349593436	ZNF492	0.144869922
JAM2	0.094194067	ZNF506	0.135415989
JUN	0.268985442	ZNF667	0.019276675
KAL1	0.092424555	ZNF681	0.234404147
KCNE4	0.0483993	ZNF69	0.045987641
KIAA1644	0.141874774	ZNF700	0.052628935
KIF26B	0.011187739	ZNF702P	0.01370892
KIF5C	0.281097007	ZNF737	0.125428752
KIT	0.005927502	ZNF781	0.019906039
L1CAM	0.206262006	ZNF788	0.083875891
LAMC2	0.277313547	ZNF793	0.269313788
LAPTM5	0.106301216	ZNF804A	0.004047341
LGI2	0.106871568	ZNF812	0.034186487
LIMA1	0.351620235	ZNF844	0.03077921
LINC00221	0.005893458	ZNF91	0.268746897
LINC00346	0.069097628	ZNF93	0.013725761

References

Adachi, Y., S. Matsubara, C. Pedraza, M. Ozawa, J. Tsutsui, H. Takamatsu, H. Noguchi, T. Akiyama and T. Muramatsu (1996). "Midkine as a novel target gene for the Wilms' tumor suppressor gene (WT1)." Oncogene **13**(10): 2197-2203.

Adriance, M. C., J. L. Inman, O. W. Petersen and M. J. Bissell (2005). "Myoepithelial cells: good fences make good neighbors." Breast Cancer Res **7**(5): 190-197.

Algar, E. M., T. Khromykh, S. I. Smith, D. M. Blackburn, G. J. Bryson and P. J. Smith (1996). "A WT1 antisense oligonucleotide inhibits proliferation and induces apoptosis in myeloid leukaemia cell lines." Oncogene **12**(5): 1005-1014.

Alva, J. A., A. C. Zovein, A. Monvoisin, T. Murphy, A. Salazar, N. L. Harvey, P. Carmeliet and M. L. Iruela-Arispe (2006). "VE-Cadherin-Cre-recombinase transgenic mouse: a tool for lineage analysis and gene deletion in endothelial cells." Dev Dyn **235**(3): 759-767.

Amini Nik, S., P. Hohenstein, A. Jadidizadeh, K. Van Dam, A. Bastidas, R. L. Berry, C. E. Patek, B. Van der Schueren, J. J. Cassiman and S. Tejpar (2005). "Upregulation of Wilms' tumor gene 1 (WT1) in desmoid tumors." Int J Cancer **114**(2): 202-208.

Ariyaratana, S. and D. M. Loeb (2007). "The role of the Wilms tumour gene (WT1) in normal and malignant haematopoiesis." Expert Rev Mol Med **9**(14): 1-17.

Armstrong, J. F., K. Pritchard-Jones, W. A. Bickmore, N. D. Hastie and J. B. Bard (1993). "The expression of the Wilms' tumour gene, WT1, in the developing mammalian embryo." Mech Dev **40**(1-2): 85-97.

Artibani (2010) “WT1 role in adult tumours” MsC thesis from The University of Edinburgh

Asselin-Labat, M. L., F. Vaillant, J. M. Sheridan, B. Pal, D. Wu, E. R. Simpson, H. Yasuda, G. K. Smyth, T. J. Martin, G. J. Lindeman and J. E. Visvader (2010). "Control of mammary stem cell function by steroid hormone signalling." Nature **465**(7299): 798-802.

Atabai, K., R. Fernandez, X. Huang, I. Ueki, A. Kline, Y. Li, S. Sadatmansoori, C. Smith-Steinhart, W. Zhu, R. Pytela, Z. Werb and D. Sheppard (2005). "Mfge8 is critical for mammary gland remodeling during involution." Mol Biol Cell **16**(12): 5528-5537.

Bae, V. L., C. K. Jackson-Cook, A. R. Brothman, S. J. Maygarden and J. L. Ware (1994). "Tumorigenicity of SV40 T antigen immortalized human prostate epithelial cells: association with decreased epidermal growth factor receptor (EGFR) expression." Int J Cancer **58**(5): 721-729.

Bandiera, R., V. P. Vidal, F. J. Motamedi, M. Clarkson, I. Sahut-Barnola, A. von Gise, W. T. Pu, P. Hohenstein, A. Martinez and A. Schedl (2013). "WT1 maintains adrenal-gonadal primordium identity and marks a population of AGP-like progenitors within the adrenal gland." Dev Cell **27**(1): 5-18.

Barragan, E., J. Cervera, P. Bolufer, S. Ballester, G. Martin, P. Fernandez, R. Collado, M. J. Sayas and M. A. Sanz (2004). "Prognostic implications of Wilms' tumor gene (WT1) expression in patients with de novo acute myeloid leukemia." Haematologica **89**(8): 926-933.

Batlle, E., E. Sancho, C. Franci, D. Dominguez, M. Monfar, J. Baulida and A. Garcia De Herreros (2000). "The transcription factor snail is a repressor of E-cadherin gene expression in epithelial tumour cells." Nat Cell Biol **2**(2): 84-89.

Bennett, M. K., J. E. Garcia-Arraras, L. A. Elferink, K. Peterson, A. M. Fleming, C. D. Hazuka and R. H. Scheller (1993). "The syntaxin family of vesicular transport receptors." Cell **74**(5): 863-873.

Bergmann, L., C. Miething, U. Maurer, J. Brieger, T. Karakas, E. Weidmann and D. Hoelzer (1997). "High levels of Wilms' tumor gene (wt1) mRNA in acute myeloid leukemias are associated with a worse long-term outcome." Blood **90**(3): 1217-1225.

Bhowmick, N. A., M. Ghiassi, A. Bakin, M. Aakre, C. A. Lundquist, M. E. Engel, C. L. Arteaga and H. L. Moses (2001). "Transforming growth factor-beta1 mediates epithelial to mesenchymal transdifferentiation through a RhoA-dependent mechanism." Mol Biol Cell **12**(1): 27-36.

Blanco, M. J., G. Moreno-Bueno, D. Sarrio, A. Locascio, A. Cano, J. Palacios and M. A. Nieto (2002). "Correlation of Snail expression with histological grade and lymph node status in breast carcinomas." Oncogene **21**(20): 3241-3246.

Borowsky, A. D. (2011). "Choosing a mouse model: experimental biology in context--the utility and limitations of mouse models of breast cancer." Cold Spring Harb Perspect Biol **3**(9): a009670.

Brabletz, T., A. Jung, S. Reu, M. Porzner, F. Hlubek, L. A. Kunz-Schughart, R. Knuechel and T. Kirchner (2001). "Variable beta-catenin expression in colorectal cancers indicates tumor progression driven by the tumor environment." Proc Natl Acad Sci U S A **98**(18): 10356-10361.

Brabletz, T., A. Jung, S. Spaderna, F. Hlubek and T. Kirchner (2005). "Opinion: migrating cancer stem cells - an integrated concept of malignant tumour progression." Nat Rev Cancer **5**(9): 744-749.

Breslow, N. E., J. R. Takashima, J. A. Whitton, J. Moksness, G. J. D'Angio and D. M. Green (1995). "Second malignant neoplasms following treatment for Wilm's tumor: a report from the National Wilms' Tumor Study Group." J Clin Oncol **13**(8): 1851-1859.

Brisken, C. and B. O'Malley (2010). "Hormone action in the mammary gland." Cold Spring Harbour Perspectives in Biology **2**(12): a003178.

Brisken, C., A. Heineman, T. Chavarria, B. Elenbaas, J. Tan, S. K. Dey, J. A. McMahon, A. P. McMahon and R. A. Weinberg (2000). "Essential function of Wnt-4 in mammary gland development downstream of progesterone signaling." Genes Dev **14**(6): 650-654.

Bruening, W. and J. Pelletier (1996). "A non-AUG translational initiation event generates novel WT1 isoforms." J Biol Chem **271**(15): 8646-8654.

Buckler, A. J., J. Pelletier, D. A. Haber, T. Glaser and D. E. Housman (1991). "Isolation, characterization, and expression of the murine Wilms' tumor gene (WT1) during kidney development." Mol Cell Biol **11**(3): 1707-1712.

Burwell, E. A., G. P. McCarty, L. A. Simpson, K. A. Thompson and D. M. Loeb (2006). "Isoforms of Wilms/' tumor suppressor gene (WT1) have distinct effects on mammary epithelial cells." Oncogene **26**(23): 3423-3430.

Caldon, C. E., C. S. Lee, R. L. Sutherland and E. A. Musgrove (2008). "Wilms' tumor protein 1: an early target of progestin regulation in T-47D breast cancer cells that modulates proliferation and differentiation." Oncogene **27**(1): 126-138.

Call, K. M., T. Glaser, C. Y. Ito, A. J. Buckler, J. Pelletier, D. A. Haber, E. A. Rose, A. Kral, H. Yeger, W. H. Lewis and et al. (1990). "Isolation and characterization of a zinc finger polypeptide gene at the human chromosome 11 Wilms' tumor locus." Cell **60**(3): 509-520.

Calvo, A., R. Catena, M. S. Noble, D. Carbott, I. Gil-Bazo, O. Gonzalez-Moreno, J. I. Huh, R. Sharp, T. H. Qiu, M. R. Anver, G. Merlino, R. B. Dickson, M. D. Johnson and J. E. Green (2008). "Identification of VEGF-regulated genes associated with increased lung metastatic potential: functional involvement of tenascin-C in tumor growth and lung metastasis." Oncogene **27**(40): 5373-5384.

Campbell, C. E., N. P. Kuriyan, R. R. Rackley, M. J. Caulfield, R. Tubbs, J. Finke and B. R. Williams (1998). "Constitutive expression of the Wilms tumor suppressor gene (WT1) in renal cell carcinoma." Int J Cancer **78**(2): 182-188.

Cardiff, R. D., D. Moghanaki and R. A. Jensen (2000). "Genetically engineered mouse models of mammary intraepithelial neoplasia." J Mammary Gland Biol Neoplasia **5**(4): 421-437.

Cardiff, R. D., M. R. Anver, B. A. Gusterson, L. Hennighausen, R. A. Jensen, M. J. Merino, S. Rehm, J. Russo, F. A. Tavassoli, L. M. Wakefield, J. M. Ward and J. E. Green (2000). "The mammary pathology of genetically engineered mice: the consensus report and recommendations from the Annapolis meeting." Oncogene **19**(8): 968-988.

Caricasole, A., A. Duarte, S. H. Larsson, N. D. Hastie, M. Little, G. Holmes, I. Todorov and A. Ward (1996). "RNA binding by the Wilms tumor suppressor zinc finger proteins." Proc Natl Acad Sci U S A **93**(15): 7562-7566.

Carpentieri, D. F., K. Nichols, P. M. Chou, M. Matthews, B. Pawel and D. Huff (2002). "The expression of WT1 in the differentiation of rhabdomyosarcoma from other pediatric small round blue cell tumors." Mod Pathol **15**(10): 1080-1086.

Cesaro, E., G. Montano, A. Rosati, R. Crescitelli, P. Izzo, M. C. Turco and P. Costanzo (2010). "WT1 protein is a transcriptional activator of the antiapoptotic bag3 gene." Leukemia **24**(6): 1204-1206.

Chakrabarti, R., Y. Wei, R. A. Romano, C. DeCoste, Y. Kang and S. Sinha (2012). "Elf5 regulates mammary gland stem/progenitor cell fate by influencing notch signaling." Stem Cells **30**(7): 1496-1508.

Chang, H., F. Gao, F. Guillou, M. M. Taketo, V. Huff and R. R. Behringer (2008). "Wt1 negatively regulates beta-catenin signaling during testis development." Development **135**(10): 1875-1885.

Charehbili, A., D. B. Fontein, J. R. Kroep, G. J. Liefers, J. S. Mieog, J. W. Nortier and C. J. van de Velde (2014). "Neoadjuvant hormonal therapy for endocrine sensitive breast cancer: a systematic review." Cancer Treat Rev **40**(1): 86-92.

Chau, Y. Y. and N. D. Hastie (2012). "The role of Wt1 in regulating mesenchyme in cancer, development, and tissue homeostasis." Trends Genet **28**(10): 515-524.

Chau, Y. Y., D. Brownstein, H. Mjoseng, W. C. Lee, N. Buza-Vidas, C. Nerlov, S. E. Jacobsen, P. Perry, R. Berry, A. Thornburn, D. Sexton, N. Morton, P. Hohenstein, E. Freyer, K. Samuel, R. van't Hof and N. Hastie (2011). "Acute multiple organ failure in adult mice deleted for the developmental regulator Wt1." PLoS Genet **7**(12): e1002404.

Chen, F., A. Li, S. Gao, D. Hollern, M. Williams, F. Liu, E. A. VanSickle, E. Andrechek, C. Zhang, C. Yang, R. Luo and H. Xiao (2014). "Tip30 controls differentiation of murine mammary luminal progenitor to estrogen receptor-positive luminal cell through regulating FoxA1 expression." Cell Death Dis **5**: e1242.

Cheng, C. W., P. E. Wu, J. C. Yu, C. S. Huang, C. T. Yue, C. W. Wu and C. Y. Shen (2001). "Mechanisms of inactivation of E-cadherin in breast carcinoma: modification of the two-hit hypothesis of tumor suppressor gene." Oncogene **20**(29): 3814-3823.

Choi, Y. S., R. Chakrabarti, R. Escamilla-Hernandez and S. Sinha (2009). "Elf5 conditional knockout mice reveal its role as a master regulator in mammary alveolar development: failure of Stat5 activation and functional differentiation in the absence of Elf5." Dev Biol **329**(2): 227-241.

Ciarloni, L., S. Mallepell and C. Brisken (2007). "Amphiregulin is an essential mediator of estrogen receptor alpha function in mammary gland development." Proc Natl Acad Sci U S A **104**(13): 5455-5460.

Clark, A. J., W. G. Dos Santos, J. McCready, M. Y. Chen, T. E. Van Meter, J. L. Ware, S. B. Wolber, H. Fillmore and W. C. Broaddus (2007). "Wilms tumor 1 expression in malignant gliomas and correlation of +KTS isoforms with p53 status." J Neurosurg **107**(3): 586-592.

Clarkson, R. W., M. T. Wayland, J. Lee, T. Freeman and C. J. Watson (2004). "Gene expression profiling of mammary gland development reveals putative roles for death receptors and immune mediators in post-lactational regression." Breast Cancer Res **6**(2): R92-109.

Clemons, M. and P. Goss (2001). "Estrogen and the risk of breast cancer." N Engl J Med **344**(4): 276-285.

Cockrell, A. S., H. Ma, K. Fu, T. J. McCown and T. Kafri (2006). "A trans-lentiviral packaging cell line for high-titer conditional self-inactivating HIV-1 vectors." Mol Ther **14**(2): 276-284.

Colombo, P. E., F. Milanezi, B. Weigelt and J. S. Reis-Filho (2011). "Microarrays in the 2010s: the contribution of microarray-based gene expression profiling to breast cancer classification, prognostication and prediction." Breast Cancer Res **13**(3): 212.

Comijn, J., G. Berx, P. Vermassen, K. Verschueren, L. van Grunsven, E. Bruyneel, M. Mareel, D. Huylebroeck and F. van Roy (2001). "The two-handed E box binding zinc finger protein SIP1 downregulates E-cadherin and induces invasion." Mol Cell **7**(6): 1267-1278.

Cook, D. M., M. T. Hinkes, M. Bernfield and F. J. Rauscher, 3rd (1996). "Transcriptional activation of the syndecan-1 promoter by the Wilms' tumor protein WT1." Oncogene **13**(8): 1789-1799.

Coosemans, A., S. A. Nik, S. Caluwaerts, S. Lambin, G. Verbist, R. Van Bree, V. Schelfhout, E. de Jonge, I. Dalle, G. Jacomen, J. J. Cassiman, P. Moerman, I. Vergote and F. Amant (2007). "Upregulation of Wilms' tumour gene 1 (WT1) in uterine sarcomas." Eur J Cancer **43**(10): 1630-1637.

Coughlin, S. S. and D. U. Ekwueme (2009). "Breast cancer as a global health concern." Cancer Epidemiol **33**(5): 315-318.

Cox, A., A. M. Dunning, M. Garcia-Closas, S. Balasubramanian, M. W. Reed, K. A. Pooley, S. Scollen, C. Baynes, B. A. Ponder, S. Chanock, J. Lissowska, L. Brinton, B. Peplonska, M. C. Southey, J. L. Hopper, M. R. McCredie, G. G. Giles,

O. Fletcher, N. Johnson, I. dos Santos Silva, L. Gibson, S. E. Bojesen, B. G. Nordestgaard, C. K. Axelsson, D. Torres, U. Hamann, C. Justenhoven, H. Brauch, J. Chang-Claude, S. Kropp, A. Risch, S. Wang-Gohrke, P. Schurmann, N. Bogdanova, T. Dork, R. Fagerholm, K. Aaltonen, C. Blomqvist, H. Nevanlinna, S. Seal, A. Renwick, M. R. Stratton, N. Rahman, S. Sangrajrang, D. Hughes, F. Odefrey, P. Brennan, A. B. Spurdle, G. Chenevix-Trench, J. Beesley, A. Mannermaa, J. Hartikainen, V. Kataja, V. M. Kosma, F. J. Couch, J. E. Olson, E. L. Goode, A. Broeks, M. K. Schmidt, F. B. Hogervorst, L. J. Van't Veer, D. Kang, K. Y. Yoo, D. Y. Noh, S. H. Ahn, S. Wedren, P. Hall, Y. L. Low, J. Liu, R. L. Milne, G. Ribas, A. Gonzalez-Neira, J. Benitez, A. J. Sigurdson, D. L. Stredrick, B. H. Alexander, J. P. Struewing, P. D. Pharoah and D. F. Easton (2007). "A common coding variant in CASP8 is associated with breast cancer risk." Nat Genet **39**(3): 352-358.

Crewe, H. K., S. W. Ellis, M. S. Lennard and G. T. Tucker (1997). "Variable contribution of cytochromes P450 2D6, 2C9 and 3A4 to the 4-hydroxylation of tamoxifen by human liver microsomes." Biochem Pharmacol **53**(2): 171-178.

Dame, C., K. M. Kirschner, K. V. Bartz, T. Wallach, C. S. Hussels and H. Scholz (2006). "Wilms tumor suppressor, Wt1, is a transcriptional activator of the erythropoietin gene." Blood **107**(11): 4282-4290.

Davar, D., J. H. Beumer, L. Hamieh and H. Tawbi (2012). "Role of PARP inhibitors in cancer biology and therapy." Curr Med Chem **19**(23): 3907-3921.

Davies, J. A., M. Ladomery, P. Hohenstein, L. Michael, A. Shafe, L. Spraggon and N. Hastie (2004). "Development of an siRNA-based method for repressing specific genes in renal organ culture and its use to show that the Wt1 tumour suppressor is required for nephron differentiation." Hum Mol Genet **13**(2): 235-246.

Davies, R. C., C. Calvio, E. Bratt, S. H. Larsson, A. I. Lamond and N. D. Hastie (1998). "WT1 interacts with the splicing factor U2AF65 in an isoform-dependent manner and can be incorporated into spliceosomes." Genes Dev **12**(20): 3217-3225.

de Cremoux, P., C. Tran-Perennou, B. L. Brockdorff, E. Boudou, N. Brunner, H. Magdelenat and A. E. Lykkesfeldt (2003). "Validation of real-time RT-PCR for analysis of human breast cancer cell lines resistant or sensitive to treatment with antiestrogens." Endocr Relat Cancer **10**(3): 409-418.

de Cremoux, P., C. Tran-Perennou, C. Elie, E. Boudou, C. Barbaroux, M. F. Poupon, Y. De Rycke, B. Asselain and H. Magdelenat (2002). "Quantitation of estradiol receptors alpha and beta and progesterone receptors in human breast tumors by real-time reverse transcription-polymerase chain reaction. Correlation with protein assays." Biochem Pharmacol **64**(3): 507-515.

de Menezes, R. F., A. Bergmann and L. C. Thuler (2013). "Alcohol consumption and risk of cancer: a systematic literature review." Asian Pac J Cancer Prev **14**(9): 4965-4972.

Dechsukhum, C., J. L. Ware, A. Ferreira-Gonzalez, D. S. Wilkinson and C. T. Garrett (2000). "Detection of a novel truncated WT1 transcript in human neoplasia." Mol Diagn **5**(2): 117-128.

Dedes, K. J., P. M. Wilkerson, D. Wetterskog, B. Weigelt, A. Ashworth and J. S. Reis-Filho (2011). "Synthetic lethality of PARP inhibition in cancers lacking BRCA1 and BRCA2 mutations." Cell Cycle **10**(8): 1192-1199.

Dejong, V., A. Degeorges, S. Filleur, S. Ait-Si-Ali, A. Mettouchi, P. Bornstein, B. Binetruy and F. Cabon (1999). "The Wilms' tumor gene product represses the transcription of thrombospondin 1 in response to overexpression of c-Jun." Oncogene **18**(20): 3143-3151.

Dennis, S. L., S. S. Manji, D. P. Carrington, D. L. Scarcella, D. M. Ashley, P. J. Smith and E. M. Algar (2002). "Expression and mutation analysis of the Wilms' tumor 1 gene in human neural tumors." Int J Cancer **97**(5): 713-715.

Devilard, E., F. Bladou, O. Ramuz, G. Karsenty, J. P. Dales, G. Gravis, C. Nguyen, F. Bertucci, L. Xerri and D. Birnbaum (2006). "FGFR1 and WT1 are markers of human prostate cancer progression." BMC Cancer **6**: 272.

Dey, B. R., V. P. Sukhatme, A. B. Roberts, M. B. Sporn, F. J. Rauscher, 3rd and S. J. Kim (1994). "Repression of the transforming growth factor-beta 1 gene by the Wilms' tumor suppressor WT1 gene product." Mol Endocrinol **8**(5): 595-602.

Dickson, C., A. Creer and V. Fantl (2000). "Mammary gland oncogenes as indicators of pathways important in mammary gland development." Oncogene **19**(8): 1097-1101.

Dixon, J. M. (2009). ABC OF BREAST DISEASES, BMJ Books.

Dohi, S., S. Ohno, Y. Ohno, S. Kyo, G. Soma, H. Sugiyama and M. Inoue (2010). "WT1 expression correlates with angiogenesis in endometrial cancer tissue." Anticancer Res **30**(8): 3187-3192.

Drummond, I. A., S. L. Madden, P. Rohwer-Nutter, G. I. Bell, V. P. Sukhatme and F. J. Rauscher, 3rd (1992). "Repression of the insulin-like growth factor II gene by the Wilms tumor suppressor WT1." Science **257**(5070): 674-678.

Easton, D. F., K. A. Pooley, A. M. Dunning, P. D. Pharoah, D. Thompson, D. G. Ballinger, J. P. Struewing, J. Morrison, H. Field, R. Luben, N. Wareham, S. Ahmed, C. S. Healey, R. Bowman, K. B. Meyer, C. A. Haiman, L. K. Kolonel, B. E. Henderson, L. Le Marchand, P. Brennan, S. Sangrajrang, V. Gaborieau, F. Odefrey, C. Y. Shen, P. E. Wu, H. C. Wang, D. Eccles, D. G. Evans, J. Peto, O. Fletcher, N. Johnson, S. Seal, M. R. Stratton, N. Rahman, G. Chenevix-Trench, S. E. Bojesen, B. G. Nordestgaard, C. K. Axelsson, M. Garcia-Closas, L. Brinton, S. Chanock, J. Lissowska, B. Peplonska, H. Nevanlinna, R. Fagerholm, H. Eerola, D. Kang, K. Y. Yoo, D. Y. Noh, S. H. Ahn, D. J. Hunter, S. E. Hankinson, D. G. Cox, P. Hall, S. Wedren, J. Liu, Y. L. Low, N. Bogdanova, P. Schurmann, T. Dork, R. A. Tollenaar, C. E. Jacobi, P. Devilee, J. G. Klijn, A. J. Sigurdson, M. M. Doody, B. H. Alexander, J. Zhang, A. Cox, I. W. Brock, G. MacPherson, M. W. Reed, F. J. Couch, E. L. Goode, J. E. Olson, H. Meijers-Heijboer, A. van den Ouweland, A. Uitterlinden, F. Rivadeneira, R. L. Milne, G. Ribas, A. Gonzalez-Neira, J. Benitez, J. L. Hopper, M. McCredie, M. Southey, G. G. Giles, C. Schroen, C. Justenhoven, H. Brauch, U. Hamann, Y. D. Ko, A. B. Spurdle, J. Beesley, X. Chen, A. Mannermaa, V. M. Kosma, V. Kataja, J. Hartikainen, N. E. Day, D. R. Cox and B. A. Ponder (2007). "Genome-wide association study identifies novel breast cancer susceptibility loci." Nature **447**(7148): 1087-1093.

Engels, F. K., A. J. Ten Tije, S. D. Baker, C. K. Lee, W. J. Loos, A. G. Vulto, J. Verweij and A. Sparreboom (2004). "Effect of cytochrome P450 3A4 inhibition on the pharmacokinetics of docetaxel." Clin Pharmacol Ther **75**(5): 448-454.

Englert, C., M. Vidal, S. Maheswaran, Y. Ge, R. M. Ezzell, K. J. Isselbacher and D. A. Haber (1995). "Truncated WT1 mutants alter the subnuclear localization of the wild-type protein." Proc Natl Acad Sci U S A **92**(26): 11960-11964.

Englert, C., S. Maheswaran, A. J. Garvin, J. Kreidberg and D. A. Haber (1997). "Induction of p21 by the Wilms' tumor suppressor gene WT1." Cancer Res **57**(8): 1429-1434.

Englert, C., X. Hou, S. Maheswaran, P. Bennett, C. Ngwu, G. G. Re, A. J. Garvin, M. R. Rosner and D. A. Haber (1995). "WT1 suppresses synthesis of the epidermal growth factor receptor and induces apoptosis." Embo j **14**(19): 4662-4675.

Essafi, A., A. Webb, R. L. Berry, J. Slight, S. F. Burn, L. Spraggon, V. Velecela, O. M. Martinez-Estrada, J. H. Wiltshire, S. G. Roberts, D. Brownstein, J. A. Davies, N. D. Hastie and P. Hohenstein (2011). "A wt1-controlled chromatin switching mechanism underpins tissue-specific wnt4 activation and repression." Dev Cell **21**(3): 559-574.

Farmer, H., N. McCabe, C. J. Lord, A. N. Tutt, D. A. Johnson, T. B. Richardson, M. Santarosa, K. J. Dillon, I. Hickson, C. Knights, N. M. Martin, S. P. Jackson, G. C. Smith and A. Ashworth (2005). "Targeting the DNA repair defect in BRCA mutant cells as a therapeutic strategy." Nature **434**(7035): 917-921.

Fata, J. E., V. Chaudhary and R. Khokha (2001). "Cellular turnover in the mammary gland is correlated with systemic levels of progesterone and not 17beta-estradiol during the estrous cycle." Biol Reprod **65**(3): 680-688.

Foster, M. R., J. E. Johnson, S. J. Olson and D. C. Allred (2001). "Immunohistochemical analysis of nuclear versus cytoplasmic staining of WT1 in malignant mesotheliomas and primary pulmonary adenocarcinomas." Arch Pathol Lab Med **125**(10): 1316-1320.

Gaiger, A., V. Reese, M. L. Disis and M. A. Cheever (2000). "Immunity to WT1 in the animal model and in patients with acute myeloid leukemia." Blood **96**(4): 1480-1489.

Gashler, A. L., D. T. Bonthron, S. L. Madden, F. J. Rauscher, 3rd, T. Collins and V. P. Sukhatme (1992). "Human platelet-derived growth factor A chain is transcriptionally repressed by the Wilms tumor suppressor WT1." Proc Natl Acad Sci U S A **89**(22): 10984-10988.

Gessler, M., A. Poustka, W. Cavenee, R. L. Neve, S. H. Orkin and G. A. Bruns (1990). "Homozygous deletion in Wilms tumours of a zinc-finger gene identified by chromosome jumping." Nature **343**(6260): 774-778.

Giardine, B., C. Riemer, R. C. Hardison, R. Burhans, L. Elnitski, P. Shah, Y. Zhang, D. Blankenberg, I. Albert, J. Taylor, W. Miller, W. J. Kent and A. Nekrutenko (2005). "Galaxy: a platform for interactive large-scale genome analysis." Genome Res **15**(10): 1451-1455.

Gillmore, R., S. A. Xue, A. Holler, J. Kaeda, D. Hadjiminas, V. Healy, R. Dina, S. C. Parry, I. Bellantuono, Y. Ghani, R. C. Coombes, J. Waxman and H. J. Stauss (2006). "Detection of Wilms' tumor antigen--specific CTL in tumor-draining lymph nodes of patients with early breast cancer." Clin Cancer Res **12**(1): 34-42.

Goodyer, P., M. Dehbi, E. Torban, W. Bruening and J. Pelletier (1995). "Repression of the retinoic acid receptor-alpha gene by the Wilms' tumor suppressor gene product, wt1." Oncogene **10**(6): 1125-1129.

Gossen, M. and H. Bujard (1992). "Tight control of gene expression in mammalian cells by tetracycline-responsive promoters." Proc Natl Acad Sci U S A **89**(12): 5547-5551.

Gown, A. M. (2008). "Current issues in ER and HER2 testing by IHC in breast cancer." Mod Pathol **21 Suppl 2**: S8-s15.

Green, J. E., M. A. Shibata, K. Yoshidome, M. L. Liu, C. Jorcyk, M. R. Anver, J. Wigginton, R. Wiltrout, E. Shibata, S. Kaczmarczyk, W. Wang, Z. Y. Liu, A. Calvo and C. Couldrey (2000). "The C3(1)/SV40 T-antigen transgenic mouse model of mammary cancer: ductal epithelial cell targeting with multistage progression to carcinoma." Oncogene **19**(8): 1020-1027.

Green, K. A. and L. R. Lund (2005). "ECM degrading proteases and tissue remodelling in the mammary gland." Bioessays **27**(9): 894-903.

Greenup, R., A. Buchanan, W. Lorizio, K. Rhoads, S. Chan, T. Leedom, R. King, J. McLennan, B. Crawford, P. Kelly Marcom and E. Shelley Hwang (2013). "Prevalence of BRCA mutations among women with triple-negative breast cancer (TNBC) in a genetic counseling cohort." Ann Surg Oncol **20**(10): 3254-3258.

Gross, I., D. J. Morrison, D. P. Hyink, K. Georgas, M. A. English, M. Mericskay, S. Hosono, D. Sassoon, P. D. Wilson, M. Little and J. D. Licht (2003). "The receptor tyrosine kinase regulator Sprouty1 is a target of the tumor suppressor WT1 and important for kidney development." J Biol Chem **278**(42): 41420-41430.

Gudmundsdottir, K. and A. Ashworth (2006). "The roles of BRCA1 and BRCA2 and associated proteins in the maintenance of genomic stability." Oncogene **25**(43): 5864-5874.

Gustafsson, E., C. Brakebusch, K. Hietanen and R. Fassler (2001). "Tie-1-directed expression of Cre recombinase in endothelial cells of embryoid bodies and transgenic mice." J Cell Sci **114**(Pt 4): 671-676.

Haber, D. A., A. J. Buckler, T. Glaser, K. M. Call, J. Pelletier, R. L. Sohn, E. C. Douglass and D. E. Housman (1990). "An internal deletion within an 11p13 zinc finger gene contributes to the development of Wilms' tumor." Cell **61**(7): 1257-1269.

Haber, D. A., R. L. Sohn, A. J. Buckler, J. Pelletier, K. M. Call and D. E. Housman (1991). "Alternative splicing and genomic structure of the Wilms tumor gene WT1." Proc Natl Acad Sci U S A **88**(21): 9618-9622.

Hajra, K. M., D. Y. Chen and E. R. Fearon (2002). "The SLUG zinc-finger protein represses E-cadherin in breast cancer." Cancer Res **62**(6): 1613-1618.

Halbritter, F., H. J. Vaidya and S. R. Tomlinson (2012). "GeneProf: analysis of high-throughput sequencing experiments." Nat Methods **9**(1): 7-8.

Hall, J. M., M. K. Lee, B. Newman, J. E. Morrow, L. A. Anderson, B. Huey and M. C. King (1990). "Linkage of early-onset familial breast cancer to chromosome 17q21." Science **250**(4988): 1684-1689.

Hammes, A., J. K. Guo, G. Lutsch, J. R. Leheste, D. Landrock, U. Ziegler, M. C. Gubler and A. Schedl (2001). "Two splice variants of the Wilms' tumor 1 gene have distinct functions during sex determination and nephron formation." Cell **106**(3): 319-329.

Hammond, M. E., D. F. Hayes and A. C. Wolff (2011). "Clinical Notice for American Society of Clinical Oncology-College of American Pathologists guideline recommendations on ER/PgR and HER2 testing in breast cancer." J Clin Oncol **29**(15): e458.

Hammond, M. E., D. F. Hayes, M. Dowsett, D. C. Allred, K. L. Hagerty, S. Badve, P. L. Fitzgibbons, G. Francis, N. S. Goldstein, M. Hayes, D. G. Hicks, S. Lester, R. Love, P. B. Mangu, L. McShane, K. Miller, C. K. Osborne, S. Paik, J. Perlmutter, A. Rhodes, H. Sasano, J. N. Schwartz, F. C. Sweep, S. Taube, E. E. Torlakovic, P. Valenstein, G. Viale, D. Visscher, T. Wheeler, R. B. Williams, J. L. Wittliff and A. C. Wolff (2010). "American Society of Clinical Oncology/College Of

American Pathologists guideline recommendations for immunohistochemical testing of estrogen and progesterone receptors in breast cancer." J Clin Oncol **28**(16): 2784-2795.

Han, X. and R. W. Chesney (2003). "Regulation of taurine transporter gene (TauT) by WT1." FEBS Lett **540**(1-3): 71-76.

Han, Y., L. Yang, F. Suarez-Saiz, S. San-Marina, J. Cui and M. D. Minden (2008). "Wilms' tumor 1 suppressor gene mediates antiestrogen resistance via down-regulation of estrogen receptor-alpha expression in breast cancer cells." Mol Cancer Res **6**(8): 1347-1355.

Han, Y., S. San-Marina, J. Liu and M. D. Minden (2004). "Transcriptional activation of c-myc proto-oncogene by WT1 protein." Oncogene **23**(41): 6933-6941.

Hanson, J., J. Gorman, J. Reese and G. Fraizer (2007). "Regulation of vascular endothelial growth factor, VEGF, gene promoter by the tumor suppressor, WT1." Front Biosci **12**: 2279-2290.

Harrington, M. A., B. Konicek, A. Song, X. L. Xia, W. J. Fredericks and F. J. Rauscher, 3rd (1993). "Inhibition of colony-stimulating factor-1 promoter activity by the product of the Wilms' tumor locus." J Biol Chem **268**(28): 21271-21275.

Hartley, J. L., G. F. Temple and M. A. Brasch (2000). "DNA cloning using in vitro site-specific recombination." Genome Res **10**(11): 1788-1795.

Harvey, J. M., G. M. Clark, C. K. Osborne and D. C. Allred (1999). "Estrogen receptor status by immunohistochemistry is superior to the ligand-binding assay for predicting response to adjuvant endocrine therapy in breast cancer." J Clin Oncol **17**(5): 1474-1481.

Hawkins, S. M. and M. M. Matzuk (2008). "The menstrual cycle: basic biology." Ann N Y Acad Sci **1135**: 10-18.

Heckman, C., E. Mochon, M. Arcinas and L. M. Boxer (1997). "The WT1 protein is a negative regulator of the normal bcl-2 allele in t(14;18) lymphomas." J Biol Chem **272**(31): 19609-19614.

Herschkowitz, J. I., K. Simin, V. J. Weigman, I. Mikaelian, J. Usary, Z. Hu, K. E. Rasmussen, L. P. Jones, S. Assefnia, S. Chandrasekharan, M. G. Backlund, Y. Yin, A. I. Khramtsov, R. Bastein, J. Quackenbush, R. I. Glazer, P. H. Brown, J. E. Green, L. Kopelovich, P. A. Furth, J. P. Palazzo, O. I. Olopade, P. S. Bernard, G. A. Churchill, T. Van Dyke and C. M. Perou (2007). "Identification of conserved gene expression features between murine mammary carcinoma models and human breast tumors." Genome Biol **8**(5): R76.

Hewitt, S. M., S. Hamada, T. J. McDonnell, F. J. Rauscher, 3rd and G. F. Saunders (1995). "Regulation of the proto-oncogenes bcl-2 and c-myc by the Wilms' tumor suppressor gene WT1." Cancer Res **55**(22): 5386-5389.

Hinck, L. and G. B. Silberstein (2005). "Key stages in mammary gland development: the mammary end bud as a motile organ." Breast Cancer Res **7**(6): 245-251.

Hohenstein, P. and N. D. Hastie (2006). "The many facets of the Wilms' tumour gene, WT1." Hum Mol Genet **15 Spec No 2**: R196-201.

Hohenstein, P., J. Slight, D. D. Ozdemir, S. F. Burn, R. Berry and N. D. Hastie (2008). "High-efficiency Rosa26 knock-in vector construction for Cre-regulated overexpression and RNAi." Pathogenetics **1**(1): 3.

Hollink, I. H., M. M. van den Heuvel-Eibrink, M. Zimmermann, B. V. Balgobind, S. T. Arentsen-Peters, M. Alders, A. Willasch, G. J. Kaspers, J. Trka, A.

Baruchel, S. S. de Graaf, U. Creutzig, R. Pieters, D. Reinhardt and C. M. Zwaan (2009). "Clinical relevance of Wilms tumor 1 gene mutations in childhood acute myeloid leukemia." Blood **113**(23): 5951-5960.

Holzer, R. G., C. MacDougall, G. Cortright, K. Atwood, J. E. Green and C. L. Jorcyk (2003). "Development and characterization of a progressive series of mammary adenocarcinoma cell lines derived from the C3(1)/SV40 Large T-antigen transgenic mouse model." Breast Cancer Res Treat **77**(1): 65-76.

Hosen, N., T. Shirakata, S. Nishida, M. Yanagihara, A. Tsuboi, M. Kawakami, Y. Oji, Y. Oka, M. Okabe, B. Tan, H. Sugiyama and I. L. Weissman (2007). "The Wilms' tumor gene WT1-GFP knock-in mouse reveals the dynamic regulation of WT1 expression in normal and leukemic hematopoiesis." Leukemia **21**(8): 1783-1791.

Hosen, N., Y. Sonoda, Y. Oji, T. Kimura, H. Minamiguchi, H. Tamaki, M. Kawakami, M. Asada, K. Kanato, M. Motomura, M. Murakami, T. Fujioka, T. Masuda, E. H. Kim, A. Tsuboi, Y. Oka, T. Soma, H. Ogawa and H. Sugiyama (2002). "Very low frequencies of human normal CD34+ haematopoietic progenitor cells express the Wilms' tumour gene WT1 at levels similar to those in leukaemia cells." Br J Haematol **116**(2): 409-420.

Hosono, S., I. Gross, M. A. English, K. M. Hajra, E. R. Fearon and J. D. Licht (2000). "E-cadherin is a WT1 target gene." J Biol Chem **275**(15): 10943-10953.

Hossain, A. and G. F. Saunders (2001). "The human sex-determining gene SRY is a direct target of WT1." J Biol Chem **276**(20): 16817-16823.

Hsu, S. Y., M. Kubo, S. Y. Chun, F. G. Haluska, D. E. Housman and A. J. Hsueh (1995). "Wilms' tumor protein WT1 as an ovarian transcription factor: decreases in expression during follicle development and repression of inhibin-alpha gene promoter." Mol Endocrinol **9**(10): 1356-1366.

Huang, T. H., D. E. Laux, B. C. Hamlin, P. Tran, H. Tran and D. B. Lubahn (1997). "Identification of DNA methylation markers for human breast carcinomas using the methylation-sensitive restriction fingerprinting technique." Cancer Res **57**(6): 1030-1034.

Huber, M. A., N. Kraut and H. Beug (2005). "Molecular requirements for epithelial-mesenchymal transition during tumor progression." Curr Opin Cell Biol **17**(5): 548-558.

Huff, V. (2011). "Wilms' tumours: about tumour suppressor genes, an oncogene and a chameleon gene." Nat Rev Cancer **11**(2): 111-121.

Huh, W. J., I. U. Mysorekar and J. C. Mills (2010). "Inducible activation of Cre recombinase in adult mice causes gastric epithelial atrophy, metaplasia, and regenerative changes in the absence of "floxed" alleles." Am J Physiol Gastrointest Liver Physiol **299**(2): G368-380.

Hunter, D. J., P. Kraft, K. B. Jacobs, D. G. Cox, M. Yeager, S. E. Hankinson, S. Wacholder, Z. Wang, R. Welch, A. Hutchinson, J. Wang, K. Yu, N. Chatterjee, N. Orr, W. C. Willett, G. A. Colditz, R. G. Ziegler, C. D. Berg, S. S. Buys, C. A. McCarty, H. S. Feigelson, E. E. Calle, M. J. Thun, R. B. Hayes, M. Tucker, D. S. Gerhard, J. F. Fraumeni, Jr., R. N. Hoover, G. Thomas and S. J. Chanock (2007). "A genome-wide association study identifies alleles in FGFR2 associated with risk of sporadic postmenopausal breast cancer." Nat Genet **39**(7): 870-874.

Hylander, B., E. Repasky, P. Shrikant, M. Intengan, A. Beck, D. Driscoll, P. Singhal, S. Lele and K. Odunsi (2006). "Expression of Wilms tumor gene (WT1) in epithelial ovarian cancer." Gynecol Oncol **101**(1): 12-17.

Ijpenberg, A., J. M. Perez-Pomares, J. A. Guadix, R. Carmona, V. Portillo-Sanchez, D. Macias, P. Hohenstein, C. M. Miles, N. D. Hastie and R. Munoz-Chapuli (2007). "Wt1 and retinoic acid signaling are essential for stellate cell development and liver morphogenesis." Dev Biol **312**(1): 157-170.

Incassati, A., A. Chandramouli, R. Eelkema and P. Cowin (2010). "Key signaling nodes in mammary gland development and cancer: beta-catenin." Breast Cancer Res **12**(6): 213.

Inoue, K., H. Ogawa, T. Yamagami, T. Soma, Y. Tani, T. Tatekawa, Y. Oji, H. Tamaki, T. Kyo, H. Dohy, A. Hiraoka, T. Masaoka, T. Kishimoto and H. Sugiyama (1996). "Long-term follow-up of minimal residual disease in leukemia patients by monitoring WT1 (Wilms tumor gene) expression levels." Blood **88**(6): 2267-2278.

Inoue, K., H. Ogawa, Y. Sonoda, T. Kimura, H. Sakabe, Y. Oka, S. Miyake, H. Tamaki, Y. Oji, T. Yamagami, T. Tatekawa, T. Soma, T. Kishimoto and H. Sugiyama (1997). "Aberrant overexpression of the Wilms tumor gene (WT1) in human leukemia." Blood **89**(4): 1405-1412.

Inoue, K., H. Sugiyama, H. Ogawa, M. Nakagawa, T. Yamagami, H. Miwa, K. Kita, A. Hiraoka, T. Masaoka, K. Nasu and et al. (1994). "WT1 as a new prognostic factor and a new marker for the detection of minimal residual disease in acute leukemia." Blood **84**(9): 3071-3079.

Iwatsuki, M., K. Mimori, T. Yokobori, H. Ishi, T. Beppu, S. Nakamori, H. Baba and M. Mori (2010). "Epithelial-mesenchymal transition in cancer development and its clinical significance." Cancer Sci **101**(2): 293-299.

Jahkola, T., T. Toivonen, I. Virtanen, K. von Smitten, S. Nordling, K. von Boguslawski, C. Haglund, H. Nevanlinna and C. Blomqvist (1998). "Tenascin-C expression in invasion border of early breast cancer: a predictor of local and distant recurrence." Br J Cancer **78**(11): 1507-1513.

Jahkola, T., T. Toivonen, K. von Smitten, C. Blomqvist and I. Virtanen (1996). "Expression of tenascin in invasion border of early breast cancer correlates with higher risk of distant metastasis." Int J Cancer **69**(6): 445-447.

Johnson, S. M., H. Grosshans, J. Shingara, M. Byrom, R. Jarvis, A. Cheng, E. Labourier, K. L. Reinert, D. Brown and F. J. Slack (2005). "RAS is regulated by the let-7 microRNA family." Cell **120**(5): 635-647.

Jones, P. L. and F. S. Jones (2000). "Tenascin-C in development and disease: gene regulation and cell function." Matrix Biol **19**(7): 581-596.

Joshi, P. A., H. W. Jackson, A. G. Beristain, M. A. Di Grappa, P. A. Mote, C. L. Clarke, J. Stingl, P. D. Waterhouse and R. Khokha (2010). "Progesterone induces adult mammary stem cell expansion." Nature **465**(7299): 803-807.

Joshi, P. A., M. A. Di Grappa and R. Khokha (2012). "Active allies: hormones, stem cells and the niche in adult mammopoiesis." Trends Endocrinol Metab **23**(6): 299-309.

Kalluri, R. and R. A. Weinberg (2009). "The basics of epithelial-mesenchymal transition." J Clin Invest **119**(6): 1420-1428.

Kang, L., L. Wang and Z. Y. Wang (2011). "Opposite regulation of estrogen receptor-alpha and its variant ER-alpha36 by the Wilms' tumor suppressor WT1." Oncol Lett **2**(2): 337-341.

Karayan-Tapon, L., M. Wager, J. Guilhot, P. Levillain, C. Marquant, J. Clarhaut, V. Potiron and J. Roche (2008). "Semaphorin, neuropilin and VEGF expression in glial tumours: SEMA3G, a prognostic marker?" Br J Cancer **99**(7): 1153-1160.

Kauff, N. D. and R. R. Barakat (2007). "Risk-reducing salpingo-oophorectomy in patients with germline mutations in BRCA1 or BRCA2." J Clin Oncol **25**(20): 2921-2927.

Keilholz, U., H. D. Menssen, A. Gaiger, A. Menke, Y. Oji, Y. Oka, C. Scheibenbogen, H. Stauss, E. Thiel and H. Sugiyama (2005). "Wilms' tumour gene 1 (WT1) in human neoplasia." Leukemia **19**(8): 1318-1323.

Khokha, R. and Z. Werb (2011). "Mammary gland reprogramming: metalloproteinases couple form with function." Cold Spring Harb Perspect Biol **3**(4).

Kim, J., D. Prawitt, N. Bardeesy, E. Torban, C. Vicaner, P. Goodyer, B. Zabel and J. Pelletier (1999). "The Wilms' tumor suppressor gene (wt1) product regulates Dax-1 gene expression during gonadal differentiation." Mol Cell Biol **19**(3): 2289-2299.

King, J. W., S. Thomas, F. Corsi, L. Gao, R. Dina, R. Gillmore, K. Pigott, A. Kaisary, H. J. Stauss and J. Waxman (2009). "IL15 can reverse the unresponsiveness of Wilms' tumor antigen-specific CTL in patients with prostate cancer." Clin Cancer Res **15**(4): 1145-1154.

King-Underwood, L. and K. Pritchard-Jones (1998). "Wilms' tumor (WT1) gene mutations occur mainly in acute myeloid leukemia and may confer drug resistance." Blood **91**(8): 2961-2968.

King-Underwood, L., J. Renshaw and K. Pritchard-Jones (1996). "Mutations in the Wilms' tumor gene WT1 in leukemias." Blood **87**(6): 2171-2179.

Kirschner, K. M., L. K. Sciesielski and H. Scholz (2010). "Wilms' tumour protein Wt1 stimulates transcription of the gene encoding vascular endothelial cadherin." Pflugers Arch **460**(6): 1051-1061.

Kispert, A., S. Vainio and A. P. McMahon (1998). "Wnt-4 is a mesenchymal signal for epithelial transformation of metanephric mesenchyme in the developing kidney." Development **125**(21): 4225-4234.

Knudson, A. G., Jr. (1971). "Mutation and cancer: statistical study of retinoblastoma." Proc Natl Acad Sci U S A **68**(4): 820-823.

Knudson, A. G., Jr. and L. C. Strong (1972). "Mutation and cancer: a model for Wilms' tumor of the kidney." J Natl Cancer Inst **48**(2): 313-324.

Koesters, R., M. Linnebacher, J. F. Coy, A. Germann, Y. Schwitalle, P. Findeisen and M. von Knebel Doeberitz (2004). "WT1 is a tumor-associated antigen in colon cancer that can be recognized by in vitro stimulated cytotoxic T cells." Int J Cancer **109**(3): 385-392.

Kossman, D. A., N. I. Williams, S. M. Domchek, M. S. Kurzer, J. E. Stopfer and K. H. Schmitz (2011). "Exercise lowers estrogen and progesterone levels in premenopausal women at high risk of breast cancer." J Appl Physiol (1985) **111**(6): 1687-1693.

Kouros-Mehr, H. and Z. Werb (2006). "Candidate regulators of mammary branching morphogenesis identified by genome-wide transcript analysis." Dev Dyn **235**(12): 3404-3412.

Kreidberg, J. A., H. Sariola, J. M. Loring, M. Maeda, J. Pelletier, D. Housman and R. Jaenisch (1993). "WT-1 is required for early kidney development." Cell **74**(4): 679-691.

Kudoh, T., T. Ishidate, M. Moriyama, K. Toyoshima and T. Akiyama (1995). "G1 phase arrest induced by Wilms tumor protein WT1 is abrogated by cyclin/CDK complexes." Proc Natl Acad Sci U S A **92**(10): 4517-4521.

Kumar-Singh, S., K. Segers, U. Rodeck, H. Backhovens, J. Bogers, J. Weyler, C. Van Broeckhoven and E. Van Marck (1997). "WT1 mutation in malignant mesothelioma and WT1 immunoreactivity in relation to p53 and growth factor receptor expression, cell-type transition, and prognosis." J Pathol **181**(1): 67-74.

Ladomery, M. R., J. Slight, S. Mc Ghee and N. D. Hastie (1999). "Presence of WT1, the Wilm's tumor suppressor gene product, in nuclear poly(A)(+) ribonucleoprotein." J Biol Chem **274**(51): 36520-36526.

Laity, J. H., J. Chung, H. J. Dyson and P. E. Wright (2000). "Alternative splicing of Wilms' tumor suppressor protein modulates DNA binding activity through isoform-specific DNA-induced conformational changes." Biochemistry **39**(18): 5341-5348.

Langlands, F. E., K. Horgan, D. D. Dodwell and L. Smith (2013). "Breast cancer subtypes: response to radiotherapy and potential radiosensitisation." Br J Radiol **86**(1023): 20120601.

Lanigan, F., D. O'Connor, F. Martin and W. M. Gallagher (2007). "Molecular links between mammary gland development and breast cancer." Cell Mol Life Sci **64**(24): 3159-3184.

Lapillonne, H., A. Renneville, A. Auvrignon, C. Flamant, A. Blaise, C. Perot, J. L. Lai, P. Ballerini, F. Mazingue, S. Fasola, A. Dehee, F. Bellman, M. Adam, M. Labopin, L. Douay, G. Leverger, C. Preudhomme and J. Landman-Parker (2006). "High WT1 expression after induction therapy predicts high risk of relapse and death in pediatric acute myeloid leukemia." J Clin Oncol **24**(10): 1507-1515.

Larsson, S. H., J. P. Charlieu, K. Miyagawa, D. Engelkamp, M. Rassoulzadegan, A. Ross, F. Cuzin, V. van Heyningen and N. D. Hastie (1995). "Subnuclear localization of WT1 in splicing or transcription factor domains is regulated by alternative splicing." Cell **81**(3): 391-401.

Laux, D. E., E. M. Curran, W. V. Welshons, D. B. Lubahn and T. H. Huang (1999). "Hypermethylation of the Wilms' tumor suppressor gene CpG island in human breast carcinomas." Breast Cancer Res Treat **56**(1): 35-43.

Lee, K., N. Gjorevski, E. Boghaert, D. C. Radisky and C. M. Nelson (2011). "Snail1, Snail2, and E47 promote mammary epithelial branching morphogenesis." Embo j **30**(13): 2662-2674.

Lee, M. R., J. N. Shin, A. R. Moon, S. Y. Park, G. Hong, M. J. Lee, C. W. Yun, D. W. Seol, S. Piya, J. Bae, J. W. Oh and T. H. Kim (2008). "A novel protein, MUDENG, induces cell death in cytotoxic T cells." Biochem Biophys Res Commun **370**(3): 504-508.

Lee, S. B., K. Huang, R. Palmer, V. B. Truong, D. Herzlinger, K. A. Kolquist, J. Wong, C. Paulding, S. K. Yoon, W. Gerald, J. D. Oliner and D. A. Haber

(1999). "The Wilms tumor suppressor WT1 encodes a transcriptional activator of amphiregulin." Cell **98**(5): 663-673.

Lee, T. H. and J. Pelletier (2001). "Functional characterization of WT1 binding sites within the human vitamin D receptor gene promoter." Physiol Genomics **7**(2): 187-200.

Li, F. P., J. F. Fraumeni, Jr., J. J. Mulvihill, W. A. Blattner, M. G. Dreyfus, M. A. Tucker and R. W. Miller (1988). "A cancer family syndrome in twenty-four kindreds." Cancer Res **48**(18): 5358-5362.

Li, R. S., G. L. Law, R. A. Seifert, P. J. Romaniuk and D. R. Morris (1999). "Ornithine decarboxylase is a transcriptional target of tumor suppressor WT1." Exp Cell Res **247**(1): 257-266.

Li, X., J. W. Law and A. Y. Lee (2012). "Semaphorin 5A and plexin-B3 regulate human glioma cell motility and morphology through Rac1 and the actin cytoskeleton." Oncogene **31**(5): 595-610.

Liaw, D., D. J. Marsh, J. Li, P. L. Dahia, S. I. Wang, Z. Zheng, S. Bose, K. M. Call, H. C. Tsou, M. Peacocke, C. Eng and R. Parsons (1997). "Germline mutations of the PTEN gene in Cowden disease, an inherited breast and thyroid cancer syndrome." Nat Genet **16**(1): 64-67.

Little, M. and C. Wells (1997). "A clinical overview of WT1 gene mutations." Hum Mutat **9**(3): 209-225.

Liu, X., M. I. Gallego, G. H. Smith, G. W. Robinson and L. Hennighausen (1998). "Functional rescue of Stat5a-null mammary tissue through the activation of compensating signals including Stat5b." Cell Growth Differ **9**(9): 795-803.

Loeb, D. M., D. Korz, M. Katsnelson, E. A. Burwell, A. D. Friedman and S. Sukumar (2002). "Cyclin E is a target of WT1 transcriptional repression." J Biol Chem **277**(22): 19627-19632.

Loeb, D. M., E. Evron, C. B. Patel, P. M. Sharma, B. Niranjan, L. Buluwela, S. A. Weitzman, D. Korz and S. Sukumar (2001). "Wilms' tumor suppressor gene (WT1) is expressed in primary breast tumors despite tumor-specific promoter methylation." Cancer Res **61**(3): 921-925.

Loonstra, A., M. Vooijs, H. B. Beverloo, B. A. Allak, E. van Drunen, R. Kanaar, A. Berns and J. Jonkers (2001). "Growth inhibition and DNA damage induced by Cre recombinase in mammalian cells." Proc Natl Acad Sci U S A **98**(16): 9209-9214.

Lu, P., M. D. Sternlicht and Z. Werb (2006). "Comparative mechanisms of branching morphogenesis in diverse systems." J Mammary Gland Biol Neoplasia **11**(3-4): 213-228.

Luengo-Fernandez, R., J. Leal, A. Gray and R. Sullivan (2013). "Economic burden of cancer across the European Union: a population-based cost analysis." Lancet Oncol **14**(12): 1165-1174.

Lund, L. R., J. Romer, N. Thomasset, H. Solberg, C. Pyke, M. J. Bissell, K. Dano and Z. Werb (1996). "Two distinct phases of apoptosis in mammary gland involution: proteinase-independent and -dependent pathways." Development **122**(1): 181-193.

Madden, S. L., D. M. Cook, J. F. Morris, A. Gashler, V. P. Sukhatme and F. J. Rauscher, 3rd (1991). "Transcriptional repression mediated by the WT1 Wilms tumor gene product." Science **253**(5027): 1550-1553.

Mailander, V., C. Scheibenbogen, E. Thiel, A. Letsch, I. W. Blau and U. Keilholz (2004). "Complete remission in a patient with recurrent acute myeloid leukemia induced by vaccination with WT1 peptide in the absence of hematological or renal toxicity." Leukemia **18**(1): 165-166.

Malhotra, G. K., X. Zhao, H. Band and V. Band (2010). "Histological, molecular and functional subtypes of breast cancers." Cancer Biol Ther **10**(10): 955-960.

Mani, S. A., W. Guo, M. J. Liao, E. N. Eaton, A. Ayyanan, A. Y. Zhou, M. Brooks, F. Reinhard, C. C. Zhang, M. Shipitsin, L. L. Campbell, K. Polyak, C. Brisken, J. Yang and R. A. Weinberg (2008). "The epithelial-mesenchymal transition generates cells with properties of stem cells." Cell **133**(4): 704-715.

Markus, M. A., B. Heinrich, O. Raitskin, D. J. Adams, H. Mangs, C. Goy, M. Ladomery, R. Sperling, S. Stamm and B. J. Morris (2006). "WT1 interacts with the splicing protein RBM4 and regulates its ability to modulate alternative splicing in vivo." Exp Cell Res **312**(17): 3379-3388.

Maroulakou, I. G., M. Anver, L. Garrett and J. E. Green (1994). "Prostate and mammary adenocarcinoma in transgenic mice carrying a rat C3(1) simian virus 40 large tumor antigen fusion gene." Proc Natl Acad Sci U S A **91**(23): 11236-11240.

Martinez-Estrada, O. M., L. A. Lettice, A. Essafi, J. A. Guadix, J. Slight, V. Velecela, E. Hall, J. Reichmann, P. S. Devenney, P. Hohenstein, N. Hosen, R. E. Hill, R. Munoz-Chapuli and N. D. Hastie (2010). "Wt1 is required for cardiovascular progenitor cell formation through transcriptional control of Snail and E-cadherin." Nature Genetics **42**(1): 89-93.

Masciari, S., N. Larsson, J. Senz, N. Boyd, P. Kaurah, M. J. Kandel, L. N. Harris, H. C. Pinheiro, A. Troussard, P. Miron, N. Tung, C. Oliveira, L. Collins, S. Schnitt, J. E. Garber and D. Huntsman (2007). "Germline E-cadherin mutations in familial lobular breast cancer." J Med Genet **44**(11): 726-731.

Maurer, U., F. Jehan, C. Englert, G. Hubinger, E. Weidmann, H. F. DeLuca and L. Bergmann (2001). "The Wilms' tumor gene product (WT1) modulates the response to 1,25-dihydroxyvitamin D3 by induction of the vitamin D receptor." J Biol Chem **276**(6): 3727-3732.

Mayo, M. W., C. Y. Wang, S. S. Drouin, L. V. Madrid, A. F. Marshall, J. C. Reed, B. E. Weissman and A. S. Baldwin (1999). "WT1 modulates apoptosis by transcriptionally upregulating the bcl-2 proto-oncogene." Embo j **18**(14): 3990-4003.

McCann, S., J. Sullivan, J. Guerra, M. Arcinas and L. M. Boxer (1995). "Repression of the c-myb gene by WT1 protein in T and B cell lines." J Biol Chem **270**(40): 23785-23789.

McCarty, G., O. Awad and D. M. Loeb (2011). "WT1 protein directly regulates expression of vascular endothelial growth factor and is a mediator of tumor response to hypoxia." J Biol Chem **286**(51): 43634-43643.

McFadyen, M. C., W. T. Melvin and G. I. Murray (2004). "Cytochrome P450 enzymes: novel options for cancer therapeutics." Mol Cancer Ther **3**(3): 363-371.

Meijers-Heijboer, H., A. van den Ouweland, J. Klijn, M. Wasielewski, A. de Snoo, R. Oldenburg, A. Hollestelle, M. Houben, E. Crepin, M. van Veghel-Plandsoen, F. Elstrodt, C. van Duijn, C. Bartels, C. Meijers, M. Schutte, L. McGuffog, D. Thompson, D. Easton, N. Sodha, S. Seal, R. Barfoot, J. Mangion, J. Chang-Claude, D. Eccles, R. Eeles, D. G. Evans, R. Houlston, V. Murday, S. Narod, T. Peretz, J. Peto, C. Phelan, H. X. Zhang, C. Szabo, P. Devilee, D. Goldgar, P. A.

Futreal, K. L. Nathanson, B. Weber, N. Rahman and M. R. Stratton (2002). "Low-penetrance susceptibility to breast cancer due to CHEK2(*)1100delC in noncarriers of BRCA1 or BRCA2 mutations." Nat Genet **31**(1): 55-59.

Menke, A. L., A. Shvarts, N. Riteco, R. C. van Ham, A. J. van der Eb and A. G. Jochemsen (1997). "Wilms' tumor 1-KTS isoforms induce p53-independent apoptosis that can be partially rescued by expression of the epidermal growth factor receptor or the insulin receptor." Cancer Res **57**(7): 1353-1363.

Menssen, H. D., E. Bertelmann, S. Bartelt, R. A. Schmidt, G. Pecher, K. Schramm and E. Thiel (2000). "Wilms' tumor gene (WT1) expression in lung cancer, colon cancer and glioblastoma cell lines compared to freshly isolated tumor specimens." J Cancer Res Clin Oncol **126**(4): 226-232.

Menssen, H. D., H. J. Renkl, M. Entezami and E. Thiel (1997). "Wilms' tumor gene expression in human CD34+ hematopoietic progenitors during fetal development and early clonogenic growth." Blood **89**(9): 3486-3487.

Micalizzi, D. S., S. M. Farabaugh and H. L. Ford (2010). "Epithelial-mesenchymal transition in cancer: parallels between normal development and tumor progression." J Mammary Gland Biol Neoplasia **15**(2): 117-134.

Mikawa, T. and R. G. Gourdie (1996). "Pericardial mesoderm generates a population of coronary smooth muscle cells migrating into the heart along with ingrowth of the epicardial organ." Dev Biol **174**(2): 221-232.

Miki, Y., J. Swensen, D. Shattuck-Eidens, P. A. Futreal, K. Harshman, S. Tavtigian, Q. Liu, C. Cochran, L. M. Bennett, W. Ding and et al. (1994). "A strong candidate for the breast and ovarian cancer susceptibility gene BRCA1." Science **266**(5182): 66-71.

Miller, R. W., J. L. Young, Jr. and B. Novakovic (1995). "Childhood cancer." Cancer **75**(1 Suppl): 395-405.

Miller-Hodges, E. and P. Hohenstein (2012). "WT1 in disease: shifting the epithelial-mesenchymal balance." J Pathol **226**(2): 229-240.

Minc, E., P. de Coppet, P. Masson, L. Thiery, S. Dutertre, M. Amor-Gueret and C. Jaulin (1999). "The human copper-zinc superoxide dismutase gene (SOD1) proximal promoter is regulated by Sp1, Egr-1, and WT1 via non-canonical binding sites." J Biol Chem **274**(1): 503-509.

Miyoshi, Y., A. Ando, C. Egawa, T. Taguchi, Y. Tamaki, H. Tamaki, H. Sugiyama and S. Noguchi (2002). "High expression of Wilms' tumor suppressor gene predicts poor prognosis in breast cancer patients." Clin Cancer Res **8**(5): 1167-1171.

Miyoshi, Y., A. Ando, Y. Takamura, T. Taguchi, Y. Tamaki and S. Noguchi (2002). "Prediction of response to docetaxel by CYP3A4 mRNA expression in breast cancer tissues." Int J Cancer **97**(1): 129-132.

Miyoshi, Y., T. Taguchi, S. J. Kim, Y. Tamaki and S. Noguchi (2005). "Prediction of response to docetaxel by immunohistochemical analysis of CYP3A4 expression in human breast cancers." Breast Cancer **12**(1): 11-15.

Moleirinho, S., N. Chang, A. H. Sims, A. M. Tilston-Lunel, L. Angus, A. Steele, V. Boswell, S. C. Barnett, C. Ormandy, D. Faratian, F. J. Gunn-Moore and P. A. Reynolds (2013). "KIBRA exhibits MST-independent functional regulation of the Hippo signaling pathway in mammals." Oncogene **32**(14): 1821-1830.

Moore, A. W., A. Schedl, L. McInnes, M. Doyle, J. Hecksher-Sorensen and N. D. Hastie (1998). "YAC transgenic analysis reveals Wilms' tumour 1 gene activity in the proliferating coelomic epithelium, developing diaphragm and limb." Mech Dev **79**(1-2): 169-184.

Moore, A. W., L. McInnes, J. Kreidberg, N. D. Hastie and A. Schedl (1999). "YAC complementation shows a requirement for Wt1 in the development of epicardium, adrenal gland and throughout nephrogenesis." Development **126**(9): 1845-1857.

Morel, A. P., M. Lievre, C. Thomas, G. Hinkal, S. Ansieau and A. Puisieux (2008). "Generation of breast cancer stem cells through epithelial-mesenchymal transition." PLoS One **3**(8): e2888.

Morrison, A. A., J. P. Venables, G. Dellaire and M. R. Ladomery (2006). "The Wilms tumour suppressor protein WT1 (+KTS isoform) binds alpha-actinin 1 mRNA via its zinc-finger domain." Biochem Cell Biol **84**(5): 789-798.

Morrison, D. J., M. A. English and J. D. Licht (2005). "WT1 induces apoptosis through transcriptional regulation of the proapoptotic Bcl-2 family member Bak." Cancer Res **65**(18): 8174-8182.

Moshier, J. A., M. Skunca, W. Wu, S. M. Boppana, F. J. Rauscher, 3rd and J. Dosescu (1996). "Regulation of ornithine decarboxylase gene expression by the Wilms' tumor suppressor WT1." Nucleic Acids Res **24**(6): 1149-1157.

Mundlos, S., J. Pelletier, A. Darveau, M. Bachmann, A. Winterpacht and B. Zabel (1993). "Nuclear localization of the protein encoded by the Wilms' tumor gene WT1 in embryonic and adult tissues." Development **119**(4): 1329-1341.

Murray, C. J., M. A. Richards, J. N. Newton, K. A. Fenton, H. R. Anderson, C. Atkinson, D. Bennett, E. Bernabe, H. Blencowe, R. Bourne, T. Braithwaite, C. Brayne, N. G. Bruce, T. S. Brugha, P. Burney, M. Dherani, H. Dolk, K. Edmond, M. Ezzati, A. D. Flaxman, T. D. Fleming, G. Freedman, D. Gunnell, R. J. Hay, S. J. Hutchings, S. L. Ohno, R. Lozano, R. A. Lyons, W. Marcenes, M. Naghavi, C. R. Newton, N. Pearce, D. Pope, L. Rushton, J. A. Salomon, K. Shibuya, T. Vos, H. Wang, H. C. Williams, A. D. Woolf, A. D. Lopez and A. Davis (2013). "UK health performance: findings of the Global Burden of Disease Study 2010." Lancet **381**(9871): 997-1020.

Nagaharu, K., X. Zhang, T. Yoshida, D. Katoh, N. Hanamura, Y. Kozuka, T. Ogawa, T. Shiraishi and K. Imanaka-Yoshida (2011). "Tenascin C induces epithelial-mesenchymal transition-like change accompanied by SRC activation and focal adhesion kinase phosphorylation in human breast cancer cells." Am J Pathol **178**(2): 754-763.

Nakatsuka, S., Y. Oji, T. Horiuchi, T. Kanda, M. Kitagawa, T. Takeuchi, K. Kawano, Y. Kuwae, A. Yamauchi, M. Okumura, Y. Kitamura, Y. Oka, I. Kawase, H. Sugiyama and K. Aozasa (2006). "Immunohistochemical detection of WT1 protein in a variety of cancer cells." Mod Pathol **19**(6): 804-814.

Narod, S. A. and W. D. Foulkes (2004). "BRCA1 and BRCA2: 1994 and beyond." Nat Rev Cancer **4**(9): 665-676.

Natoli, T. A., A. McDonald, J. A. Alberta, M. E. Taglienti, D. E. Housman and J. A. Kreidberg (2002). "A mammal-specific exon of WT1 is not required for development or fertility." Mol Cell Biol **22**(12): 4433-4438.

Neve, R. M., K. Chin, J. Fridlyand, J. Yeh, F. L. Baehner, T. Fevr, L. Clark, N. Bayani, J. P. Coppe, F. Tong, T. Speed, P. T. Spellman, S. DeVries, A. Lapuk, N. J. Wang, W. L. Kuo, J. L. Stilwell, D. Pinkel, D. G. Albertson, F. M. Waldman, F. McCormick, R. B. Dickson, M. D. Johnson, M. Lippman, S. Ethier, A. Gazdar and J.

W. Gray (2006). "A collection of breast cancer cell lines for the study of functionally distinct cancer subtypes." Cancer Cell **10**(6): 515-527.

Neville, M. C., T. B. McFadden and I. Forsyth (2002). "Hormonal regulation of mammary differentiation and milk secretion." J Mammary Gland Biol Neoplasia **7**(1): 49-66.

Nichols, K. E., G. G. Re, Y. X. Yan, A. J. Garvin and D. A. Haber (1995). "WT1 induces expression of insulin-like growth factor 2 in Wilms' tumor cells." Cancer Res **55**(20): 4540-4543.

Nistico, P., M. J. Bissell and D. C. Radisky (2012). "Epithelial-mesenchymal transition: general principles and pathological relevance with special emphasis on the role of matrix metalloproteinases." Cold Spring Harb Perspect Biol **4**(2).

Oakes, S. R., H. N. Hilton and C. J. Ormandy (2006). "The alveolar switch: coordinating the proliferative cues and cell fate decisions that drive the formation of lobuloalveoli from ductal epithelium." Breast Cancer Res **8**(2): 207.

Oftedal, O. T. (2002). "The mammary gland and its origin during synapsid evolution." J Mammary Gland Biol Neoplasia **7**(3): 225-252.

Ogawa, H., H. Tamaki, K. Ikegame, T. Soma, M. Kawakami, A. Tsuboi, E. H. Kim, N. Hosen, M. Murakami, T. Fujioka, T. Masuda, Y. Taniguchi, S. Nishida, Y. Oji, Y. Oka and H. Sugiyama (2003). "The usefulness of monitoring WT1 gene transcripts for the prediction and management of relapse following allogeneic stem cell transplantation in acute type leukemia." Blood **101**(5): 1698-1704.

Oh, S., Y. Song, J. Yim and T. K. Kim (1999). "The Wilms' tumor 1 tumor suppressor gene represses transcription of the human telomerase reverse transcriptase gene." J Biol Chem **274**(52): 37473-37478.

Ohno, S., S. Dohi, Y. Ohno, S. Kyo, H. Sugiyama, N. Suzuki and M. Inoue (2009). "Immunohistochemical detection of WT1 protein in endometrial cancer." Anticancer Res **29**(5): 1691-1695.

Oji, Y., S. Nakamori, M. Fujikawa, S. Nakatsuka, A. Yokota, N. Tatsumi, S. Abeno, A. Ikeba, S. Takashima, M. Tsujie, H. Yamamoto, M. Sakon, R. Nezu, K. Kawano, S. Nishida, K. Ikegame, M. Kawakami, A. Tsuboi, Y. Oka, K. Yoshikawa, K. Aozasa, M. Monden and H. Sugiyama (2004). "Overexpression of the Wilms' tumor gene WT1 in pancreatic ductal adenocarcinoma." Cancer Sci **95**(7): 583-587.

Oji, Y., T. Suzuki, Y. Nakano, M. Maruno, S. Nakatsuka, T. Jomgeow, S. Abeno, N. Tatsumi, A. Yokota, S. Aoyagi, T. Nakazawa, K. Ito, K. Kanato, T. Shirakata, S. Nishida, N. Hosen, M. Kawakami, A. Tsuboi, Y. Oka, K. Aozasa, T. Yoshimine and H. Sugiyama (2004). "Overexpression of the Wilms' tumor gene W T1 in primary astrocytic tumors." Cancer Sci **95**(10): 822-827.

Oji, Y., Y. Miyoshi, S. Koga, Y. Nakano, A. Ando, S. Nakatsuka, A. Ikeba, E. Takahashi, N. Sakaguchi, A. Yokota, N. Hosen, K. Ikegame, M. Kawakami, A. Tsuboi, Y. Oka, H. Ogawa, K. Aozasa, S. Noguchi and H. Sugiyama (2003). "Overexpression of the Wilms' tumor gene WT1 in primary thyroid cancer." Cancer Sci **94**(7): 606-611.

Oka, Y., A. Tsuboi, T. Taguchi, T. Osaki, T. Kyo, H. Nakajima, O. A. Elisseeva, Y. Oji, M. Kawakami, K. Ikegame, N. Hosen, S. Yoshihara, F. Wu, F. Fujiki, M. Murakami, T. Masuda, S. Nishida, T. Shirakata, S. Nakatsuka, A. Sasaki, K. Udaka, H. Dohy, K. Aozasa, S. Noguchi, I. Kawase and H. Sugiyama (2004). "Induction of WT1 (Wilms' tumor gene)-specific cytotoxic T lymphocytes by WT1 peptide vaccine and the resultant cancer regression." Proc Natl Acad Sci U S A **101**(38): 13885-13890.

Oka, Y., K. Udaka, A. Tsuboi, O. A. Elisseeva, H. Ogawa, K. Aozasa, T. Kishimoto and H. Sugiyama (2000). "Cancer immunotherapy targeting Wilms' tumor gene WT1 product." J Immunol **164**(4): 1873-1880.

Osborne, C. K., K. Hobbs and J. M. Trent (1987). "Biological differences among MCF-7 human breast cancer cell lines from different laboratories." Breast Cancer Res Treat **9**(2): 111-121.

Oskarsson, T., S. Acharyya, X. H. Zhang, S. Vanharanta, S. F. Tavazoie, P. G. Morris, R. J. Downey, K. Manova-Todorova, E. Brogi and J. Massague (2011). "Breast cancer cells produce tenascin C as a metastatic niche component to colonize the lungs." Nat Med **17**(7): 867-874.

Palmer, R. E., A. Kotsianti, B. Cadman, T. Boyd, W. Gerald and D. A. Haber (2001). "WT1 regulates the expression of the major glomerular podocyte membrane protein Podocalyxin." Curr Biol **11**(22): 1805-1809.

Parkin, D. M. and L. M. G. Fernández (2006). "Use of Statistics to Assess the Global Burden of Breast Cancer." Breast Journal **12**: S70-S80.

Paschka, P., G. Marcucci, A. S. Ruppert, S. P. Whitman, K. Mrozek, K. Maharry, C. Langer, C. D. Baldus, W. Zhao, B. L. Powell, M. R. Baer, A. J. Carroll, M. A. Caligiuri, J. E. Kolitz, R. A. Larson and C. D. Bloomfield (2008). "Wilms' tumor 1 gene mutations independently predict poor outcome in adults with cytogenetically normal acute myeloid leukemia: a cancer and leukemia group B study." J Clin Oncol **26**(28): 4595-4602.

Peinado, H., D. Olmeda and A. Cano (2007). "Snail, Zeb and bHLH factors in tumour progression: an alliance against the epithelial phenotype?" Nat Rev Cancer **7**(6): 415-428.

Pelletier, J., M. Schalling, A. J. Buckler, A. Rogers, D. A. Haber and D. Housman (1991). "Expression of the Wilms' tumor gene WT1 in the murine urogenital system." Genes Dev **5**(8): 1345-1356.

Perez-Pomares, J. M. and R. Munoz-Chapuli (2002). "Epithelial-mesenchymal transitions: a mesodermal cell strategy for evolutive innovation in Metazoans." Anat Rec **268**(3): 343-351.

Perou, C. M., T. Sorlie, M. B. Eisen, M. van de Rijn, S. S. Jeffrey, C. A. Rees, J. R. Pollack, D. T. Ross, H. Johnsen, L. A. Akslen, O. Fluge, A. Pergamenschikov, C. Williams, S. X. Zhu, P. E. Lonning, A. L. Borresen-Dale, P. O. Brown and D. Botstein (2000). "Molecular portraits of human breast tumours." Nature **406**(6797): 747-752.

Peto, J., N. Collins, R. Barfoot, S. Seal, W. Warren, N. Rahman, D. F. Easton, C. Evans, J. Deacon and M. R. Stratton (1999). "Prevalence of BRCA1 and BRCA2 gene mutations in patients with early-onset breast cancer." J Natl Cancer Inst **91**(11): 943-949.

Pierobon, M. and C. L. Frankenfeld (2013). "Obesity as a risk factor for triple-negative breast cancers: a systematic review and meta-analysis." Breast Cancer Res Treat **137**(1): 307-314.

Plath, K., S. Mlynarczyk-Evans, D. A. Nusinow and B. Panning (2002). "Xist RNA and the mechanism of X chromosome inactivation." Annu Rev Genet **36**: 233-278.

Polyak, K. and J. Garber (2011). "Targeting the missing links for cancer therapy." Nat Med **17**(3): 283-284.

Prall, F. (2007). "Tumour budding in colorectal carcinoma." Histopathology **50**(1): 151-162.

Prat, A. and C. M. Perou (2009). "Mammary development meets cancer genomics." Nat Med **15**(8): 842-844.

Prat, A., J. S. Parker, O. Karginova, C. Fan, C. Livasy, J. I. Herschkowitz, X. He and C. M. Perou (2010). "Phenotypic and molecular characterization of the claudin-low intrinsic subtype of breast cancer." Breast Cancer Res **12**(5): R68.

Pritchard-Jones, K., S. Fleming, D. Davidson, W. Bickmore, D. Porteous, C. Gosden, J. Bard, A. Buckler, J. Pelletier, D. Housman and et al. (1990). "The candidate Wilms' tumour gene is involved in genitourinary development." Nature **346**(6280): 194-197.

Qi, X. W., F. Zhang, X. H. Yang, L. J. Fan, Y. Zhang, Y. Liang, L. Ren, L. Zhong, Q. Q. Chen, K. Y. Zhang, W. D. Zang, L. S. Wang, Y. Zhang and J. Jiang (2012). "High Wilms' tumor 1 mRNA expression correlates with basal-like and ERBB2 molecular subtypes and poor prognosis of breast cancer." Oncol Rep **28**(4): 1231-1236.

Radisky, D. C. and L. C. Hartmann (2009). "Mammary involution and breast cancer risk: transgenic models and clinical studies." J Mammary Gland Biol Neoplasia **14**(2): 181-191.

Rauscher, F. J., 3rd, J. F. Morris, O. E. Tournay, D. M. Cook and T. Curran (1990). "Binding of the Wilms' tumor locus zinc finger protein to the EGR-1 consensus sequence." Science **250**(4985): 1259-1262.

Regan, J. and M. Smalley (2007). "Prospective isolation and functional analysis of stem and differentiated cells from the mouse mammary gland." Stem Cell Reviews **3**(2): 124-136.

Regan, J. L., H. Kendrick, F. A. Magnay, V. Vafaizadeh, B. Groner and M. J. Smalley (2012). "c-Kit is required for growth and survival of the cells of origin of Brca1-mutation-associated breast cancer." Oncogene **31**(7): 869-883.

Regan, J. L., T. Sourisseau, K. Soady, H. Kendrick, A. McCarthy, C. Tang, K. Brennan, S. Linardopoulos, D. E. White and M. J. Smalley (2013). "Aurora A kinase regulates mammary epithelial cell fate by determining mitotic spindle orientation in a Notch-dependent manner." Cell Rep **4**(1): 110-123.

Rehman, M. and L. Tamagnone (2013). "Semaphorins in cancer: biological mechanisms and therapeutic approaches." Semin Cell Dev Biol **24**(3): 179-189.

Reizner, N., S. Maor, R. Sarfstein, S. Abramovitch, W. V. Welshons, E. M. Curran, A. V. Lee and H. Werner (2005). "The WT1 Wilms' tumor suppressor gene product interacts with estrogen receptor-alpha and regulates IGF-I receptor gene transcription in breast cancer cells." J Mol Endocrinol **35**(1): 135-144.

Renshaw, J., L. King-Underwood and K. Pritchard-Jones (1997). "Differential splicing of exon 5 of the Wilms tumour (WTI) gene." Genes Chromosomes Cancer **19**(4): 256-266.

Renwick, A., D. Thompson, S. Seal, P. Kelly, T. Chagtai, M. Ahmed, B. North, H. Jayatilake, R. Barfoot, K. Spanova, L. McGuffog, D. G. Evans, D. Eccles, D. F. Easton, M. R. Stratton and N. Rahman (2006). "ATM mutations that cause ataxia-telangiectasia are breast cancer susceptibility alleles." Nat Genet **38**(8): 873-875.

Reynolds, P. (2013). "Smoking and breast cancer." J Mammary Gland Biol Neoplasia **18**(1): 15-23.

Richard, D. J., V. Schumacher, B. Royer-Pokora and S. G. Roberts (2001). "Par4 is a coactivator for a splice isoform-specific transcriptional activation domain in WT1." Genes Dev **15**(3): 328-339.

Richert, M. M., K. L. Schwertfeger, J. W. Ryder and S. M. Anderson (2000). "An atlas of mouse mammary gland development." J Mammary Gland Biol Neoplasia **5**(2): 227-241.

Roberts, A. B., F. Tian, S. D. Byfield, C. Stuelten, A. Ooshima, S. Saika and K. C. Flanders (2006). "Smad3 is key to TGF-beta-mediated epithelial-to-mesenchymal transition, fibrosis, tumor suppression and metastasis." Cytokine Growth Factor Rev **17**(1-2): 19-27.

Robinson, G. W. (2007). "Cooperation of signalling pathways in embryonic mammary gland development." Nat Rev Genet **8**(12): 963-972.

Rodrigues, P. C., S. N. Oliveira, M. B. Viana, E. I. Matsuda, A. E. Nowill, S. R. Brandalise and J. A. Yunes (2007). "Prognostic significance of WT1 gene expression in pediatric acute myeloid leukemia." Pediatr Blood Cancer **49**(2): 133-138.

Rodriguez-Antona, C. and M. Ingelman-Sundberg (2006). "Cytochrome P450 pharmacogenetics and cancer." Oncogene **25**(11): 1679-1691.

Rose, E. A., T. Glaser, C. Jones, C. L. Smith, W. H. Lewis, K. M. Call, M. Minden, E. Champagne, L. Bonetta, H. Yeger and et al. (1990). "Complete physical map of the WAGR region of 11p13 localizes a candidate Wilms' tumor gene." Cell **60**(3): 495-508.

Roy, P., L. J. Yu, C. L. Crespi and D. J. Waxman (1999). "Development of a substrate-activity based approach to identify the major human liver P-450 catalysts of cyclophosphamide and ifosfamide activation based on cDNA-expressed activities and liver microsomal P-450 profiles." Drug Metab Dispos **27**(6): 655-666.

Rupprecht, H. D., I. A. Drummond, S. L. Madden, F. J. Rauscher, 3rd and V. P. Sukhatme (1994). "The Wilms' tumor suppressor gene WT1 is negatively autoregulated." J Biol Chem **269**(8): 6198-6206.

Ryan, G., V. Steele-Perkins, J. F. Morris, F. J. Rauscher, 3rd and G. R. Dressler (1995). "Repression of Pax-2 by WT1 during normal kidney development." Development **121**(3): 867-875.

Sadanandam, A., M. L. Varney, S. Singh, A. E. Ashour, N. Moniaux, S. Deb, S. M. Lele, S. K. Batra and R. K. Singh (2010). "High gene expression of semaphorin 5A in pancreatic cancer is associated with tumor growth, invasion and metastasis." Int J Cancer **127**(6): 1373-1383.

Savagner, P., K. M. Yamada and J. P. Thiery (1997). "The zinc-finger protein slug causes desmosome dissociation, an initial and necessary step for growth factor-induced epithelial-mesenchymal transition." J Cell Biol **137**(6): 1403-1419.

Saxen, L. and H. Sariola (1987). "Early organogenesis of the kidney." Pediatr Nephrol **1**(3): 385-392.

Schade, B., T. Rao, N. Dourdin, R. Lesurf, M. Hallett, R. D. Cardiff and W. J. Muller (2009). "PTEN deficiency in a luminal ErbB-2 mouse model results in dramatic acceleration of mammary tumorigenesis and metastasis." J Biol Chem **284**(28): 19018-19026.

Scharnhorst, V., P. Dekker, A. J. van der Eb and A. G. Jochemsen (1999). "Internal translation initiation generates novel WT1 protein isoforms with distinct biological properties." J Biol Chem **274**(33): 23456-23462.

Schedl, A. (2007). "Renal abnormalities and their developmental origin." Nat Rev Genet **8**(10): 791-802.

Schittenhelm, J., J. Thiericke, C. Nagel, R. Meyermann and R. Beschorner (2010). "WT1 expression in normal and neoplastic cranial and peripheral nerves is independent of grade of malignancy." Cancer Biomark **7**(2): 73-77.

Schmid, D., G. Heinze, B. Linnerth, K. Tisljar, R. Kusec, K. Geissler, C. Sillaber, K. Laczika, M. Mitterbauer, S. Zochbauer, C. Mannhalter, O. A. Haas, K. Lechner, U. Jager and A. Gaiger (1997). "Prognostic significance of WT1 gene expression at diagnosis in adult de novo acute myeloid leukemia." Leukemia **11**(5): 639-643.

Schmidt, E. E., D. S. Taylor, J. R. Prigge, S. Barnett and M. R. Capecchi (2000). "Illegitimate Cre-dependent chromosome rearrangements in transgenic mouse spermatids." Proc Natl Acad Sci U S A **97**(25): 13702-13707.

Seal, S., D. Thompson, A. Renwick, A. Elliott, P. Kelly, R. Barfoot, T. Chagtai, H. Jayatilake, M. Ahmed, K. Spanova, B. North, L. McGuffog, D. G. Evans, D. Eccles, D. F. Easton, M. R. Stratton and N. Rahman (2006). "Truncating mutations in the Fanconi anemia J gene BRIP1 are low-penetrance breast cancer susceptibility alleles." Nat Genet **38**(11): 1239-1241.

Sekiya, M., M. Adachi, Y. Hinoda, K. Imai and A. Yachi (1994). "Downregulation of Wilms' tumor gene (wt1) during myelomonocytic differentiation in HL60 cells." Blood **83**(7): 1876-1882.

Semprini, S., T. J. Troup, N. Kotelevtseva, K. King, J. R. Davis, L. J. Mullins, K. E. Chapman, D. R. Dunbar and J. J. Mullins (2007). "Cryptic loxP sites in mammalian genomes: genome-wide distribution and relevance for the efficiency of BAC/PAC recombineering techniques." Nucleic Acids Res **35**(5): 1402-1410.

Seredina, T. A., O. B. Goreva, V. O. Talaban, A. Y. Grishanova and V. V. Lyakhovich (2012). "Association of cytochrome P450 genetic polymorphisms with neoadjuvant chemotherapy efficacy in breast cancer patients." BMC Med Genet **13**: 45.

Shackleton, M., F. Vaillant, K. J. Simpson, J. Stingl, G. K. Smyth, M. L. Asselin-Labat, L. Wu, G. J. Lindeman and J. E. Visvader (2006). "Generation of a functional mammary gland from a single stem cell." Nature **439**(7072): 84-88.

Shearer, P., G. Kapoor, J. B. Beckwith, J. Takashima, N. Breslow and D. M. Green (2001). "Secondary acute myelogenous leukemia in patients previously treated for childhood renal tumors: a report from the National Wilms Tumor Study Group." J Pediatr Hematol Oncol **23**(2): 109-111.

Shimamura, R., G. C. Fraizer, J. Trapman, C. Lau Yf and G. F. Saunders (1997). "The Wilms' tumor gene WT1 can regulate genes involved in sex determination and differentiation: SRY, Mullerian-inhibiting substance, and the androgen receptor." Clin Cancer Res **3**(12 Pt 2): 2571-2580.

Silberstein, G. B., G. R. Dressler and K. Van Horn (2002). "Expression of the PAX2 oncogene in human breast cancer and its role in progesterone-dependent mammary growth." Oncogene **21**(7): 1009-1016.

Silberstein, G. B., K. Van Horn, P. Strickland, C. T. Roberts and C. W. Daniel (1997). "Altered expression of the WT1 Wilms tumor suppressor gene in human breast cancer." Proc Natl Acad Sci U S A **94**(15): 8132-8137.

Silverthorn, D. U. (2004). Human physiology : an integrated approach. San Francisco, Pearson/Benjamin Cummings.

Sim, E. U., A. Smith, E. Szilagi, F. Rae, P. Ioannou, M. H. Lindsay and M. H. Little (2002). "Wnt-4 regulation by the Wilms' tumour suppressor gene, WT1." Oncogene **21**(19): 2948-2960.

Simpson, L. A., E. A. Burwell, K. A. Thompson, S. Shahnaz, A. R. Chen and D. M. Loeb (2006). "The antiapoptotic gene A1/BFL1 is a WT1 target gene that mediates granulocytic differentiation and resistance to chemotherapy." Blood **107**(12): 4695-4702.

Soerjomataram, I., J. Lortet-Tieulent, D. M. Parkin, J. Ferlay, C. Mathers, D. Forman and F. Bray (2012). "Global burden of cancer in 2008: a systematic analysis of disability-adjusted life-years in 12 world regions." The Lancet **380**(9856): 1840-1850.

Song, J. (2007). "EMT or apoptosis: a decision for TGF-beta." Cell Res **17**(4): 289-290.

Sorlie, T., C. M. Perou, R. Tibshirani, T. Aas, S. Geisler, H. Johnsen, T. Hastie, M. B. Eisen, M. van de Rijn, S. S. Jeffrey, T. Thorsen, H. Quist, J. C. Matese, P. O. Brown, D. Botstein, P. E. Lonning and A. L. Borresen-Dale (2001). "Gene expression patterns of breast carcinomas distinguish tumor subclasses with clinical implications." Proc Natl Acad Sci U S A **98**(19): 10869-10874.

Sorlie, T., R. Tibshirani, J. Parker, T. Hastie, J. S. Marron, A. Nobel, S. Deng, H. Johnsen, R. Pesich, S. Geisler, J. Demeter, C. M. Perou, P. E. Lonning, P. O. Brown, A. L. Borresen-Dale and D. Botstein (2003). "Repeated observation of breast tumor subtypes in independent gene expression data sets." Proc Natl Acad Sci U S A **100**(14): 8418-8423.

Srinivas, S., T. Watanabe, C. S. Lin, C. M. William, Y. Tanabe, T. M. Jessell and F. Costantini (2001). "Cre reporter strains produced by targeted insertion of EYFP and ECFP into the ROSA26 locus." BMC Dev Biol **1**: 4.

Stanhope-Baker, P. and B. R. Williams (2000). "Identification of connective tissue growth factor as a target of WT1 transcriptional regulation." J Biol Chem **275**(49): 38139-38150.

Stark, K., S. Vainio, G. Vassileva and A. P. McMahon (1994). "Epithelial transformation of metanephric mesenchyme in the developing kidney regulated by Wnt-4." Nature **372**(6507): 679-683.

Sternlicht, M. D. (2006). "Key stages in mammary gland development: the cues that regulate ductal branching morphogenesis." Breast Cancer Res **8**(1): 201.

Stratton, M. R. and N. Rahman (2008). "The emerging landscape of breast cancer susceptibility." Nat Genet **40**(1): 17-22.

Stuchell, M. D., J. E. Garrus, B. Muller, K. M. Stray, S. Ghaffarian, R. McKinnon, H. G. Krausslich, S. G. Morham and W. I. Sundquist (2004). "The human endosomal sorting complex required for transport (ESCRT-I) and its role in HIV-1 budding." J Biol Chem **279**(34): 36059-36071.

Stute, P., S. Sielker, C. E. Wood, T. C. Register, C. J. Lees, F. N. Dewi, J. K. Williams, J. D. Wagner, U. Stefenelli and J. M. Cline (2012). "Life stage differences in mammary gland gene expression profile in non-human primates." Breast Cancer Res Treat **133**(2): 617-634.

Summers, K., J. Stevens, I. Kakkas, M. Smith, L. L. Smith, F. Macdougall, J. Cavenagh, D. Bonnet, B. D. Young, T. A. Lister and J. Fitzgibbon (2007). "Wilms' tumour 1 mutations are associated with FLT3-ITD and failure of standard induction chemotherapy in patients with normal karyotype AML." Leukemia **21**(3): 550-551; author reply 552.

Takahara, A., S. Koido, M. Ito, E. Nagasaki, Y. Sagawa, T. Iwamoto, H. Komita, T. Ochi, H. Fujiwara, M. Yasukawa, J. Mineno, H. Shiku, S. Nishida, H. Sugiyama, H. Tajiri and S. Homma (2011). "Gemcitabine enhances Wilms' tumor gene WT1 expression and sensitizes human pancreatic cancer cells with WT1-specific T-cell-mediated antitumor immune response." Cancer Immunol Immunother **60**(9): 1289-1297.

Takeichi, M., K. Nimura, M. Mori, H. Nakagami and Y. Kaneda (2013). "The transcription factors Tbx18 and Wt1 control the epicardial epithelial-mesenchymal transition through bi-directional regulation of Slug in murine primary epicardial cells." PLoS One **8**(2): e57829.

Tamagnone, L. (2012). "Emerging role of semaphorins as major regulatory signals and potential therapeutic targets in cancer." Cancer Cell **22**(2): 145-152.

Tan, D. S., C. Marchio and J. S. Reis-Filho (2008). "Hereditary breast cancer: from molecular pathology to tailored therapies." J Clin Pathol **61**(10): 1073-1082.

Tatsumi, N., Y. Oji, N. Tsuji, A. Tsuda, M. Higashio, S. Aoyagi, I. Fukuda, K. Ito, J. Nakamura, S. Takashima, Y. Kitamura, S. Miyai, T. Jomgeow, Z. Li, T. Shirakata, S. Nishida, A. Tsuboi, Y. Oka and H. Sugiyama (2008). "Wilms' tumor gene WT1-shRNA as a potent apoptosis-inducing agent for solid tumors." Int J Oncol **32**(3): 701-711.

Tessari, A., D. Palmieri and S. Di Cosimo (2013). "Overview of diagnostic/targeted treatment combinations in personalized medicine for breast cancer patients." Pharmgenomics Pers Med **7**: 1-19.

Thiery, J. P., H. Acloque, R. Y. Huang and M. A. Nieto (2009). "Epithelial-mesenchymal transitions in development and disease." Cell **139**(5): 871-890.

Thompson, D. and D. Easton (2004). "The genetic epidemiology of breast cancer genes." J Mammary Gland Biol Neoplasia **9**(3): 221-236.

Tiede, B. and Y. Kang (2011). "From milk to malignancy: the role of mammary stem cells in development, pregnancy and breast cancer." Cell Res **21**(2): 245-257.

Timar, J., L. Meszaros, Z. Orosz, A. Albini and E. Raso (2005). "WT1 expression in angiogenic tumours of the skin." Histopathology **47**(1): 67-73.

Tischkowitz, M., B. Xia, N. Sabbaghian, J. S. Reis-Filho, N. Hamel, G. Li, E. H. van Beers, L. Li, T. Khalil, L. A. Quenneville, A. Omeroglu, A. Poll, P. Lepage, N. Wong, P. M. Nederlof, A. Ashworth, P. N. Tonin, S. A. Narod, D. M. Livingston and W. D. Foulkes (2007). "Analysis of PALB2/FANCN-associated breast cancer families." Proc Natl Acad Sci U S A **104**(16): 6788-6793.

Trimboli, A. J., K. Fukino, A. de Bruin, G. Wei, L. Shen, S. M. Tanner, N. Creasap, T. J. Rosol, M. L. Robinson, C. Eng, M. C. Ostrowski and G. Leone (2008). "Direct evidence for epithelial-mesenchymal transitions in breast cancer." Cancer Res **68**(3): 937-945.

Trka, J., M. Kalinova, O. Hrusak, J. Zuna, O. Krejci, J. Madzo, P. Sedlacek, V. Vavra, K. Michalova, M. Jarosova and J. Stary (2002). "Real-time quantitative PCR detection of WT1 gene expression in children with AML: prognostic significance, correlation with disease status and residual disease detection by flow cytometry." Leukemia **16**(7): 1381-1389.

Tsuboi, A., Y. Oka, H. Ogawa, O. A. Elisseeva, H. Li, K. Kawasaki, K. Aozasa, T. Kishimoto, K. Udaka and H. Sugiyama (2000). "Cytotoxic T-lymphocyte responses elicited to Wilms' tumor gene WT1 product by DNA vaccination." J Clin Immunol **20**(3): 195-202.

Tuna, M., A. Chavez-Reyes and A. M. Tari (2005). "HER2/neu increases the expression of Wilms' Tumor 1 (WT1) protein to stimulate S-phase proliferation and inhibit apoptosis in breast cancer cells." Oncogene **24**(9): 1648-1652.

Udtha, M., S. J. Lee, R. Alam, K. Coombes and V. Huff (2003). "Upregulation of c-MYC in WT1-mutant tumors: assessment of WT1 putative transcriptional targets using cDNA microarray expression profiling of genetically defined Wilms' tumors." Oncogene **22**(24): 3821-3826.

Ueda, T., Y. Oji, N. Naka, Y. Nakano, E. Takahashi, S. Koga, M. Asada, A. Ikeba, S. Nakatsuka, S. Abeno, N. Hosen, Y. Tomita, K. Aozasa, N. Tamai, A. Myoui, H. Yoshikawa and H. Sugiyama (2003). "Overexpression of the Wilms' tumor gene WT1 in human bone and soft-tissue sarcomas." Cancer Sci **94**(3): 271-276.

Uesugi, K., Y. Hiasa, Y. Tokumoto, T. Mashiba, Y. Koizumi, M. Hirooka, M. Abe, B. Matsuura and M. Onji (2013). "Wilms' tumor 1 gene modulates Fas-related death signals and anti-apoptotic functions in hepatocellular carcinoma." J Gastroenterol **48**(9): 1069-1080.

Utomo, A. R., A. Y. Nikitin and W. H. Lee (1999). "Temporal, spatial, and cell type-specific control of Cre-mediated DNA recombination in transgenic mice." Nat Biotechnol **17**(11): 1091-1096.

Vainio, S. and Y. Lin (2002). "Coordinating early kidney development: lessons from gene targeting." Nat Rev Genet **3**(7): 533-543.

Van Driessche, A., Z. N. Berneman and V. F. Van Tendeloo (2012). "Active specific immunotherapy targeting the Wilms' tumor protein 1 (WT1) for patients with hematological malignancies and solid tumors: lessons from early clinical trials." Oncologist **17**(2): 250-259.

Van Keymeulen, A., A. S. Rocha, M. Ousset, B. Beck, G. Bouvencourt, J. Rock, N. Sharma, S. Dekoninck and C. Blanpain (2011). "Distinct stem cells contribute to mammary gland development and maintenance." Nature **479**(7372): 189-193.

van Staveren, W. C., D. Y. Solis, A. Hebrant, V. Detours, J. E. Dumont and C. Maenhaut (2009). "Human cancer cell lines: Experimental models for cancer cells in situ? For cancer stem cells?" Biochim Biophys Acta **1795**(2): 92-103.

Varanasi, R., N. Bardeesy, M. Ghahremani, M. J. Petruzzi, N. Nowak, M. A. Adam, P. Grundy, T. B. Shows and J. Pelletier (1994). "Fine structure analysis of the WT1 gene in sporadic Wilms tumors." Proc Natl Acad Sci U S A **91**(9): 3554-3558.

Vargo-Gogola, T. and J. M. Rosen (2007). "Modelling breast cancer: one size does not fit all." Nat Rev Cancer **7**(9): 659-672.

Verma, S., M. L. Salmans, M. Geyfman, H. Wang, Z. Yu, Z. Lu, F. Zhao, S. M. Lipkin and B. Andersen (2012). "The estrogen-responsive Agr2 gene regulates mammary epithelial proliferation and facilitates lobuloalveolar development." Dev Biol **369**(2): 249-260.

Visvader, J. E. (2009). "Keeping abreast of the mammary epithelial hierarchy and breast tumorigenesis." Genes Dev **23**(22): 2563-2577.

Wagner, K. D., N. Wagner, V. P. Sukhatme and H. Scholz (2001). "Activation of vitamin D receptor by the Wilms' tumor gene product mediates apoptosis of renal cells." J Am Soc Nephrol **12**(6): 1188-1196.

Wagner, K. J., C. E. Patek, C. Miles, S. Christie, A. J. Brookes and M. L. Hooper (2001). "Truncation of WT1 results in downregulation of cyclin G1 and IGFBP-4 expression." Biochem Biophys Res Commun **287**(4): 977-982.

Wagner, K. U., A. Krempler, A. A. Triplett, Y. Qi, N. M. George, J. Zhu and H. Rui (2004). "Impaired alveologenesis and maintenance of secretory mammary epithelial cells in Jak2 conditional knockout mice." Mol Cell Biol **24**(12): 5510-5520.

Wagner, K. U., K. McAllister, T. Ward, B. Davis, R. Wiseman and L. Hennighausen (2001). "Spatial and temporal expression of the Cre gene under the control of the MMTV-LTR in different lines of transgenic mice." Transgenic Res **10**(6): 545-553.

Wagner, N., J. F. Michiels, A. Schedl and K. D. Wagner (2008). "The Wilms' tumour suppressor WT1 is involved in endothelial cell proliferation and migration: expression in tumour vessels in vivo." Oncogene **27**(26): 3662-3672.

Waldstrom, M. and A. Grove (2005). "Immunohistochemical expression of wilms tumor gene protein in different histologic subtypes of ovarian carcinomas." Arch Pathol Lab Med **129**(1): 85-88.

Walker, C., F. Rutten, X. Yuan, H. Pass, D. M. Mew and J. Everitt (1994). "Wilms' tumor suppressor gene expression in rat and human mesothelioma." Cancer Res **54**(12): 3101-3106.

Wang, L. and Z. Y. Wang (2008). "The Wilms' tumor suppressor WT1 inhibits malignant progression of neoplastigenic mammary epithelial cells." Anticancer Res **28**(4b): 2155-2160.

Wang, Z. Y., Q. Q. Qiu and T. F. Deuel (1993). "The Wilms' tumor gene product WT1 activates or suppresses transcription through separate functional domains." J Biol Chem **268**(13): 9172-9175.

Wang, Z. Y., S. L. Madden, T. F. Deuel and F. J. Rauscher, 3rd (1992). "The Wilms' tumor gene product, WT1, represses transcription of the platelet-derived growth factor A-chain gene." J Biol Chem **267**(31): 21999-22002.

Wang, Z., M. Gerstein and M. Snyder (2009). "RNA-Seq: a revolutionary tool for transcriptomics." Nat Rev Genet **10**(1): 57-63.

Wansbury, O., A. Mackay, N. Kogata, C. Mitsopoulos, H. Kendrick, K. Davidson, C. Ruhrberg, J. S. Reis-Filho, M. J. Smalley, M. Zvelebil and B. A. Howard (2011). "Transcriptome analysis of embryonic mammary cells reveals insights into mammary lineage establishment." Breast Cancer Res **13**(4): R79.

Ward, A., J. A. Pooler, K. Miyagawa, A. Duarte, N. D. Hastie and A. Caricasole (1995). "Repression of promoters for the mouse insulin-like growth factor II-encoding gene (Igf-2) by products of the Wilms' tumour suppressor gene wt1." Gene **167**(1-2): 239-243.

Watson, C. J. (2006). "Post-lactational mammary gland regression: molecular basis and implications for breast cancer." Expert Rev Mol Med **8**(32): 1-15.

Webster, N. J., Y. Kong, P. Sharma, M. Haas, S. Sukumar and B. L. Seely (1997). "Differential effects of Wilms tumor WT1 splice variants on the insulin receptor promoter." Biochem Mol Med **62**(2): 139-150.

Weigelt, B., F. C. Geyer and J. S. Reis-Filho (2010). "Histological types of breast cancer: how special are they?" Mol Oncol **4**(3): 192-208.

Wellner, U., J. Schubert, U. C. Burk, O. Schmalhofer, F. Zhu, A. Sonntag, B. Waldvogel, C. Vannier, D. Darling, A. zur Hausen, V. G. Brunton, J. Morton, O. Sansom, J. Schuler, M. P. Stemmler, C. Herzberger, U. Hopt, T. Keck, S. Brabletz and T. Brabletz (2009). "The EMT-activator ZEB1 promotes tumorigenicity by repressing stemness-inhibiting microRNAs." Nat Cell Biol **11**(12): 1487-1495.

Wells, J., M. N. Rivera, W. J. Kim, K. Starbuck and D. A. Haber (2010). "The predominant WT1 isoform (+KTS) encodes a DNA-binding protein targeting the planar cell polarity gene Scribble in renal podocytes." Mol Cancer Res **8**(7): 975-985.

Werner, H., F. J. Rauscher, 3rd, V. P. Sukhatme, I. A. Drummond, C. T. Roberts, Jr. and D. LeRoith (1994). "Transcriptional repression of the insulin-like growth factor I receptor (IGF-I-R) gene by the tumor suppressor WT1 involves binding to sequences both upstream and downstream of the IGF-I-R gene transcription start site." J Biol Chem **269**(17): 12577-12582.

Werner, H., G. G. Re, I. A. Drummond, V. P. Sukhatme, F. J. Rauscher, 3rd, D. A. Sens, A. J. Garvin, D. LeRoith and C. T. Roberts, Jr. (1993). "Increased expression of the insulin-like growth factor I receptor gene, IGF1R, in Wilms tumor is correlated with modulation of IGF1R promoter activity by the WT1 Wilms tumor gene product." Proc Natl Acad Sci U S A **90**(12): 5828-5832.

Wooster, R., G. Bignell, J. Lancaster, S. Swift, S. Seal, J. Mangion, N. Collins, S. Gregory, C. Gumbs and G. Micklem (1995). "Identification of the breast cancer susceptibility gene BRCA2." Nature **378**(6559): 789-792.

Wooster, R., S. L. Neuhausen, J. Mangion, Y. Quirk, D. Ford, N. Collins, K. Nguyen, S. Seal, T. Tran, D. Averill and et al. (1994). "Localization of a breast cancer susceptibility gene, BRCA2, to chromosome 13q12-13." Science **265**(5181): 2088-2090.

Xie, G., A. Ji, Q. Yuan, Z. Jin, Y. Yuan, C. Ren, Z. Guo, Q. Yao, K. Yang, X. Lin and L. Chen (2014). "Tumour-initiating capacity is independent of epithelial-mesenchymal transition status in breast cancer cell lines." Br J Cancer **110**(10): 2514-2523.

Xu, C., C. Wu, Y. Xia, Z. Zhong, X. Liu, J. Xu, F. Cui, B. Chen, O. D. Roe, A. Li and Y. Chen (2013). "WT1 promotes cell proliferation in non-small cell lung cancer cell lines through up-regulating cyclin D1 and p-pRb in vitro and in vivo." PLoS One **8**(8): e68837.

Xu, Z., W. Wang, C. X. Deng and Y. G. Man (2009). "Aberrant p63 and WT-1 expression in myoepithelial cells of pregnancy-associated breast cancer: implications for tumor aggressiveness and invasiveness." Int J Biol Sci **5**(1): 82-96.

Yamagami, T., H. Sugiyama, K. Inoue, H. Ogawa, T. Tatekawa, M. Hirata, T. Kudoh, T. Akiyama, A. Murakami and T. Maekawa (1996). "Growth inhibition of human leukemic cells by WT1 (Wilms tumor gene) antisense oligodeoxynucleotides: implications for the involvement of WT1 in leukemogenesis." Blood **87**(7): 2878-2884.

Yanada, M., S. Terakura, T. Yokozawa, K. Yamamoto, H. Kiyoi, N. Emi, K. Kitamura, A. Kohno, M. Tanaka, T. Tobita, T. Takeo, H. Sao, T. Kataoka, M. Kobayashi, A. Takeshita, Y. Morishita, T. Naoe and I. Sugiura (2004). "Multiplex real-time RT-PCR for prospective evaluation of WT1 and fusion gene transcripts in newly diagnosed de novo acute myeloid leukemia." Leuk Lymphoma **45**(9): 1803-1808.

Yang, J., S. A. Mani, J. L. Donaher, S. Ramaswamy, R. A. Itzykson, C. Come, P. Savagner, I. Gitelman, A. Richardson and R. A. Weinberg (2004). "Twist, a master regulator of morphogenesis, plays an essential role in tumor metastasis." Cell **117**(7): 927-939.

Yang, L., Y. Han, F. Suarez Saiz and M. D. Minden (2007). "A tumor suppressor and oncogene: the WT1 story." Leukemia **21**(5): 868-876.

Yue, W., R. J. Santen, J. P. Wang, Y. Li, M. F. Verderame, W. P. Bocchinfuso, K. S. Korach, P. Devanesan, R. Todorovic, E. G. Rogan and E. L. Cavalieri (2003). "Genotoxic metabolites of estradiol in breast: potential mechanism of estradiol induced carcinogenesis." J Steroid Biochem Mol Biol **86**(3-5): 477-486.

Zaia, A., G. C. Fraizer, L. Piantanelli and G. F. Saunders (2001). "Transcriptional regulation of the androgen signaling pathway by the Wilms' tumor suppressor gene WT1." Anticancer Res **21**(1a): 1-10.

Zamora-Avila, D. E., M. A. Franco-Molina, L. M. Trejo-Avila, C. Rodriguez-Padilla, D. Resendez-Perez and P. Zapata-Benavides (2007). "RNAi silencing of the WT1 gene inhibits cell proliferation and induces apoptosis in the B16F10 murine melanoma cell line." Melanoma Res **17**(6): 341-348.

Zapata-Benavides, P., M. Tuna, G. Lopez-Berestein and A. M. Tari (2002). "Downregulation of Wilms' tumor 1 protein inhibits breast cancer proliferation." Biochem Biophys Res Commun **295**(4): 784-790.

Zavadil, J. and E. P. Bottinger (2005). "TGF-beta and epithelial-to-mesenchymal transitions." Oncogene **24**(37): 5764-5774.

Zhang, T. F., S. Q. Yu, L. S. Guan and Z. Y. Wang (2003). "Inhibition of breast cancer cell growth by the Wilms' tumor suppressor WT1 is associated with a destabilization of beta-catenin." Anticancer Res **23**(5a): 3575-3584.

Zhou, B., Q. Ma, S. Rajagopal, S. M. Wu, I. Domian, J. Rivera-Feliciano, D. Jiang, A. von Gise, S. Ikeda, K. R. Chien and W. T. Pu (2008). "Epicardial progenitors contribute to the cardiomyocyte lineage in the developing heart." Nature **454**(7200): 109-113.

Zhuang, Z., M. J. Merino, A. O. Vortmeyer, B. Bryant, A. E. Lash, C. Wang, M. T. Deavers, W. F. Shelton, S. Kapur and R. S. Chandra (1997). "Identical genetic changes in different histologic components of Wilms' tumors." J Natl Cancer Inst **89**(15): 1148-1152.